Universität der Bundeswehr München
Fakultät für Luft- und Raumfahrttechnik
Institut für Mechanik

Thermo-oxidative ageing of elastomers

A contribution to the experimental investigation and modelling

M.Sc. Alexander Kurt Herzig

Vollständiger Abdruck der von der Fakultät für Luft- und Raumfahrttechnik der Universität der Bundeswehr München zum Erlangen des akademischen Grades eines

Doktor-Ingenieurs (Dr.-Ing.)

genehmigten Dissertation.

Vorsitzender:	Univ.-Prof. Dr. rer. nat. Michael Pfitzner
1. Gutachter:	PD Dr.-Ing. habil. Michael Johlitz
2. Gutachter:	Univ.-Prof. Dr. Sci. (Tech.) Leif Kari

Die Dissertation wurde am 28.10.2019 bei der Universität der Bundeswehr München eingereicht und durch die Fakultät für Luft- und Raumfahrttechnik am 26.02.2020 angenommen. Die mündliche Prüfung fand am 06.03.2020 statt.

Acknowledgement

The work presented was developed during my time as an external research assistant of the Institute of Mechanics, Department of Aerospace Engineering, at the University of the Bundeswehr München. I would like to thank everybody who supported me both technically and mentally during preparing this work.

I would like to express all my gratitude to my supervisor PD Dr.-Ing. habil. Michael Johlitz for his advice and supervision. I am particularly grateful for the technical discussions and its support during this work. The confidence he showed and the freedoms he allowed to me made it possible to realise this scientific project as an external research assistant. I took this privilege never as granted and always enjoyed an equal or even a better treatment as a full-time present research assistant. Besides his enormous expertise in this field and his structured approach to complex problems he provided me a comprehensive academical education and opened the door to international conferences and cooperation.

The head of the Institute of Mechanics Univ.-Prof. Dr.-Ing. habil. Alexander Lion is gratefully acknowledged for paving the way and always supporting this work. He enabled me to start this work as an external research assistant despite all organisational difficulties. His extraordinary ability to abstract complex scientific problems and his fascination to scientific work stood always as an example to me.

Further, I would like to show my gratitude to Univ.-Prov. Dr. Sci. (Tech.) Leif Kari for accompanying me during my whole scientific career and his special interest in my work. The constructive and inspiring discussions with him had been a great source of help and contributed significantly to the development of this work.

Special thanks go to Univ.-Prof. Dr.-Ing. Karl-Christian Thienel who advised and supported me during the whole period of my academic education. His knowledge and vision in the field of scientific work was a great help to me. I appreciate his honest opinion and patience which guided me during my work in the last years or slowed me down when I was once again running in danger to overshoot the mark.

Finally, I would like to thank my fiancée Janina who supported me during the whole time of this project and had to endure a lot of privation in the last years. This work would not have been possible without her incredible patience and her understanding.

Alexander Herzig

Spring 2020

Abstract

In recent decades, elastomer ageing behaviour become enormously important due to their use in increasingly complex and high load applications. In particular, the influence of oxygen and elevated temperature limits the long service life behaviour of elastomer components and increase interest in predicting a material's properties as well as the mechanism behind it. In this work, elastomers thermo-oxidative ageing was analysed in detail by approaching the topic via several disciplines including: engineering, material science and chemistry. After providing a broad fundamental understanding of polymer ageing, oxygen ingress and diffusion into the elastomer is described and forms the basis of experimental investigation and modelling.

Experimental investigation started with the absorption of oxygen by the elastomer sample. A test setup using a respirometer was constructed to measure the quantity of oxygen molecules are taken up by the elastomer during exposure. Test results showed the time dependent absorption rate and clarified the behaviour of certain elastomer types, as well as, the influence of antioxidants. Oxygen adsorption was found as a temperature mediated process with a variable absorption rate during ageing. In order to include information about the spatial distribution in the material, the behaviour of oxygen in the elastomer is also explored. Since diffusion was thought to be very important for the overall oxidation and Diffusion-Limited-Oxidation (DLO) represents a key process when dealing with thermo-oxidative ageing, investigations were expanded to include test methods aimed at understanding nonhomogeneous oxidation. Computer tomography was introduced as a novel approach to give an insight to local changes in density but serves as an indicator for heterogenous ageing only. A closer view on the chemical changes occurring was given by infrared spectroscopy (FT-IR) which provides spatial changes in the adsorption behaviour of functional groups, like carbonyl. The results showed surface oxidation occurring while the interior is only slightly affected. Furthermore, the effects of chemical changes were shown by mechanical testing of aged elastomer samples.

Analogously to the experimental approach, modelling was conducted along the chain of causation. Oxygen absorption was described by Henry's law, with solubility influenced by the progress of ageing. In order to include nonhomogeneous effects, a modular model was developed which is based on a diffusion-reaction equation. Reactivity was coupled with the presence of oxygen and the level of oxidation. The latter represents saturation effects which occur when oxidative reactions proceed. Furthermore, reaction rate decreases due to decreasing number of reaction partners. Diffusivity was described as a function of the level of oxidation. As a measure of oxidation, ageing parameters for network degradation and reformation were introduced. The model was able to describe experimental testing results for which ageing parameter for network degradation was theoretically equal to the carbonyl nitrile ratio obtained by FT-IR analysis. In the course of this work the model was critically reviewed steadily and continuously adjusted to optimise performance and reduce the degree of phenomenology.

Nonhomogeneous oxidation is visualised by plotting ageing parameters over the sample's cross-

section which clearly shows the effect of diffusion-limited oxidation. The outcome was used to describe spatial mechanical properties and clarified the dualism of network degradation and reformation. Moreover, the ageing profiles were coupled with the amount of the absorbed oxygen providing further understanding of thermo-oxidative ageing.

Zusammenfassung

Mit dem zunehmenden Einsatz von Elastomeren in komplexen und sicherheitskritischen Anwendungen stieg die Bedeutung ihres Alterungsverhaltens in den letzten Jahrzehnten stetig an. Insbesondere der Einfluss von Sauerstoff und erhöhter Temperatur kann das Langzeitverhalten von Elastomerbauteilen essentiell beeinflussen und stärkte das Interesse, die sich verändernden Materialeigenschaften vorherzusagen sowie die dahinterstehenden Mechanismen zu verstehen. In dieser Arbeit wurde die thermo-oxidative Alterung von Elastomeren detailliert analysiert, indem das Thema aus verschiedenen Blickwinkeln wie den Disziplinen Konstruktion, Materialwissenschaften und Chemie beleuchtet wurde. Nach der Einführung in die Grundlagen der Alterung von Polymeren, wurde die thermo-oxidative Alterung entlang des Weges beschrieben, über den Sauerstoffmoleküle aus der Umgebung ins Innere eines Elastomers gelangen. Dies bildete die Grundlage für experimentelle Untersuchungen und die Entwicklung bzw. Weiterentwicklung eines Materialmodels.

Der Beginn der Oxidation mit der Aufnahme von Sauerstoffmolekülen aus der Umgebung setzte den Startpunkt für die experimentellen Untersuchungen in dieser Arbeit. Es wurde ein Versuchsstand konstruiert, welcher mit Hilfe eines Respirometer die Sauerstoffmenge maß, die von einer Elastomerprobe während der Auslagerung aufgenommen wurde. Die experimentellen Ergebnisse zeigten, dass die Sauerstoffaufnahme sich mit zunehmender Auslagerungsdauer veränderte und verdeutlichten das Verhalten verschiedener Elastomerarten sowie den Einfluss von Antioxidantien. Um Informationen über Auswirkungen der räumlichen Verteilung des aufgenommenen Sauerstoffes im Material zu erhalten, wurde der Weg des Sauerstoffs im Elastomer weiterverfolgt. Dabei lag der Fokus auf der Untersuchung der inhomogenen Oxidation, welche durch Diffusionsprozesse, im speziellen der Diffusion-Limited-Oxidation (DLO), verursacht werden kann.

Lokale Dichteveränderungen wurden mittels Computertomographie nach verschiedenen Alterungsstufen untersucht und erwies sich als eine neue Möglichkeit zur Indikation von heterogenen Alterserscheinungen. Eine genauere Betrachtung der auftretenden chemischen Veränderungen erfolgte durch Infrarotspektroskopie (FT-IR). Die Veränderungen im Hinblick auf funktionelle Gruppen wie Carbonyl lieferten Erkenntnisse über den Grad der Oxidation und zeigten bei erhöhten Temperaturen eine Konzentration der Oxidation an der Probenoberfläche, während der Innenraum geringfügiger beeinflusst wurde. Die Auswirkungen der chemischen Veränderungen konnten durch mechanische Tests an gealterten Elastomerproben gezeigt werden.

Analog zum experimentellen Ansatz folgte die Materialmodellierung ebenfalls dem Weg des Sauerstoffes von der Absorption aus der Umgebung bis zur Reaktion mit dem Elastomer. Um inhomogene Effekte einzubeziehen, wurde ein modulares Modell entwickelt, das auf einer Diffusionsreaktionsgleichung basiert. Der Reaktionsterm wurde in Abhängigkeit der Sauerstoffkonzentration und der bereits stattgefundenen Oxidation formuliert. Letzteres repräsentiert Sättigungseffekte, die auftreten, wenn die Reaktionsgeschwindigkeit aufgrund der abnehmenden Anzahl von Reaktionspartnern abnimmt. Des Weiteren wurde der Diffusionskoeffizient als Funktion des Ox-

idationsgrades beschrieben. Als Maß für die Oxidation wurden Alterungsparameter für den Netzwerkabbau und die Reformation eingeführt. Das Modell ermöglichte es, die experimentellen Testergebnisse zu simulieren. Dabei wurde der Alterungsparameter für den Netzwerkabbau mit dem aus FT-IR-Analysen ermittelten Carbonyl-Nitril-Verhältnis gleichgesetzt. Eine kontinuierliche Reflektion und Anpassung des Modells während der hier beschriebenen Arbeit trug zur stetigen Optimierung und Verringerung des Anteils bei, der nur phänomenologisch beschrieben werden konnte.

Die inhomogene Oxidation wurde mittels der ortsabhängigen Alterungsparameter dargestellt und verdeutlichte so den Effekt der Diffusion-Limited-Oxidation. Die Ergebnisse wurden zur Beschreibung der mechanischen Eigenschaften und des Dualismus von Netzwerkabbau und Neubildung verwendet. Darüber hinaus wurden die Alterungsprofile mit der Menge des absorbierten Sauerstoffs gekoppelt, um ein besseres Verständnis der thermo-oxidativen Alterung zu erzielen.

Contents

1 Introduction

Approximately 3500 years before Charles Nelson Goodyear discovered the process of vulcanisation Mesoamerican peoples struggled with similar problems when using natural rubber. The raw material, dried latex, became brittle at low temperatures and sticky at elevated temperatures which makes it unsuitable for most practical applications. Deficiencies in strength, elasticity and durability of natural rubber produced from the Castilla elastica tree hindered a technical usage and made the Mesoamericans to be resourceful. By mixing raw latex with extract from the morning glory vine Ipomoea alba the Mayas discovered that the properties of the rubber can be improved and manufacturing of usable devices, for instance, rubber balls, sandal soles or adhesive bands became possible. Furthermore, the Mayas adjusted the mixture ratio to obtain rubber with different properties for specific needs. This made them the first known pioneers which were able to manufacture processed rubber [1]. Producing bouncing rubber balls was important for the Mayas since they needed them for religious ballgames which took place at big stone courts like the one at Chichen Itza, Mexico (Figure 1). The sulphur-containing amino acids of the morning glory vine provoked a cross-linking process in the latex from the rubber trees on molecular level similar to what Goodyear discovered centuries later and gave the material the typical rubberlike behaviour. There is almost no information about the longevity and ageing behaviour of the Mayan rubber balls but probably most of the players did not care about that since they got the honour to be sacrificed after the game.

Figure 1: Left: Mayan ballcourt goal at Chichen Itza, Mexico; right: a centuries-old latex ball made by the Olmec, Mexico (right picture: National Geographic)

During discovering the American continent in the 15th century the European explorers came in contact with natural rubber for the first time, which was used by the natives for various applications. Later in time, the European sailors recognised the potential of this new material and brought it to Europe, but during the journey the natural rubber became viscous and hard. In addition, the dried latex was highly temperature dependent, which was a serious disadvantage of the products made from it.

In the 19th century, one of the people working with natural rubber was Charles Nelson Goodyear who produced rainwear and other products. Initially, he was not very successful with these

products since on one hand the clothes became stiff and brittle at cold temperatures and on the other hand the material could not withstand summerlike temperatures. In 1839 he merged natural rubber (latex) and sulphur probably in an act of coincidence and exposed the mixture to elevated temperatures. As a result, he obtained an odourless material, which was elastic and solid at a broad temperature range. This was the first time vulcanised rubber was produced and the success story of rubber started.

With progressive development in the subsequent decades, the technical and economical requirements for rubber materials increased more and more. Hence, the research on the initial properties after manufacture was extended to durability and ageing phenomena. Changing properties during storage and application gained attention in a way which was much higher than known from metals. Thus, a new field of research emerged which deals with the prediction and simulation of aged elastomers or more broadly formulated of polymers. Due to the variety of different types of elastomers, admixtures and impact factors an all-embracing solution to this problem is highly challenging and will probably not exist in the next few decades.

The following work focuses on the influence of oxygen on elastomer materials. On this account, the work aims not on a singular solution but provides fundamental knowledge and proposals to handle the phenomena of oxidative ageing. Furthermore, specific examples of experimental investigations and constitutive modelling are given.

This work starts from the basics of polymer ageing by explaining and classifying different impact factors in subsection 3.1 as well as different kinds of polymer ageing in subsection 3.2 before the ageing of elastomers comes into focus (subsection 3.3). Subsequently, oxidation is introduced as only one among many types of elastomer ageing in section 4. Thermo-oxidative ageing is handled from a theoretical point of view by following the mechanism by which oxygen molecules penetrate the elastomer material and cause chemical reactions. This forms the basis for experimental investigations in this field. In order to execute measurements on oxygen absorption of elastomers, a testing setup was developed for this work which is explained in subsection 5.1. Afterwards, spatial phenomena are considered by investigating heterogeneous effects of oxidation (subsection 5.2) before a brief introduction to ageing-induced changes in mechanical properties is given in subsection 5.3. Chapter six deals with the simulation of the phenomena investigated experimentally. Subsequently, subsection 6.1 starts by examining the oxygen absorption behaviour. In subsection 6.2 modelling of heterogeneous oxidation is investigated by describing the diffusion-reaction behaviour of exposed elastomers.

For reasons of clarity, critical reflection of the developed setup as well as detailed discussions of the experimental and theoretical outputs are given at the end of the corresponding chapters. A summarised reflection and an outlook at the end conclude this work.

2 State of the Art

In the last decades polymers became enormously important in the industrial field of material science and engineering. The reasons for this success are their diverse, including advantages in material properties such as: plasticity, flexibility and good adhesion. Consequently, they have been used in a broad range of technical applications from cheap disposables to complex and highly loaded components such as: vibration absorbers, vehicle tires, gaskets, matrix material in composites, coatings or adhesive bonding agents. Based on progressive research and increasing knowledge in polymer science, the material is intensively used in highly stress load-bearing applications as well as safety critical components. For instance, polymer coatings are used in medical applications including biocompatible surfaces of implants [2][3], main supporting adhesive bonds in aircrafts [4][5], elastomer sealings and electrical isolations in nuclear power plants [6], and filling material for concrete repair in civil engineering [7]. Most of these applications place stringent requirements on the structural integrity and durability of the material. Whereas the fatigue or ageing behaviour of a plastic fork attracts limited attention, the failure mechanism of car or aircraft tires can result in fatal consequences. Therefore, with ongoing deployment of highly loaded and exposed polymer components, research on durability, changing properties and lifetime prediction moves into focus more and more.

A challenge and highly relevant aspect during the entire lifetime of polymer components is the more or less distinctive process of degradation. The accompanying changes in material properties are described as “ageing”, which can be both chemical and physical phenomena. In order to understand these almost unavoidable changes a broad multidisciplinary approach from morphology, chemistry and material science is required. Especially for issues affecting service live a closer look on the chemical composition and the effects on it caused by ageing is necessary. Degradation of polymers is induced by several processes running in parallel which can amplify or compensate each other depending on the materials composition, the dimension of the component as well as external factors like contact to different medias, high temperatures, pressure or radiation [8]. This makes ageing a complex and hard to predict challenge.

Besides irreversible changes polymers also show reversible processes which affect their behaviour based on the aspiring of a thermodynamic equilibrium state by macromolecular relaxation processes [9][10][11]. From a lifetime limiting point of view physical ageing plays a tangential role but nevertheless for applications with respect to mechanical properties a precise description of this behaviour is essential. Examples to describe physical ageing based on a free energy approach are provided for example by Lion et al. [12] and Mittermeier et al. [13].

Degradation is caused mostly by environmental influences which exist during manufacturing and service life. Especially an oxygen containing environment affects the material and provokes irreversible degradation. This type of chemical ageing is the dominant and most relevant ageing process in many applications even due to the fact that an oxygen containing environment is usually present as ambient air [14][15]. Chemical reactions are known to affect the molecular

structure of the polymer which result in changes of mechanical properties. Since oxidation is not a uniform chemical process but depends on the polymer material and the reactions' boundary conditions, several more or less simplified reaction schemes and kinetic models are considered to describe the reaction kinetics [16][17][18]. The pure existence of different reactions schemes makes clear that there is a need for a closer look on the individual oxidation behaviour of different types of polymers, since material composition and morphology play an important role.

Especially for elastomers the degradation process and therefore the restriction in operation time is driven by chemical ageing. One of the earliest studies on the ageing of elastomers was conducted by Tobolsky et al. [19][20]. Changes in mechanical properties have been explained by breaking up and linking of the carbon chains as well as the cross-linkings between them. This approach is still used for the characterisation of elastomers nowadays but reaches its limit more and more since various effects cannot be explained due to the lack of considering diverse chemical reactions or inhomogeneous processes.

The influence of oxygen on elastomers which will be in the scope of the following work can strongly affect the material with respect to changes in mechanical properties, permeability to gases or fatigue behaviour [20][21]. Main research challenge regarding polymer ageing is the qualitative and quantitative description of altering properties over the lifetime of elastomer components to predict the end of usage, prevent unintentional failure and optimise maintenance costs. Thus, material models are required which simulate the ageing behaviour and establish a connection between the sources and effects of oxidative degradation. This implies a detailed knowledge of the ongoing physical and chemical processes as well as suitable experimental methods to identify the correlations as well as causations and to describe reliably the static and dynamic behaviour of the material under ageing. In the case of elastomers this is still a huge challenge particularly for viscoelasticity and chemo-rheological properties [22].

Since degradation of mechanical properties is mainly caused by oxidation a lot of research was already done on this issue [23][24][25]. Usually experimental investigations with samples exposed at elevated temperatures were executed to accelerate the ageing process and shorten testing time. The question arises if degradation can simply be accelerated by increased temperature or if the experiments lose their predictive value [26]. Investigations showed that oxygen absorption, chemical reactivity and the influence of antioxidants are functions of the ageing temperature. Thus, experimental testing on ageing is performed above service temperature to accelerate ageing and finally predict the behaviour of the polymer under usage conditions for much longer periods in time [11][23][26][27][28]. This extrapolation is based on appropriate mathematical models, e.g. an Arrhenius relationship [14]. In the case of changing reaction mechanisms due to different temperature levels the method described reaches its limit and forecasts become inaccurate. One reason is that activation temperature of certain degradative reactions is solely reached under testing conditions since they are not important in a lower temperature regime [23][29][30][31].

Another reason making predictions difficult is the influence of developing degradation on the ongoing ageing process. Here, the degree of ageing has influence on the subsequent ageing be-

haviour. This is important when processes do not occur homogeneously throughout the material. Hence, a more or less heterogeneous ageing can be observed depending on certain circumstances. For oxidation that can be relevant if diffusivity of the polymer is influenced since oxygen is usually absorbed from the ambient environment and diffuses into the material before oxidative reactions occur or if antioxidants migrate due to concentrations gradients which arise during exposure. Other reasons are morphological variations due to e.g. changes in the degree of crystallisation. Heterogeneous effects can also be provoked by catalyst residues or isolated thermal reactions due to an inhomogeneous temperature field. In general, impact factors which take effect on the polymer from the outside like gases or fluids as well as radiation cause higher levels of degradation at the outer region before the latter continues into the interior or are even is limited to the surface layer [21][32]. The interaction of processes running in parallel add complexity to the investigation and complicate the modelling of polymer ageing.

The phenomena of oxygen being unable to penetrate to the core of the elastomer component due to oxidation is known as diffusion-limited-oxidation (DLO). The declined diffusivity can be explained either by a spatial reduction of the diffusion coefficient or the binding of oxygen molecules by oxidative reactions in the surface layer. Both effects hinder oxygen molecules from being distributed homogeneously and hinder oxidation progressing into the core of the sample. As a result, oxidation is limited to the superficial region and the interior of the material is less affected.

The fact that oxidation starts with the absorption of oxygen molecules by the polymers surface has motivated methods to avoid ageing by blocking the diffusion process or subsequent oxidative reactions. Therefore, waxes are used which function as a physical barrier and gave gases no access to the elastomers surface. Another possibility are additives which prevent the chemical reaction of the oxygen with the polymers. Usually, technical applications combine both methods or apply several antioxidants in parallel [33]. A technical application of polymers, especially elastomers, without any antioxidant is almost impracticable due to the high propensity to oxidation as well as other types of ageing. Therefore, antioxidants should always be considered when research focuses on the durability of polymers. For one thing, antioxidants are usually handled like a substance being solved in the polymer with the ability of diffusion as well as reaction with oxygen [34]. On the other hand, antioxidants are often not considered separately and their effects are detached to the oxidative reaction kinetics which means chemical reactivity of oxidation is considered being slightly lower due to the presence of antioxidants [35][36][37].

As mentioned, most rates of physical and chemical processes depend on temperature and therefore oxygen absorption, diffusion and reaction can be accelerated by elevated temperatures. Generally, two heat sources can be distinguished, heat flux from the ambient due to elevated environmental temperature and heat sources in the material due to chemical reactions or dissipative heating. The latter is important for dynamically loaded elastomers since the internal temperature can be high compared to the ambient one [38]. A modelling approach which links mechanical strain to dissipative heating was developed by Johlitz and Dippel [39][40]. Due to various external load applications and non-trivial shapes of elastomer components, complex states

of stress can occur. Further an inhomogeneous and changeable temperature field also fosters heterogeneous ageing.

Once oxygen infiltrates the elastomer a sequence of chemical reactions can occur. The chemical reactions provoke changes in the macromolecular structure of the elastomer which in the end are responsible for changes in polymer properties. Therefore, detailed knowledge about the ongoing chemical reactions is essential. Investigations by infrared spectroscopy showed that the amount of certain functional groups change during ageing [41]. Measuring these changes can be used to determine the degree of ageing. For example, functional groups like carbonyl and hydroxyl as well as the amount of carbon-carbon double bonds can serve as qualitative and quantitative gages [21][25][42][43][44].

This is the onset of the following work which provides a contribution to the oxidative ageing of elastomers and constitutive modelling of these phenomena. Therefore, approaches to the topic from various angles were introduced and discussed including the engineering point of view as well as physical and chemical processes. Since degradation of elastomers is a multidisciplinary issue special attention is given on a clear and logical structure following the chain of causation. The primary challenge is the fact that essential processes are taking place on different scales. Thus, microscopic effects are considered as well as macroscopic ones without losing focus on technical application of the material from an engineering point of view.

3 Ageing of polymers

3.1 Ageing and lifetime prediction

Ageing describes chemical and physical changes which affect the properties of a material over time. Ever since polymers were used in key applications durability and end of service time or lifetime came to the forefront. Therefore, knowledge of the ageing behaviour, or changing properties as a function of time becomes an important aspect to the polymeric material. Additionally, in safety critical applications a huge effort is spent on the prediction of material properties and durability. In order to ensure a valid prediction a closer look at the chemical composition of the material and its microscopic structure is as necessary as the exact knowledge about loads affecting the polymer. All in all, service conditions must be known to choose the appropriate material for the certain application.

In general, polymers are distinguished in four different categories which are quite different in their properties and fields of application. The four types are as follows: thermoplastics, thermoplastic elastomers, elastomers and thermosets, which all consist of entangled molecular chains. The structure of the molecular chains and their entanglement as well as the cross-linking of them result in the classification of the polymers. A detailed description of the different types of polymers is not the focus of this work since it is given in detail elsewhere [45][46][47]. Of course, durability is different for the types of polymers and ageing of thermoplastics is mostly different from ageing of elastomers or stiff thermosets. Nevertheless, the mechanisms described in the following are valid for polymers in general and a fundamental understanding is given which is expanded for the case of elastomers subsequently.

The causes of ageing can be distinguished in intrinsic and extrinsic aspects. Intrinsic aspects are based on an interior state of non-equilibrium or contamination, which occur during manufacturing. Such unstable thermodynamic states can result, from internal stresses due to non-homogeneous morphology like the degree of crystallisation, or incomplete synthesis. Unequal distribution of additives during manufacturing and their limited miscibility are additional reasons which provoke changes in the material. These effects can hardly be avoided and are pervasive during manufacturing and application. The unstable thermodynamic states are also present in the raw material and come from the physical structure of the polymer and occur in all kinds of plastics. Extrinsic aspects of ageing mostly need thermal activation to provoke measurable variations of the polymer's properties. Hence, it seems that these kind of changes can be attributed to thermal ageing effects but in fact elevated temperature is mostly not the origin but an accelerating factor [11][47][48].

Extrinsic factors represent the influence of the ambient environment or external loads which affect the polymer during lifetime. Therefore, it is important to know the expected load range and environmental conditions during application. Examples for extrinsic factors which impact the polymer from the environment are: heat input, weathering (including moisture), radiation

and biological or chemical exposure. Perhaps the most important influence is that of oxygen which is part of the atmosphere. It is absorbed by the polymer and reacts chemically with the polymer, called thermo-oxidative ageing [11][38]. In general, extrinsic factors are mostly unavoidable since the environmental conditions are a consequence of a certain application. An example of this is rubber gaskets of an oil conducting tube system at the boundary of rubber and oil or protective coatings which guard a metallic component against weathering, for instance.

A summary and visualisation of intrinsic and extrinsic ageing factors is given in Figure 2. Thereby it should be shown that extrinsic factors result from the ambient environment and intrinsic ones are related to the material condition. Of course, a sharp separate consideration is not possible due to the interaction of intrinsic and extrinsic factors. An example is the relaxation of internal stresses which only can proceed above a certain temperature or chemical structure which is affected by ozone and oxygen in parallel. The factors listed in Figure 2 shall be explained and discussed briefly to widen the understanding of the exposure of polymers and establish the basis for the subsequent chapters. First the extrinsic and afterwards the intrinsic factors are presented.

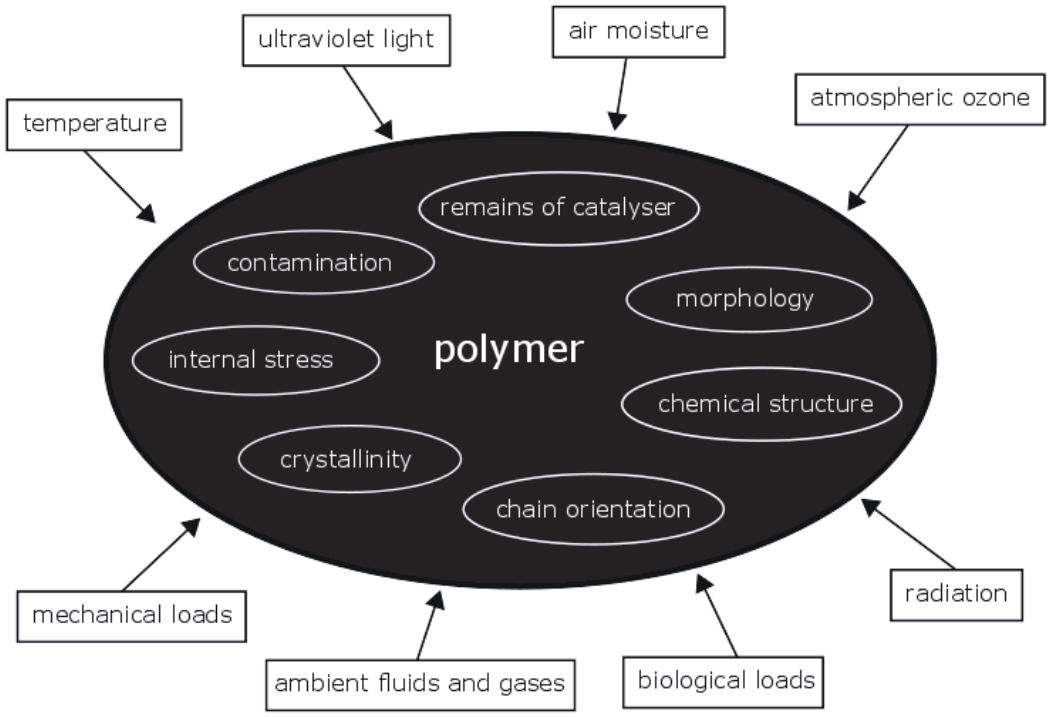

Figure 2: Examples of intrinsic and extrinsic factors influencing polymer materials [48]

3.1.1 Extrinsic factors

An omnipresent factor when dealing with the ageing of polymers is the influence of temperature. Elevated molecular movement and the acceleration of chemical reactions put temperature in perspective when talking about polymer ageing. During the polymer lifetime, temperature plays

an important role starting from the manufacturing process, where elevated temperatures are used to initiate cross-linking reactions and nonhomogeneous heat distribution can result in non-uniform cross-linking density. Further, cooling from the melt can cause states of imbalance which become important if the polymer is later exposed to elevated temperatures. Heat input and temperature cycles during storage and use have impact on the properties of the material and affect its long-term stability. These elevated temperatures can cause thermal degradation which affects the chemical bonds in the molecular chain of the polymer. The bonds are stresses due to thermally induced molecular vibration up to breakage. Additionally, incomplete cross-linking which results in residual cross-linking agents can provoke post cross-linking that counteracts thermal degradation [20]. As a result, elevated temperature is often used to accelerate the ageing process and in general to shorten exposure time during testing. For elastomers as well as for glassy polymers the experimental exposure is done above glass transition temperature or above the melting point for semi-crystalline polymers. At these temperatures reactions and mechanisms can be activated which are not relevant at service temperatures. Thus, the extrapolation of results obtained at higher to lower temperature is highly questionable [49].

The most relevant kind of radiation polymers are exposed to are UV-radiation and highly energetic radiation. The former is usually part of sunlight and hence a widespread factor. The latter mainly means nuclear radiation and hence is only important in high specialised applications like nuclear power plants [6][50]. UV-radiation affects the molecular makeup and causes chain scission, network reformation and the formation of functional groups. Usually the effect is limited to the surface layer and does not affect the whole material evenly.

In Figure 2 the influence of water is split up into effects of humidity and liquid water. Water can affect polymers physically by means of swelling and extraction of soluble substances like additives. Other kinds of ageing can be intensified for instance oxidation. On the other hand, in maritime applications water can be the only medium in the ambient environment of the elastomer and thus prevent the polymer from other impacts like oxygen or ozone. The absorption of water by the polymer can cause a gain in weight and corresponding swelling [51][52] which affects the materials density. The increase in weight of elastomers was demonstrated to be different for distilled water and salt water [53]. Further, water provokes different levels of heat dissipation and has an impact on the fatigue behaviour of elastomers [54]. Besides its physical impact water can cause chemical changes due to hydrolysis which splits functional groups such as esters in polyurethane. This results in the decrease of the molecular weight and consequently in the degradation of mechanical properties [11].

In many application polymers are used since they offer unique mechanical properties. Elastomers are of particular interest due to their deformability and elasticity. Nevertheless, such deformations can cause straining of bond angle and bond distance upon failure of the molecular chain [11]. Furthermore, mechanical loads can influence other ageing mechanisms for instance, diffusivity [55]. These types of effects are not well understood yet. In the case of thermo-oxidative ageing mechanical loads can provoke a decrease of oxygen diffusion and hence decelerate degradation but in parallel chain scission and the formation of radicals enhance ageing. This dualism

is an example of the complexity of competing effects between mechanical and other loads. Depending on the polymer and circumstances of exposure predictions are difficult. Ageing can also influence the mechanical properties such as cracks which are formed at an embrittled surface due to mechanical loads or shrinkage. Consequently, stress condition and the surface area which is in contact with the ambient medium changes and affects the subsequent ageing behaviour [29][56].

Biological impact on polymers is rather insignificant compared to others. Nevertheless, their chemical structure based on hydrocarbons poses breeding ground for living organism which can be a problem particularly in regions with tropical climate. Besides the disadvantage this fact also offers new opportunities regarding biodegradation for a sustainable usage of polymers [57] or usage in special fields like pharmaceutical applications [58].

Several ageing mechanisms are hidden behind the influence of fluids and gases. The effect of water and moisture was already discussed above but in combination with corrosive gases like for instance nitrogen oxide, sulphur dioxide or ozone, diluted acid solutions can emerge which affect polymer material. Such acids cause deterioration of the molecular structure via chain scission which results in embrittlement. In a more concentrated form, acid can attack the polymer when polymers are exposed to pure chemicals. This can be found in more specialised applications or were such materials are used to protection against such substances like for example in the form of rubber gloves. In this context lubricants should be mentioned as well. Polymers in contact with oil are often found in automotive technology and where the oil affects the material in different ways. Besides a barrier effect isolating the polymer from other environmental influences the oil itself can penetrate into the material and accelerate or decelerate chain-scission and network reformation. Further extraction and reaction with additives can occur especially for elastomers [59].

The most important and common deterioration of polymers is caused by oxygen and ozone which are omnipresent in atmosphere. The latter particularly affects unsaturated hydrocarbons and provokes effects comparable to oxidation. Oxidation causes chemical changes due to the reaction of oxygen with the molecular structure resulting in chain-scission, network reformation and chain branching. In the further course of this work oxidation of elastomers will be analysed more detailed.

All in all, extrinsic ageing aspects mostly generate heterogenous conditions due to the external impact. Besides material composition and potential coupling with other effects penetration and diffusion effects must be considered for a detailed analysis. In contrast to the extrinsic factors the intrinsic ones deal with the interior condition of the polymer and contain the physical and chemical structure as well as substances and contaminations contained [8].

3.1.2 Intrinsic factors

The chemical structure of polymers can be influenced by ageing phenomena as mentioned before. In addition the chemical structure itself has huge impact on the degradation behaviour. Effects of external factors highly depend on the materials composition. As an example, radical reactions mainly attack CH-bonds and functional groups like hydroxyl, ester or amide usually increase the sensitivity to chemical deterioration [11]. Susceptibility of polymers is high for branched molecule chains and otherwise saturated unbranched hydrocarbons which are quite resistant against the influence of oxygen. Further, methyl and phenyl groups are examples for decelerating oxidation by providing a shielding effect. Polymers containing double bonds are most susceptible to chemical deterioration [60]. Thus, the type of polymer and the chemical composition plays a major role in the ageing behaviour. Moreover, the manufacturing process has huge impact on the chemical constitution and heterogeneity in the material. This influences morphology and causes nonhomogeneous molecular mass distribution which has an impact on the thermo-oxidative ageing since oxygen absorption behaviour is affected [11]. The latter is also influenced by cross-linking density and distribution governing the permeation behaviour [61].

Morphology describes the physical or rather the supramolecular structure of polymers and hence depicts the causal linkage between chemical and physical aspects. This includes amongst others chain orientation and crystallinity as well as vacancies usually due to manufacturing. Chain orientation has an impact on diffusion behaviour of gases and fluids penetrating the polymer as well as the swelling behaviour. Internal stresses can occur if polymers are cooled from the melt without sufficient time to achieve equilibrium. During polymer lifetime, tensions relieve and morphology changes.

Although crystallinity is a special form of morphology, it should be mentioned separately due to its importance for polymer materials. Since the most energetic condition is the tightest packing density, polymer molecular chains try to align in parallel which results in partial areas of close arrangement. If molecules are close together, penetration of fluids and gases is impeded and diffusivity is low [62]. Amorphous structures usually show a higher diffusivity. Crystallinity can occur non-homogeneously and produce gradients due to nonuniform heat distribution during the manufacturing process. Furthermore, during service application elevated temperatures, mechanical loads and chemical degradation can cause so called post-crystallisation due to partial enabling of molecular rearrangements.

Contaminations are usually unintended but occur during production or postprocessing of the polymer. Metallic impurities can have an especially catalytic effect and serve as starting point of oxidation. Contaminations are also a significant reason for absorption of UV-radiation and hence warm the material. Furthermore, the undesired soiling of the polymer substances can also be a left over from the manufacturing process if not fully reacted. For example, catalysts can remain unreacted in the polymer and cause chemical reactions at a later stage especially when thermally activated. This leads to chemical changes like post-cross-linking which provokes alteration of mechanical properties. Sometimes such effects are intended and the residual catalyst

counteracts ageing induced chain-scission [21].

After introducing intrinsic and extrinsic factors it should be clarified that the actual ageing process is always taking place in the material itself and the differentiation here is based on the origin of the trigger that causes the time-dependent changes in the polymer's properties. When dealing with ageing of polymers a broad multidisciplinary approach is required taking into account morphology, chemistry, and material science. All in all, usage conditions and the functional purpose are the selection criteria for the polymer applied in a certain application. Since polymers are categorised as organic matter a macroscopic as well as a microscopic point of view is required [48]. The knowledge of both material composition and ambient conditions are necessary to enable a suitable selection of the polymer and predict service life.

3.1.3 Challenges of lifetime prediction

The influence of thermal loads strongly affects the other intrinsic and extrinsic aspects presented. Individual ageing processes can be accelerated or suppressed by temperature which can lead to diverse the timeline of ongoing physical and chemical changes. That means, one particular environmental or internal effect can dominate the process of ageing. In most technical applications polymers are affected by several ageing processes in parallel which interact and are dependent on other factors such as the progress of ageing itself. Since it is difficult to separate individual ageing processes and to investigate them isolated as well as measure them in a quantitative way, experimental research is still a challenge. This is for reason, various processes which are interlinked in a complex interlocking manner that is not completely understood yet [48]. Different experimental approaches like mechanical, chemical, or calorimetric investigations are used to achieve a better understanding of the ageing behaviour of a certain polymer. Nevertheless, the specific environmental conditions must always be considered for any prediction regarding service time of polymer components or adhesive bonds. Therefore, it is recommended to carry out investigations on exactly the material used in the desired application and under the expected environmental conditions. Further, shape and dimensions should be chosen on the same principles to achieve robust results. Unfortunately, this can cause practical difficulties for laboratory investigations, for instance, slow ageing under real conditions or the final shape of the component is quite big or not suitable for usual testing setup, i.e. car tires. Adapting the experimental condition should be done thoughtfully since extracting specimens from a given component or producing new samples in test-specimen shape as well as accelerating the ageing process by intensifying extrinsic factors can provoke a different ageing behaviour and hence distort the predictions. For reasons of fundamental research, it is advisable to execute analysis on well-known, simple material samples to avoid an accumulation of too many combinations of ageing processes and to keep the interpretation as simple as possible. An example is the partial omission of additives and antioxidants to achieve a better understanding of how these additives influence the ageing behaviour. This is especially evident when dealing with diffusion phenomena, heterogeneous vs. homogenous ageing processes, or liquid-state vs. solid-state kinetics [26].

Besides the challenge of simulating and accelerating ageing conditions as closely as possible to real conditions, lifetime prediction has the difficult task to characterise the deterioration and define limits which represent the end of usability. One possibility is testing the same material under equal conditions as exposed in reality. Testing until failure requires very long ageing durations which is mostly inconvenient. Therefore, ageing is done only for a limited duration and extrapolation is used to predict material properties for longer exposure times. This requires models which are able to extrapolate the experimental findings to extended ageing durations. Furthermore, this method has to be iterated for each material and service conditions which makes it very time consuming and costly. Hence, samples are usually exposed to laboratory conditions which provoke accelerated ageing and reduce testing time. The most common exposure is to elevated temperatures which is used to simulate ageing at lower temperatures but for longer durations. Therefore, models are required which allow such a time shifting. Furthermore, when passing physical or chemical transition zones like glass transition temperature this can be quite difficult. All in all, lifetime prediction needs the definition of failure criteria which usually depends on the specific application. It is very difficult to define a certain parameter which is used to measure the degree of ageing and a threshold which describes the end of life time especially for different types of polymers and different applications.

Although it is difficult to define firm criteria for the end of polymers lifetime some examples should be given. Kawashima et al. [43] used the quantity of carbon-carbon bonds as a quantitative measure. He defined the end of service time when the absorbance of infrared spectroscopy is reduced to 45 % compared to virgin state (see also subsubsection 5.2.2). Blanco [63][64] introduced a degradation value in percent which is based on activation energy and mass loss to describe the degree of ageing. DIN 53383 describes the testing of thermo-oxidative ageing of polyethylene and defines an oxidation index of 2 as lifetime limit. The oxidation index is measured by infrared spectroscopy and uses the quantity of carbonyl groups in the material (see also paragraph 5.2.2.1). Dobkowski [65] uses the oxidation induction time (OIT) as a measure of thermo-oxidative stability which finally is based on the activation energy. Several more approaches exist to quantify the degree of degradation which are based, for instance, on mechanical properties like ultimate elongation, tensile strength or colour change [66]. The fact that it is quite hard to find specific values for the end of lifetime underlines the difficulty of this problem. Depending on the application purpose and the polymer itself lifetime prediction is an individual process which cannot be answered in a general and all-embracing manner.

3.2 Different kinds of polymer ageing

Different ways exist to subdivide polymer ageing regarding source or consequence of the ageing process. The following explanations were gathered during the research for this project and have been published in [48]. This chapter should give an overview over the field of polymer ageing and highlight possible approaches that should help to get a closer understanding.

A possible classification of ageing phenomena was already given in the previous subsection 3.1 by

distinguishing the origin of ageing in intrinsic and extrinsic ones (see also Figure 2). An obvious way to elucidate the ageing behaviour is to ask the basic question: How can the deterioration of a polymer be reduced or avoided? The answer is both simple and complicated at the same time. An alleged easy solution would be to isolate the polymer from the influencing factors and consequently prevent ageing mechanism to initiate. A problem would be to accomplish keeping heat or mechanical loads away from an elastomeric vibration absorber or atmospheric influences from a coating. For many applications that is not useful and does not represent a practical solution.

Besides the fact that most extrinsic aspects cannot be avoided it is essential to consider them during design phase. A priori knowledge of loads and boundary conditions are essential to choose the ideally suited material for a certain application. Some polymers are more resistant to a given environment than others and are more capable of handling certain loads. An example are adhesives in aircraft engineering which are often made from epoxy-based structural film adhesives which are characterised by good mechanical behaviour and temperature stability. In contrast, silicon adhesives are used when stiffness is less important but oil resistance is required [5]. Another example are applications in maritime engineering which involve other requirements regarding salt water resistance and humidity than construction or civil engineering. The latter uses polymers, e.g. as adhesives for grout injection into cracks or as surface coating [7]. However, distinguishing ageing regarding intrinsic and extrinsic factors does not consider the nature of the ageing process. Hence, a further possibility exists for classification.

The most common classification of polymer ageing considers physical and chemical ageing regarding the processes that occur on molecular level. Sometimes mechanical ageing is listed as a third category. Hence, in the following ageing will be classified in three fundamental groups wherein mechanical ageing is often not accepted as an own category of ageing and typically allocated to physical ageing and fatigue:

- Physical ageing
- Chemical ageing
- Mechanical ageing

3.2.1 Physical Ageing

Physical ageing describes variations of polymers in a so-called thermoreversible manner. Mainly these are characteristic material functions which are altered with time in morphology, molecular orientation or concentration ratios of components (in the case of multi-component systems). These could be: specific volume, heat capacity, or the relaxation function of a polymer in the glassy state. Physical ageing is more distinct for temperatures close to the glass transition temperature T_g of the material as explained more in detail below [67]. Increasing temperature

above T_g can reverse physical ageing due to the thermoreversible nature of the process. Neither the polymers' chains nor the cross-links between them are broken up by physical ageing but the structural arrangement and orientation of the molecular chains is affected. Elevated molecular movement due to elevated temperatures allows the molecular structure and the backbone chains to align in a more energetically favourable way which consequently results in relaxation of residual stresses. Furthermore, the molecular chains often have a production-related preferential direction in the material, which originate from flow processes during moulding. Due to the entropy-elastic recovery, reorientation processes take place, which can lead to distortion and tearing of the material [19]. Typical representatives of physical ageing are [11][68]:

- Chain re-orientation
- Relaxation of residual stresses
- Post-crystallisation and decrease of glass-transition temperature
- Diffusion and emitting of additives like plasticiser

Post-crystallisation of plastics occurs especially at elevated temperatures between glass transition and the melting region by striving for a thermodynamically more stable state. Besides the change of material properties, the formation of a denser molecular package must be taken into account since the latter can also lead to shrinkage and associated cracking. In Figure 3 physical ageing is illustrated and the difference to chemical ageing is differentiated. The graphic indicates that physical ageing is a reversible process without any chemical changes. The changes in morphology are shown as alignment changes of the carbon chains which can be reversed by heating the polymer above glass transition temperature.

From a thermodynamic point of view, physical ageing is based on non-equilibrium states which are created by cooling the polymer from the melt. The material is transferred from an entropy-elastic or liquid state into a stiffy glass state. Thereby the polymer tries to reach a thermodynamic equilibrium state by macromolecular movements. Such relaxation processes require thermal activation. During cooling from the melt, the relaxation is not possible in that short time span and hence internal stresses and chain segment orientation are locked. Subsequently, relaxation processes occur during service time due to the stresing of the material to reduce this non-equilibrium state. As a consequence, property and volume changes occur which are known effects of physical ageing. Even going further, shrinkage and expansion induced damages like of fracture can occur. Indeed these are irreversible changes despite physical ageing itself being thermally reversible [67].

Rearrangements of molecular chains as caused by crystallisation or orientation changes affect the polymers diffusivity. Usually the diffusion coefficient declines if the molecular chain entanglement and network becomes denser [11][62]. This is an example for the interaction of physical and chemical ageing and proves that an isolated focus on either one is inadvisable. During the whole

lifetime, physical and chemical ageing influence each other although both phenomena run on different timescales.

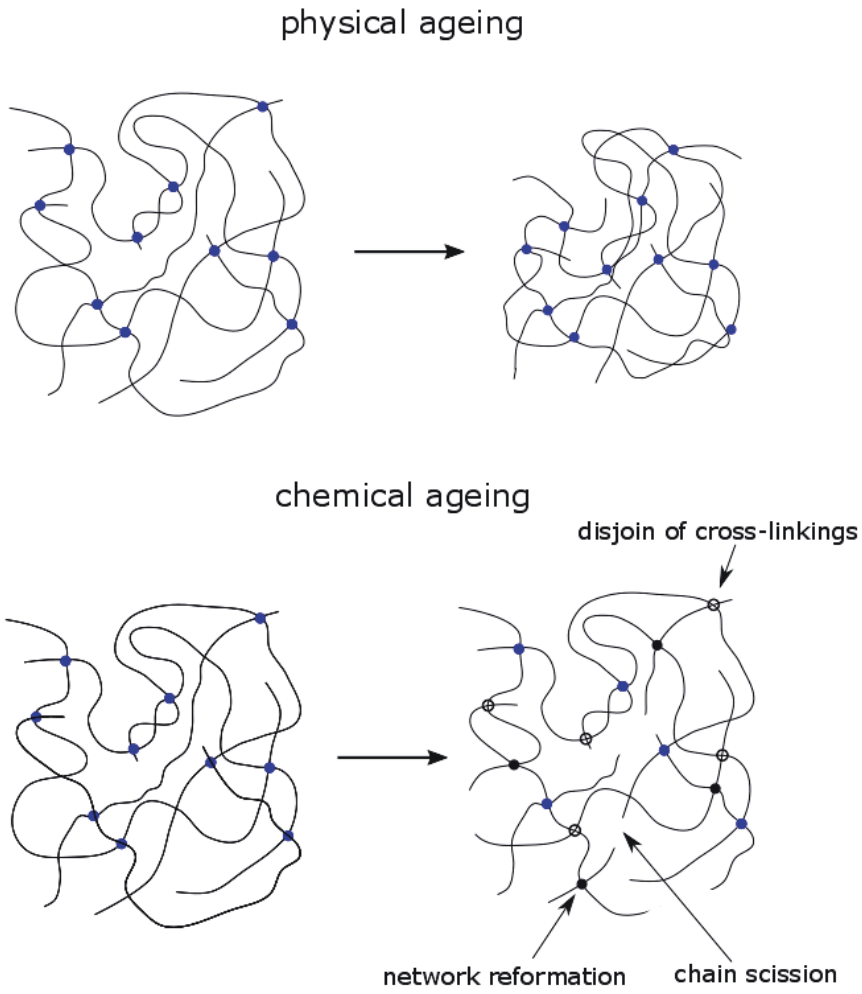

Figure 3: Schematic illustration of physical and chemical ageing [48]

The effect of physical ageing on polymers is exemplified in the following by differential scanning calorimetry (DSC) data of a powder coating material (amorphous thermosetting epoxy–polyester system) measured by Johlitz [67]. Figure 4 shows the calorimetric response of the material by plotting the heat capacity as a function of decreasing temperature while cooling rate is controlled. The maximum heat capacity, known as enthalpy relaxation peak, at approximately 70-75 °C is characterised by a distinctive rate dependence. Glass transition of the material is within this temperature range. The data reveal that the enthalpy relaxation peak is more prominent the slower the cooling rate is chosen. That is explained by the molecular structure having more time to relax than at higher cooling rates [9]. For accelerated cooling the entanglement of the molecular chains is hampered due to insufficient time and the molecular configuration reaches a less dense state. As a consequence, less thermal energy is necessary to convert the polymer into the entropy-elastic equilibrium state.

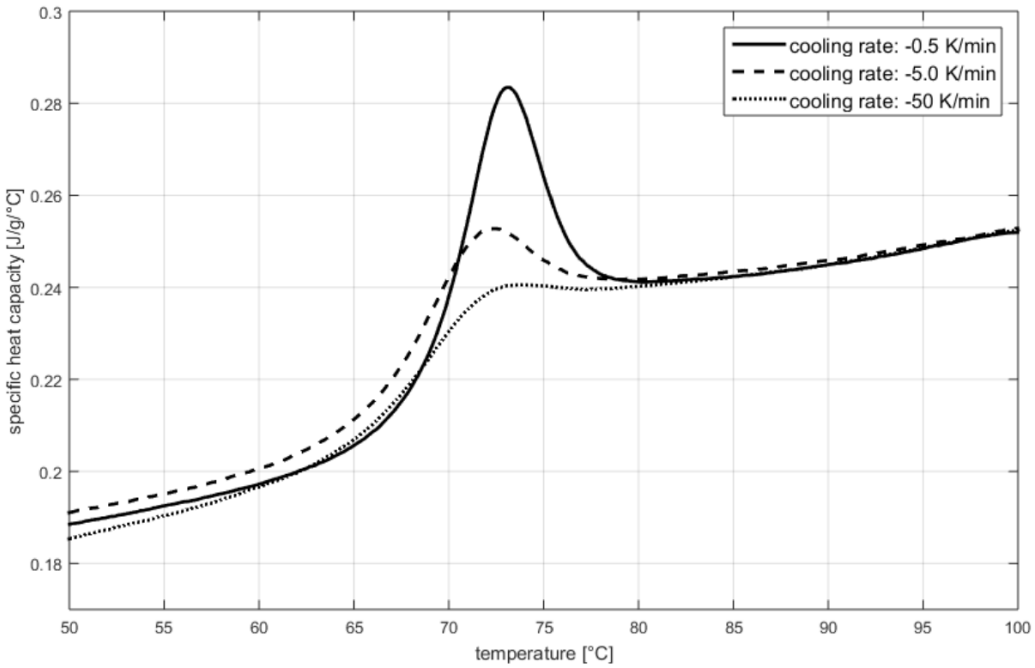

Figure 4: Specific heat capacity of a polymeric coating material as a function of cooling rate (based on [67]); preceding heating rate was 10 K/min. Temperature profiles: annealing for 10 min at 160 °C; quenching to 30 °C with a cooling rate of -50 K/min; heating up to 120 °C with 10 K/min with measuring heat capacity; repeating cycle with cooling rates of -5 K/min and -0.5 K/min [48]

The glass transition temperature is a significant property of a polymer and is important when dealing with physical ageing. A possible explanation of this effect based on free volume is given by Ehrenstein and Pongratz [11]. Molecular movement needs two prerequisites, thermal energy and free volume. The former provides the energy which enables mobility of molecules and the second is needed to ensure the space required for these movements. Although free volume follows the temperature it can be decreased faster by quenching than thermal energy is reduced. Consequently, mobility drops abruptly when the lower limit of volume is reached and changes in the orientation and location of the molecules are no longer possible. The reduced mobility also provokes a delay in the rate of decrease of the free volume. This means by cooling below the glass transition temperature, molecules still possess a certain amount of energy, but free volume declines in a way such that mobility is effecitvely reduced, and the polymer becomes glassy. Hence, passing the glass transition temperature has huge impact on the physical processes at a molecular level, and mechanical properties of the polymer alter suddenly. Due to reduced molecular mobility, the capability of reaching an energetically more favourable state is stunted. A state of nonequilibrium fixed until relaxation processes occur which are known as a type of physical ageing, or the material is again heated above T_g. Only then can the imbalance be relieved corresponding to a reverse of physical ageing mentioned above. Owing to this fact, it is obvious that the physical state of a polymer depends on the cooling rate when passing T_g.

3.2.2 Chemical Ageing

Any unintended changes in the chemical composition, molecular structure or molecular size of polymers during storage or application are referred to as chemical ageing. These processes are irreversible which means heating above T_g or melting temperature does not reverse the changes occurred [19][68]. Chemical ageing can manifest in different ways which all degrade the molecular structure. According to [68] and [11] the following degradation processes can be distinguished:

- Chain scission: cleavage of the molecular backbone, which is particularly induced by light irradiation and/or oxygen as well as elevated temperatures; molecular weight is reduced
- Cross-linking or ring formation (cyclisation reaction) as a consequence of preceding chain scission
- Secession of monomers or low molecular weight compounds due to depolymerisation or separation of side groups
- Alteration of existing or formation of new functional groups, i.e. as a result of secession or reaction with ambient substances like oxygen

Chemical ageing is shown in Figure 3 by a simplified illustration of a cross-linked polymer network whose chains are broken up due to chain scission or a disjoin of the crosslinks. In parallel, new cross-links are built which cause network reformation. Here, the influence of chemical ageing on the mechanical properties becomes obvious. The number of crosslinks (crosslinking density) and the length of the molecular chains (molecular weight) are crucial for the behaviour of polymers under load. Backbone chain scission facilitates molecular disentanglement and reduces its stabilising effect. Below a certain molecular mass limit, M_{nc}, carbon chains become too short and entanglement loses the stabilising function which causes an abrupt deterioration of mechanical properties. This is shown in Figure 5 by plotting fracture strength σ_B over molecular weight M. Above M_{nc} the influence of molecular weight or rather the average chain length has linear influence on fracture strength [67][69][70]. A change in the macromolecular structure also has great influence on optical and rheological properties [19]. Of course, the reactions mentioned depend on environmental influences as already discussed above.

On one hand, scission of the molecular backbone reduces the stability but on the other hand other chemical reactions can provoke new crosslinking which counteract the degradation of the polymer network. These new bonds link carbon chains and increase cross-linking density. This is done in a stress-free state which means cross-links are created in the current condition of molecular network without any loads applied on the bonds. Comparisons of intermittent and continuous relaxation tests on aged polymers prove this like shown by Johlitz [67][71] and Tobolsky [20] for the case of elastomeric material. Depending on the circumstances of ageing the one or the other effect dominates, and completely different changes in properties can occur.

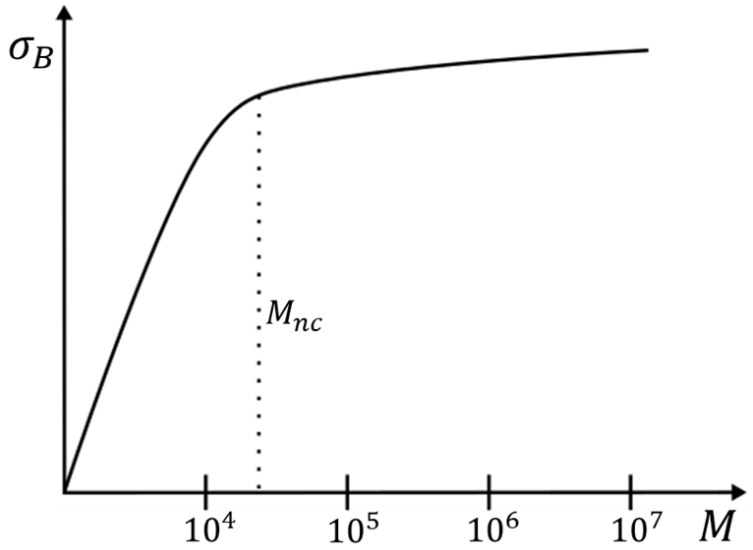

Figure 5: Influence of molecular weight on the fracture strength of polymer [69]

Besides the carbon backbone or rather the molecular main chain, functional groups are affected, or new ones created by chemical ageing. These can affect mechanical, electrical or optical properties of the polymer. Further, it can represent the initial step for reaction chains like that of oxidation which will be shown more in detail later (see section 4). The formation of functional groups can be used as an indicator and measure for the degradation of polymers (see subsubsection 5.2.2). Moreover, separation of monomers or low molecular weight compounds as a consequence of chain scission or other degradative reactions also affects the mechanical properties and can cause odour emission [72].

3.2.3 Mechanical Ageing

Mechanical ageing aggregates all changes and damages which are caused by mechanical loads, though the influence of mechanical loads applied to the polymer on the durability is not completely understood yet. A common approach from an engineering point of view is equalising mechanical ageing with fatigue and hence excluding it from the topic of ageing. The answer is to be found somewhere in between and requires a more differentiated consideration. Mechanical ageing has various reasons such as a shift in the equilibrium influencing the chemical conformation or mechanical loading of the molecular structure which deforms the bonds between atoms or molecules. Furthermore, dissipative heating appears due to alternating loads [39][73]. The latter results in an elevation of the materials temperature and accelerates other ageing processes which is discussed above in subsubsection 3.1.1 when introducing extrinsic factors. Moreover, changes in the material temperature affect the mechanical properties, especially the viscoelastic ones. Elevated temperature causes the molecular structure to be more flexible which results in increased deformability. Improved ductility implies a better compatibility of the polymer with mechanical loads and the probability of crack formation is reduced.

In general, mechanical loads can be distinguished in single loads and alternating loads of a certain frequency spectrum. High single loads can damage the molecular structure as well as result in crack formation which affects the stress state and also subsequent ageing processes. Further, mechanical loads can provoke as well as encourage the formation of radicals and thus accelerate the thermo-oxidative ageing (see also subsection 4.2) [11]. Mechanical loads can directly cause damage to the polymer as well as initiate or affect other ageing processes. A further example is the effect on certain structural characteristics like diffusivity. Free-volume can be influenced by compression load or high stretching and hence for example penetration of oxygen is affected [55].

Summarising, mechanical ageing describes diverse phenomena. A lot of them influence chemical and physical ageing processes. Nevertheless, other aspects allow a clear separation from these two categories of ageing and justify the definition of an own field of polymer degradation. One possibility is considering the term of mechanical ageing for all changes provoked by external mechanical loads. Another approach is equating mechanical ageing with dissipative heating or rather the influence of temperature during cycling loading.

3.2.4 Further Ageing Classification

An overview of the classification in chemical, physical and mechanical ageing, is provided in Figure 6. Polymer ageing is subdivided in these three subtypes and further distinguished in the characteristics which are affected. Subsequently the properties changing or the phenomena occurring are listed. Of course, Figure 6 provides no guarantee for completeness but illustrates the subdivision introduced previously.

Dissipative heating and penetration of ambient media give rise to the question of whether ageing occurs heterogeneously in the material or not. Obviously, absorption of media starts at the surface and heating either from outside or due to mechanical loading do not rise temperature identical everywhere, at least in the beginning of exposure. Ageing factors which have been introduced usually occur in a more independent way regarding the position in the material such as post-vulcanisation, relaxation of residual stresses or the effect of remnants of cross-linking agents and contaminations. Thus, ageing can be divided with respect to the place of its occurrence:

- Homogeneous ageing
- Heterogeneous ageing

Space independent degradation can be caused by both chemical and physical ageing. Nevertheless, nonhomogeneous effects are usually caused by extrinsic factors which initially penetrate the polymer starting at its surface. Thus, it is possible that ageing phenomena already occur at the surface leaving the interior of the component is unaffected. Radiation, e.g. ultraviolet radiation,

is such an example. Probably the most common way causing heterogeneous ageing are diffusion based processes that occur by weathering or generally when stored in media [67]. These can be, for instance: oxygen, ozone, water or oil. Amongst these, oxidation is an important type of ageing and an omnipresent factor when considering lifetime of polymer materials. Furthermore, non-homogeneities can also exist as a result of the production process, e.g. when the polymer is cooled down quickly and temperature gradients occur which cause space-dependent residual stresses or different morphologies. The latter can be evoked from an unsteady degree of curing or crystallisation when parts of the polymer have more time for molecular chain rearrangement than others. Consequently, different properties and ageing resistance are generated in superficial and interior regions.

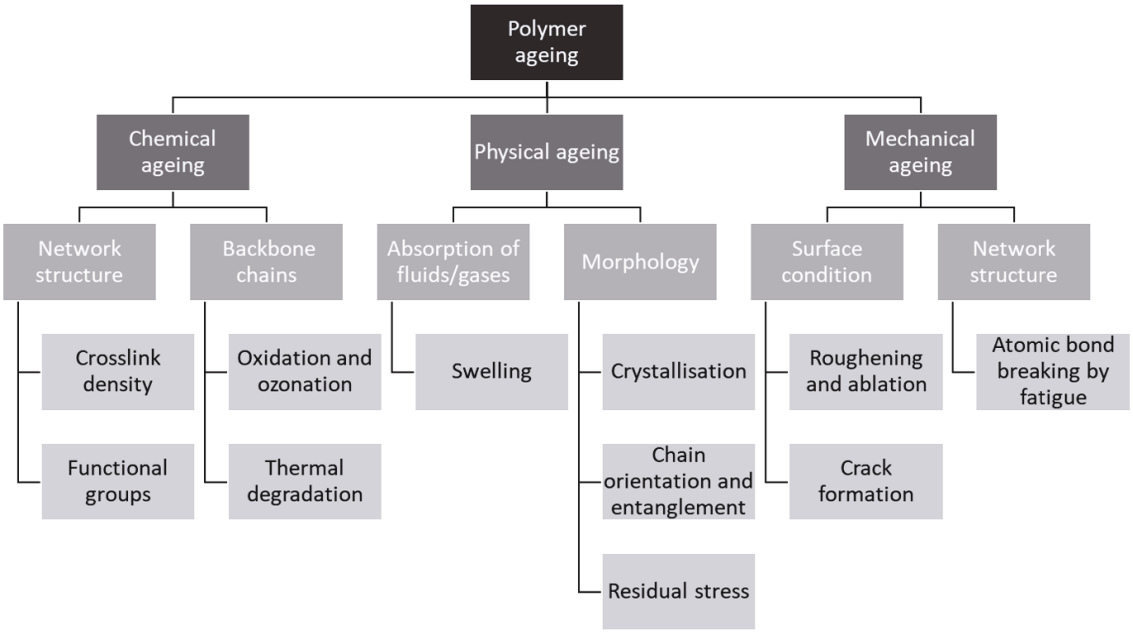

Figure 6: Overview of polymer ageing by classification in chemical, physical and mechanical phenomena

The classification of ageing phenomena is not a general law, but it tries to distinguish different kinds of polymer deterioration in a structured way. Here a possibility should be demonstrated regarding the topic of different ageing effects and their reasons can be handled. Of course, unclear boundaries occur since some effects cannot be exclusively allocated to a single subtype. Depending on the individual environmental conditions and the polymer used, a complex ageing characteristic can emerge. Furthermore, different types of ageing can influence the polymer material in parallel. Subdividing these processes helps to assess the ageing of polymers and indicates contributing factors.

Moreover, several ageing processes running in parallel make investigations difficult. A possible approach is the separation of individual types of ageing to find out more about how they are affecting durability. For example, elastomer specimens are exposed at elevated temperature in an air containing environment and compared to samples aged in vacuum. Testing of these factors can

be effortful, but one cannot exclude these ageing processes which occur in a different manner in an isolated condition since individual ageing phenomena interact which each other. Consequently, a broad range of different testing methods compared with detailed knowledge of the boundary conditions occurring during in service usage is required to enable reliable statements about durability.

3.3 Ageing of Elastomers

A brief overview of the ageing behaviour of elastomers will be given here since the following work deals with the ageing or rather oxidation of elastomers. At first, some basics about this kind of polymer are provided and then characteristics of elastomer deterioration are introduced.

Elastomers are crosslinked polymers whose glass transition temperature is generally below 0 °C. Below that temperature freezing of the Micro-Brownian-Motion occurs which results in non-appearance of thermal movement in the elastomer. The atoms therefore no longer have any significant temperature-dependent motion. Above the transition range, chain mobility is given and thus entropy-elastic behaviour up to the decomposition temperature occurs. Macro-Brownian-Motions are virtually inhibited because chain molecules are fixed among each other by chemical cross-linkings. Hence, macromolecules are not completely independent of each other but three-dimensional and wide-meshed cross-linked. A special property of elastomers permits highly reversible deformations which are provoked by external forces. After discharge, the macromolecules usually return to their original shape. This behaviour can be explained by the orientation of the molecular chains, which are highly disordered and heavily coiled in the unloaded state. They can be easily aligned since they have only very weak bonds among each other, as mentioned above. The alignment corresponds to a higher order of the molecules. After discharge, the original disordered state is restored. Other types of plastic can also show such a rubber-elastic behaviour, but usually only in a very limited temperature range. For elastomers this is true for a very wide range. Below glass transition temperature elastomers show a shear modulus, for instance, of 104-106 N/mm^2 while at higher temperatures up to decomposition temperature it is 0.1 to 102 N/mm^2 and almost independent of temperature [74].

Elastomers are produced of natural rubber or synthetic rubber by means of cross-linking at elevated temperature of approximately 150 °C to 210 °C. Typically, sulphur serves as cross-linking agent but also metal oxides, amines, alkali soaps or other cross-linker products are possible. By adding small amounts of sulphur, about 3 parts of sulphur per 100 parts of rubber (3 phr) the chain molecules of natural rubber are cross-linked by sulphur bonds and form a soft elastomer. At sulphur levels above 5 phr the soft rubber area is left and an elastomer with leathery quality and low elasticity is obtained. With sulphur content being further increased to 25 to 40 phr there is such a high degree of crosslinking that the rubber elasticity disappears, and hard rubber is obtained [75]. The cross-linking process (also called vulcanisation) is a quite important step between raw and finished elastomeric products. Among other factors of the vulcanisation process, temperature and reaction time influence the number of cross-links formed

(state of cure). The latter is responsible for the rubber elastic behaviour as well as many other properties of elastomers. In order to visualise the effect of cross-linkings in elastomers, an uncured and a cured sample are compared schematically in Figure 7. The left part of the graphic shows a simplified entanglement of molecular chains which are stretched by an external load. The chains become more oriented and slip off due to the force applied. After unloading, molecular chains strive back to the original state but a plastic deformation remains. In contrast to this, a cross-linked network which is stretched to the same strain returns to its original shape after unloading since a slipping off and therefor a disentangling of the molecular chains is prevented by the cross-linkings. Moreover, Figure 7 gives an idea how chemical ageing can affect the properties of elastomers if chemical cross-linkings, chain length or entanglement are affected. Of course, this is a schematic and very simplified illustration which does not consider the details of elastomeric systems and their ageing behaviour.

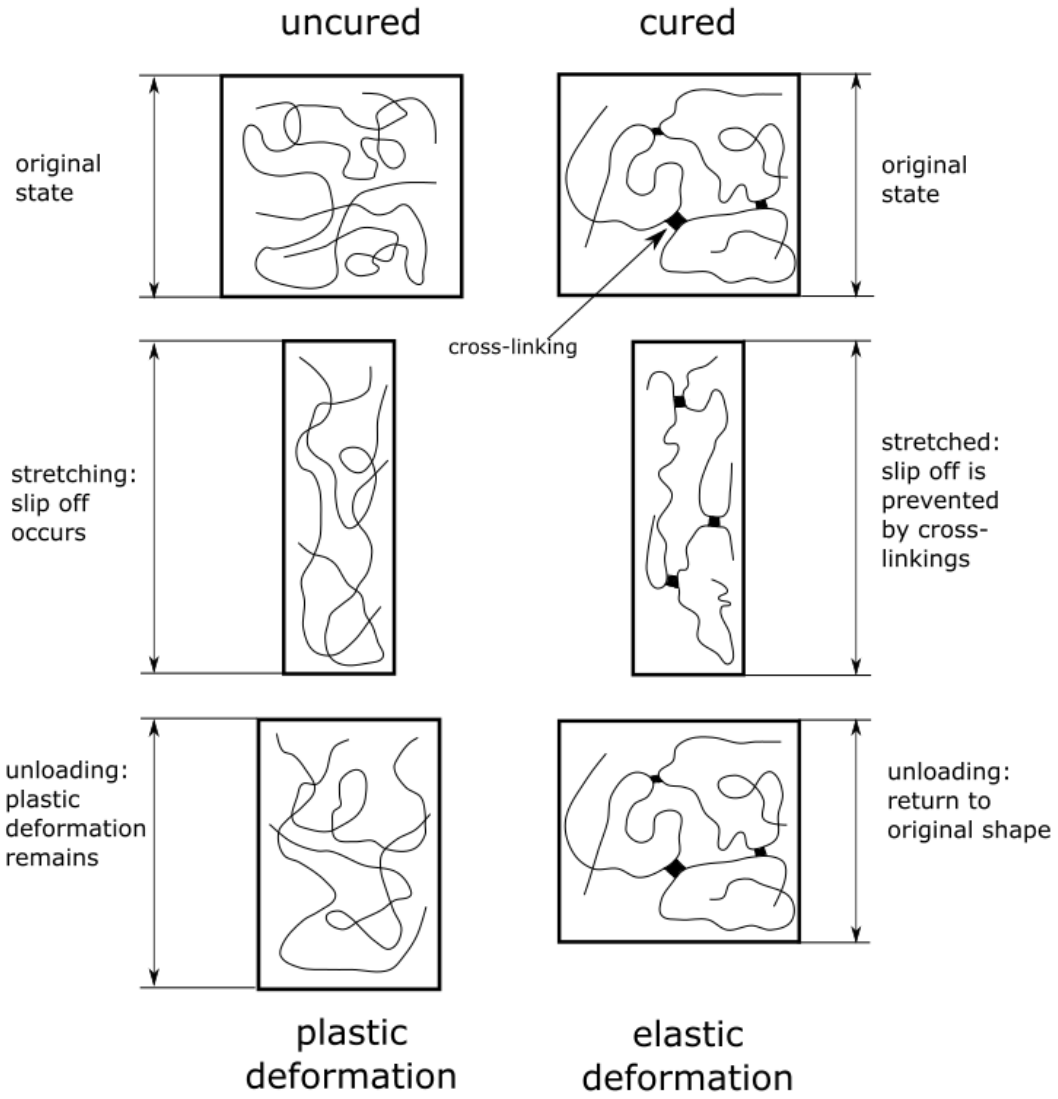

Figure 7: Deformation behaviour of a cured and uncured molecular network

As already mentioned, common technical elastomers do not only consist of natural rubber but are

often a mixture of several substances. Pure rubber is unusable by itself for technical applications and obtains its desired properties only with other substances added and subsequent curing. The composition determines the basic properties such as ageing resistance, flexibility or resistance again media like lubricants, fuel or water. By adding additives certain properties can be changed or improved, for instance: low temperature flexibility, impact resilience, compression set or heat and swelling resistance. The ultimate properties of elastomers are governed by the type of rubber, the blend composition, and the method of making that blend. Certain components are listed subsequently, which are relevant for the properties of elastomers and therefore also for their ageing behaviour, according to [75][76]:

- Type of rubber
  Represents the main component of elastomers and has huge impact on the characteristic properties. It determines the level of the mechanical properties and dictates the range of the application temperature as well as the durability against environmental impacts. The selection of the type of rubber defines the basic properties which are adjusted by additives. Since it is the largest portion it is also the main cost driver.

- Reclaimed rubber
  Rubber waste which is reprocessed and vulcanisable by chemical processes. Previously, it was added to reduce the amount of rubber needed and to save material costs. Nowadays it is used for technical reasons as to improve the processing behaviour. Larger amounts often degrade the mechanical behaviour.

- Fillers
  Solid particles of mostly submicroscopic size which can be active or inactive according to size and surface condition. Active fillers are fine (about 20-100 nm) and bind rubber molecules to their surface. Thus, elasticity is reduced but in turn strength and abrasion resistance is improved. Such fillers are for example special carbon blacks and silicic acids. Without these active carbon blacks, today's mileage of car tires would not be possible. Coarse-grained fillers (about 0.8-3 μm) are inactive fillers which provoke no improvement in mechanical properties. They are used as cheap extenders and promote electrical insulation.

- Plasticisers
  Plasticisers boost the mobility of the molecular chains and thus reduce the viscosity as well as the hardness, increase the elasticity and improve the low temperature behaviour. They are usually added as liquid component and dissolve in the rubber mixture. Adding too much degrades the mechanical properties and may further cause undesirable side effects. Plasticisers can evaporate if temperatures are too high and lead to hardening or embrittlement of the material. Even contact with liquids can lead to unwanted reactions. Larger amounts of plasticizers are added only if an improvement in cold flexibility should be achieved and material costs should remain low. However, side effects in the other parameters must always be kept in mind which makes compromises unavoidable.

- Catalysts
  Accelerators reduce the time needed for vulcanisation. Further, reaction temperature and the amount of curing agent is reduced with catalyst addition, which improves curing quality and ageing resistance. The latter is due to less sulphur required for the development of the cross-linking network which provokes less weak points for oxidative attacks.

- Processing adds
  Some adds are used to ensure a better processing of the elastomer during manufacturing or subsequent treatment. These include: resins, soaps, solid hydrocarbons, fatty acids and factice (polymerisation product of unsaturated oils and fats with sulphur and hydrogen chloride). In principle, processing adds can be counted as plasticisers. Reclaimed rubber can also positively influence processing of the elastomer. Hence, processing adds should not be considered in isolation, but it should be mentioned that some additives are used to simplify processing.

- Antioxidants
  In spite of their name antioxidants are not limited to the prevention of oxidation but the term is often used to denote all anti-ageing additives which counteract deterioration. They are used to prevent the influence of oxygen or ozone as well as for the protection against light, fatigue or hydrolysis. A closer look on the mechanism of antioxidants is provided in subsection 4.4.

- Curing agents
  Vulcanising- or crosslinking-agents are substances which are needed for the curing of the elastomer. Without these additives, no cross-linking between the rubber molecules would be possible. Sulphur is still the most common vulcanising agent to date but can only be used with rubber types having double bonds in the main chain or in the side chains. The elasticity of the elastomer depends on the number of sulphur bonds. The more there are, the harder and inelastic the rubber becomes. The number of sulphur cross-links depends on the amount of sulphur added and the duration of the vulcanisation. If the rubber has no double bonds, peroxides which contain oxygen-oxygen bonds are an option to be used as a curing agent for compounds. They produce polymer chains with a radical which subsequently form a covalent carbon-carbon bond with another polymer chain. This results in a good heating performance but has no benefit regarding oxidation. In contrast, sulphur creates sulphur-carbon bonds which allow post-crosslinking of remaining curing agent. The reaction schemes of both peroxide- and sulphur-based curing are illustrated in Figure 8.

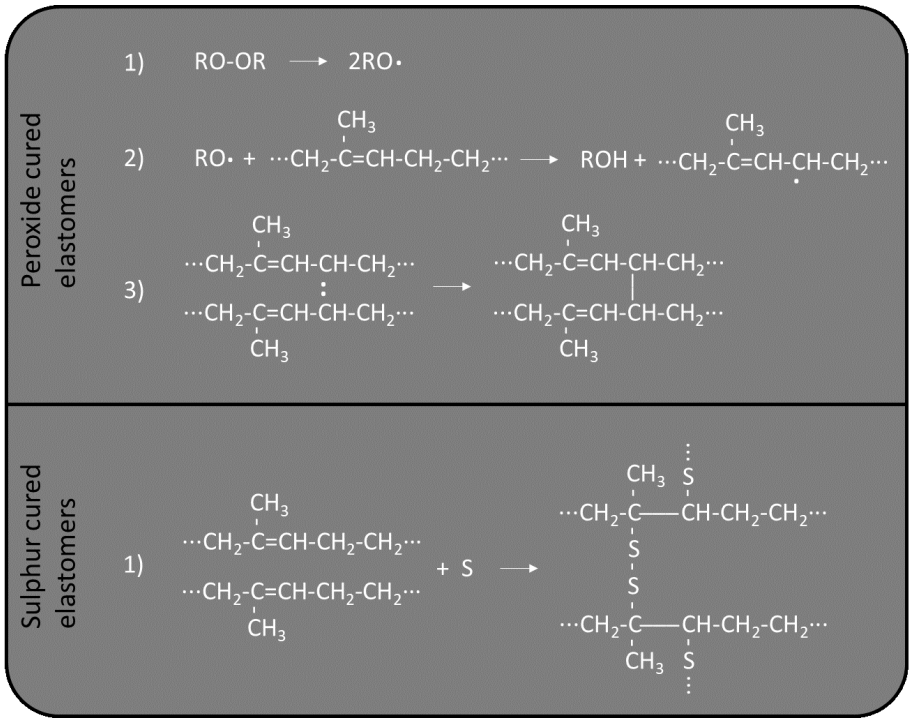

Figure 8: Simplified reaction scheme of peroxide- and sulphur-cured elastomers

Peroxides contain oxygen-oxygen bonds which are broken when exposed to heat. Then, radicals are formed (in Figure 8 " · " denotes an unshared and unpaired electron) which are highly reactive. These radicals attack the weakly bound hydrogens and separate them from the molecular chain. Consequently, polymer chain radicals are produced which react among each other and create chemical crosslinks.

Sulphur curing is based on the mixture of pure sulphur or compounds which contain sulphur. At elevated temperatures sulphur is linked to the carbon chains which contain double bonds. Thereby, the elastomer chains are not cross-linked directly but rather by means of sulphur-crosslinks consisting of one or more sulphur atoms. The reaction process is accelerated by higher amounts of sulphur which also results in crosslinks containing more than one sulphur atom. This represents bonds of lower strength. Figure 8 shows a sulphur crosslink consisting of two sulphur atoms. Covalent bonds build by peroxide curing between carbons is stronger (350 kJ) than sulphur-carbon bonds (285 kJ) or sulphur-sulphur bonds (155-270 kJ) created during sulphur vulcanisation. Thus breaking them requires more energy which improves the heat resistance of peroxide cured elastomers [47][77].

- Further additives
  Besides the additives mentioned above there are a lot more which should not be described here in detail. These include: activators, vulcanisation retarders, pigments, masticators, propellants, fragrances, flame retardants, adhesive agents, preserving agents or desiccants.

Ageing of elastomers make service and lifetime predictions difficult since influencing factors have to be weighted differently for each type of elastomer or varying fields of application. Elastomers used in applications like tires, dampers, gaskets or conveyor belts are exposed to diverse loads. In most cases of elastomer ageing, ambient temperature, time of exposure and media in contact are dominant factors. More specifically, in practical use, ageing of elastomers is very often influenced by elevated temperatures and ambient oxygen which provoke irreversible changes [8][22]. Besides these factors elastomers are influenced by moisture, solar radiation or ozone [11]. At lower temperatures ageing effects often exhibit reversible character or rather physical ageing dominates. If temperature increases ageing decreases rubber elasticity irreversibly [22] and hardness increases [78]. This is undesirable if isolation properties of e.g. dampers are of interest [79][80]. In general, influence of ageing is more pronounced for elastic than for viscoelastic properties and therefore usually neglected for the latter in a first approach [20][81].

Durability of elastomers is mainly controlled by three factors [11]:

1. Basic polymer material composition (kind of atoms, saturation level of the molecular main chains, ...)

2. Way of chemical cross-linking (e.g. peroxide or sulphur-based curing, ...)

3. Additional compounds (heavy-metal compounds, fillers, anti-ageing additives, ...)

Elastomers with carbon-carbon double bonds are particularly very sensitive to attacks by oxygen and ozone. If there are no double bonds in the molecular main chain ageing resistance is generally higher for these types of elastomers. Examples for elastomers containing double bonds are nitrile rubber (NBR) or styrene-butadiene rubber (SBR). Double bonds are broken up during the ageing process and degraded to single bonds. The free electron pair generated subsequently results in chemical attachment of the reactant. Besides this agglomeration of atoms or molecular groups irreversible processes affecting elastomers are chain scission, cross-linking and breaking as well as reformation of covalent bonds of the polymer network. Both scission and reformation processes can provoke contrary consequences. Chain scission results in a decrease of stiffness whereas reformation leads to the opposite effect. This can give an easy start for micro-cracking and superficial cracks as well as embrittlement and discolouration [8][11]. In combination with mechanical loads, the chemical degradation makes reversible chain movements and relaxation processes easier to occur. Moreover, in an unlikely case mechanical loads can influence the processes of ageing. Tobolsky showed that chemical ageing is independent of strain in the range up to 200 % [20]. Since the condition of the polymer network in combination with fillers and the material composition governs the technical properties of elastomer ageing has huge influence on the behaviour of elastomer.

Moreover, the process of crack initiation is essential regarding the lifetime of elastomers. Formation of cracks can occur far below tensile strength due to cyclic loading. In other words, as ageing increases the risk of crack initiation increases. As already mentioned, oxidation is quite

often the reason for that degradation. Oxygen ingress from the ambient environment oxidation is based on absorption, diffusion and permeation processes. This can cause heterogeneous ageing effects and profiles starting from the surface and reaching into the interior of the material. Such an aged surface layer represents also a so called “crack initiation zone” for elastomers [8]. If diffusion processes are influenced by the ongoing change the influence of oxygen can be limited to a superficial layer. This increases complexity of elastomer ageing and underlines the question already posed: can degradative reactions in an oxygen containing environment be easily accelerated [26]? This is a basic question of the following work. Before, this question shall be answered a detailed look will be provided on the oxidative ageing of elastomers in the following chapter.

4 Oxidative ageing of elastomers

After introducing the fundamentals of polymer technology and elastomer ageing the next section will focus on the influence of oxygen on elastomers. This will provide a detailed base of information for the subsequent part of this work dealing with the thermo-oxidative ageing of rubber materials. Oxidation of elastomers is a multi-process phenomenon including both physical and chemical phenomena. Therefore, this chapter will describe the flow of oxygen molecules from the ambient environment into the elastomer or will follow the chain of causation. The process is seperated into a sequence of steps including the absorption and diffusion of molecules from the ambient environment, the oxidative reactions with the polymer and their consequences on the mechanical properties as well as the role of antioxidants on this process. Outlining the chain of causation, oxidation can by simplified by the following depiction [11][16][48][56][82]:

1. Oxygen absorption
2. Diffusion process and induction period
3. Initialisation reaction
4. Chain scission and reformation
5. Termination reaction

The following subchapters will take up these individual steps and provide a comprehensive view on the oxidative ageing of elastomers.

4.1 Oxygen absorption and diffusion

The prerequisite of oxidation is the presence of oxygen molecules which are present in most applications due to air surrounding the elastomer. There can be oxygen already in the elastomer due to contaminations caused for instance during the manufacturing process. The latter should be kept in mind but is not discussed within this chapter. Oxygen molecules have to dissolve at the elastomers surface before penetrating the material. The driving force for adsorption is the surface affinity of the elastomer for oxygen molecules and a difference in oxygen concentration between polymer and ambient medium. After absorption a gradient of oxygen is created in the surface layer of the elastomer which provokes diffusion taking place. For visualisation the process is shown schematically in Figure 9.

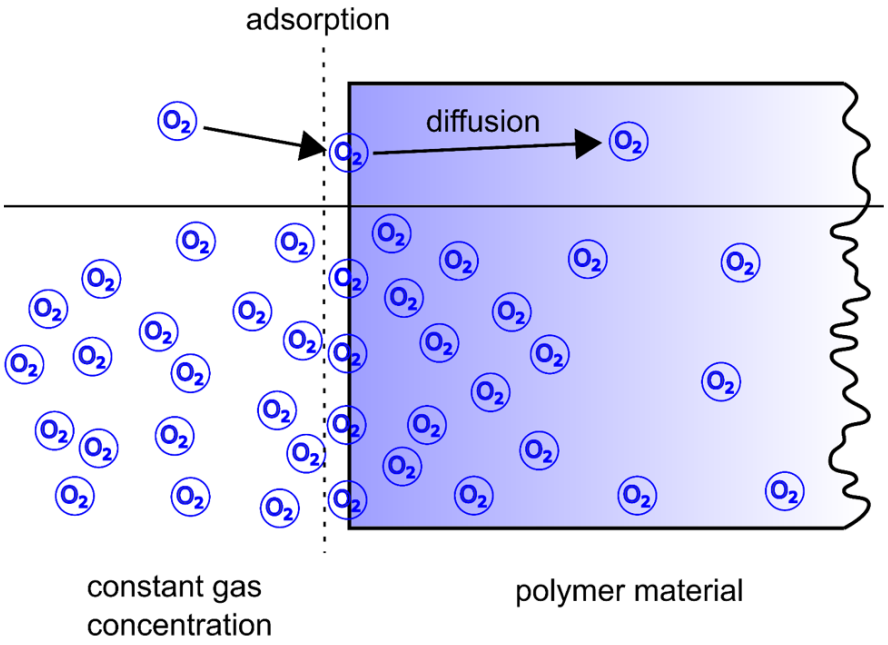

Figure 9: Schematic illustration of oxygen absorption and diffusion in elastomers

From a chemical point of view the process of adsorption can be distinguished in physisorption and chemisorption. The former describes weak links like van der Waals bonds which bind oxygen to the polymer surface without influencing the chemical structure of the adsorbate or the polymer. Since the oxygen is only weakly attached to the surface of the polymer further transportation into the material is possible. In contrast chemisorption describes the chemical binding of an adsorbate to the polymer's surface. These linkages are much stronger and hinder subsequent permeation of oxygen into the elastomer [48][83].

Another approach describes the adsorption of oxygen at the elastomers surface as solubility which generally is described by means of Henry's law (Equation (1)). This uses solubility as a material parameter and formulates the oxygen concentration at the outer surface of the material as a linear function of the ambient pressure.

$$C_S = S\, p_{ox} \tag{1}$$

C_S is the equilibrium concentration of oxygen at the elastomers surface, S the solubility rate coefficient and p_{ox} the partial oxygen pressure [84]. The amount of oxygen absorbed does not completely represent the amount of oxygen reacted with the elastomer since oxygen molecules can also be dissolved in the elastomer without any reaction occurring. This can have several reasons, for instance, saturation effects due to previous oxidative reactions or a activation energy not high enough which decelerates the reaction rate [84]. Besides the ambient oxygen pressure and the type of elastomer, oxygen uptake is also a function of temperature as well as ageing duration and the progress of ageing [85]. Although there is not a lower temperature limit it is possible to decelerate oxygen uptake to a neglectable level [28]. A further possibility to characterise solvent

of media in polymers is given by Flury-Huggins theory which describes the thermodynamic of polymer solution by a mathematical model based on entropy mixing [61][86].

Solubility is difficult to be determined experimentally since it always occurs in parallel with diffusion. The most common way to measure permeability of elastomers is given by the method called time-lag experiment. Thereby a thin elastomer film separates two chambers. One of these chambers is charged with gas of a certain pressure while the other one is monitored regarding concentration changes over time caused by gas penetrating through the film. The elastomer is assumed to be completely free of oxygen at the beginning of testing and diffusivity is supposed to be constant over time and depth of penetration [56]. If such experimental results are used to predict the lifetime of elastomers under real conditions further phenomena should be taken into account like the aspect of turbulent air flow favouring the oxygen uptake contrary to static conditions [28].

As already mentioned solubility S cannot be considered separately since it always goes along with diffusion processes D. Hence, uptake and transportation, better known as adsorption and diffusion are usually summarised under the term of permeation. Permeation P includes the whole process of oxygen molecules getting from the ambient environment into the elastomer and is described by Equation (2).

$$P = S\,D \tag{2}$$

The type of elastomer and the material composition has major impact on the permeation behaviour of elastomers. For instance, the presence of methyl groups and polar groups reduce permeability [17][62]. That means, affecting the chemical structure of elastomers by changing functional groups can alter the permeation behaviour. Therefore, chemical ageing can influence the oxygen uptake and consequently the subsequent oxidation. Furthermore, the polymer network and morphology has an impact on the diffusion behaviour since oxygen molecules have to pass through the entanglement of polymer chains. A tight network impedes this and reduces diffusivity. Thus, crystalline structures reduce permeation [11][62] as well as a more oriented arrangement of molecular chains like provoked by high strain. Compression has a similar effect since molecular structure is densified and free volume for diffusion between the polymer chains is reduced [17]. Diffusion can also be influenced by the size of the gas molecules. Molecules with smaller radii penetrate the polymer network more easily. Solubility and diffusion under the influence of ageing cannot be handled by the common methods and require a more sophisticated model.

The description of diffusion is mostly done by means of Fick's first law which uses a diffusion coefficient to quantify diffusivity. Elevated temperatures increase the diffusion coefficient and diffusivity and consequently a conflict arises with ageing running in parallel. Oxidation is accelerated at elevated temperatures which usually reduces the diffusion coefficient [87][88]. Thus, increasing temperature accelerates both diffusion and oxidative reactions. This dualism

is shown schematically in Figure 10. Accelerated oxidation provokes a higher consumption of oxygen molecules which then are no longer available for further diffusion. In other words, accelerated reactivity causes oxygen molecules to react with the polymer shortly after adsorption which concentrates oxidation in the surface layer. Depending on which of the processes dominate oxidation occurs more or less heterogeneously. The effect of accelerated oxidation at the superficial layer has an impact on the entire ageing of the elastomer because a protective layer concentrates and limits oxidative reactions to the edge of material. This process is called diffusion-limited oxidation (DLO) [26][29][89]. In a distinctive way the interior can be unaffected even for long ageing durations.

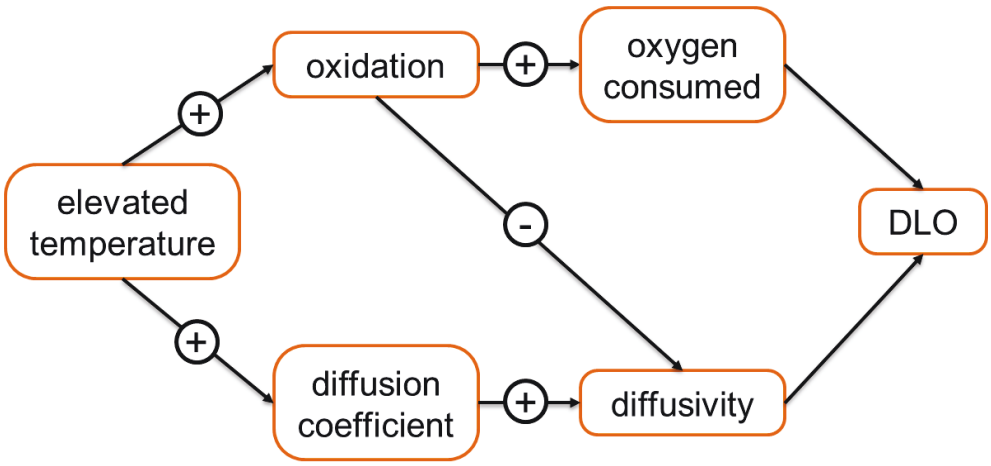

Figure 10: Schematic illustration of diffusion-limited-oxidation (DLO)

The intensity of DLO depends on the elastomers composition especially the presence of antioxidants, temperature, ageing duration, ambient oxygen pressure, mechanical loads as well as sample geometry and size [90]. The effect of DLO can, for instance, be shown by experimental investigation on the mechanical properties. A pronounced gradient of the elastic modulus can be observed by modulus profiling on aged samples (see also subsubsection 5.3.1) [89][91]. For longer periods of ageing and/or higher temperatures the gradient becomes more distinctive.

Since elastomers are often used at room temperature oxidation is performing at a slower rate and lengthened time scales. As introduced before DLO is highly temperature dependent and hence lifetime prediction is difficult. The influence of DLO is usually increased by elevated temperatures since the chemical activation energy of diffusion is lower than the chemical activation energy of oxidative reactions. Therefore, oxidative reactions are triggered or accelerated during artificial ageing in a way that would not occur during usage. Thermal activation of diffusion can be imagined as an energy limit required to push the elastomer molecules far enough apart for enabling infiltration by oxygen molecules [61][62].

Based on DLO, size effect is a sufficient method to protect elastomer components against oxidation (see also paragraph 6.2.4.3). The bigger the sample the higher the ratio of material which is not degraded by oxidation. This countermeasure has its practical limits but motivates the introduction of a critical sample thickness below which DLO effects become insignificant. Demanding

90 % of the sample being oxidised homogeneously would be an example for such a limit [29].

Although oxygen absorption and diffusion are important processes to describe elastomer oxidation considering the chemical reaction of oxygen with the material is indispensable. On the one hand oxygen being dissolved does not or almost not influence the mechanical properties and on the other hand reactions bind oxygen chemically which influences further diffusion as shown in Figure 10.

4.2 Oxidative reaction

The understanding of oxidative reactions in elastomers remains a challenge. The fact that several approaches exist to describe and simplify the reaction process indicates the diversity and complexity of this topic. The most common approach is the "Basic Autooxidation Scheme" (BAS) which is based on the reaction of free radicals with the molecular backbone chains. This is similar to the procedure of low molecular weight hydrocarbons. 'Autooxidation' depicts the autocatalytic oxidation of elastomers which can be subdivided in three steps as briefly mentioned at the very beginning of section 4: initialisation, continuation by chains scission and reformation as well as termination reaction. The initiation and continuation of the process is illustrated in a schematic manner by the basic oxidation scheme in Figure 11 [11][16][37]. The reactions follow a hierarchy which depends on the circumstances of ageing (e.g. physical conditions, chemical composition of the elastomer, influence of other reactants such as ozone, mechanical loads) and whether network degradation or reformation dominates. BAS is only one example of a conceivable process of oxidative schemes. Further ones are discussed by Verdu [17].

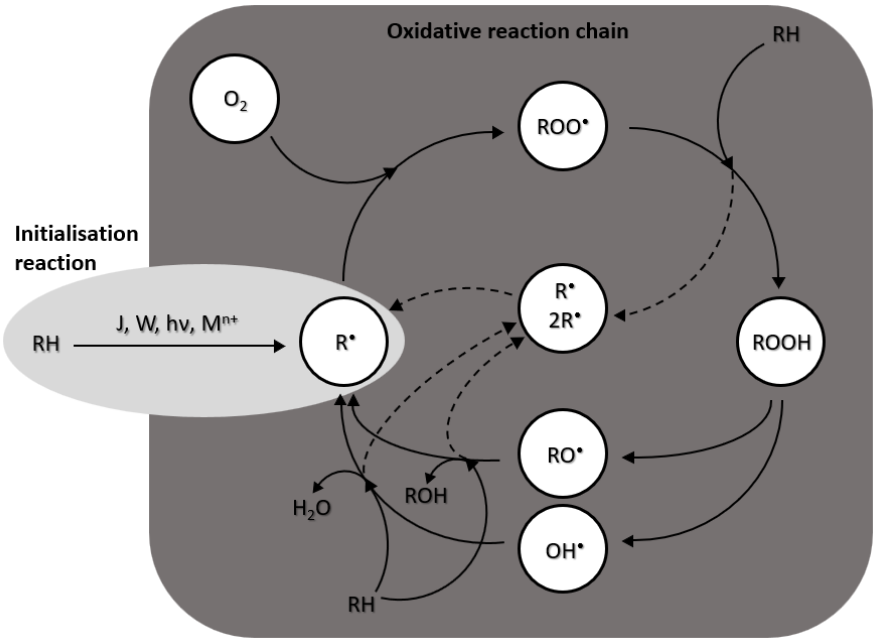

Figure 11: Schematic illustration of the basic oxidation scheme [48]

Start of the reaction is the creation of free radicals R• who emerge from the breakage of chemical bonds due to diverse loads. The impact of thermal energy J, electromagnetic energy $h\nu$, mechanical loads W, or metal ions M^{n+} that remained from manufacturing are considered as potential reasons for the creation of radicals [11][16][17]. The origin is still not completely elucidated. On molecular level a hydrogen atom of the elastomer chain is split off which creates an elastomer molecule with a free unpaired electron [37]. Another possibility is the scission of a C-C bond in the molecular backbone which forms an alkyl macroradical.

Due to their high reactivity the evolved radicals immediately react with the oxygen dissolved in the elastomer and build aggressive macroalkyl peroxyradical ROO•. This is only possible if enough oxygen is provided by the absorption and diffusion process. Due to its reactivity ROO• takes a neighbouring proton H• from its own chain or from an adjacent macromolecule and builds a hydroperoxide ROOH group. This step determines the velocity of the whole autooxidation process since the activation energy for forming the hydroperoxide by reaction of macroalkyl peroxyradical with the elastomer is higher than the reaction of the free radical R• with oxygen [37].

Hydroperoxides are more stable but contain quite weak oxygen-oxygen bonds which can be split easily into two alkoxyradicals (RO• and OH•). This step drives forward the reaction by attacking hydrogen atoms of the molecular backbone and hence increases the number of radicals (RH + RO• → ROH + R• and RH + OH• → HOH + R•). In general, the number of new radicals is decisive for the reaction rate. The reaction mechanism is autocatalytic and is therefore called autoxidation [11]. After a moderate beginning the oxidation is accelerated by producing radicals on its own which drives forward the reaction process. This enables BAS to describe the induction period usually observed during elastomer oxidation.

In principle, this scheme is only a model which simplifies the process of oxidation and cannot be fully used for all types of elastomers. This is demonstrated by the mere fact that several schemes exist which all provide an approach for describing the reaction scheme for thermo-oxidative ageing. In reality the reaction mechanisms for network degradation and reformation are much more complicated [22]. Especially, the origin of the initial radicals is unclear. Nevertheless, a direct reaction of oxygen molecules with the elastomer backbone without any intermediate step can be precluded due to the thermodynamic aspects [19].

The last step of the autooxidation scheme is the termination reaction which is not shown in Figure 11 for clarity reasons. It bases on the recombination of two radicals. Under usual conditions two macroalkyl peroxyradical ROO• react due to higher availability than free radicals R•. This is a consequence of the lower reactivity of ROO• as mentioned above. In the case of limited provision of oxygen, the availability of ROO• is reduced and recombination of R• becomes dominant. Hence, the termination reaction depends on the amount of oxygen molecules available or rather is a function of the diffusion process [16][37]. As a consequence, oxidation is stopped as a result of oxygen molecules being consumed faster by reaction than supplied by diffusion which was shown before in Figure 10 as a mechanism of DLO.

The scheme introduced depicts the effect on the molecular structure. Embrittlement and hardening are caused by chain scission when radicals are generated at the beginning or by recombination of radicals at the end of reaction process. BAS reaches its limit when DLO occurs and oxidation is dominated by the provision of oxidation [34][62][92].

4.3 Effects of oxidation on the properties of elastomers

Although oxidation is an omnipresent topic when elastomers are used, engineers and users are less interested in the actual oxidation mechanisms compared to the consequences. For example, most elastomers are applied due to their mechanical properties and hence changes of them are eyed critically. This chapter should offer a bridge between the previous explanations on oxidation and its influence on the macroscopic properties. The content of this chapter was partly published in [48].

First of all, different elastomer properties which can be differed during ageing and oxidation are introduced in Table 1. Depending on the application, certain properties are more desirable than others. Thus, examples of typical applications and loads are included in the listing according to the characteristic [17][48]. The following properties include only those which are relevant for the technical function of the material and should clearly be distinguished. For example, oil resistance is an interesting characteristic but does not represent a function of the elastomer. Imagine a gasket which is used to seal an engine component. The properties of interest are elasticity, changes in dimension and permeability. Influence of oil can affect these properties but is not a function of the gasket as discussed here.

As can be seen in Table 1 molecular network and filler materials are mainly responsible for the properties listed. Oxidation affects the chemical structure of the elastomer and as a result changes occur in the molecular network. Thus, oxidation can influence essential properties of elastomer materials. Changes in the molecular network due to oxidation are relevant mechanisms which motivates a closer look at it.

As already described in previous chapters the term ‘molecular network’ summarises different effects and conditions on molecular scale. These are based on chemical and morphological aspects. For example, the average length of the molecular chains (molecular weight), chemical bonds between the chains (cross-linking density), the entanglement and orientation of the chains, the degree of branching and functional groups attached to the chains, the chemical composition of the chains, non-covalent bonds between the chains (Van der Waal forces) and energetic aspects of chain alignment (e.g. crystallisation). Oxidative reactions affect the polymer network by scission and reformation of different bonds which has a major impact on the aspects mentioned. Further, additives contained like filler material are influenced. The loss of plasticiser can also cause an increase in stiffness but only as a contributing factor due to its low amount [41]. Some of the points mentioned are not affected by oxidation at first glance but indirect implications can occur. For example, when molecular weight is decreased by chain-scission the elastomer

chains can more easily be arranged in parallel and more pronounced effects of strain induced crystallisation or short-chain crystallisation occur [11].

Table 1: Technical relevant properties of elastomers

Elastomer property	Effect	Structural aspects involved	Typical applications of interest
mechanical properties	the most important one; includes lots of sub-properties like elasticity, relaxation behaviour or hardness	molecular network (molecular weight, entanglement, cross-linking density); filler material	damper, sealings or tyres
fracture properties and permeability	very close to mechanical properties; includes inter alia thermal fracture, abrasion and permeability; embrittlement, crack initiation and propagation are caused	molecular network; chemical composition; filler material	tyres, brake pads of bicycles, conveyor belts and sealing material
optical properties	discolouration due to fading; not critical from a technical point of view but aesthetically relevant	molecular network (e.g. crystallisation); filler material	all applications where the visual appearance of the elastomer is important
electrical properties	electrical insulation and dielectric strength, electrical conductivity and antistatic agent	filler material	rubber hoses, cable insulation, conductive rubber for keyboards, antistatic mats or antistatic shoes
changes in density and volume	includes changes in weight and dimension; loss of substance and additives as well as changes molecular structure; absorption of ambient media	molecular network; filler material	coating material and sealings like O-rings

The tensile properties of the molecular network are mainly determined by the chemical bonds created during curing which are stronger than physical ones or entanglements. When these bonds are affected by ageing the materials' characteristic is altered significantly (see also subsection 3.2, Figure 3). As explained in the previous chapter, during the mechanism of oxidative reactions both chain-scission and forming of chemical bonds occur simultaneously. Depending on which of the two processes dominate the resulting properties can differ widely, even resulting in contrary effects. For example, thermo-oxidative ageing provokes a decrease in stiffness for Natural Rubber whereas Government Rubber-Styrene (GR-S) becomes stiffer. Polybutadiene rubber shows that both processes run in parallel since at the beginning of exposure stiffness increases and with further ageing softening occurs. Since the oxidative reactions and the mechanical behaviour is highly temperature dependent these statements cannot be generalised for all situations and should only give a heuristic. The new bonds are synonymous to a secondary network which

is newly built in the current state and hence stress-free. Only if reformation is very strong volume shrinkage can occur which results in stresses. Experimental investigations on the effects of network degradation and reformation are usually accomplished by relaxation testing. Continuous and intermittent relaxation tests are used whereas the former is not able to detect the effects of reformation [20]. Furthermore, intermittent tests consider both effects together but are not able to distinguish between them. Thus, both types of investigation are required to obtain a complete set of information about network changes occurring during ageing. The specific behaviour of these effects is pronounced in the case of different types of elastomers. Figure 12 qualitatively shows the normalised stress responses of different kinds of rubber as a function of ageing time. Ageing is assumed at an elevated temperature of 130 °C and testing performed at room temperature. The information of this graphic is based on the results of Tobolsky [20].

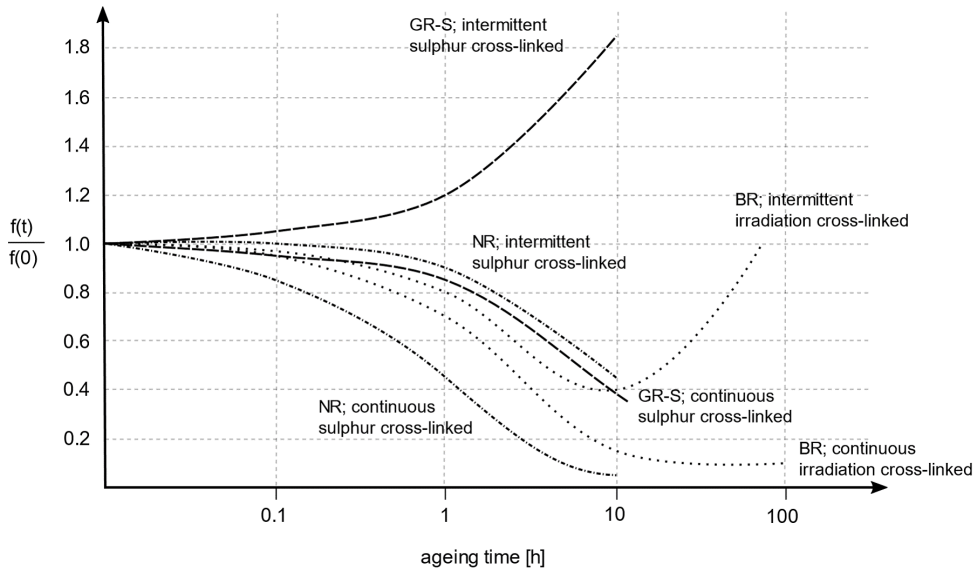

Figure 12: Continuous and intermittent relaxation tests at 130 °C ageing temperature on sulphur and irradiation crosslinked elastomers; polybutadiene rubber (BR), natural rubber (NR), Government Rubber-Styrene (GR-S) (information based on [20]; published in [48])

A fact which can be observed in Figure 12 is that continuous tests generally show lower stresses compared to intermittent ones. This effect can be explained by non-consideration of network reformation during continuous testing due to the reasons argued. The processes on molecular level ongoing during oxidation can also be explained using the example of compression set. Like continuous relaxation experiments, deformation is applied such that stresses evolve. In this compressed status oxidative reactions provoke a degradation of the original network and stresses are relieved. In parallel, new bonds are built between the elastomer chains in the current alignment which restrain the material from going back to the initial state after loads are taken away. These considerations are shown schematically in Figure 13.

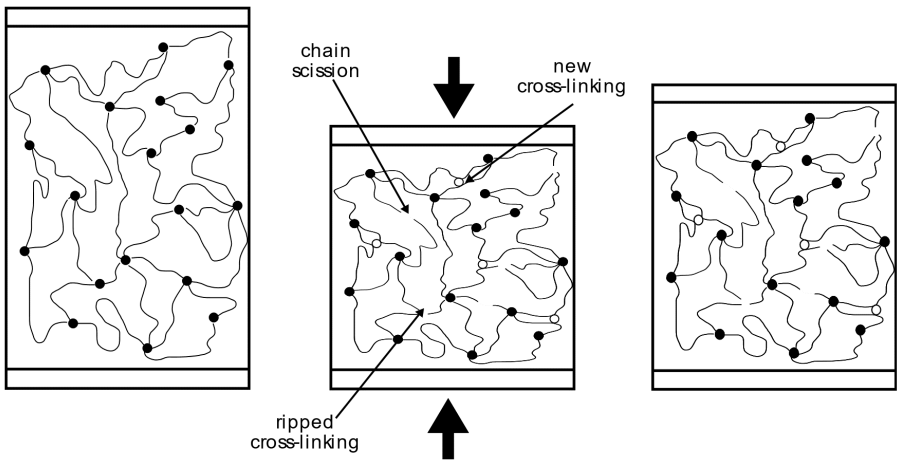

Figure 13: Schematic illustration of chain-scission and reformation during compression set; (left) virgin condition, (centre) compression and ongoing ageing, (right) unloaded sample after ageing [48]

Due to the molecular structure based on entangled molecular chains the mechanical response varies by the velocity of load applied. The effects of ageing on stiffness, relaxation behaviour and compression set also indicate influences on the elastomer's viscoelasticity. Nevertheless, changes in the viscoelasticity of elastomers due to ageing are less pronounced than that of the elastic behaviour and hence usually are neglected [20][81].

Beside the tensile behaviour oxidation also has influence on the hardness of elastomers. Commonly this effect is mentioned along with embrittlement of elastomeric materials but has to be carefully differentiated. Oxidative reactions affecting the molecular network have a major impact on the hardness by ripping bonds and creating new ones [50][93]. Therefore, oxygen increases cross-linking density which forms a stiffer network and consequently affects hardness. Since oxidation is mostly a diffusion-based phenomena hardness is influenced in an inhomogeneous way. Especially at elevated ageing temperatures polymers can show heterogeneous behaviour (see also subsection 5.2). At the surface of elastomer samples additional hardening can occur due to secondary degradation mechanism which may not have the same intensity as oxidation based effects [29]. Other effects influencing hardness of elastomer materials are post-vulcanisation and the loss of plasticisers or other additives [8].

Increased hardness goes hand in hand with spatially increased stresses provoking crack initiation since stiffer material carries higher load than other parts of the component. This is important since partly oxidised elastomers can become susceptible to cracking even at a low level of ageing. Therefore, fatal failure can occur even if degradation is less proceeded. Thus, inhibition of crack formation or stop of crack propagation is strived. Different countermeasures have been developed to prevent the cracking at the superficial layer e.g. by antioxidants (see subsection 4.4). Tyre industry is quite interested in the effect of crack initiation and propagation since it is essential for the mileage of car tyres. Cracks behave like a very sharp notch and result in an increased stress field ahead the crack tip which provoke local strain hardening. The strain hardening can

behave like a reinforcement and decelerate or stop the crack propagation [94].

Cracking can be important even for elastomers not primarily used as load carrying components. Due to spatial oxidation and/or an inhomogeneous temperature field micro-cracks can emerge. These cracks are cavities for ambient medium getting deeper into the elastomer or permeating through the material. Furthermore, permeability is also influenced by oxidation. Usually the diffusion of oxygen is based on the free volume in the elastomer as explained in subsection 4.1. Similar effects occur when dealing with elastomers as a sealing material. Changes in segmental mobility of polymer chains due to oxidative reactions affect the permeability of the elastomer since chain interactions, cross-linking density, molecular weight of the chains or the degree of crystallisation can be differed. Moreover, the existence of bulky and polar groups can decrease permeability as well as the presence of filler material [56][95]. Of course, the relevance of these permeability changing processes depends on the application or rather the ambient medium which should be stored or kept out.

Discolouration can be a good indicator that degradation occurred, but precise conclusions on the mechanical properties are limited. More often it is an unwanted effect of fading induced by oxidation in the superficial layer which impairs the visual appearance and the optical quality. The fading, yellowing and brown colouring are caused by the formation of functional groups during oxidation. The oxidation of double bonds and the creation of conjugated double bonds is another reason for the characteristic discolouration. The presence of plasticisers influences this discolouration. Figure 14 shows samples of EPDM before ageing and after exposure to oxygen containing environment at 100 °C for 508 hours. The aged samples show a distinctive brown colouring. After discolouration occurred the radiation absorption is varied due to the altered colour which could result in a changed heat input and hence in accelerated ageing due to the elevated temperature [11].

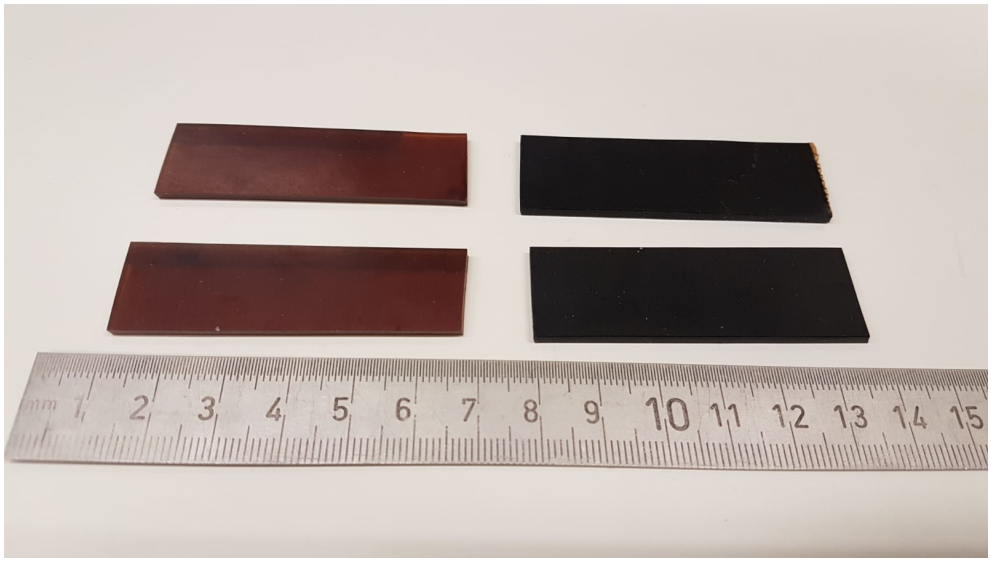

Figure 14: Discolouration of EPDM samples after exposure; right: unaged, left: aged at 100 °C for 508 h

Besides the mechanical properties, elastomers are also used due to their electrical properties. Mostly, elastomers are electric isolators and used in various applications to insulate voltage-carrying parts. Electric conductivity can be increased by filler materials like carbon black, carbon nanotubes, graphite or graphene [96]. These conductive particles provoke elastomers to transform from an isolator to a conductor by the formation of a filler network. Interactions between polymer chains and filler particles play a major role as well as particle size, structure, concentration, dispersion and orientation of the filler. The latter can be influenced by strain applied to the elastomer. In the case of moderate stretching electrical resistivity can be increased due to carbon black network structure breakdown. Besides the usage as an isolator or conductor important electrical properties can be dielectric strength, antistatic behaviour, electrical volume resistivity and surface resistivity [11][97]. During ageing the filler distribution, the interaction of filler material and molecular network can be impacted, and thus electrical properties can change. Oxidation induced embrittlement and fracture can also become relevant regarding electrical aspects. An example would be cable isolation breaking up and consequently metal conductor being bared. This is not an electrical property of the elastomer in the first place but worth mentioning in this context.

The last point mentioned in Table 1 are changes in the density and volume occurring during oxidative ageing. This includes changes in weight and dimension of the elastomer component. Using the visual representation of elastomers as an entanglement of molecular chains two mechanisms can change the macroscopic properties of density and volume. The molecular chains can be arranged in a denser package with less free volume in between or the substances can be absorbed from or resorbed to the ambient environment. Examples would be maritime applications for example elastomer coating of submarines for suppression of underwater echoes. Changes in the molecular structure by oxidation during operation on the sea surface can accelerate swelling of such a coating material and hence changes in the dimension and density of the rubber sheets can occur. Further, loss of substance and additives as well as changes in molecular structure can affect the spatial expansion or the weight of the elastomer. Critical applications are for instance sealings like O-rings which need resistance in the dimension to ensure tightness.

4.4 The role of antioxidants

Since changes provoked by oxidation are undesirable as presented in the previous chapter effort is put on the prevention of such ageing phenomena. Basically, this can be achieved by three different methods:

1. Preventing oxygen from reaching the elastomer

2. Suppression of oxidative reaction mechanisms

3. Initiation of measures which counteract the oxidation induced property changes

Most of these methods are realised by the admixture of certain additives which are distinguished by their different protective effects. Some are used to prevent the dissolution of oxygen in the elastomer by a physical barrier or to avoid oxidative reactions occurring in the interior. Usually, a combination of different antioxidants is used in a rubber compound in parallel [33]. Besides the prevention of oxidation anti-ageing agents are also developed to protect against ozone, UV-radiation, fatigue or hydrolysis. Thereby the expression 'antioxidant' is sometimes used for all these kinds of anti-ageing agents. In the following the expression 'antioxidant' will be used for additives preventing ageing by oxygen only to clearly separate it from other anti-ageing mechanisms.

One way to prevent oxidation of elastomers is shielding the material from ambient oxygen. Especially applications in atmospheres without oxygen or constructive solutions which inhibit the contact of the elastomer and the surrounding air do have less problems with oxidative reactions and hence are aspired. Unfortunately, such conditions are rare and cannot be ensured in most cases. Therefore, protection waxes are used to prevent oxygen coming in contact with the elastomer. They can be applied externally to the rubber and form a protective film or are added to the elastomer compound during the mixing process. The latter migrate to the surface in the finished vulcanisates due to their low solubility. Unfortunately, waxes evaporate at high temperatures or migration is hindered at low temperatures. Hence, usage is only possible in a limited temperature range. Although they offer no safe and lasting protection, they are widely used, especially in the storage of rubber articles. A similar effect can be achieved by impermeable coatings which hinder oxygen absorption from the ambient atmosphere. The latter is difficult to implement in the case of elastomers due to the high elasticity of the rubber material. Moreover, the diffusion of oxygen should be inhibited as much as possible if oxygen cannot be kept away from the elastomer in order to reduce ageing of the interior of the sample [82].

The second approach bases on the suppression and deceleration of oxidative reactions. Thereby primary and secondary antioxidants are distinguished. In the case of primary antioxidants, radical species are bound and stop the reaction chain of oxidation introduced in subsection 4.2. Thus, antioxidants act as radical catchers and are consumed during this process. In the case of phenols, a hydrogen is abstracted from the antioxidant by reaction with macroalkyl peroxyradical $ROO\bullet$ and form a bond with a free radical $R\bullet$. This results in a stable product instead of reacting with a hydrogen from a polymer chain, which would result in a reactive macro radical [33]. Aromatic amines are a further type of antioxidants acting as a radical scavenger and results in the formation of nitrogen compounds. Secondary antioxidants as for example phosphites react with hydroperoxides ROOH and prevent them from being decomposed into reactive products. As a consequence, radical formation is reduced, and oxidative reaction mechanism is decelerated. Further, the reduction of radicals by secondary antioxidants reduced the consumption of primary antioxidants which can be beneficial especially for long term applications [16].

Further, oxidative reactions can be prevented when no initial radicals are formed, or reaction rate is kept very low. This can be ensured by controlled environmental conditions, above all the temperature and UV-radiation. During storage before lab testing this is often used to hinder

pre-ageing and elastomers are put in refrigerators where it is dark and cold. In general, any method which hinders or decelerates the initialisation reaction can be used as an anti-oxidation method.

For reasons of illustration Figure 15 shows the antioxidants points of attack in the reaction scheme introduced before (see also Figure 11). Starting at the initialisation reaction environmental conditions can be chosen to prevent the formation of initial radicals. This can be done by controlling the influencing factors mentioned which are assumed to trigger radical formation. Moreover, avoiding oxygen in the ambient atmosphere as well as the usage of protective waxes can also prevent oxidation. Further, Figure 15 illustrates the function of radical scavengers which react with the radical species and hence eliminate them. The oxidation is interrupted at that point and reaction terminates. A similar effect is achieved by hydroperoxide decomposers.

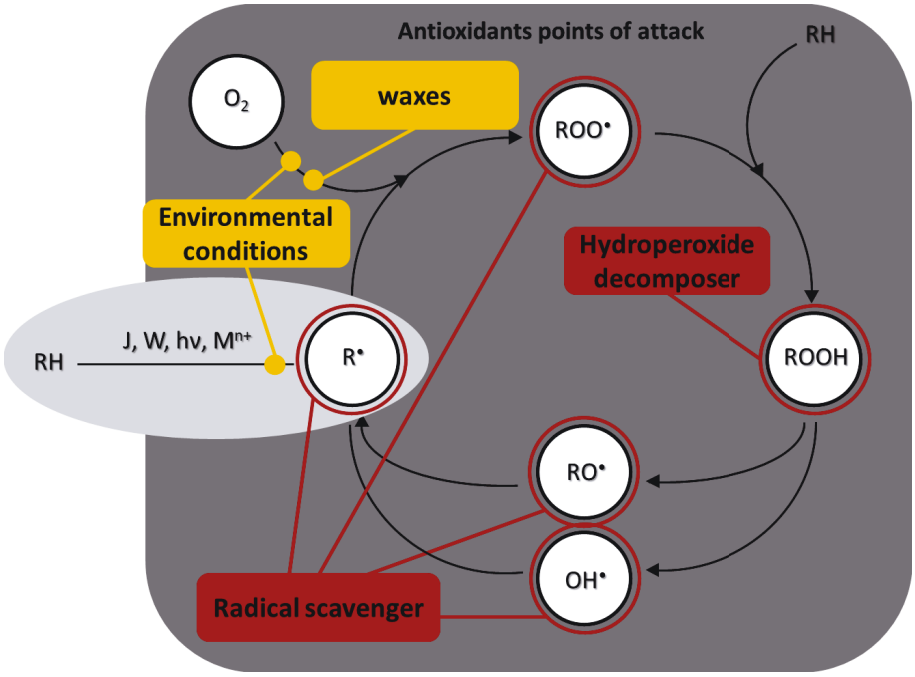

Figure 15: Antioxidants points of attack in the BAS scheme

For the case that oxidation could not be avoided, and ageing occurred measures which counteract the oxidation induced property changes are aspired. For example, remained curing agent from manufacturing can cause post-vulcanisation which counteracts the ageing induced chain scission process. For such an anti-ageing method a detailed understanding of the material, the ageing processes as well as the in-service conditions is mandatory.

A disadvantage of antioxidants can be the discolouration of the rubber material for example when using aromatic amines. Unfortunately, in light-coloured mixtures the most effective ones can therefore eventually be used in a limited way only. During ageing of filler-containing elastomers undesired interaction of antioxidants and the surface of the filler particles can occur which is poorly studied up to now [78].

Antioxidants are consumed during the protection process especially in areas of high oxygen concentration. Therefore, a gradient of antioxidant concentration arises in the sample and diffusion processes of antioxidants can occur [34][93]. Since anti-ageing agents are added in low concentrations and are limited in their effect to the close molecular environment a homogeneous distribution in the material is prerequisite for sufficient protection [16].

In general, adding anti-ageing agents must not initiate any secondary unfavourable processes in terms of stability or alteration of the polymer's physical properties. Further, it has to be compatible with the polymer and other additives in the elastomer and shall not cause any unintended effects like being highly toxic [17]. In almost all technical relevant applications of elastomers anti-ageing agents or rather antioxidants are indispensable. Therefore, a coordinated and adjusted mixture of antioxidants is required for the certain application and the type of elastomer used. Since, antioxidants are omnipresent their mechanism or rather their effect must be considered when dealing with oxidation of elastomers. This makes the analysis and interpretation of experimental investigations difficult since several processes occur in parallel, overlap and influence each other. Consequently, a conflict arises when elastomers with no or a minimum of antioxidants are manufactured for reason of research since the material is quite different to the ones used in technical applications.

5 Experimental investigation

5.1 Oxygen absorption

Since the process of oxygen uptake from the ambient environment is an essential step of the oxidation process an experimental method was needed which enables a qualitative and quantitative view on this phenomenon. If the elastomer contains little or no oxygen after the manufacturing process, the amount of oxygen molecules being absorbed from the ambient environment is an indicator for oxidation. Unfortunately, the quantity of oxygen absorbed does not allow for any conclusions to be drawn regarding reactions taking place in the polymer or changes of the chemical structure. Nevertheless, this method is described as the most direct and fundamental experimental way to approach polymer oxidation [28].

In general, investigations are distinguished by whether they are carried out under constant volume (isochoric) of oxygen or constant pressure (isobaric). Measuring under constant volume requires detecting changes in oxygen partial pressure of the ambient medium, when the volume of the surrounding medium remains unaffected i.e. no replacement of oxygen. The constant pressure method quantifies the volume of oxygen required to maintain isobaric conditions during oxidation by achieving compensation of the oxygen consumed. An overview of previously used methods up to an accuracy of approximately $2 \times 10^{-5}\,\mathrm{mol\,O_2}$ is provided by Scheirs et al. [28]. Besides these methods based on pressure measurement, other types exist using gravimetric analysis [98], gas chromatography [85] or electrode sensors to measure oxidation rates, as e.g. reported by Assink et al. [15][99].

Yet another method measuring oxygen uptake of polymers is based on respirometry which is not influenced by generated gases since only oxygen molecules are detected [14][15][16][44][99]. This highly sensitive and accurate method is usually used in biological research for e.g. measuring the respiratory cycles of small animals or mammalian cell lines [100] as well as for high-precision atmospheric oxygen measurements [101][102].

Since a finished test system for measuring oxygen absorption during ageing of elastomers is not commercially available an own setup was developed here. Based on a respirometer, an OXZILLA II Differential Oxygen Analyser from Sable Systems International (Las Vegas, NV), an experimental setup was defined and build up. Therefore, the requirements had to be defined which met the requirements or rather the principal goal of investigation. Then the design and details of the setup's structure as well as a testing process were developed which all had to be brought in accordance to each other. The development process and the functional description of the experimental setup were published in [103].

5.1.1 Requirements for the testing setup

The aim of the development was to define the universal applicability of the system which provides as much experimental scope as possible for subsequent variations of the testing procedure. Above all, the desired experimental conditions as well as the basic device OXZILLA were decisive for the design of the setup. The latter requires certain preconditions for meaningful measurements and was the only component that was preselected due to its high resolution enabling the detection even of smallest changes in oxygen concentration. During the definition and development phase the following requirements were identified and imposed:

- Possibility of continuous and static measurement to provide the option of two fundamentally different approaches. Since there is no known experimental design which allows a permanent flow around the elastomer sample and the success of this approach is unknown static measurements should be possible as well.

- The samples used should have the same dimension as those for other experiments, e.g. subsequent intermittent relaxation testing to allow a combination of different measurements on the same sample. Hence, a direct linkage of oxygen absorption and changes in other properties should be feasible.

- The experimental setup should be as independent as possible from location and equipped only with conventional connections which are available in standard laboratories.

- The entire system should have optimum accuracy to obtain results of high quality. In detail the high resolution of the respirometer should be meet by the supporting setup structure to fully exploit the potential.

- No influence on the measurement by built-in elastomer components, e.g. O-ring seals should origin from the setup. Reliable sealing of the fittings and components should ensure to prevent the ingress of ambient air which may affect the measurements.

- The known drift effect of the respirometer should be considered, and suitable countermeasures should be defined.

- Digital data acquisition and storage should be implemented.

- The control of the entire setup by means of all in one self-developed program should ensure a fully automated test procedure.

- The testing time and effort should be kept as low as possible.

- Easy and inexpensive maintenance should be ensured.

Based on these general demands on the experimental setup requirements and properties of in-

dividual components could be derived. Ambient air is chosen as the flowing medium as it best corresponds to natural ageing conditions and is available endlessly. This reduces external dependency and running costs compared to nitrogen. Some components still require pre-processing of the air flowing through. It must be dried, compressed and filtered in order not to alter the measurement and avoid damaging the devices installed. In addition, the air must be free of oil and any particles which cannot be ensured by the conventional central compressed air supply system.

5.1.2 Basic design and components

There are only a few applications which require oxygen measurements with such an accuracy like the one presented in this work. Hence, the respirometer used was not primarily designed for material science but for biological and environmental investigations. For atmospheric studies detailed descriptions of the experimental design are available, which unfortunately are only partially transferable to the configuration required here [104][105][106][107]. However, there are also studies which investigate the oxygen uptake of material samples, but the experimental setup is described more or less superficially only [15][82][108]. Figure 16 shows a simplified scheme of the developed setup in this work.

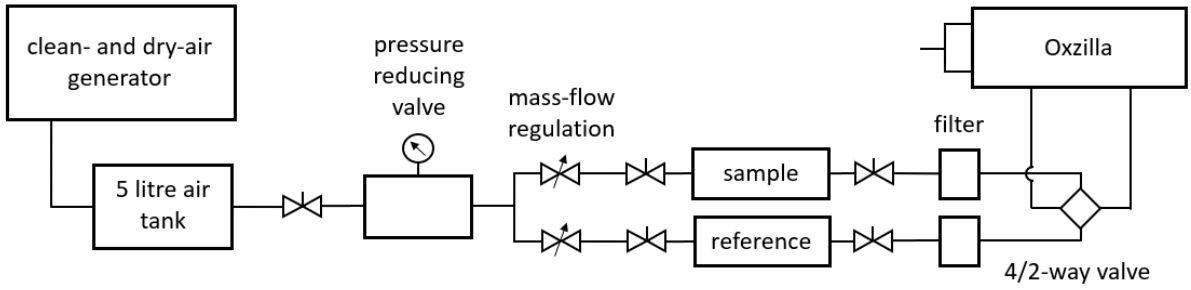

Figure 16: Schematic structure showing the measurement set-up [103]

The main device of the experimental setup is a respirometer, an OXZILLA II Differential Oxygen Analyser. It allows measurements of the absolute oxygen content of the air flowing through at two separated inputs. The analyser has its highest potential in determining the difference between the two lines (accuracy $\pm 0.1\,\%$ O_2, resolution $0.0001\,\%$ O_2). Therefore, the OXZILLA is operated with a sample and a reference mass flow here. The flow rate must be chosen between 5 and 2000 ml/min. Figure 17 illustrates the OXZILLA II Differential Oxygen Analyser and gives an overview of its connections and control elements.

Figure 17: Differential oxygen analyser "OXZILLA II" from Sable Systems International (Las Vegas, NV)

The functional principle is based on two fuel cells made out of a gold cathode and a lead anode, at which an electrical voltage linearly proportional to the oxygen partial pressure of the conducted air is created. The net reaction taking place at the electrolyte of the fuel cells reads as follows [102]:

$$O_2 + 4H^+ + 2Pb \rightarrow 2H_2O + 2Pb^{++}$$

This so-called "galvanic oxygen sensor" reacts with supplied oxygen and generates a certain voltage. The equation shown here only represents the relevant part of the chemical conversion. It should be noted that the lead of the anode is consumed by the reaction. Thus, this device is of limited life time and the fuel cells have to be replaced after about two to three years. A reason for using fuel cells as a basis for oxygen detection is their excellent accuracy and resolution. Nevertheless, these advantages come along with some challenges like drift effects and high sensitivity to environmental conditions like temperature. Such effects motivated the installation of two fuel cells in one device and the operation as a differential oxygen analyser to avoid distortions in the best possible way [105]. Any falsifying influence of polymer pipes inside the OXZILLA is not to be expected since in the present version already all wetted parts are made from stainless steel.

However, the maximum accuracy can only be achieved by the accurate control of the boundary conditions. For this purpose, the pressure and temperature of the inflowing air as well as the mass flow has to be considered and controlled. Although the pressure is measured at the inputs of both fuel cells and taken into account to correct the oxygen concentration displayed, differences should be avoided wherever possible. A deviation in the mass flow of both lines, sample and reference (see Figure 16), is critical for accurate measurements since a larger air flow initiates the generation of more charges resulting in the fuel cells indicating a higher oxygen content. Thus, constant mass flows are ensured by high-precision mass flow controllers described below.

In order to avoid distorting effects by temperature, the structure of the setup is chosen so that there are no heat sources in the vicinity of medium carrying lines. The general conditions in the laboratory ensure a stable room temperature and the 5-litre tank serves as a thermal inertia. Moreover, the temperature of both lines is monitored by the mass flow controllers and fuel cells are placed in a temperature-controlled housing.

In order to prevent pressure differences in the ambient pressure both lines are connected downstream to the respirometer which ensures a common pressure level at the outlet [107].

In summary, a certain effort is required to take full advantage of the OXZILLA's accuracy and resolution. Besides the points mentioned, ambient drafts and direct solar radiation have to be avoided. All the points stated have been considered during the development of the experimental setup. In the following the individual components chosen are presented and described.

An external compressed air supply was eliminated as an option because the air would have to be elaborately prepared to avoid any variation in the measurement or damage to the devices. The measurement requires a very low degree of moisture, that means a very low dew point and absolutely oil- and particle-free air. Condensing of air moisture could even cause damage to the fuel cells. Therefore, the compressed air is produced by the setup itself not using the existing laboratory connections. Due to the small mass flows of approximately 100 ml/min a pure compressed air generator represents the most compact and most favourable solution. Clean-Dry-Air-Packages are usually designed for producing small amounts of compressed air and meet the requirements here. An appropriate device is Model CDA10 from Twin Tower Engineering (Broomfield, CO) which was selected here. Separation of oil is not necessary since it is an oil-free compressor. Central compressed air supplies usually admix oil for the sake of corrosion protection. The Clean-Dry-Air-Package delivers an air mass of 5 standard litres per minute (SLPM) at a pressure of about 5.5 bar in normal operation. Maximum operation provides 10 SLPM. Subsequently, the compressed air of the oil free reciprocating type compressor is quenched and dried to a dew point of less than -73 °C. This is accomplished in two steps, first by a coalescing filter and then by means of a two-chamber adsorption dryer (heatless desiccant air dryer) which dehumidifies the air flow alternately in one chamber using a desiccant and meanwhile the second chamber is regenerated again. In order to avoid continuous operation of the compressor a reservoir of five litre capacity was installed downstream. Furthermore, the reservoir ensures constant air properties for short time investigations.

Further downstream in Figure 16 a shut-off valve and a pressure reducer are installed before the line is split up in two lines, sample and reference line. The shut-off valve is used to stop the air flowing through the lines when needed by the measurement process. The pressure reducer decreases the air pressure from approximately 5 to 2 bar in order to protect the subsequent mass flow controllers.

One of the most important parts of the setup are two mass flow controllers which ensure that the same amount of air flows through the two lines. Usually mass flow controllers are used where the

volume of a medium flowing through has to be precisely controlled. There are various operating principles that differ fundamentally and are more or less well suited to the conditions of use. Since gas temperatures of up to 100 °C should be possible here, most mass flow controllers that rely on thermal processes fail. Another method is based on the pressure decrease along a laminar flow element. Discovered by Hagen-Poiseuille, the volume flow of a gas can be determined by differential pressure determination. Therefore, a constriction in the measuring device is used to generate a laminar and turbulence-free flow. The key is that the flow depends linearly on the pressure drop and thus it can be described by means of Poiseuille's equation.

$$Q_V = \frac{(p_1 - p_2)\pi r^4}{8\eta L} \tag{3}$$

Q_V is the volume flow, p_1 and p_2 the static pressure at inlet and outlet, r the radius of the constriction, η the absolute viscosity of the medium and L the length of the constriction. Since geometry is not changing the equation can be rewritten using K as a constant of geometric properties.

$$Q_V = K\frac{\Delta p}{\eta L} \tag{4}$$

The rest of the equation shows the proportional dependence of the volume flow on the differential pressure and on the reciprocal of the absolute viscosity. The pressure drop is measured at two holes. The gas viscosity which depends on the medium and temperature has to be determined. Viscosity of air changes only negligibly with changing pressure below 6 bar, whereas the variation of the temperature T has great influence. Hence, mass flow controllers have to compensate temperature effects for a precise functionality. The following equation can be used for air as an approximation [109].

$$\eta(T)_{air} = 14.58\frac{T^{3/2}}{110.40 + T} \tag{5}$$

As described above the fuel cells of the respirometer are sensitive to oxygen molecules, hence it is important to ensure a constant mass flow. Therefore, the volume flow Q_V has to be converted to the mass flow Q_M by means of the continuity equation and the density conversion according to the thermodynamic gas law.

$$Q_M = \rho\, Q_V \qquad \text{with} \qquad \rho = \frac{m}{V} = \frac{p}{ZR_ST} \tag{6}$$

Thereby the density ρ is calculated by using mass m and volume V or rather pressure p, compressibility factor Z and individual gas constant R_S. In such applications Q_M is usually desig-

nated as standard volume flow using the unit SCCM (standard cubic centimetre per minute) which corresponds to the mass flow normalised to standard conditions.

Figure 18 illustrates the method using a laminar flow element. The laminar flow is generated by means of a capillary bundle and the values described are measured by sensors.

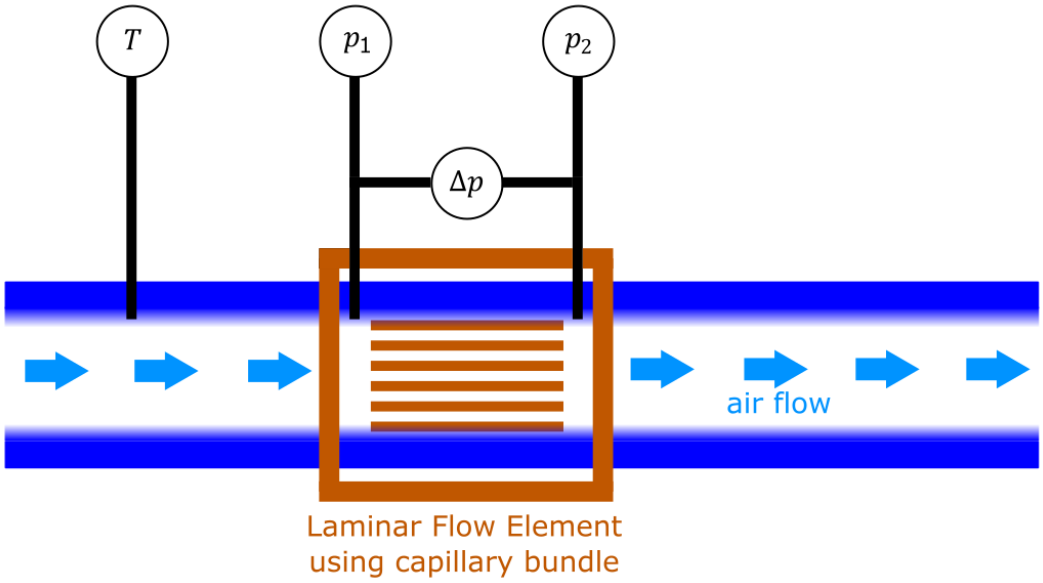

Figure 18: Schematic illustration of a laminar flow element used in mass flow controllers

This description of flow measurement using a Laminar Flow Element is valid in a limited temperature range only. In order to consider moisture and higher temperatures effects viscosity should be calculated according to Kestin-Whitelaw and the pressure calibration should be performed by “universal flow” method based on the Reynolds number.

Due to the experimental setup requirements, a mass flow controller based on a laminar flow element from Natec Sensor GmbH (Munich, Germany) was chosen. Unfortunately, there is a practical upper temperature limit for the medium of 50 °C, which is not due to the measurement method, but the electronic components used. A special manufacture with outsourced electronics allows temperatures of up to 100 °C. Figure 19 shows the mass- and volume controller of the Natec Sensor M-V/M-VC series. It consists of the housing containing the laminar flow element and the control valve which conducts the gas flow and regulates the mass flow. Here, the connections for the power supply and the interface for communication are located. The temperature-sensitive electronics including display and control panel for regulation are outsourced via a ribbon cable.

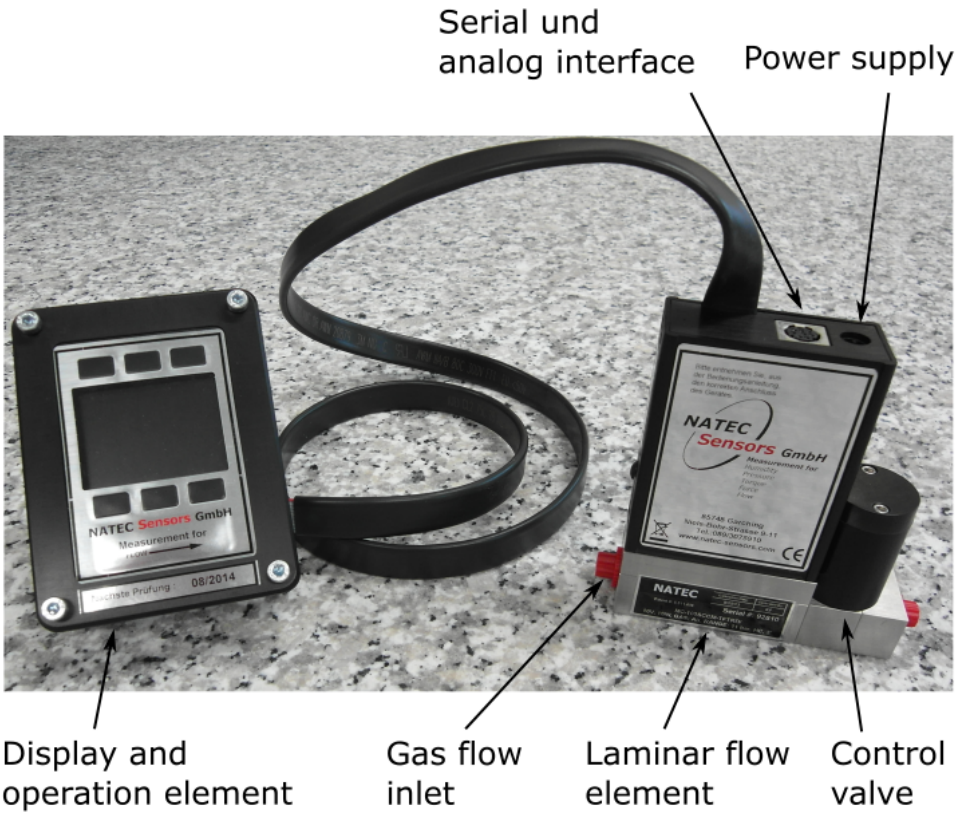

Figure 19: Mass and volume flow controller for gases of Natec Sensor GmbH M-V/M-VC series with detached electronic

Shut-off valves are installed in front of and behind the sample respectively the reference chamber to precisely control the start and end of the flow. The valves are electrically driven to automate the measurement process and ensure closing and opening of all valves simultaneously. In addition to a good seal of the valves in the closed state, especially a short switching time, minimum dead space and minimum pressure loss are important. As a sealing material polytetrafluoroethylene (PTFE) is used, which is better known under the trade name Teflon. It is an inert material and therefore extremely resistant. The housing is made of stainless steel and contains no oil or grease for lubrication. The installed valves are closed in the basic state and open only when voltage is applied. The nozzle size is 1 mm, which also results in a small coil capacity. Thus, an uncontrolled heat input of the four valves on the medium is kept as small as possible.

The sample material to be examined is placed in a chamber during exposure and measurement. In general, two types of measurement intermittent and continuous have been demanded during development. For continuous testing the processed air flows around the sample which absorbs oxygen with very low flow rates. In intermittent experiments the filled sample chamber is completely closed and exposed to e.g. elevated temperatures for ageing. After a certain duration the chamber is connected to the experimental setup and the air in the chambers is blown through the OXZILLA. This is done by flooding the chamber with processed air and conducting the mixture with present air to the respirometer.

Both ways require the possibility to open the chambers in order to equip them with the material to be examined. Therefore a high tightness of the chambers is important and should be guaranteed even after repeated use and at elevated temperatures. Further it is important to avoid any unnecessary dead space and barriers in the chambers to prevent turbulence and ensure a complete and prompt evacuation. The external ageing, i.e. disconnection of the chamber from the setup and exposure in an ageing furnace, requires a plug-in connection of the sample chambers to the setup. During external exposure the chambers have to be absolutely tight ensuring that no leakage air can penetrate. Since the sample surface area also has an influence on the oxygen uptake, the position of the elastomer in the chamber should be considered. Therefore, the samples are held in position by a wire to ensure a complete air flow around the sample, avoiding contact with the chamber wall.

The cylindrical sample chambers designed for this purpose are shown in Figure 20. They can be opened on one end using a removable screw-on cover. Besides the screw thread, an individually produced PTFE gasket is used for additional sealing. Inlet and outlet are contructed with two self-sealing quick couplings with additional stainless-steel bellows sealed valves. The latter avoids any leakage and pressure loss during external ageing. After being attached to the setup they are opened manually.

Figure 20: Hermetic sample chamber for oxygen absorption measurements; right-hand side of the tube can be opened by means of a screw-on cover

The size of the chambers was selected such that common specimens can be used and thus there is maximum freedom in the design of experiments. The cylindrical interior space has a length of 80 mm and a diameter of 30 mm. This represents the volume where the material tested is placed. The actual size of the sample has to be smaller to ensure an unhindered gas flow during measuring. Furthermore, the volume ratio of sample to the test air has to be kept small to avoid measuring errors as described later. All in all, the chambers are designed that oxygen absorption can be measured, and mechanical tests can subsequently be performed on the samples.

Downstream, the chambers filter elements are installed in both lines which clean the air of the smallest impurities. They use a sintered metal element with a pore size of 0.5 μm.

In order to counteract the natural drift of the fuel cells during continuous tests the two input lines are alternated periodically [101][104]. This is realised by means of an electronically controlled

cross valve. It consists of a 4-way stainless steel ball valve driven by an actuator. Figure 21 shows the flow chart of the valve used. By turning the ball screw the valve is switched between the two positions shown. Thus, input 1 is connected once to output 1 and in the other case to output 2. The same applies to input 2. During the switching time, the valve is momentarily shut off until the channels reach the position of the other holes. Further, the cross valve also provides more opportunities and flexibility for intermittent testing. This is discussed later when the testing procedure is explained.

Besides the functional components fittings and pipes are important elements of the experimental setup. Screw connections and air-carrying lines must be as reliable as the more complex electronical measuring and control technology. Each thread and sealing connection is a potential location for leakage. In order to avoid the use of elastomer-based sealing material for screw connections NPT (National Pipe Thread) were used wherever possible. This is a US thread standard for self-sealing metal-only pipe fittings. The sealing effect is provided by a conical arrangement of the threads and does not require a sealing material like PTFE or hemp. If it was not possible to use this technique, conventional cylindrical threads are sealed with PTFE tape.

In places where components cannot be connected directly, pipelines are used. In the experimental setup described two sizes are installed. Stainless steel tube with an outside diameter of 8 mm are used for the lines up to the mass flow controllers. The diameter is chosen in this dimension so that the flow rate remains low and pressure-changing influences e.g. at the T-branch have little or even no influence. These tubes supply both sample and reference lines with clean air without major pressure losses.

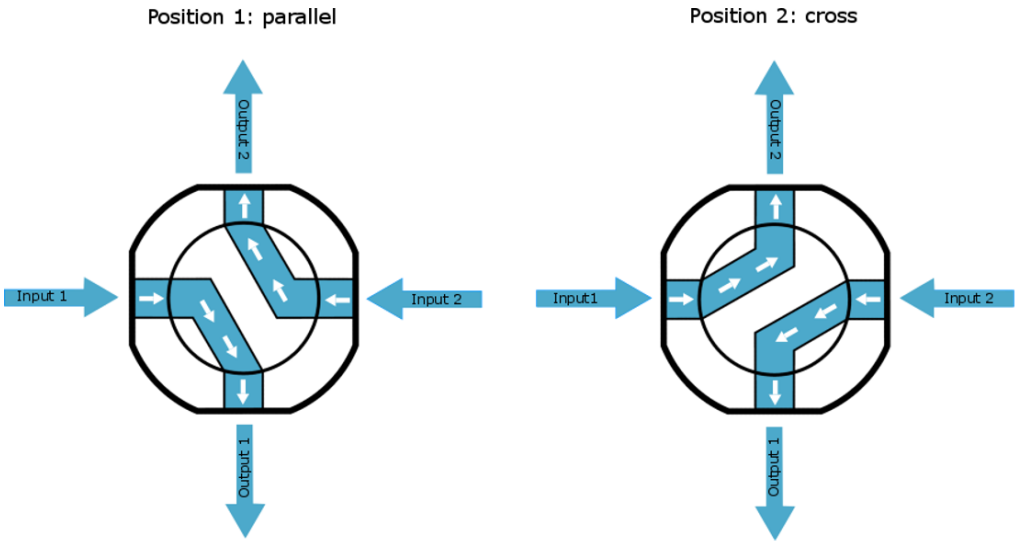

Figure 21: Schematic diagram of the 4-way ball valve

After the mass flow controllers 1/16-inch pipes made out of stainless steel are used. They are of the same size as the tubes installed in the OXZILLA and conduct the air for the oxygen measurement. In this case, a very small diameter is used to have as little air mass in the system

as possible and to ensure rapid flushing of the pipes and valves.

Furthermore, the connection to pipelines is exclusively done by compression fittings. The company Swagelok (Solon, OH) offers a patented system which uses two clamping rings and guarantees absolute tightness without using anything other than stainless steel.

In summary, almost all surfaces coming into contact with the fluid are constructed of corrosion resistant steel (e.g. stainless steel V4A). For connections, NPT threads and clamping ring sealings are used. If this was not possible, inert material like PTFE was used for gaskets. No lubricant greased valves are incorporated in the entire setup.

For measurement process reasons the setup is controlled by a self-developed program written in the programming language LabView. It controls centrally the following components:

- receiving, processing, graphical representation and storing of the information produced by the differential oxygen analyser
- control and read out of the mass flow controllers including information about temperature and pressure
- control of the shut of valves
- control of the 4-way ball valve including automatically periodic switching

The differential oxygen analyser and the mass flower controllers are connected to the computer by serial interfaces. Using the interface control documents of the component suppliers, the LabView program was developed to translate and generate the serial strings which are required for communication of the control program and the devices. The electrical valves are also controlled by the same program, thus a relay board is inserted which regulates the current flow to the valves. This board is also controlled via a serial interface and hence the whole experimental procedure can be controlled and monitored by a single program. This is important to allow precisely controlled and reproducible test sequences as described below. Furthermore, the self-developed control and monitoring software provides the possibility of modifications to adjust the program, as well as, the user interface for special needs and high automated processes. Figure 22 shows the user interface of the current version used for the measurement in this work. It provides the possibility to check different input signals and plots several output signals to provide a summary of the ongoing measurement. Further, the mass flow controllers and the valves can be driven individually or in defined sequences.

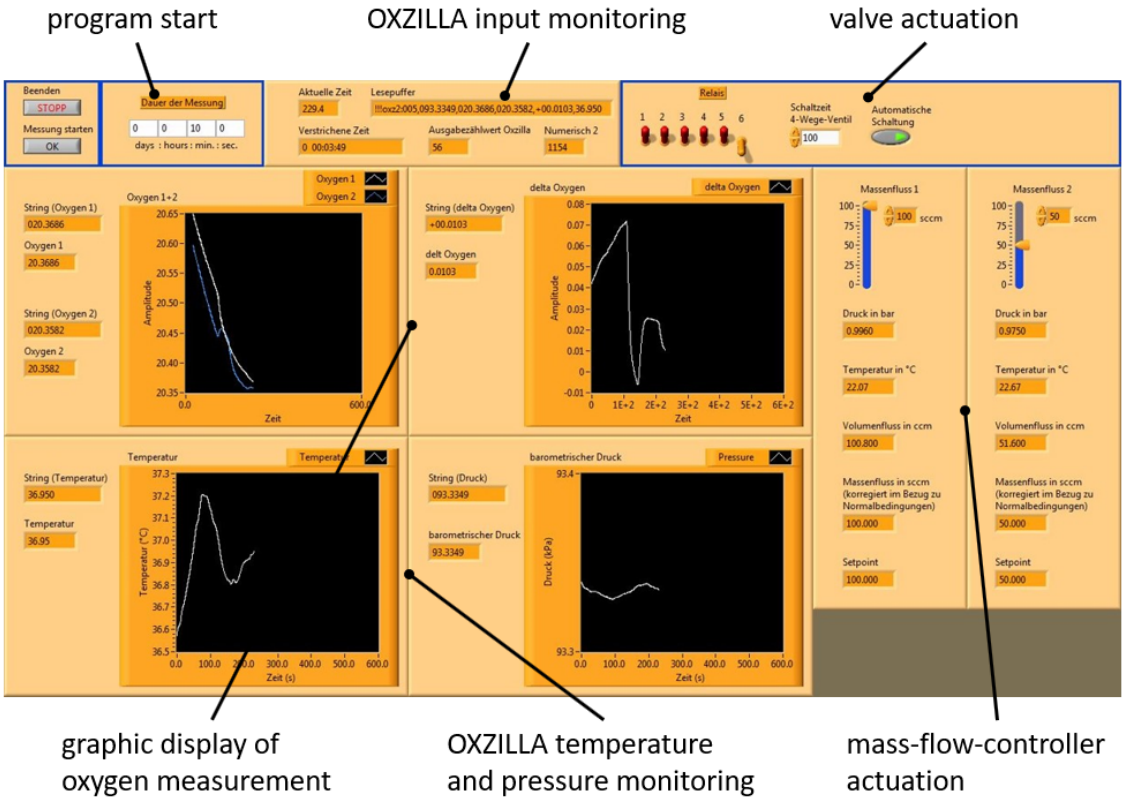

Figure 22: User interface of the self-developed control and monitoring program implemented in LabView®; the software allows an all in one control of the experimental setup including OXZILLA oxygen analyser, electric driven valves and mass-flow controllers

5.1.3 Testing procedure

As mentioned previously, flexibility and adaptability are main objectives during the design phase. Basically, the setup allows for different types of investigation, e.g. intermittent and continuous testing. In this subchapter, the procedure for intermittent testing used for measurements in this work will be presented. Moreover, the further processing and analysis of the measurement outputs will be explained. Aim of the investigation is measuring the amount of oxygen molecules being absorbed by a certain elastomer sample as a function of ageing duration and temperature.

First step is the preparation of the sample. Usually the raw material is vacuum-packed, and stored at low temperatures to prevent any pre-ageing or contamination with oxygen before being exposed to ageing conditions. Directly before ageing starts the sample is unpacked and cut to the desired shape. As already mentioned, this can be a geometry which is required for subsequent mechanical testing e.g. bone-shaped tensile specimen. In general, only measurements on identical shaped specimen should be compared since the surface-to-volume ratio as well as the geometry has influence on the oxygen absorption (see paragraph 6.2.4.3). Of course, differently shaped specimens of the same elastomer compound can be compared to investigate the influence of geometry and surface area on the oxygen absorption behaviour. Usually simple

shaped specimens like plates are used and the dimensions as well as the masses are noted before the start of the test. The chamber is preheated to the ageing temperature in open condition to avoid any delay in heating when starting exposure and to adjust the pressure in the chamber to ambient pressure. After preparation, the specimens are placed on a wire mesh in the preheated chamber (Figure 20) to minimise the contact of sample with the chamber. The valves at the chamber are closed and the chamber cover is positioned without the screw cap being fully closed. Then the chamber is put back in the air circulated furnace. After a few minutes the chamber has to be completely closed. This helps to ensure constant ageing temperature and ambient pressure in the chamber during the whole time of ageing. The chamber is exposed for the defined duration. Subsequently, it is removed from the oven and let cool down at room temperature. Therefore, it is important to consider the time of cooling as an additional ageing time since room temperature is not achieved immediately. During the whole chamber handling it is important to avoid rotating the chamber since the sample is not fixed in the chamber and displacing it could change the position of the specimen, which could affect the amount of ageing surface during exposure and the flow conditions during measuring. Natural cooling to room temperature takes several hours depending on the ageing temperature. Accelerated quenching is not suitable because it can jeopardies tightness of the valves and the screw cap. Since there is no thermometer in the chamber sufficient time is necessary to ensure a complete cooling down. A rule of thumb figured out during development of the setup is a cooling time of not less than five hours. Mostly the chambers were taken out of the oven and laid to rest overnight. Ensuring measurements at room temperature is important since the oxygen detection is sensitive to temperature. Different testing temperatures would impede the comparison of exposure tests at different ageing temperatures. At least three samples should be aged each in its own chamber to get some statistically reliable data and chambers without elastomeric material serving as a reference which get identical treatment as the loaded ones.

The latter is done to compensate any pressure effects. The chamber is closed under ambient pressure and ageing temperature. It remains sealed during cooling down later which induces a reduction of the pressure depending on the ageing temperature exposed before. Since the OXZILLA is sensitive to oxygen partial pressure this effect requires special attention. The same effect can be observed for the reference chamber and the measured value can be used to compensate the effect. The difference between sample and reference chamber indicates the amount of oxygen absorbed by the elastomer sample.

The respirometer has to be prepared for measurement before the test chambers are connected to it. This is necessary due to the characteristic of the fuel cell based test method. Along with long time measurements, drifting effects can distort the results. Usually the respirometer is turned on at least four hours before testing starts to stimulate the fuel cells by conducting clean and dry air through the respirometer. Therefore, empty chambers are installed which are flooded and serve as a transit for the air. The output signal stabilises with ongoing time which can be monitored by the control software. In order to avoid drifting effects during this procedure called “baselining” the 4-way valve is changed over periodically. Here a sequence of 100 seconds was found to be convenient. Figure 23 illustrates such a stabilisation phase by showing the difference

of oxygen concentration between both fuel cells as a function of time. The changeover of the 4-way valve is clearly visible as well as the usual offset between the fuel cells which can be eliminated easily by calibrating the respirometer [103]. Due to this preparation the fuel cells are sensitive to even smallest changes in oxygen concentration which is necessary for the subsequent testing.

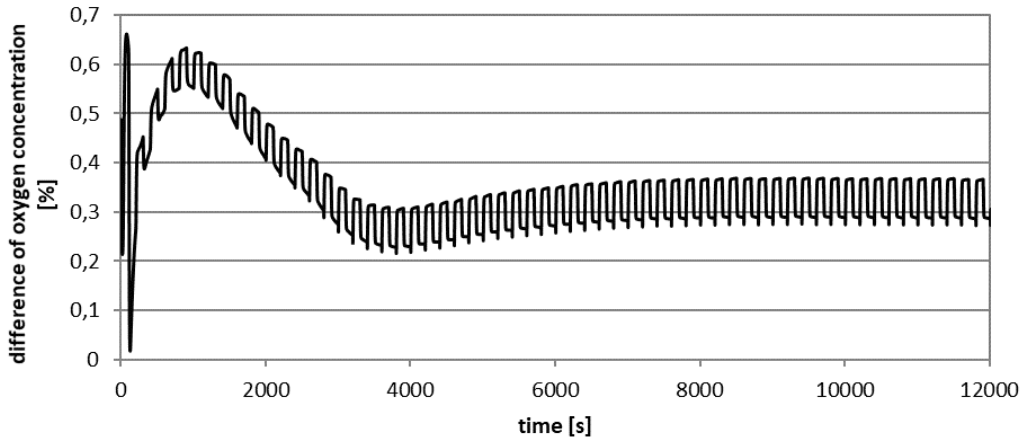

Figure 23: Stabilisation phase of the respirometer and offset effect between fuel cells [103]

Several approaches exist for the method and sequence in which the chambers are connected to the setup and oxygen concentration is measured. One possibility is explained in [103] which uses one reference chamber for each sample chamber. Both are simultaneously connected to the setup and flooded in parallel. Therefore, all four shut-off valves are closed, and the dummy chambers are replaced by the sample and reference chamber. Then recording is started, and the valves are opened.

Figure 24 shows an example for the outcome of such a measurement for a standard elastomer aged for 89 h at 60 °C. Both fuel cells detect a decrease in the oxygen concentration of the air flows after all four shut-off valves are opened approximately 100 seconds after recording started. An offset can be observed between the two signals from the beginning of the recording which does not disturb the measurement. In the moment where the valves are opened (app. at 100 s), the oxygen concentration rises shortly before falling again. This short rising is caused by the respirometer which is drifting during the time the valves are completely closed and effects due to the negative pressure in the chambers which shortly draw air in the opposite direction of flow. Afterwards the graphs of both signals decline because the air in the chambers had a reduced oxygen partial pressure. This is due to the depression in the sealed chambers resulting from the cooling after ageing. The difference between sample and reference line represents the amount of absorbed oxygen (between 100 and 200 s). The air in the chambers is mixed with cleaned and dried air from the generator and is slowly deflated to the respirometer. As soon as most of the consumed air is evacuated the oxygen concentration increases again (app. at 130 s) until the value of the air from the generator is reached (app. at 200 s). A slight difference in the oxygen concentration before and after the drop can be observed which is a consequence of fuel cell

drifting caused by discontinuous air flow due to the measuring procedure described. One should be aware of these effects to consider them during analysis of the results.

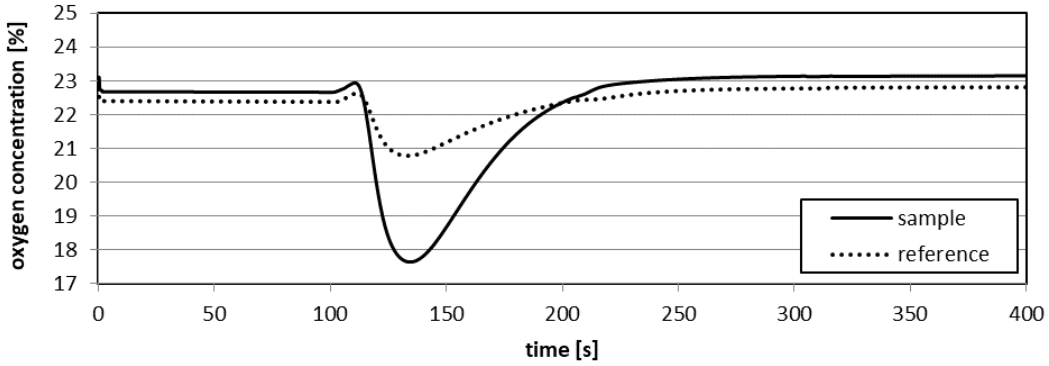

Figure 24: Oxygen concentration drop for an elastomer aged over 89 h at 60 °C [103]

The difference between both graphs is the value of interest since it represents the amount of oxygen molecules being absorbed by the elastomer. Figure 25 shows the difference of oxygen concentration (ΔOx) between both fuel cells for the above measurement. Since the mass flow is accurately controlled to 100 sccm/min it becomes possible to quantify the absorbed oxygen. The hatched area in Figure 25 is a measure for the oxygen absorption during the period of ageing. After the chambers are completely evacuated the signal stabilises at a constant value only showing a little offset when the 4-way valve switches. Besides this demonstrates that the accuracy of the setup is appropriately sensitive for that kind of measuring [103].

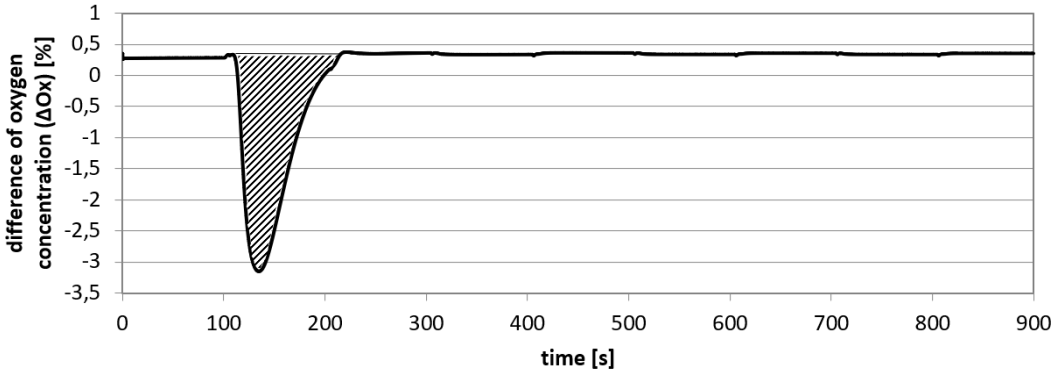

Figure 25: Difference in oxygen concentration of an elastomer aged over 89 h at 60 °C [103]

5.1.4 Calculation of the oxygen consumption

The amount of absorbed oxygen is usually expressed by the values named 'oxygen consumption' and 'oxygen consumption rate'. Caution is needed since the expression 'consumption' can also mean the amount of oxygen molecules which have chemically reacted with the material. Here, it is used as a synonym for absorption.

In order to calculate these values from the concentration graphs the oxygen deficiency of the

sample chamber can be determined by multiplying the gas flow rate by the integral of the oxygen concentration versus flow time (i.e. the area between the two curves of Figure 24 or rather the hatched area in Figure 25). Then the volume of oxygen was converted to moles of oxygen and divided by the sample weight (and ageing time to obtain the rate) to provide a normalised value (see also [14][15][103]), using the following equations.

$$oxygen\ consumption \left[\frac{\text{mol}}{\text{g}}\right] = \frac{\dot{m} \int \Delta Ox(t)dt}{m_{sample}} = \frac{\dot{m} \frac{A}{100\%}}{m_{sample}} \tag{7}$$

$$oxygen\ consumption\ rate \left[\frac{\text{mol}}{\text{g s}}\right] = \frac{\dot{m} \int \Delta Ox(t)dt}{m_{sample} \cdot t_{ageing}} \tag{8}$$

Starting point is the area between the two curves A which has the unit [%s]. This area can be calculated by means of a spreadsheet programme using a simple integration scheme (Riemann sum, midpoint rule). The mass flow $\dot{m}$ is given by the experimental setup and usually adjusted to 100 sccm/min. It has to be converted to sccm/s and the volume sccm to litre as shown by Equation (9). Division by 100 % eliminates the unit percent. In order to convert the volume into the amount of substance usually ideal gas and standard conditions STP (standard temperature and pressure) are assumed and molar gas volume ν of 22.4 l/mol is used. The result is the amount of oxygen molecules which are absorbed during ageing per weight of the sample.

$$\begin{aligned} \frac{A\,[\%\text{s}] \cdot \dot{m}\left[\frac{\text{sccm}}{\text{min}}\right]}{100\% \cdot m_{sample}\,[\text{g}]} &= \frac{A\,[\%\text{s}] \cdot \dot{m}\left[\frac{\text{sccm}}{\text{min}}\right] \cdot \frac{1}{60}\left[\frac{\text{min}}{\text{s}}\right] \cdot \frac{1}{1000}\left[\frac{\text{l}}{\text{sccm}}\right]}{100\% \cdot m_{sample}\,[\text{g}] \cdot \nu\left[\frac{\text{l}}{\text{mol}}\right]} \\ &= A \cdot \frac{\dot{m} \cdot 1\,\text{mol}}{100 \cdot 60 \cdot 1000 \cdot 22.4 \cdot m_{sample}\,[\text{g}]} \\ &= A \cdot \frac{1\,\text{mol}}{60 \cdot 1000 \cdot 22.4 \cdot m_{sample}\,[\text{g}]} \widehat{=} \left[\frac{\text{mol}}{\text{g}}\right] \end{aligned} \tag{9}$$

Analogue for the oxygen consumption rate:

$$\frac{A\,[\%\text{s}] \cdot \dot{m}\left[\frac{\text{sccm}}{\text{min}}\right]}{100\% \cdot m_{sample}\,[\text{g}] \cdot t_{ageing}\,[\text{s}]} = A \cdot \frac{1\,\text{mol}}{60 \cdot 1000 \cdot 22.4 \cdot m_{sample}\,[\text{g}] \cdot t_{ageing}\,[\text{s}]} \widehat{=} \left[\frac{\text{mol}}{\text{g s}}\right] \tag{10}$$

Equation (9) and Equation (10) show the conversion of the respirometer's output into the value mol/g or rather mol/g/s typically used for oxygen consumption. It describes the amount of oxygen molecules missing in the elastomers ambient air after exposure and represents a first indicator for oxidation. Of course, this experimental method, or more precisely, the experimental setup developed has to be critically analysed to be aware of the full potential as well as its limits.

5.1.5 Critical reflection of the method and the setup

In the following, information and thoughts are provided which emerged during design and construction of the setup and the development of the test procedure. It is necessary to be aware of advantages and disadvantages as well as limitations of the setup to be able to exploit the maximum potential and avoid incorrect measurements or misinterpretation of the results.

In general, the unit mol/g is widely used in the context of gas absorption of solid materials mostly without any questioning. Unfortunately, less information about the unit mol/g for oxygen absorption is available and usually it is used without any statement. Therefore, the question arises if it is the best suitable unit for the amount of oxygen absorbed in the case considered here.

The unit mol/g does not take into account any effect of geometry or surface which makes the value less informative if elastomer components are compared which have equal mass but different surface areas. Since the oxygen molecules are taken up by the surface of the sample, surface area has an impact on the adsorption or rather the absorption behaviour. Complex diffusion and reaction processes influence the oxygen absorption and can make oxidation a highly inhomogeneous effect. Therefore, the determination of oxygen absorption by the quotient of amount of substance and mass n/m [mol/g] is only meaningful for investigations on samples of the same geometry and material type. For different shapes of sample, a more sophisticated consideration deems necessary.

When focusing on the adsorption of molecules while neglecting any diffusion of oxygen into the interior of the sample then oxygen uptake is a function of surface area only. That implicates that the dimension n/A [mol/mm^2] would better meet the demands. Further, one should bear in mind that any influence of surface roughness is neglected here.

Since the oxygen uptake is a combination of adsorption and absorption it is not only a function of the surface area but also depends on the surface-to-volume ratio. Imagine a thin film and a sphere both having the same surface area. The oxygen uptake is different because the film becomes saturated much faster than the sphere since the latter has more volume to absorb oxygen molecules. Therefore, an adequate dimension which considers this fact could be n/A/V [mol/mm^2/mm^3]. A weak point of this unit is still the fact that complex geometries can cause local saturation, for example a bulk with lamellae. Moreover, the effects of absorption and diffusion cannot be clearly separated any better as before and a comparison of samples out of different materials and with different geometries is still very complicated.

Another idea would be the unit n/A/m [mol/mm^2/g] additionally considering the density of the material while trying to incorporate the tightness in the reflections. This approach was born when trying to modify the volume-to-mass ratio in order to gather as much information as possible about the properties of the specimens. That means a value which represents the amount of molecules being absorbed per surface area, volume and density. There are almost

no advantages to this approach, and difficulties could occur if materials of different densities are compared. Example: Imagine two samples, same surface area, mass and amount of oxygen molecules absorbed. The value n/A/m wouldn't be the same only due to the different densities.

A problem is that an elastomers quantitative oxygen absorption behaviour is a function of many things, including: material, surface area and volume, volume distribution, surface distribution and mass distribution. The latter is important to consider for spatial diffusion effects of complex geometries consisting of both bulky and lattice parts. It is almost impossible to consider such a complex behaviour by a single measurement value.

In summary, it can be said that only a comparison of samples differing in a single characteristic (size, shape or material) is meaningful. All in all, it can be recommended to use the basic unit mol/g since it is widely accepted and therefore appropriate for comparison with data from literature. But it should be always kept in mind that surface area, geometry and surface-volume-ratio have to be considered when comparing absolute amounts of oxygen uptake. Using the unit mol/g without appreciation of backgrounds and limitations could cause problems.

At standard conditions, the molar gas volume ν_{sc} of an ideal gas is 22.4 l/mol. Here, the chambers are sealed at elevated temperatures after pre-heating. Therefore, no standard conditions exist in the chamber during exposure. After exposure in the oven the chamber is cooled down to room temperature and pressure decreases. Since the chamber is sealed during the whole process standard conditions neither exist right before the measurement procedure starts.

In order to consider the effect of ageing temperature T_{ageing} on the molar gas volume, the following equation can be used. It is assumed that ambient pressure and ageing temperature exist at the moment of sealing. Thus, the question arises which value of molar gas volume has to be used in context of the consideration made here.

$$\nu \left[\frac{\mathrm{l}}{\mathrm{mol}}\right] = \frac{\nu_{sc}\left[\frac{\mathrm{l}}{\mathrm{mol}}\right]}{273.15\,\mathrm{K}} T_{ageing} = \frac{22.4\,\frac{\mathrm{l}}{\mathrm{mol}}}{273.15\,\mathrm{K}} T_{ageing} \tag{11}$$

Examples:

$$\begin{aligned} T_{ageing} &= 170\,^{\circ}\mathrm{C} \qquad v = 36.34\,\tfrac{\mathrm{l}}{\mathrm{mol}} \\ T_{ageing} &= 150\,^{\circ}\mathrm{C} \qquad v = 34.70\,\tfrac{\mathrm{l}}{\mathrm{mol}} \\ T_{ageing} &= 100\,^{\circ}\mathrm{C} \qquad v = 30.60\,\tfrac{\mathrm{l}}{\mathrm{mol}} \end{aligned}$$

Nevertheless, for calculation of the absorbed amount of oxygen 22.4 mol/l is sufficient since the test-air, which is mixed with the consumed chamber air, is assumed to have ambient pressure

and temperature. Effects of different oxygen partial pressure due to ageing temperature are compensated by the reference measurement using the chamber without a sample.

A general point regarding the principle of measurement is the fact that the amount of oxygen molecules which have been absorbed by the sample is measured and no statement about the amount of oxygen molecules which have reacted with elastomer can be made. Hence, the output is an indicator for oxidation but not suitable to determine any reliable statement with respect to the exact level of oxidation. Furthermore, due to the indirect measurement by detecting changes in the oxygen concentration of the ambient air the results do not include any information about oxygen being absorbed and subsequently emitted.

Another point is the unknown oxygen concentration of the air when closing the chamber. Hence, the exact amount of oxygen in the chamber during ageing is undefined. This effect is compensated by using an empty reference chamber which is closed simultaneously with the sample chamber under identical conditions. Nevertheless, effects of different oxygen partial pressures in the ambient air of the sample on the oxygen absorption behaviour are not controlled.

A similar problem occurs when oxygen is absorbed by the elastomer in the sealed chamber and consequently the oxygen concentration reduced. Since the sealed chambers are closed at the very beginning of exposure, enclosed air is not refreshed during the entire ageing duration. The oxygen concentration in the material raises whereas the amount of oxygen molecules in the surrounding air decreases. Consequently, the question arises if the absorption during ageing reduces the oxygen amount in a magnitude that subsequent absorption is affected.

The effect of oxygen partial pressure on the oxygen absorption is described by Henry's law [55][56].

$$C_S = S\, p_{ox} \tag{12}$$

C_s describes the equilibrium oxygen concentration, S the solubility and p the oxygen partial pressure. Solubility can further be written as a function of temperature T.

$$S = S_0 e^{-\frac{E_s}{RT}} \tag{13}$$

Since the oxygen absorption behaviour is influenced by the oxygen partial pressure, the question can be rewritten in order to address how much the oxygen partial pressure is reduced by the absorption process. In other words: how much of the oxygen in the surrounding air is absorbed by the elastomer? This should be analysed on a standard testing executed to get a first impression of the effects.

Therefore, the initial volume of the chamber V_{ch} is determined:

$$V_{ch} = \pi \left(\frac{d}{2}\right)^2 l = \pi \left(\frac{15\,\mathrm{mm}}{2}\right)^2 80\,\mathrm{mm} = 56548\,\mathrm{mm}^3 \tag{14}$$

Volume of a usual cuboid sample:

$$V_{sa} = w\,l\,h = 20 \times 55 \times 2\,\mathrm{mm} = 2200\,\mathrm{mm}^3 \tag{15}$$

Volume of surrounding air:

$$V_{air} = V_{ch} - V_{sa} = 56548\,\mathrm{mm}^3 - 2200\,\mathrm{mm}^3 = 54348\,\mathrm{mm}^3 \tag{16}$$

At standard conditions, the gas volume ν_{sc} is 22.4 l/mol. In order to consider other ageing temperatures T_{air} (here for instance 170 °C) Equation (11) introduced above is used:

$$\nu \left[\frac{\mathrm{l}}{\mathrm{mol}}\right] = \frac{22.4\,\frac{\mathrm{l}}{\mathrm{mol}}}{273.15\,\mathrm{K}}\,T_{air} = \frac{22.4\,\frac{\mathrm{l}}{\mathrm{mol}}}{273.15\,\mathrm{K}}\,443.15\,\mathrm{K} = 36.34\,\frac{\mathrm{l}}{\mathrm{mol}} \tag{17}$$

Amount of air molecules in V_{air}:

$$n_{air} = \frac{V_{air}}{\nu} = \frac{54348\,\mathrm{mm}^3}{36.34\,\frac{\mathrm{l}}{\mathrm{mol}} \times 100^3\,\frac{\mathrm{mm}^3}{\mathrm{l}}} = 1.496 \times 10^{-3}\,\mathrm{mol} \tag{18}$$

For example, the OXZILLA measurement of a broadly used elastomer (EPDM) showed an oxygen absorption of $1.80 \times 10^{-5}\,\frac{\mathrm{mol}}{\mathrm{g}}$ after 16 h ageing at 100 °C. The ratio of oxygen molecules absorbed from the surrounding air can be calculated (sample weight 2.5 g) as follows:

$$n_{air} = \frac{1.80 \times 10^{-5}\,\frac{\mathrm{mol}}{\mathrm{g}} \times 2.5\,\mathrm{g}}{1.496 \times 10^{-3}\,\mathrm{mol} \times 0.21} = 0.143 \mathrel{\widehat{=}} 14.3\,\% \tag{19}$$

Thus, approximately 14 % of the oxygen molecules in the ambient air are absorbed by the polymer during ageing here. It is important to know about this effect especially if it is intended to investigate elastomers with a high absorption affinity. The oxygen absorption rate is decelerated by the decline of the ambient oxygen partial pressure for this kind of testing procedure. This has to be considered especially when comparing investigation of a particular elastomer at different temperatures. In order to get a first impression of this effect's magnitude, the rough calculation introduced above offers a basic assessment. A further step towards the consideration of this effect is a subsequent correction of the measurement results using Henry's law which will not

be shown in detail here. In this work, the effect of changing oxygen partial pressure in the air surrounding the sample is considered but not used in modifying the calculation of the output.

Apart from this, oxygen absorption is measured as function of ageing duration and temperature, which requires a precise control of these parameters. It is a considerable challenge to regulate the temperature especially during heating and cooling phase. Preheating the chamber and no immediate sealing after inserting the specimen ensure a predictable starting point of exposure. The latter ensures a constant temperature of chamber, specimen, mesh grid and air at the starting point of ageing. Besides, an undefined duration of exposure exists during the cooling phase which is executed by removing the chamber from the furnace and letting it cool down at room temperature. Depending on the previous ageing temperature in the furnace the duration and therefore the heat input on the sample during the cooling of the chamber differs until ambient temperature is reached. This is less important for long-term tests but has to be considered for short ageing cycles when ageing time is for instance 16 hours. Therefore, the cooling from ageing temperature to ambient temperature can take several hours, effectively extending the net heat input.

A logistical disadvantage of the procedure is the limited test capacity since one chamber is used for a single specimen for the whole time of exposure. This makes long-term testing a laborious process and necessitates a large number of chambers. Hence, carrying out large test series is very time consuming or increases the costs of the setup due to the needed number of chambers including expensive stainless-steel valves and quick couplings.

At last, in the case of a leakage, especially during the cooling phase, the pressure in the chamber increases up to ambient pressure and air is flowing in and out which causes a complete loss of experimental results. This is very unfavourable particularly at the end of long-term test. Nevertheless, this case of failure is apparent and testing results can be rejected and measurements repeated. Hence, the low-pressure occurring during the cooling phase is a good indicator for the quality of sealing and ensures that no leakage air disturbed the ageing process as well as the measurement.

5.1.6 Test results

The developed setup was used to run several experimental series using different types of elastomers. The general aim was the investigation of the oxygen absorption behaviour with regard to ageing temperature and duration. A descriptive way to illustrate the data of such tests is plotting the absolute amount of oxygen molecules absorbed relative to the weight of the sample in mole per gram, as a function of ageing duration. Each measured value is obtained by a sample exposed in an individual chamber as described above. Hence, high measuring effort is necessary for a single graph showing the absorption characteristic of a material especially if several repetitions due to statistical factors are required.

During the commissioning of the setup, experiments were executed using simple shaped samples with a large surface area to achieve clear results. Mostly, elastomer specimen of the cuboid dimension 25x55x2 mm^3 were used which were cut out of a 2 mm sheet as well as type 1A tension rods (also known as S2 tension rod). The first results obtained were published in [103] which confirmed the basic functionality and gave a first impression of the magnitude of elastomers oxygen absorption (Figure 26).

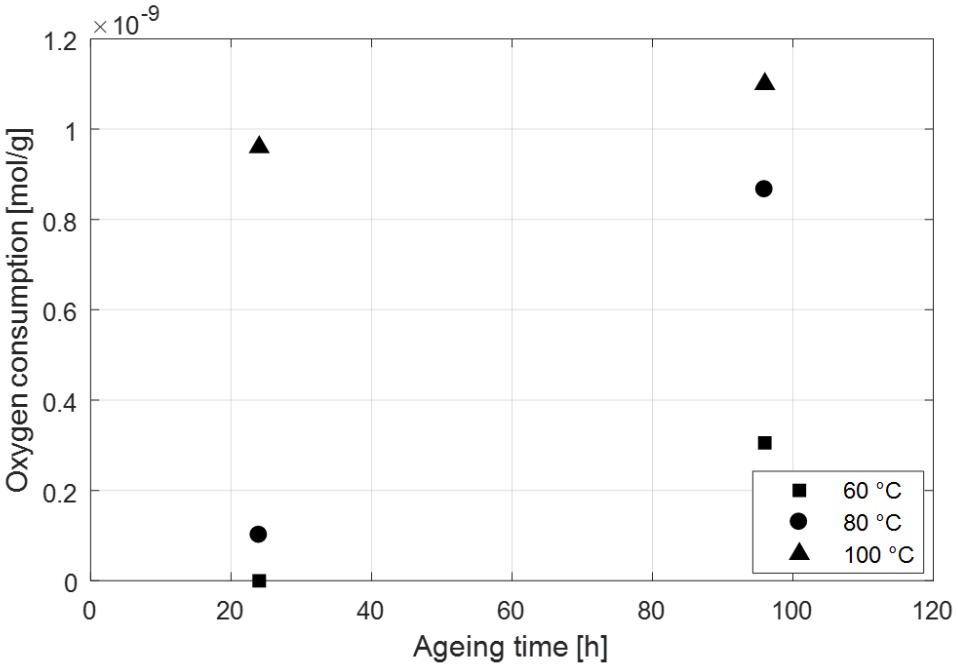

Figure 26: Initial oxygen absorption measurements on the experimental setup of an elastomer material without antioxidants as function of ageing temperature and duration [103]

A standard elastomer (Natural Rubber) was taken which is widely used in the automotive industry with the modification of containing no antioxidants. Three tension rod samples were placed simultaneously in one chamber to increase surface area and thus to increase the measured amount of oxygen absorbed. The scale of the results coincides with values from literature [16]. Moreover, general conclusions about the absorption behaviour can be drawn. The elastomer absorbs more oxygen with increasing time of ageing and higher temperatures. A closer interpretation and discussion of the first experimental results should not be done here since several sources of error were eliminated during the further improvement of the setup and accuracy of the first measurements has to be questioned. With experience obtained over time, sealing of the chambers was improved and measurement procedure was optimised.

After commissioning, the first adjustments and improvements further measurement series were planned and executed. The first one presented here was used to test a so-called Standard Vietnam Rubber (SVR), which is based on a natural rubber as a raw material (NR SVR CV69). The results were the basis for the publications [84][90][92]. Glass transition temperature of this sulphur cross-linked material is -58 °C. The material is widely used in technical applications

especially in vehicle engineering. Therefore, usually antioxidants are added to decelerate the ageing process and increase service life. Here, both SVR with and without the addition of antioxidants were investigated to obtain a comprehensive monitoring of the oxidation behaviour. The elastomer contains 50 phr (parts per hundred rubber) carbon black to improve mechanical properties and resistance. Further, additional sulphur is used as a post-cross-linking agent to reinforce the polymers network during lifetime and counteract degradation. In addition, the material used contains zinc oxide (ZnO) and stearic acid as vulcanisation activators as well as n-cyclohexyl-2-benzothiazole sulfenamide (CBS) and tetrabenzyl thiuram disulfide (TBzTD) for acceleration of the cross-linking process.

Specimen of the dimensions 25x55x2 mm^3 were aged in the sealed chambers described before at temperatures of 70 °C, 120 °C and 150 °C for periods up to 72 hours. The amount of oxygen was measured, and the results received are plotted over ageing time in Figure 27.

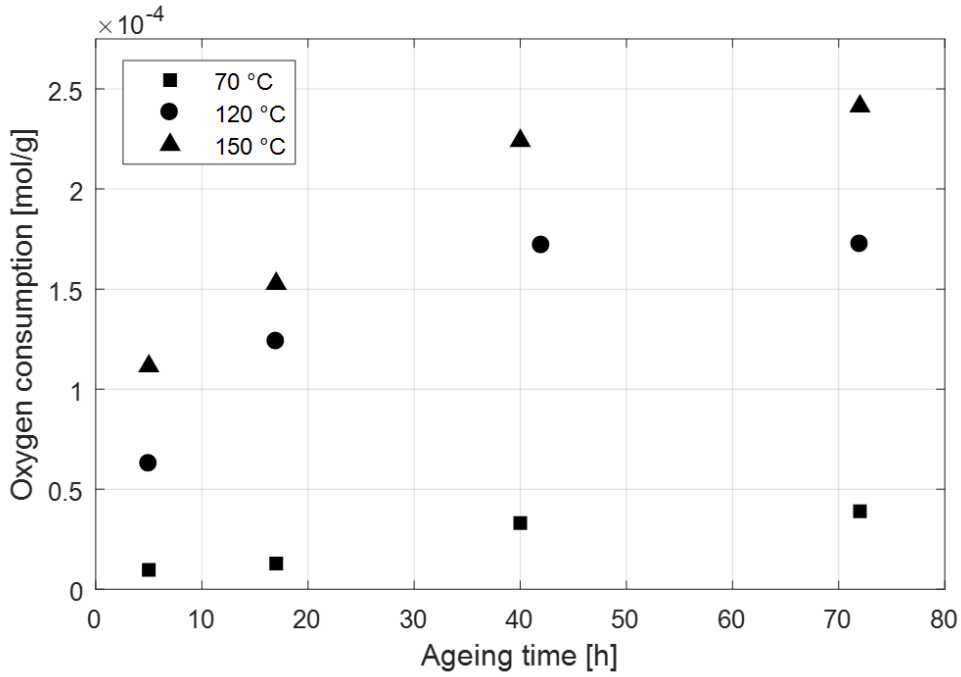

Figure 27: Oxygen absorption of Standard Vietnam Rubber without antioxidants as function of ageing temperature and duration

The results obviously show that the oxygen absorption is thermal activated. The higher the temperature the higher the amount of oxygen absorbed. During the time of exposure oxygen is taken up steadily that is clearly pronounced for high temperatures 120 °C and 150 °C whereas minimal oxygen absorption is observed for 60 °C. This behaviour is also confirmed by other elastomers when fluorelastomer O-rings were tested and only neglectable oxygen absorption was observed below approximately 60 °C [14]. Most of the oxygen is absorbed in the first period of exposure and oxygen absorption decelerates with ongoing ageing duration. A levelling appeared at the end of the investigation period which indicates a kind of saturation. This phenomena is not generally confirmed by previous works on other types of elastomer like polyurethane foam

or fluorelastomer which revealed a steady oxygen absorption at least in the considered period [14][15].

Besides the depiction in mole per gram the illustration of the oxygen absorption rate using mole per gram and second is used which shows the oxygen absorption at a certain time step during ageing and represents the velocity of the process. The oxygen absorption rate is shown in Figure 28. The results highlight the non-steady state nature of the oxygen absorption process which is highly dependent on temperature and duration of exposure. Furthermore, oxygen absorption is observed to be concentrated to the first hours of exposure. The decline in oxygen absorption rate is more pronounced with higher temperatures and the uptake process seems to be inhibited more and more. This can be explained by an increasing oxygen concentration in the surface area and the setting in of DLO effects.

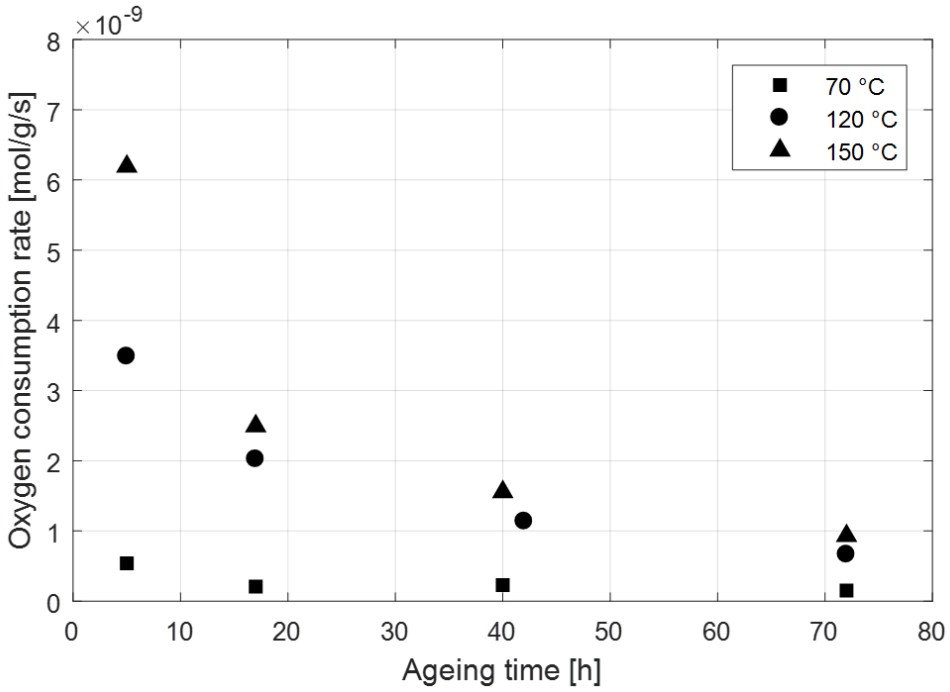

Figure 28: Oxygen absorption rate of Standard Vietnam Rubber without antioxidants as function of ageing temperature and duration

Antioxidants influence the oxygen absorption behaviour since they can for instance hinder the initial uptake or bind oxygen molecules and hence suppress further diffusion. Thus, the DLO effect can be partly or totally inhibited. In order to investigate the effects of antioxidants on the oxygen absorption behaviour the Standard Vietnam Rubber used above was tested a second time including antioxidants. Therefore, the same material was used but different to the previous testing antioxidants were not excluded during manufacturing. In detail three different antioxidants are added N-Isopropyl-N'-phenyl-p-phenylendiamin (IPPD), 2,2,4-Trimethyl-1,2-Dihydroquinoline polymer (TMQ) and a blend of paraffins as well as micro-waxes (Antilux). IPPD is used to protect natural and synthetic elastomers against an oxidative and ozone influence and as an antiflex for the protection against catalytic degradation caused by heavy metals.

TMQ is an antioxidant for nearly all elastomer types in a variety of applications in a wide range of temperatures. Its persistence provides a long-term heat aging resistance to elastomers. Antilux is an additive which protects rubber against influences due to ozone and weathering in general. It migrates to the surface of the elastomer and forms a protective wax layer which remains stable up to temperatures of approximately 50 °C. The antioxidants included are common for this material in technical applications. In conclusion, this mixture is used to protect the elastomer mainly against its three most prominent adversaries, oxidation/ozonation, thermal degradation and weathering/radiation. Figure 29 includes both investigations with and without added antioxidants for better comparison.

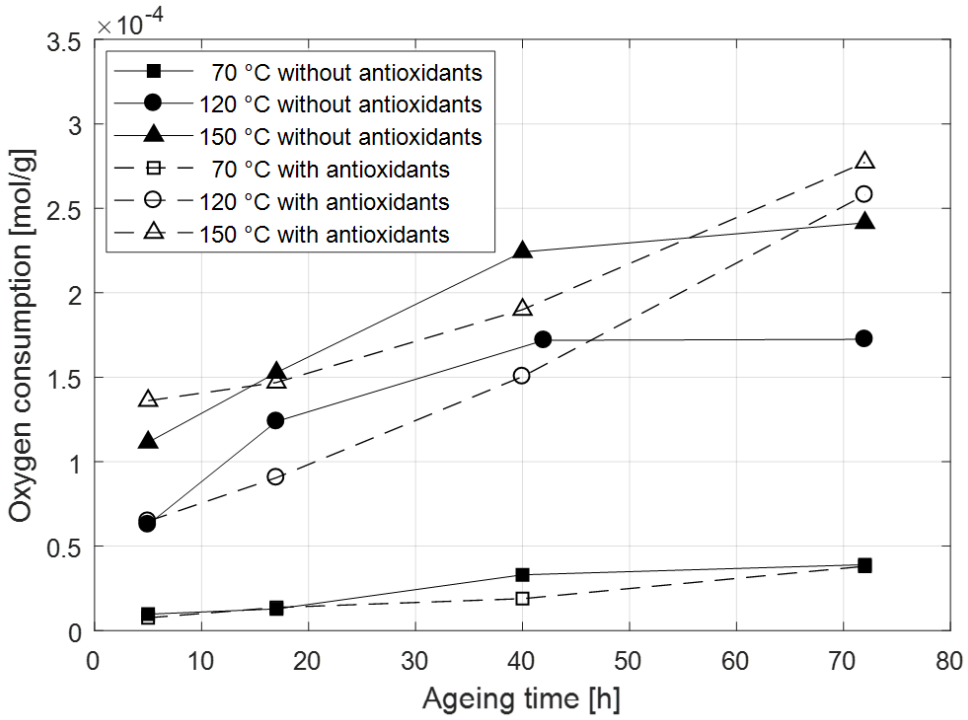

Figure 29: Comparison of the oxygen absorption of Natural Rubber (Standard Vietnam Rubber) with and without antioxidants

In general, it can be noted that the ageing temperature accelerates the oxygen absorption. For ageing at 70 °C the oxygen absorption with and without antioxidants does not practically differ and shows only a slight increase of the amount of oxygen being absorbed over ageing duration. At temperatures of 120 °C and 150 °C the magnitude of oxygen absorbed for both types of material has roughly the same order, but the shape of the graphs differs. Without antioxidants, the oxygen absorption rate decreases as depicted above (see also Figure 28). Adding antioxidants shows no decline of the oxygen absorption but it does gradually increase during ageing, at least for the period of investigation. In the beginning, oxygen absorption is similar and a significant amount of oxygen is absorbed during the first five hours of exposure. Antioxidants do not seem to have large influence in this phase. Afterwards antioxidants inhibits the oxygen absorption, but with ongoing ageing duration this effect declines and finally the amount of oxygen absorbed exceeds the values of the material without antioxidants. This behaviour gives an idea why no general

statement about elastomers oxygen absorption behaviour is possible and different shapes of oxygen absorption graphs can be observed in literature [14][15][28][89][110]. In order to explain the observations a detailed understanding of the interaction between solubility, diffusion and oxidative reaction under the presence of antioxidants as well as the thermal activation of these processes is required.

In order to achieve a better understanding about the oxygen absorption of elastomers results of further elastomer types are presented here. The materials are selected to get an idea about its specific oxidation behaviour. Further, the results help to figure out similarities and differences in the oxygen absorption behaviour and identify systematics or mechanisms. Ethylene Propylene Diene Monomer Rubber (EPDM) is known to be excellent resistant to weathering, thermal ageing and chemical exposure combined with acceptable tensile behaviour. This distinguishes it from Natural Rubber which is susceptible to degradation.

EPDM was tested in the course of a commissioning by Freudenberg Technology Innovation SE & Co. KG, Corporate R&D. In Figure 30 the oxygen absorption of EPDM was normalised to the highest value measured. However, the scale of absolute oxygen absorption is similar to that of Natural Rubber shown above. When comparing the outcome with the results of Natural Rubber already presented one has to pay attention to the longer ageing times and higher ageing temperatures. The graphs in Figure 30 show a similar characteristic as for Natural Rubber without antioxidants (Figure 29). A closer comparison of the measurements at 100 °C and 120 °C as well as at 150 °C points out a similar qualitative behaviour of Natural Rubber and EPDM but it takes approximately ten times longer for the latter. It seems that the better durability of EPDM can qualitatively been equated with a more susceptible elastomer like Natural Rubber without antioxidants. Deceleration occurs after a very fast phase of absorption at the beginning of the exposure. Ageing at 170 °C underlines the observation that oxygen absorption is highly temperature dependent.

At the beginning of the ageing process of EPDM oxygen absorption increases with temperature from 100 °C via 150 °C to 170 °C (Figure 30). As the ageing time progresses oxygen absorption rate decreases. Whether the oxygen uptake levels and which stationary value is approached is not apparent from the series of measurements due to limited number of measurement points because of the costly exposure time.

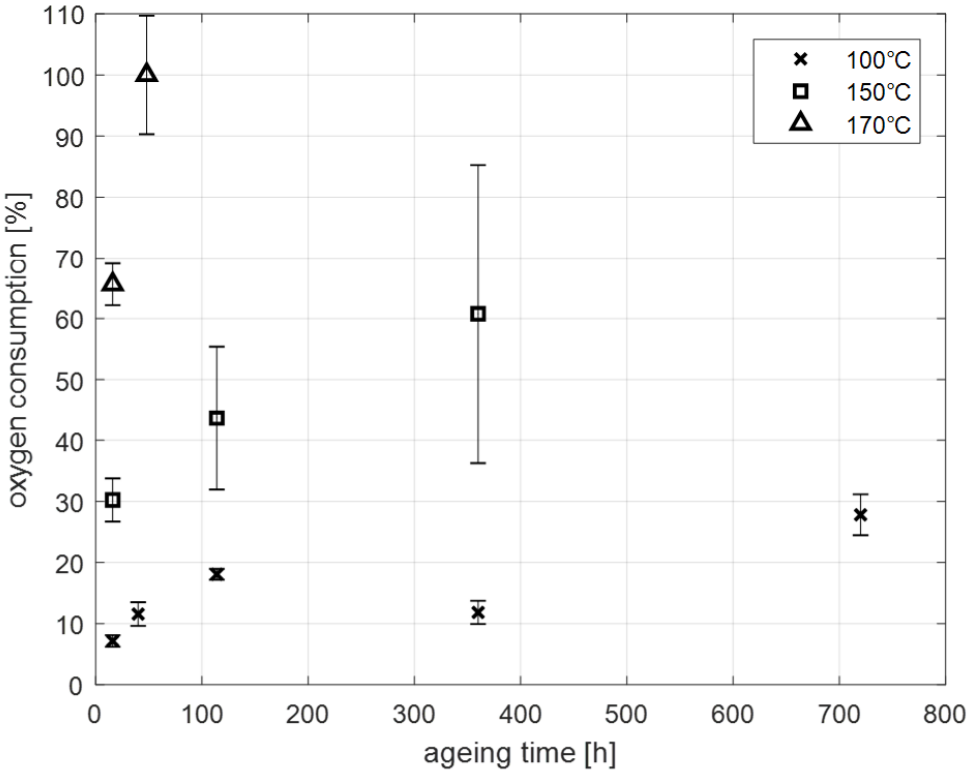

Figure 30: Oxygen absorption of Ethylene Propylene Diene Monomer Rubber (EPDM) as a function of ageing temperature and duration; measurement scatter included by standard deviation

As a third example for oxygen absorption of elastomers investigations of Nitrile Rubber (NBR) were executed and presented here. An unfilled and unstabilised peroxide-cured nitrile rubber containing one third acrylonitrile was aged at 100 °C and 120 °C up to 21 days. A 1 phr polymerised 1,2-dihydro-2,2,4-trimethylquinoline (TMQ) was mixed as antioxidant to the compound of NBR and dicumyl peroxide. The oxygen absorption as a function of ageing time and temperature is shown in Figure 31. The outcome is different to the previous investigation and was quite unexpected. The rule of elevated temperatures always resulting in more oxygen uptake is not applicable here. At first the exposure and testing at 100 °C was executed. The results show a high absorption rate at the beginning which decelerates with ongoing ageing as expected for an elastomer containing antioxidants. For a slightly elevated temperature of 120 °C a faster and higher uptake had been expected as already observed when investigating other elastomers. The outcome presented in Figure 31 diverges significantly from expectations. Significantly less oxygen was absorbed during ageing at 120 °C than at 100 °C. In the very first period up to 24 hours of exposure the oxygen absorption at both temperatures are similar. Afterwards the oxygen uptake at 120 °C does not progress and remains almost on the same level. Due to the surprising findings, test results have been checked accurately. Nevertheless, there is a systematic error since oxygen absorption shall not decline while standard deviation is very low which can be traced back to undefined boundary conditions during closing of the ageing chambers or other effects during experimental procedure. Of course, the alternating values could also be explained

by oxygen being emitted after previous absorbing, which is considered to be very unlikely. Several subsequent checks and low scattering of the measurement values confirm the correctness of the outcome.

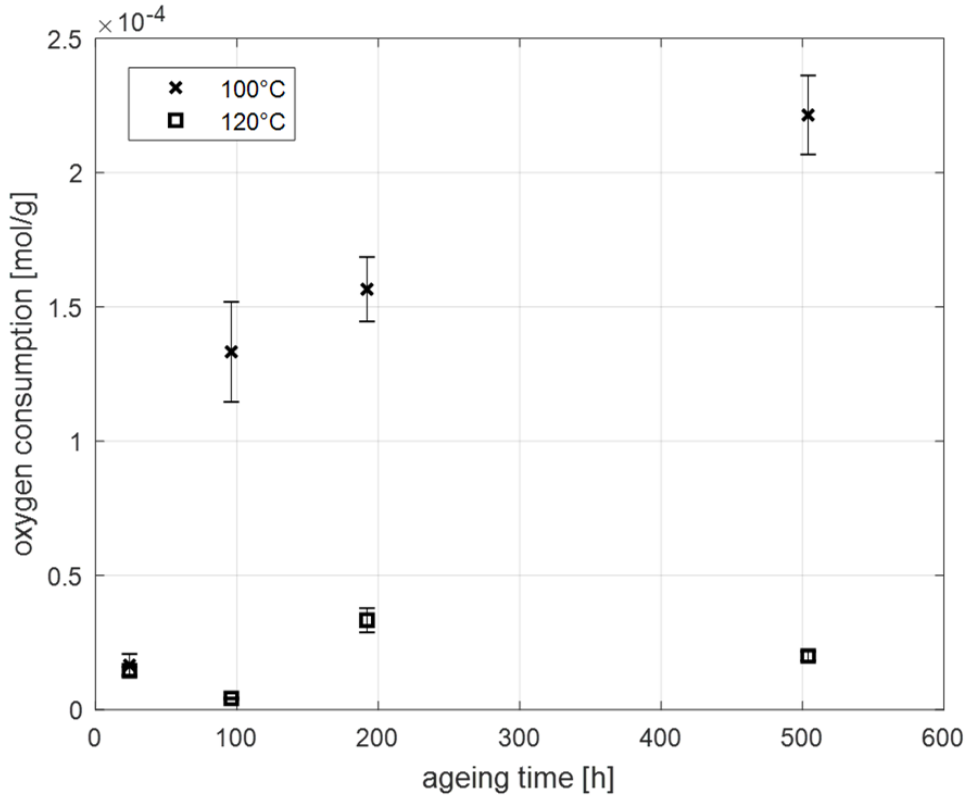

Figure 31: Oxygen absorption of unstabilised peroxide-cured nitrile rubber containing one third acrylonitrile as a function of ageing temperature and duration

5.1.7 Discussion

The outcome of testing on Natural Rubber (Standard Vietnam Rubber) with and without antioxidants seems to be paradoxical at first glance (Figure 29) since antioxidants are expected to protect the elastomer against the effect of oxidation and reduce oxygen uptake. The former is correct, the latter is not generally true. As mentioned before, oxygen uptake does not mean that the oxygen has reacted with the elastomer's molecular structure, but that oxygen is absorbed by the bulk material. Considering Figure 28 depicts that there must be at least one process which reduces the oxygen absorption rate without the presence of antioxidants. Deceleration takes place during ageing which means that the oxidation process itself has to be involved.

On the one side permeability is reduced by oxidative reactions and on the other side an unhindered reactivity causes a concentration of the oxidation process to the elastomers surface layer. That means solubility and diffusivity can be reduced which limit oxygen molecules to surface region. Furthermore, the elevated concentration in the outer region shows a high oxygen concentration compared to the rest of the elastomer and hence the concentration gradient between

ambient area and bulk elastomer is reduced. This is a classic phenomenon of DLO causing the decline observed in Figure 29. The effect of protection waxes like Antilux is neglectable at temperatures of 120 °C and 150 °C. The presence of antioxidants reduces the effect of DLO since oxidative reactions are avoided. Hence, oxygen is restrained to react with the elastomer and diffusion is enabled to the interior. Of course, waxes have influence on the oxygen absorption but above 50 °C the effectiveness is strongly reduced. The increase in oxygen absorption rate between five and 70 hours ageing time probably is caused by antioxidants trying to hinder the absorption process, but the effect is rapidly reduced due to temperature. The high oxygen absorption within the first five hours is almost not affected by the presence of antioxidants. That can be explained by an initial uptake process at the surface before any antioxidant is able to bind oxygen molecules and reduce concentration gradient between ambient atmosphere and surface layer.

EPDM shows a similar oxygen absorption behaviour as Natural Rubber but with longer ageing times which can be explained by a general higher resistance of the elastomer against oxidation. The shape of the curve in Figure 30 can be equated with that of Natural Rubber without antioxidants (Figure 27). A possible explanation is that higher resistance of EPDM causes delayed oxidation hence changes in material behaviour take longer. Nevertheless, oxygen is absorbed, and oxidative effects occur which affect the oxygen absorption behaviour. Furthermore, raising oxygen concentration in the material and at the surface reduces the concentration gradient, as well as the affinity of absorption. This explanation leaves some questions, which cannot be answered at this point of research. For example, there are no findings about the distribution of oxygen in EPDM and natural rubber. Hence, higher oxygen absorption does not mean a higher concentration in the entire sample. Further, oxygen absorption does not allow a statement about the degree of oxidation and hence predicting other properties like mechanical ones based on the findings presented should be treated with caution.

At first sight the oxygen absorption behaviour of unstabilised peroxide-cured nitrile rubber seems to be based on a different mechanism than the materials investigated before. Especially the outcome of ageing at 120 °C follows not the expectation raised by the results of the previous investigations. The question arises regarding what causes such a complex behaviour and which temperature dependent effects have such a dominant influence on the oxygen absorption. Obviously, the mechanism is activated by passing a certain activation temperature somewhere between 100 °C and 120 °C. Reaching this activation energy results in an abrupt decline of oxygen absorption based on a changed solubility and/or diffusion behaviour. Perhaps the effect can also be influenced by moisture that is adsorbed in the polymer. The antioxidant can be excluded as a direct reason of the effect since its field of action already begins at room temperature and furthermore TMQ act as an alkyl radical scavenger stopping the oxidative reactions. Indirectly, it could be possible that at a certain temperature the antioxidant completely loses its effect and oxidation can run unhindered. Then, an increased reactivity due to the elevated temperature can occur. Combining both effects can result in a strong rise of oxidative reactions. Consequently, oxygen absorption is decreased after a short time of ageing which can explain the oxygen absorption presented in Figure 31.

The experimental data and explanations presented in this subchapter give an insight in the oxygen absorption behaviour of elastomers. The results show that different types of elastomers exhibit significantly different oxygen uptake characteristics. In summary, it is shown that general rules are difficult to state due to the complexity of the oxidation mechanism (see also section 4). Distinct behaviour can be observed regarding the oxygen absorption of different elastomer types. Solubility and diffusivity vary between raw material like e.g. Natural Rubber, EPDM or NBR [62][88]. Moreover, additives are used for different reasons. Fillers like carbon black are used to adjust mechanical properties. Different antioxidants are added to avoid degradation. All these points result in a complex thermal influenced oxygen absorption behaviour. Even going further, the ambient partial oxygen pressure, the influence of dynamical mechanical loads and the shape of the elastomer component (surface-volume-ratio) provoke a highly nonlinear behaviour. All this underline the challenging field of predicting the ageing behaviour of elastomers.

All in all, it is possible to explain the outcomes by means of the oxidative chain of causation introduced in (section 4). Depending on the type of rubber and the dominating ageing processes oxygen absorption behaviour can be quite different in occurrence. Nevertheless, it is possible to explain the results by the mechanisms shown before, for example the dualism of DLO (subsection 4.1). In parallel, this makes clear how important it is to consider inhomogeneous effects when dealing with the oxidative ageing of elastomers.

5.2 Heterogeneous oxidation

Besides the total amount of oxygen absorbed, information about the spatial oxidation level is essential for interpreting the ageing mechanism in more detail. At this point it should be mentioned that experimental investigations on the ageing behaviour of elastomers can be subdivided into two categories: results of ageing and reasons for ageing. The former aims on the consequences of ageing, for example changing mechanical properties. The latter focuses on the triggers or prerequisites of the ageing process, like the amount of oxygen molecules absorbed [48]. The linkage of both types of results is important and challenging at the same time since same consequences can be caused by different types of ageing. For instance, changes in tensile properties can be affected by thermal and oxidative ageing in parallel.

Several approaches exist to examine spatial differences in the level of oxidation. Probably the most common is modulus profiling which is used for measuring the change in modulus across a sample. This method measures the local differences of a mechanical property of the elastomer which can be affected by ageing. Thus, modulus profiling is a classical representation of a result measuring method. A test body indents the sample while load and displacement are recorded. Therefore, an aged specimen is cut in cross-section and modulus is measured along the profile. An example for modulus profiling on unfilled nitrile rubber obtained by Celina et al. [89] is shown in Figure 32.

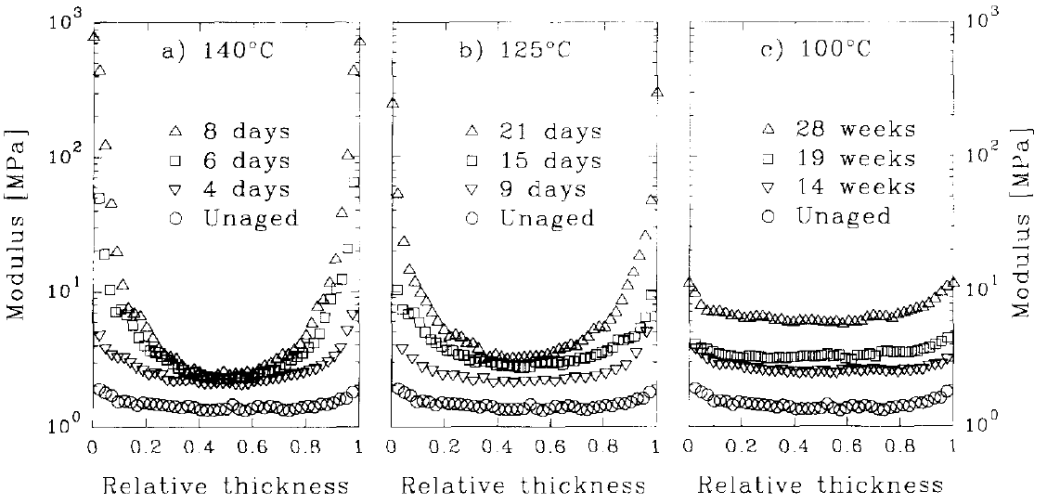

Figure 32: Modulus profiles of unfilled nitrile rubber aged at 140, 125 and 100 °C up to 28 days [89]

Other methods to investigate heterogeneous effects are: density profiling [91], chemiluminescence [55][111][112] or pinpoint dynamical mechanical analysis [21]. Heterogeneity in density can also be measured by using computer tomography as will be shown subsequently since this technique reaches high enough resolution nowadays [92].

In general, almost every method which is available for detecting bulk material properties can be used for investigations of heterogeneous effects since the elastomer sample can be cut in thin slices which are individually tested afterwards. Unfortunately, cutting rubber represents a challenge especially if the material must not be influenced by the cutting process itself. Producing slices with only few millimetres of thickness is possible with conventional methods and manageable effort. Even thinner slices can be obtained by, for instance, embedding the material, cooling by means of liquified nitrogen and cutting by using a microtome. But even with such an advanced method any impact on the subsequent testing results is difficult to predict.

Since destructive testing entails certain disadvantages like thermal impact or loss of subsequent testing, only non-destructive investigations with respect to heterogeneous oxidation are considered in the following. Therefore, two examples of spatial approaches are introduced which allow investigations on inhomogeneous changes in the material due to thermo-oxidative ageing.

5.2.1 Computer Tomography

5.2.1.1 Test method

Besides density determination on bulk materials based on density gradients or Archimedes approach, progressive improvements in computer tomography (CT) technology opened a new field of density measurement [50]. Up to now, CT is mostly known as an imaging method from med-

ical examinations to obtain 3D-pictures representing differences in density of different materials stacked together. CT played a tangential role in polymer science because of the weak X-ray absorbance and the resulting poor contrast of this material [113]. Due to continuous improvements of accuracy and resolution in the past decade detection of minor changes in density was enabled and thus a new scope for application arose. Initial investigations of materials consisting of different raw materials composed like fibre-reinforced polymers [114] or containing pores like foamed elastomers [115] were performed as well as investigations on fatigue cracks and structural damage [116][117]. In these applications non-destructive testing methods were used to detect defects and voids as well as to measure fibre orientation and porosity. Further improvements allowed the detection of small continuously distributed changes like dispersion analysis of filler materials or the distribution of chemical admixtures in elastomers [118].

X-ray radiation is absorbed differently by materials of unequal density, or rather as a function of the atomic number of the material tested. For the case of regions with lower density like amorphous ones less X-ray radiation is absorbed than by crystalline regions. Shrinkage due to post-crosslinking can cause regions with elevated density. Consequently, changes in material density are used to monitor the level of ageing as shown by Gillen et al. [50] on cable jackets and insulation material of nuclear power plants. This is possible due to ageing causing a density increase in most cable materials. Micro X-ray CT specialised on material analysation has reached a sensitivity and a resolution high enough (approximately 7–8 μm spatial resolution) to use the method for such investigations on aged materials. The method is based on detecting density changes provoked by cross-linking and chain scission reactions which are used as a measure for oxidation and hence enable the non-destructive investigation of heterogeneous ageing [48][50][92][119]. Besides alterations in the cross-linking which causes shrinkage, oxidative reactions replace light hydrogen atoms (atomic weight of 1) along the carbon chain with heavier oxygen atoms (atomic weight of 16) [50]. Furthermore, density is also affected by elimination and diffusion of solvents or additives, for instance antioxidants which are consumed during oxidation. For example, degradation of binder was found to cause an increase in polymer density of more than 2 % over material lifetime [29]. Additionally, elastomers density of other types of polymers can be affected by post-crystallisation resulting in a denser packing [11].

5.2.1.2 Test results

Aged Standard Vietnam Rubber containing antioxidants was tested by means of a micro X-ray analyser, Bruker Skyscan 1173 X-ray micro tomography. In addition to carbon black as filler material, sulphur is used as a post-cross-linking agent to elicit degradation effects during lifetime. Results and details have been published in [90]. The samples are the same as used for the analysis by respirometer before and allow a quick analysis since the samples are already aged (compare subsubsection 5.1.6, Figure 29). Micro X-ray tomography was performed to analyse density changes in the cross-section of the bar shaped samples. The results of this natural rubber aged at 60 and 80 °C for different durations are illustrated in Figure 33. The graphic shows an increased density at the surface regions of the samples for ageing times above five

months whereat the interior is almost not affected by exposure. Local areas of high density at low ageing times are artefacts due to the exposure in circulating air furnaces where the samples are flown against by the ventilated air. Hot air circulation seems to promote acceleration effects of superficial density changes which are limited to the exposed side of the sample. Besides this non-intentional effect, the density map of the cross-section at 60 °C shows a homogeneous appearance which is not influenced by the continuous exposure. Raising the temperature to 80 °C provokes more pronounced circulation artefacts and for ageing times greater than five months the superficial area of higher density encloses the whole sample. Heterogeneity is well expressed for ageing at ten months at a temperature of 80 °C. The results depict the influence of elevated temperature and the presence of air containing environment on the mass density of the material. The unintended artefacts show that the presence of air has impact on the sample. Density is increased by the thermo-oxidative ageing at the outer region of the sample and continues to the interior. For the aged specimen here, the interior of the most exposed sample (10 months, 80 °C) is almost on the same level of density as the least aged one (1 month, 60 °C).

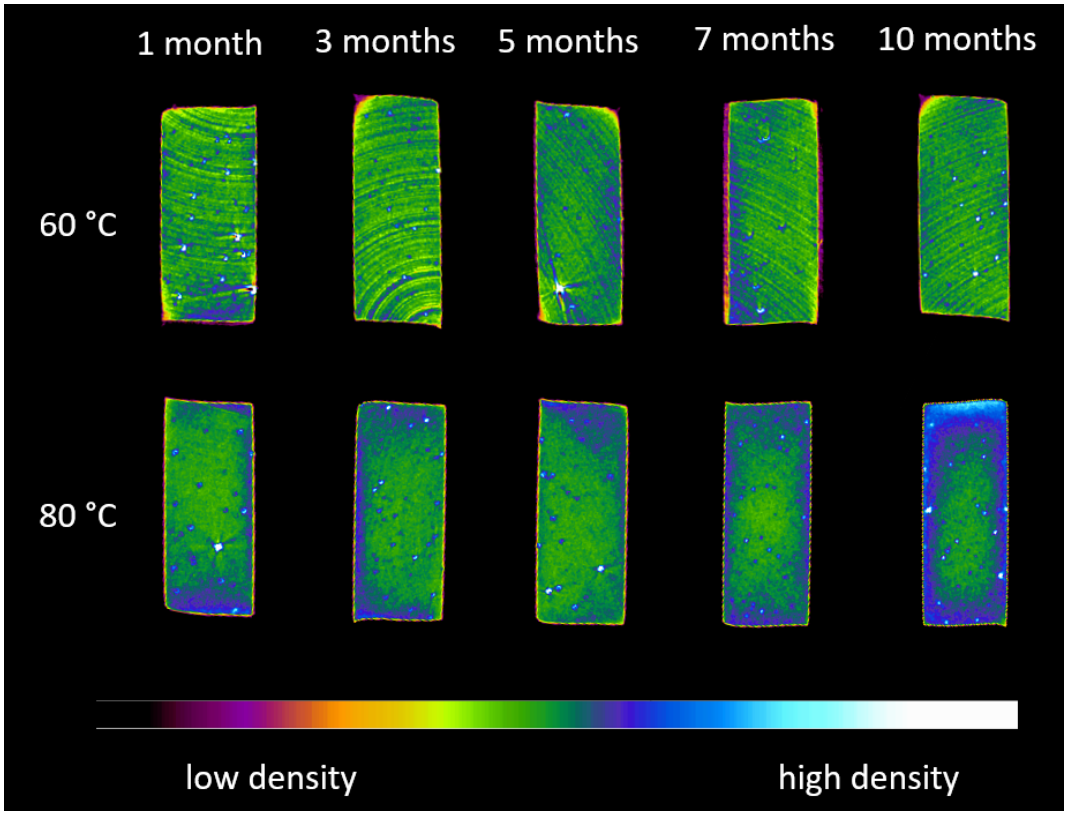

Figure 33: Micro-computed tomography investigation on Standard Vietnam Rubber containing antioxidants aged at 60 and 80 °C up to 10 months

The graphical representation of the spatial density Micro-CT allows a quantitative determination of the density and hence enables the creation of density profiles over the cross-section of the sample. Therefore, the density is represented by an index which results from the absorption behaviour of the X-ray beam and which is proportional to the mass density of the material. In order to get the absolute values of mass density a reference object has to be used for calibration which is not done here. Hence, the absolute values of the density index have no significance and

can only be compared within measurements under same conditions, which mean that several samples are put in the micro CT together and X-ray investigation was done simultaneous or rather measurements are done under equal conditions and settings. This was done for all measurements shown in one diagram here. Therefore, the density index was chosen as zero for the interior of the sample and deviations at the outer regions are indicated relative to it. Aim was to get a first measure of the relative density changes due to different levels of ageing and between the inner and outer zone of the sample. It is sufficient to get a first impression of the density gradient and to evaluate the kind of investigation in this field of research. Figure 34 shows the density profiles of the samples aged at 60 °C, Figure 35 at 80 °C along the thinner width of the cross-section shown in Figure 33. At first, density profiles at 60 °C occur more homogeneous than at 80 °C. Although the density indices of the samples show an unstable behaviour, density increases at the edges can be observed. Comparing the density indices of ageing at 60 °C and 80 °C reveals more heterogeneous density profiles for the higher temperature and longer ageing durations whereas the interior of the samples remain at the initial level.

Besides the density profiles the graphs also show the effect of shrinkage when comparing the percentage of distance of the very last measurement points (90 to 100 %). Density is determined at equidistant points over the distance from one air-exposed surface to the opposite side with the thickest sample being scaled to 100 %. The samples exhibit a reduced thickness caused by ageing which corresponds to the explanations of density increases due to exposure given above.

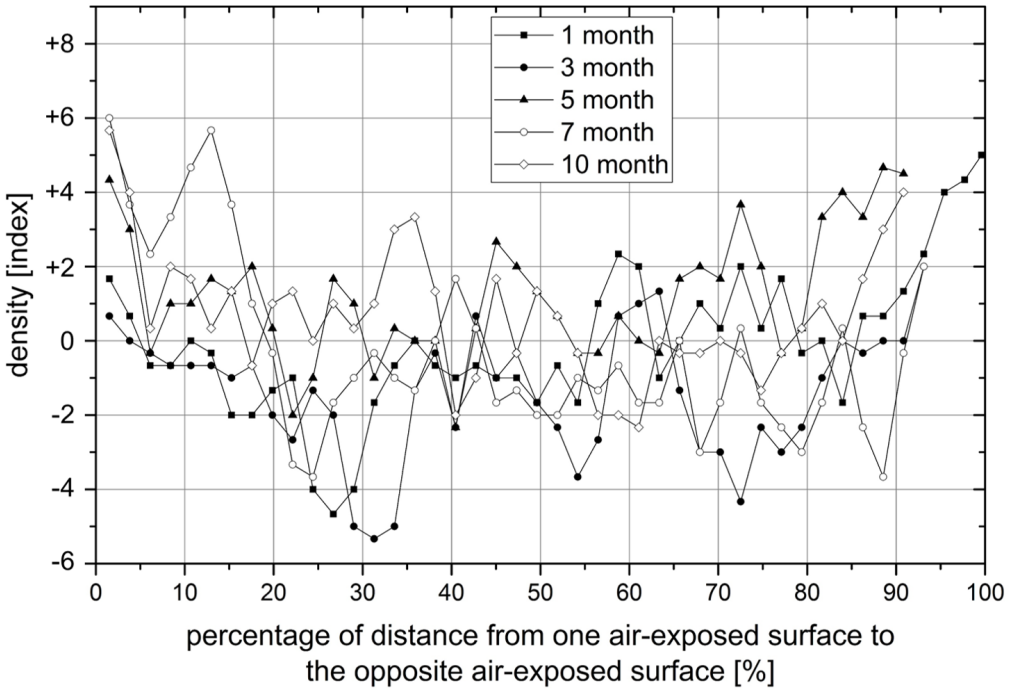

Figure 34: Cross-section density profiles of Standard Vietnam Rubber containing antioxidants aged at 60 °C up to 10 months

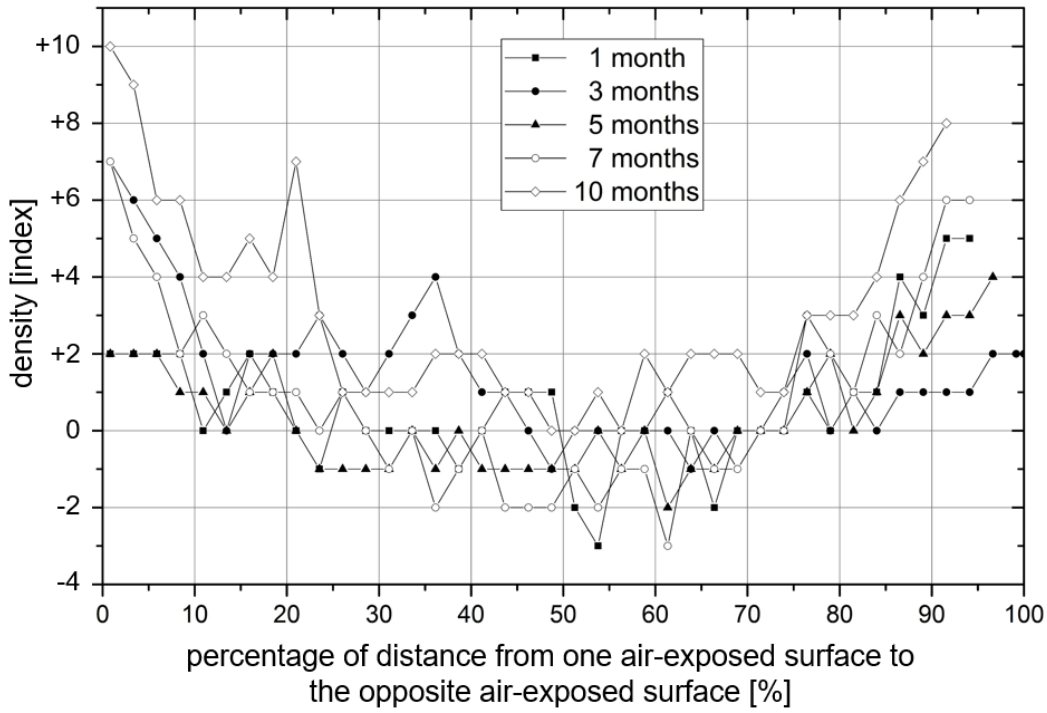

Figure 35: Cross-section density profiles of Standard Vietnam Rubber containing antioxidants aged at 80 °C up to 10 months [90]

Figure 34 and Figure 35 depict that generally longer exposure causes an increase in density. Particularly, the values at the outer regions having a 0 to 10 % distance from air exposed surface show elevated density. The most aged sample, 10 months ageing at 80 °C, clearly highlights the heterogeneous density increase in the superficial layer. In the core of the sample density is largely unaffected and on a similar level than for shorter exposure times. The graphs of Figure 34 and Figure 35 confirm the observations made in Figure 33.

In order to emphasise the effect of temperature CT-scans of samples aged at different temperatures for nine months were done. Temperature was chosen from room temperature up to 100 °C and visualisation of the results is given in Figure 36. Exposure at ambient temperature and 60 °C show no visible difference in density and lead to a homogeneous appearance. At 80 °C density increases in the surface layer and leaves the core unaffected like shown before. Exposure of the material to a more elevated temperature of 100 °C causes a contrary behaviour. Density mapping exhibits a clear inhomogeneous appearance and the interior is still almost not affected. The density in the outer region did not increase as expected but decreased instead to a level even lower than the interior of the sample and the lowest ageing condition shown. Hence, the variation in temperature provoked a completely different behaviour of the elastomer.

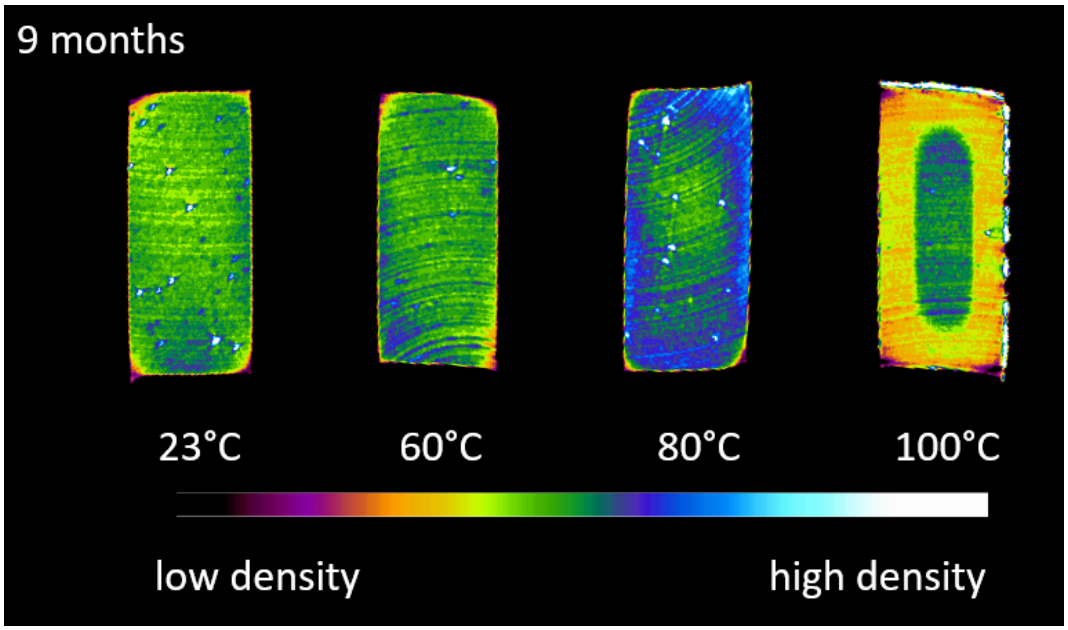

Figure 36: Micro-computed tomography investigation on Standard Vietnam Rubber containing antioxidants aged at temperatures up to 100 °C for 9 months

The quantitative profile plots of the density are shown in Figure 37. The results verified that the interior of the sample remains on the same level between approximately 30 to 70 % for all temperatures. For elevated temperatures densities increase especially at the edge of the samples. Results of the measurements after ageing up to 80 °C show the expected behaviour of higher temperatures resulting in a higher density but for samples aged at 100 °C the density decreases apart from the interior zone and confirm the findings of density mapping in Figure 36. The outcome for 100 °C looks as expected for the interior being on a similar level than the other measurements and an absolute value of the density index of 4 to 5 at the edges. However, the profile of the latter occurs upside down which means the density decreases unexpectedly. Since all data shown in Figure 36 or rather Figure 37 were collected by a single measurement an error can be excluded. All samples were put in the CT chamber simultaneously to obtain comparably density indexes.

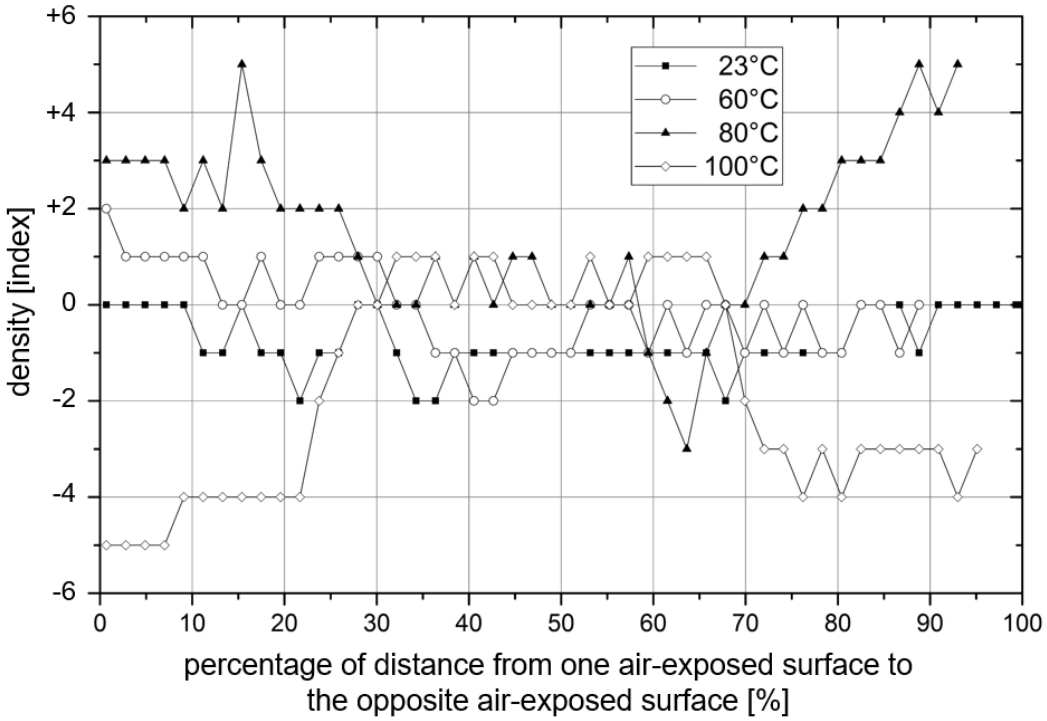

Figure 37: Cross-section density profiles of Standard Vietnam Rubber containing antioxidants aged for nine months at different temperatures [90]

5.2.2 FT-IR Spectroscopy

5.2.2.1 Test method

A direct method to investigate consequences of ageing requires a closer look on the spatial chemical changes of elastomers. This is enabled by Fourier Transformed Infrared Spectroscopy (FT-IR) which can be done on microtome films or by using microscopy equipment (FT-IR-microscopy) [21][89]. FT-IR spectroscopy monitors the vibration spectrum of molecules or rather functional groups which depend on their atomic mass and bond strength. The molecules are excited by a spectrum of infrared radiation which is varied by means of an interferometer. The latter ensures a stepless variation of the wavelength. A mathematical transformation, a Fourier transform, of the interferogram provides a so called single-beam spectrum [120]. The signal received shows the intensity over the wavenumber and is analysed with regard to changes caused by absorbance effects due to the excitation of molecules. This frequency spectrum obtained is a characteristic quantity for the chemical composition of the material [121]. Usually the recorded spectra are compared with a database to aid in compound identification. Furthermore, FT-IR can be used to detect changes in the chemical structure of the elastomer and to identify individual groups that arise or disappear during ageing [48][122].

An example of the effects of ageing on a FT-IR spectrum is given in Figure 38. Absorbance of infrared radiation is plotted over the wavenumber for an NBR rubber containing 18 wt%

acrylonitrile for unaged condition and after exposure at 100 °C for 4032 h (168 d). Measurements are done at the surface of the aged samples. The graphs are shifted vertically to avoid overlap for reasons of clarity. The absorbance at a certain wavenumber is a measure for the existence of vibrations in this range of frequency. These vibrations are a function of the atomic mass of the atoms participating and the bonding between them. Further, different kind of vibrations like stretching, bending and rotating of the bonding as well as surrounding conditions which influence the oscillation mode by interacting with other atoms or rather functional groups result in various vibration frequencies. Consequently, a FT-IR spectrum is a complex fingerprint of the materials composition which should always be viewed in its entirety. Nevertheless, it is possible to attribute different sections of the spectrum to different groups of bonds which is accomplished in Figure 38 for the case of elastomers. At the lower frequencies or rather the higher wavenumbers (app. 4000-2400 cm^{-1}) the hydrogen bonds predominate like hydroxyl (O-H), secondary amino group (NH) or methylene (CH_2). Around app. 2400-1900 cm^{-1} triple bonds are located like nitrile (C≡N). At lower wavenumbers (app. 1900-1400 cm^{-1}) double bonds can be found like carbonyl (C=O) which is important regarding oxidation. Single bonds and scaffold vibrations can be found primarily at wavenumbers below 1500 cm^{-1}. There, carbon-carbon double bonds and diverse bonds containing oxygen can be found. In general, the analysation of FT-IR spectra is not a trivial task and rarely it appears clear at initial investigation. Chemical reactions cause changes on molecular level which provoke diverse variations in a spectrum like those shown in Figure 38. Overlapping or intensifying and diminishing of different effects make the analyse to a challenging task. However, certain functional groups or rather their intensity at a certain wavenumber in the spectra are found to be representative for ageing in elastomers.

As shown in Figure 38, air exposure results in changes of the FT-IR spectrum of NBR. The evolution of the most important vibrational bands from an elastomer ageing point of view are listed in the following. Absorbance of methylene (CH_2) decreases when comparing the unaged (graph a) with the aged condition (graph b). Same holds for carbon-carbon double bonds (C=C) which are part of the molecular backbone of elastomers. They are reduced due to thermo-oxidative ageing and thus the dominant peak in figure at approximately 1000-900 cm^{-1} declines significantly. Representative for oxidative ageing is the formation of carbonyl (C=O), which is often chosen as a relative measure for the degree of oxidation. That means the quantity of carbonyl groups is compared for unaged and aged condition. For the aged sample the peak at app. 1700 cm^{-1} is increased and suggests the occurrence of oxidation. Since the absolute value of absorbance can hardly be compared between two measurements especially on two different samples it is stated comparatively to a stable molecular group. Mostly this is nitrile (C≡N) which usually is not affected by ageing conditions and therefore chosen as an internal reference band [25][123]. Of course, this can be different for other material compositions or ageing circumstances [43].

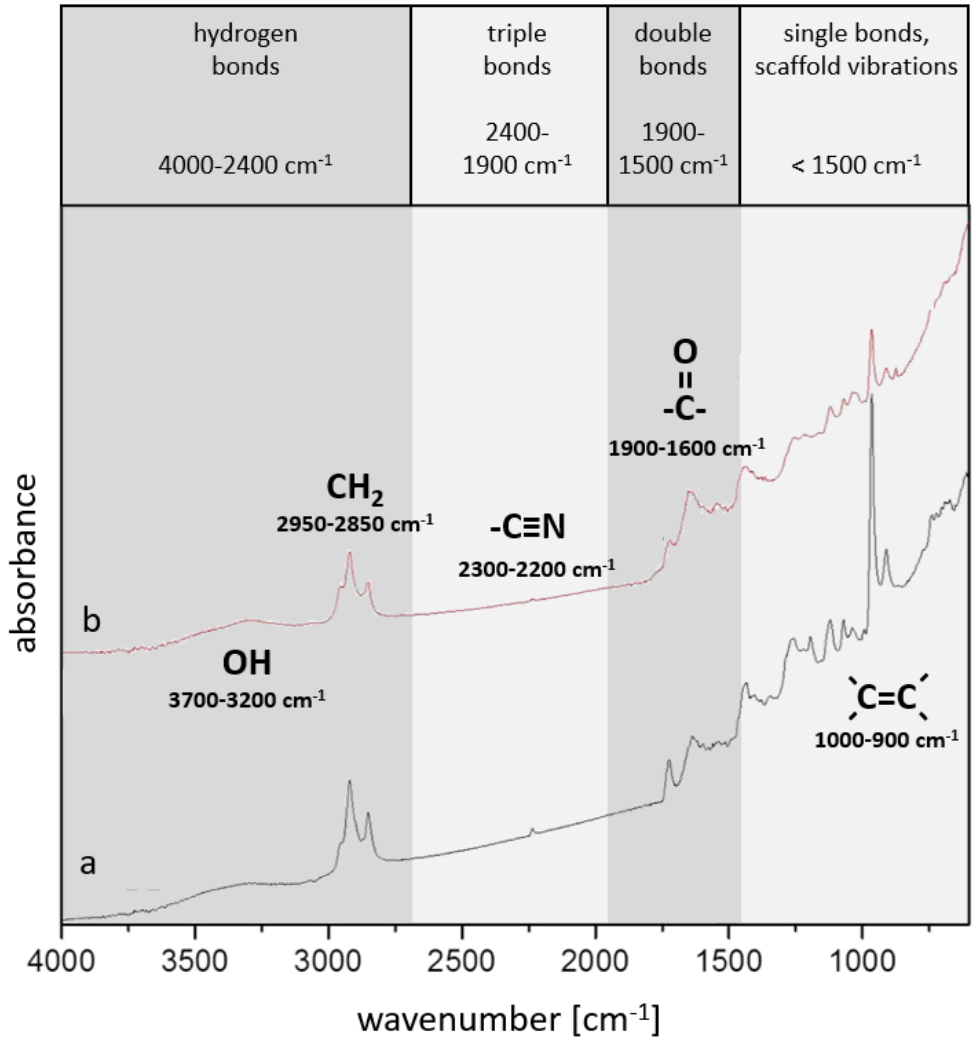

Figure 38: FT-IR spectra of NBR rubber containing 18 wt% acrylonitrile for unaged condition (a) and after exposure at 100 °C for 4032 h (b); division of different spectral ranges including some exemplary functional groups

Hence, changes in the FT-IR spectrum are always specified relative to a stable band. This motivates the introduction of indexes like an oxidation index [11]. Either the absorbance is considered at a specific wavenumber or rather a peak or the average value is calculated in a certain range of wavenumbers. That means the area under the curve is calculated in a certain wavenumber range of interest by drawing a baseline using two point tangent. Subsequently, the values are divided by a value or rather a range area of a stable band. For the material shown in Figure 38 this could be for example:

$$oxidation\ \ index = \frac{A_{1800\ to\ 1700\,\mathrm{cm^{-1}}}}{A_{2300\ to\ 2200\,\mathrm{cm^{-1}}}} \tag{20}$$

$$oxidation\ \ index = \frac{I_{1720\,\mathrm{cm^{-1}}}}{I_{2235\,\mathrm{cm^{-1}}}} \tag{21}$$

On the one side $A_{1800\,to\,1700\,cm^{-1}}$ represents the carbonyl groups which results from the absorption of carboxylic acid ($1790\,cm^{-1}$), esters ($1763\,cm^{-1}$), aldehyde ($1728\,cm^{-1}$) and ketones ($1715\,cm^{-1}$) [11]. On the other side $I_{1720\,cm^{-1}}$ is the peak of the carbonyl group and $I_{2235\,cm^{-1}}$ the nitrile group which is observed to be stable during ageing.

With this basic approach it should be mentioned that there is no general scale which can be used for every kind of elastomer and degradation. Hence, interpretation of FT-IR spectra must be performed for individual polymer types and requires both effort and experience. Nevertheless, standards exist like for instance DIN 53383-2 which defines the oxidation stability testing of polyethylene by means of infrared spectroscopy. It uses a carbonyl ratio which is the quotient of $I_{1720\,cm^{-1}}$ and a characteristic band of the polymer (polyethylene: $I_{2020\,cm^{-1}}$, polypropylene: $I_{1250\,cm^{-1}}$, polystyrene: $I_{1870\,cm^{-1}}$). As stated in subsubsection 3.1.3 before, for carbonyl ratio reaching the value two, the end of lifetime is supposed to be reached due to extensive embrittlement of polyethylene [11]. In the case of NBR, Kawashima et al. [43] define the end of lifetime when absorbance of carbon-carbon double bound is reduced to 45 % of its initial value.

In the following spatial molecular changes of NBR during ageing will be examined. Therefore, a literature research was conducted to get an idea about the chemical changes of elastomers to be expected in the course of various exposure scenarios. The most important results are shown in the following table [11][25][43][89][93][123][124][125][126][127].

Table 2: Technical relevant properties of elastomers

functional group		type of vibration	freqeuncy range [cm^{-1}]	trend of absorption due to ageing	potential reasons for change
hydroxyl	−OH	streching vibration	3600−3200	↗	oxidation
methylene	−CH2	stretching vibration	3000−2800	↘	cross-linking; loss of additives
		bending vibration	1480−1400	↘	
nitrile	−C≡N	stretching vibration	2300−2200	→	unchanged reference band
				↘	cyclisation
carbonyl	−C=O	stretching vibration	1900−1600	↗	oxidation; formation of aldehyde, ester, ketones, acid
carbon-carbon double bonds	C=C	stretching vibration	1700−1600	↗ ↘	crosslinking reactions; influence of antioxidants
		bending vibrations	970−960		scission reactions, oxidative attack; consumption of antioxidants
ester	O=C−O	stretching vibration	1200−1050	↗	oxidation

The changes on molecular level listed in Table 2 are examples of the ones occurring during thermo-oxidative ageing. Depending on the type of elastomer and the circumstances like ageing temperature the molecular changes differ in their way and intensity. Usually the most representative indicator for thermo-oxidative ageing is the formation of hydroxyl and carbonyl groups which is used in almost every investigation of the literature referenced. Another functional group which can be formed by oxidation is ester. Besides the formation of new characteristic groups already existing ones can be degraded like methylene as well as the carbon backbone of the elastomer itself. The latter is affected by both chain scission and network reformation reactions. They are in dualism to each other and depending on the circumstance one of them can be more pronounced.

5.2.2.2 Test results

Since measurements at the surface of the sample only, (Figure 38) provide no information about the condition in the interior of the sample further experimental testing is required. Therefore, a 2 mm sheet of NBR aged at 100 and 120 °C up to 21 days was sliced to films of 20 μm thickness using a Leica RM2255 microtome for subsequent IR spectroscopy. Before slicing was performed the specimen was mounted in epoxy resin discs to ensure clean cuts. Every fifth slice was analysed by FTIR spectroscopy to receive data with a spatial resolution of 100 μm. That means starting from the centre of the sample and working to the edge, for a total of ten points across one half of the cross-section. Usually, analysing one half of the cross-section is sufficient since ageing is expected to occur symmetrically. In order to confirm this one sample (120 °C, 8 d) was tested over the whole cross-section. Spectra were collected by using a Varian 620-IR FTIR Imaging Microscope in transmission mode, with four scans at a resolution of 4 cm^{-1} in the range between 4000-400 cm^{-1}. The FTIR data of the surface layer are measured separately by means of an ATR FTIR with diamond attachment (Nicolet iS10 FTIR spectrometer). Figure 39 shows the spectra collected over half of the cross-section.

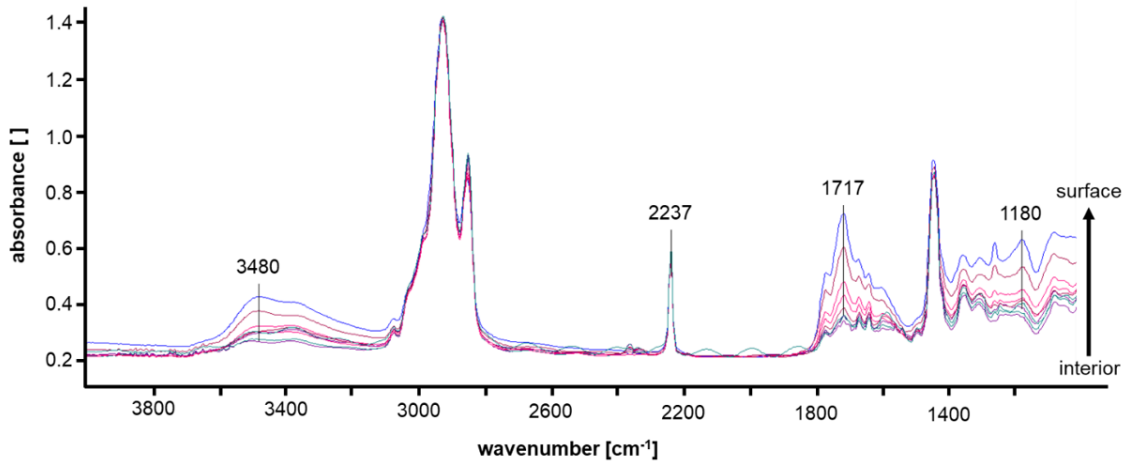

Figure 39: FTIR spectra at different points of the cross section of a NBR-sample containing 33 wt% acrylonitrile aged at 120 °C for 21 days

The spectra are shown all together in one graphic for reasons of direct comparison. At a first glance it can be seen that the spectra change at certain bands of wavenumber continuously from the core of the sample to the surface whereas other bands remain constant. Further, the absorbance of nitrile (2237 cm^{-1}) does not change which means it is constant over the cross-section of the sample. Nitrile was identified as a reference band and used to baseline all spectra for reasons of better comparability. Three key functional groups have been identified in Figure 39: hydroxyl (3480 cm^{-1}), carbonyl (1717 cm^{-1}) and ester (1180 cm^{-1}). They all increase in absorption from the inside to the outside of the sample. The peak ratios of carbonyl ($I_{1717\,cm^{-1}}$) and nitrile ($I_{2237\,cm^{-1}}$) are calculated as oxidation index and the result for samples aged at 100 °C and 120 °C are illustrated in Figure 40.

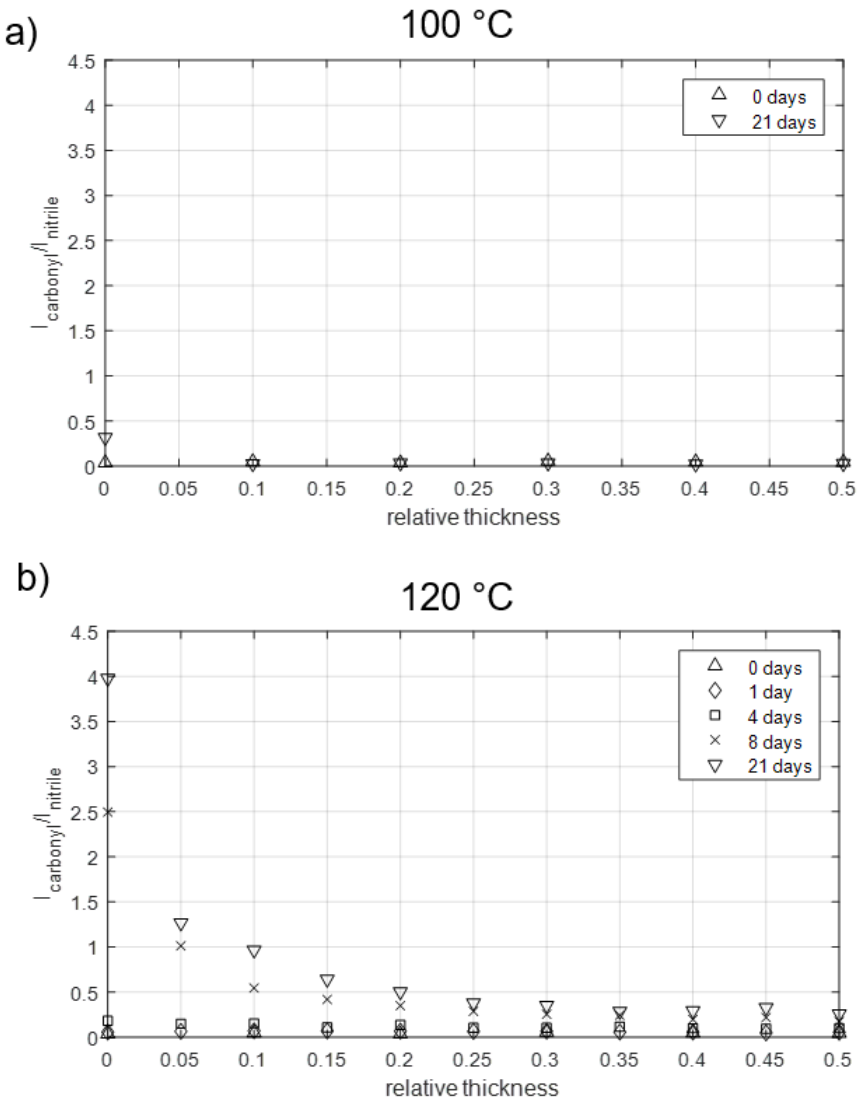

Figure 40: Oxidation index (carbonyl-nitrile ratio) profiles of NBR aged at 100 °C (a) and 120 °C (b) up to 21 days

The samples aged at 100 °C barely exhibited noticeable change in the oxidation index along the profile after 21 days of exposure. For this reason, FTIR spectroscopy was not executed for 1, 4 and 8 days at 100 °C. The low oxidation index in Figure 40 (a) demonstrates that the sample has

been minimally oxidised at the surface. Behind the surface layer there is no noticeable increase in absorption of the carbonyl band. Figure 40 (b) makes clear that increasing the temperature to 120 °C has a pronounced impact on the ageing process and oxidation index appears to be more heterogeneous with ongoing increasing ageing duration. Oxidation profile increases slightly over the entire cross-section up to 4 days. Afterwards oxidation proceeds more intensive at the surface and the rubber is least oxidised at the centre of the sample. After 21 days oxidation index reaches approximately the value 4 at the very outside whereas the interior of the sample is still hardly affected, and a large gradient of the oxidation profile occurs in the outer 10 percent of the samples cross-section.

Comparing the results of Figure 40 (a) and (b) depicts the rate of surface ageing being much higher at 120 °C than at 100 °C. Further, a kind of induction period seems to occur up to at least 4 days of ageing. After an initial phase of mild homogeneous oxidation, a rapid step of oxidation occurs (120 °C, 8 and 21 days) which is concentrated to the edge of the material.

In order to emphasise the heterogeneity of the oxidation index, after aerobic ageing at 120 °C the results over the whole sample thickness are presented in Figure 41. The data after 8 days of ageing are used from the verification test over the whole cross-section. The other profiles are generated by reflecting the data on the middle line assuming symmetry of the carbonyl profiles. The outcome visualises that carbonyl formation is low and quite homogeneous in between approximately 25 % to 75 % of the elastomer sheet tested. Further, the increase of oxidation index at the surface is remarkable since its value is more than double after 8 days or rather more than three times after 21 days of ageing compared to the next deeper measurement point at 5 %.

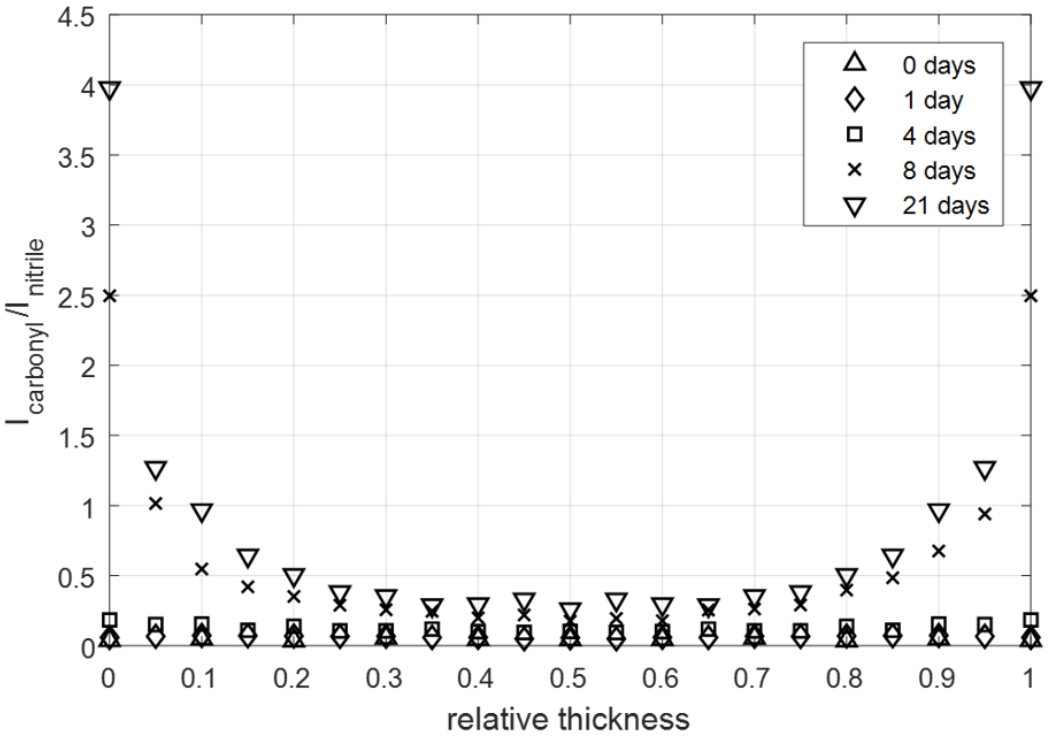

Figure 41: Full carbonyl profile development of NBR aged at 120 °C up to 21 days

5.2.3 Discussion

CT was introduced as a novel approach to investigate nonhomogeneous oxidation. Oxidative degradation density changes can be caused by other processes such as swelling or loss of plasticisers. Hence, the results of CT serve as an indicator for heterogeneous ageing only. The CT analysis is not a direct measure to derive the level of oxidation from and hence should not be used as the only method when investigating the degree if oxidation. Nevertheless, it provides an additional non-destructive insight in aged elastomer material and delivers profile information. Although Figure 34 depicts a wider dispersion of the values than Figure 35 some basic information can be drawn from the results. Longer ageing conditions result in a more nonhomogeneous density profile with smaller effects on the interior of the sample. This corresponds with the supposition that the oxygen is taken up from the ambient environment and induces oxidation in the superficial layer of the sample. This is exacerbated by elevated temperatures and results in a high reactivity of oxygen in the superficial region and a decrease in oxygen permeability. Consequently, oxygen molecules are hindered to get in the interior or in other words: DLO occurs.

Investigations for nine months at different temperatures (Figure 36 and Figure 37) confirm the previous results but ageing at 100 °C shows a completely different behaviour by density decreasing at the superficial region. This converse observation is explained by several processes running in parallel. Depending on the ageing temperature, certain processes may dominate which causes contrary outputs. Usually, most exposed elastomers exhibit a density increase due to the reasons explained before. Here, ageing causes a reduction of density which could for example be explained by chain-scission reactions being more dominant than cross-linking reactions or outward diffusion of one or more elements. The latter is caused by the loss of additives or the migration of antioxidants [21][42].

The effects on the chemical structure of the elastomer are amongst others caused by thermo-oxidative ageing but not limited to it. Since the density highly depends on the constituent atoms chemical reactions are important especially if atoms are replaced by others of different atomic mass. The average atomic mass of a material is an important factor for its density and other effects like free volume or crystallinity are circumstantial. Consequently, polymers which initially include lots of heavy atoms are less sensitive to altering the atomic mass by oxidation. The addition of oxygen atoms to materials mainly consisting of lighter atoms like carbon or hydrogen effects on density are noticeable [17].

Consequently, the suitability of density determination for investigations on thermo-oxidative ageing depends on the type of the elastomer since density changes can be more or less pronounced. Apart from this, it is necessary to investigate any alterations in density correlate with changes in the other properties. Hence, at this point it can be stated that density measurement by micro CT is an indirect method which enables new possibilities of no-destructive testing and can be used as an indication method for heterogeneity. In order to improve significance further investigations are necessary which should elaborate the correlation of thermo-oxidative ageing,

changes in mass density and e.g. mechanical properties.

One possibility to further probe the ongoing chemical changes during ageing is the use of FTIR spectroscopy. This direct method provides an insight of what is going on from a chemical point of view or rather in which way the material composition is affected. Besides the elastomers itself the presence, distribution and quantity of additives like antioxidants, plasticisers and filler material can be investigated. In the case of a high carbon black filler content analysis can be difficult since other signals are superimposed by those of carbon black and preceding extraction process can be required.

Although FTIR does not deliver absolute values, in general relative measurements provide a very powerful tool when examining effects of oxidation. Comparing FTIR spectra of different ageing states as shown in Figure 39 indicates dynamic and static wavelength bands whereas it is more difficult to make points based on a single spectrum only. On that account, oxidation indices are used to provide an absolute value of oxidation after analysis of a single spectrum. It is more challenging to draw conclusions concerning the level of oxidation by one FTIR measurement than by comparing different states of ageing. Further, oxidation indices presented consider only a single band (e.g. carbonyl group). Oxidation processes can be far more complex especially when comparing ageing at different temperatures or in different media. In general, such ratios are a good relative measure but if several processes alter the chemical structure in parallel or different processes are triggered by different conditions of exposure a more global picture is needed than a single oxidation ratio. Further still, defining the end of lifetime by using an oxidation ratio can be a good heuristic but reaching the end of operating life depends on the properties needed in a certain application. In a first approach Table 2 gives an idea what can be of interest when analysing ageing phenomena of elastomers. However, it provides only an overview of possibilities and must be critically reflected for each individual type of elastomer and its additives.

The investigations on NBR by FTIR reveal a pronounced temperature dependency and heterogeneity. Differences between 100 °C and 120 °C in Figure 40 can be traced back to activation energy reached above 100 °C which triggers or accelerates the formation of carbonyl groups. The distinctive temperature dependency can also be based on antioxidants which lose their function by exceeding the ageing temperature of 100 °C. Further, consumption of antioxidants can be accelerated in such a way that their protective effect disappears after a certain time of exposure. Such a mechanism can explain the still poor level of oxidation within the first four days of exposure at 120 °C. Afterwards functionality of the antioxidants decreases, and the oxidation rate begins to increase. Subsequently, the oxidation rate reaches its peak and decreases with ongoing duration. Comparing the curves of 8- and 21-day ageing in Figure 40 b depicts a decreasing oxidation rate. That means a saturation effect occurs with ongoing ageing or diffusion of further oxygen into the elastomer is prevented by DLO. The latter statement is additionally supported by the heterogeneity being more pronounced for 120 °C/21 days ageing. Oxidation is concentrated on the superficial region and oxidation ratio increases only slightly in the interior. This can be seen when comparing the values of ageing at 120 °C for 8 and 21 days in a depth of 20 %. Saturation effects in the outer region which do not also affect the diffusion process does

not explain the decelerated ageing behaviour in the interior.

Slight oxidation in the whole sample after short ageing duration, as shown in Figure 41, for one to four days cannot be explained by diffusion processes during exposure. Nevertheless, the presence of oxygen is a prerequisite for the formation of carbonyl groups. Oxidation effects without any oxygen provided during exposure from the ambient environment can be explained by previous contamination during manufacturing and/or oxygen absorption and diffusion prior to controlled exposure.

In order to reach a conlcusion regarding when a polymer's end of lifetime is reached further information and investigations are required. Depending on the type of application, for instance as an O-Ring sealing, the mechanical properties changing during the processes of oxidation are of interest like, for example, compression set or relaxation time.

5.3 Mechanical properties

5.3.1 Overview of mechanical testing

Thermo-oxidative ageing as introduced in section 4 considers changing properties and the end of lifetime as last steps following the chain of causation or more precisely, elastomer properties which are of interest for the actual usage. As previously mentioned these properties usually are mechanical ones which are the primary reason for choosing the material in a certain application. An illustrative example is the elastic modulus, which in an initial approach was shown to be proportional to the cross-linking density [86][128][129]. This effect is visualised in Figure 42 by a simplified model of a molecular chain network under tensile load. Two elastomer samples with different cross-linking densities are loaded by equal tensile stress. The figure shows the molecular chains and cross-linkings between them without considering any effects of entanglement. By applying a load the molecular chains orient in the tensile stress direction which is limited by the cross-linkings. Hence, a higher cross-linking density results in lower ability of chain mobility which is equivalent to a higher elastic modulus.

When predicting changes in the mechanical properties two approaches can be distinguished. The first one considers the mechanical behaviour of the whole sample. This means inhomogeneities are not considered or rather are included in an encompassing description. Such an approach is mostly chosen when the final application is of interest. For example, when searching for a suitable engine bearing during the design phase or defining the end of lifetime criteria the overall behaviour of the bearing is of interest. The second way considers the mechanical properties from a more detailed point of view. Heterogeneous changes of mechanical properties are preferred since they are closer to the real condition of the elastomer component, which is required for developing constitutive models and giving precise predictions. Experimental investigations in both ways are reasonable and necessary to obtain a comprehensive view on the changing properties during oxidation.

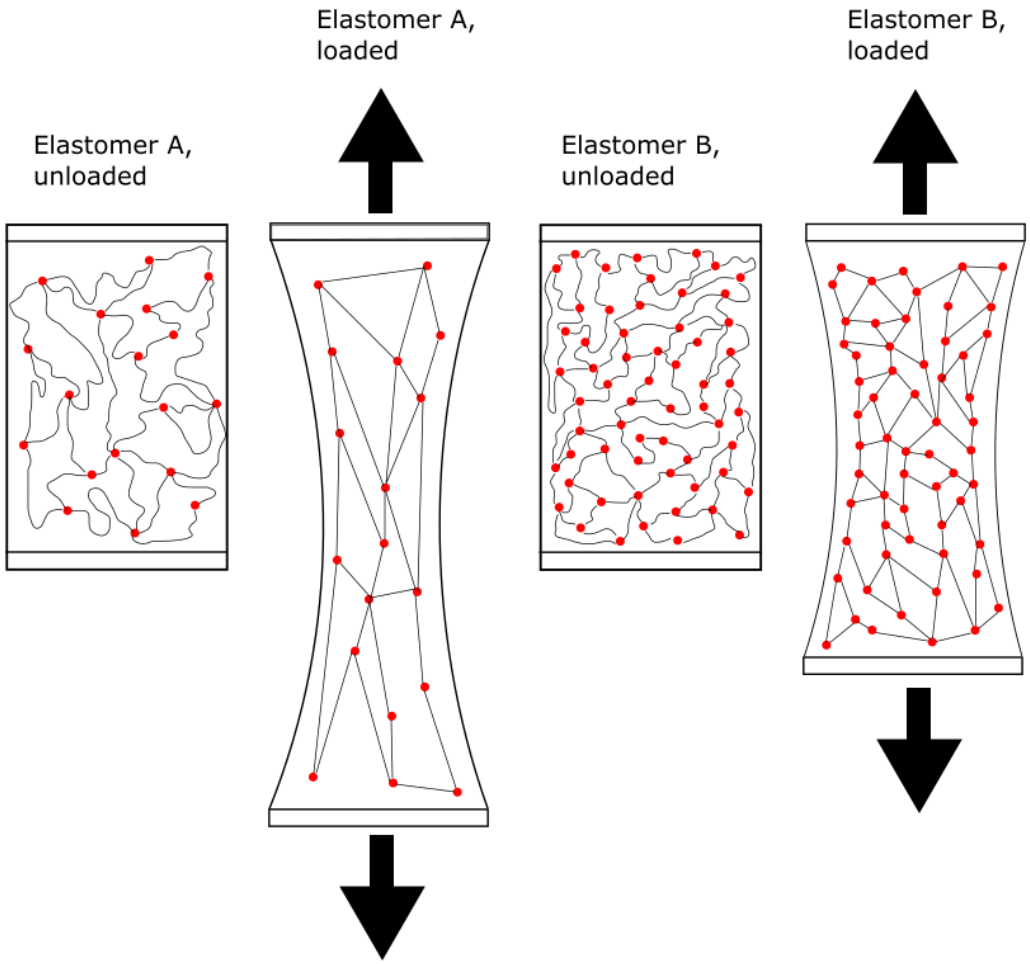

Figure 42: Tensile test on elastomer samples of different cross-linking density (based on [68])

Most research projects aim to adress the mechanical testing of elastomers after exposure. This is obvious since the main interest of such investigations is in the degree of degradation of mechanical properties due to ageing. Unfortunately, these investigations do often not provide any insight to the mechanisms of the changes in mechanical properties. Mechanical testing of elastomers after oxidation is not a main part of this work but quite important since it is the most popular part or rather a result of oxidation. For this reason, this chapter should give a brief overview of possibilities to test mechanical changes. Further, examples will be given including relaxation testing and compression set.

Mechanical testing represents an indirect way of investigating oxidation which aims on the consequences caused by ageing. Of course, the following examples are not restricted to investigations on ageing but are used to analyse elastomers in general [48]:

- Tensile, compression and shear test
  Ageing-induced changes in the quasistatic mechanical material behaviour are analysed after elastomer samples are aged under stress-free conditions. These basic test methods are also applicable for investigations on the viscoelastic behaviour when considering the

factor of time besides stress and strain [8][20][38][67].

- Relaxation and creep tests
  These time-dependent tests provide detailed information about the viscoelastic material properties. Elastomer samples are loaded with a constant strain or stress by monitoring the corresponding stress or strain signal. Such tests can be run in an intermittent or continuous way.

- Dynamic Mechanical Analysis (DMA)
  This technique aims on the material behaviour under harmonic stress- or strain-controlled loading. Hence, DMA can be used to analyse the ageing induced changes on the dynamic mechanical material behaviour. Stress and strain being in phase represents the storage modulus, which describes the dynamic elastic properties. Further, the part of stress being in phase with the strain rate is used to determine the loss modulus describing the dissipation properties of the elastomer [120].

- Compression set test
  Samples are stored under compression while the ageing proceeds and the resultant stress decreases due to the ongoing degradation. After a certain time, the samples are removed from the clamping and the height is measured after a short period of viscoelastic recovery. The difference between height before and after ageing is used to calculate the compression set, which represents a relative measure of the permanent deformation [38].

- Hardness test
  This non-destructive investigation method aims on the consequences of ageing at the sample surface. Indenting the sample by a test body and registering load and displacement provides information about the mechanical properties at the surface or rather slightly below the surface. The method is also be used to deduce information about elastic modulus. An advantage is the possibility to obtain measurements of spatial resolution which is known as modulus profiling [21][89]. In order to provide information about gradients in the interior the samples have to be cut first.

5.3.2 Examples of mechanical testing

5.3.2.1 Relaxation test

As described in subsection 5.1 oxygen consumption measurements were performed on samples which are shaped in such a way that further tests are enabled subsequently. A common way to get information about the mechanical properties changing during ageing is given by intermittent relaxation tests. As an example, tension rods were tested directly after oxygen absorption was measured (compare subsubsection 5.1.6, Figure 26). Therefore, the samples were clamped into a tension testing machine and preloaded with 0.3 N (0.033 N/mm^2) to straighten the specimens

and to achieve comparable initial conditions. Afterwards a tensile strain of 20 % was applied and kept constant. The induced stress was measured by the load cell of the tensile testing machine for a period of one hour. The results after a preceding ageing time of 24 h at 60 °C, 80 °C and 100 °C are illustrated in Figure 43. In the beginning tension of all samples increases up to approximately 0.75 to 0.80 MPa. After a few seconds relaxation initiates, and tension decreases until a state of balance is reached at approximately 0.65 MPa which means a reduction of roughly 15 % compared to initial tension.

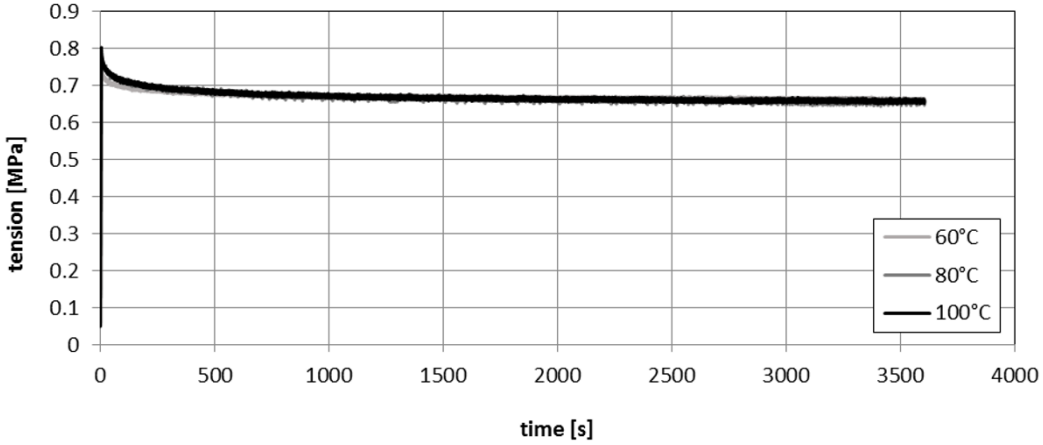

Figure 43: Relaxation test on natural rubber after 24 h ageing at elevated temperatures

Figure 43 depicts that ageing for 24 h resulted in minimal difference in behaviour of the subsequent relaxation test between the ageing temperatures. Hence, relaxation tests were also performed at samples aged for longer durations. Consequently, Figure 44 shows the results of the intermittent relaxation tests run on samples aged for 96 h at 60 °C, 80 °C and 100 °C. After this duration of exposure, the mechanical behaviour of the samples differs clearly. The tension resulting from 20 % stretching is different for each temperature. The initial tension is highest for 60 °C and lowest for 100 °C. Compared to the tests after 24 h ageing the absolute values are higher for 60 °C and 80 °C and little lower for 100 °C. In general, Figure 44 shows a higher stiffness for lower ageing temperatures which is an unexpected behaviour only known from some peroxidically cured systems. Equilibrium stresses measured after relaxation of 1 h shows the same behaviour as the initial tension and is highest for 60 °C ageing and lowest for 100 °C. Further, tensile relaxation is approximately 15 % lower than initial tension which is of the same magnitude as measured after 24 h ageing, which was shown previously. Nevertheless, conclusions if or in which way the ageing influences the relaxation behaviour can hardly be drawn based on the Figure 43 and Figure 44 due to the low amount of experiments.

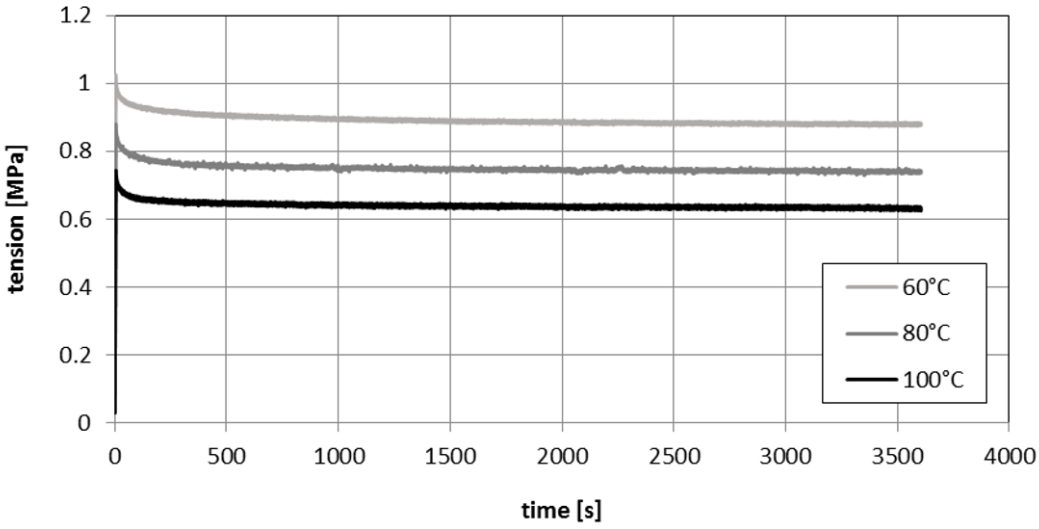

Figure 44: Relaxation test after 96 h ageing at elevated temperatures

The results clearly indicate that there is no trivial explanation for the changes of relaxation behaviour caused by ageing, but it shows that exposure has an apparent consequence on the effect of mechanical properties. As mentioned before, intermittent relaxation tests are able to consider both network degradation and reformation. Hence, they are appropriate to give a good overview of the tensile behaviour of elastomers. Nevertheless, there are other types of loads which can be better investigated by other tests. An example for compression tests is given next.

5.3.2.2 Compression set test

Compression set of polyurethane was measured after different durations and temperatures of ageing. Therefore, cylindrical samples were prepared and compressed by a self-developed clamping device as shown in Figure 45. The compression applied was about 23 % and height was measured before, during and after exposure.

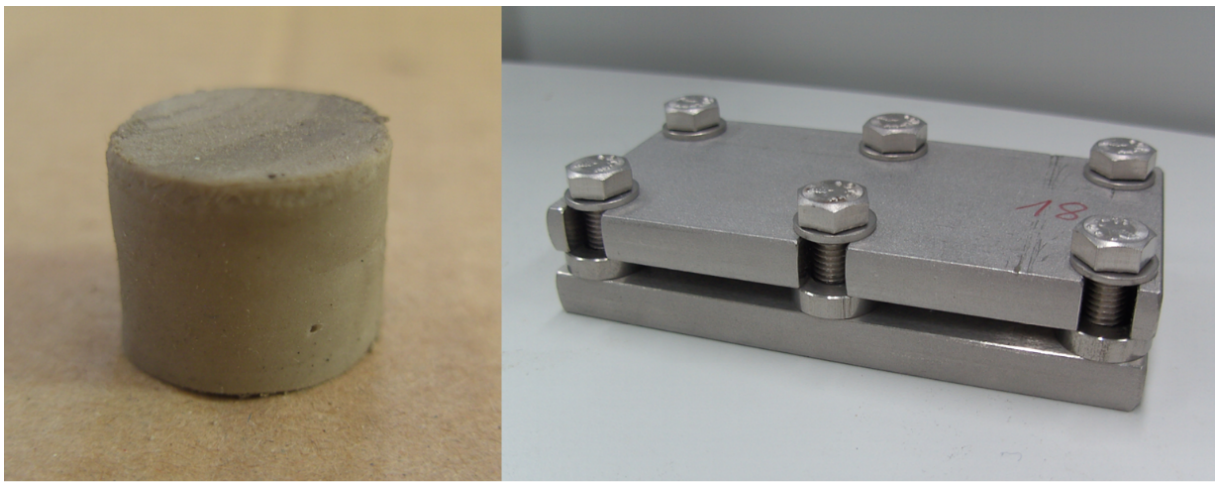

Figure 45: Polyurethane samples (left) and clamping device (right) for compression set testing

Afterwards, the ratio of non-reversible deformation known as compression set CS was calculated using the following equation with h_0 as the initial height, h_1 as the compressed height and h_2 as the height after ageing and unclamping.

$$CS = \frac{h_0 - h_2}{h_0 - h_1} \tag{22}$$

The results for ageing of polyurethane samples at 60 and 80 °C up to a duration of 33 days are illustrated in Figure 46. Compression set appears as a function of temperature and ageing time. Ageing influences the behaviour of the elastomer in both test series. More precisely, compression set increases with higher temperature and ageing time. The latter appears as a non-linear process and saturation seems to occur with increasing ageing time. Experiments at both temperatures depict a rapid increase of compression set after a short time which is not fully reflected in Figure 46 since the first measurements do not start at ageing time zero. The gradient of the curve becomes progressively smaller with increasing duration and it appears that the curves converge to a certain level.

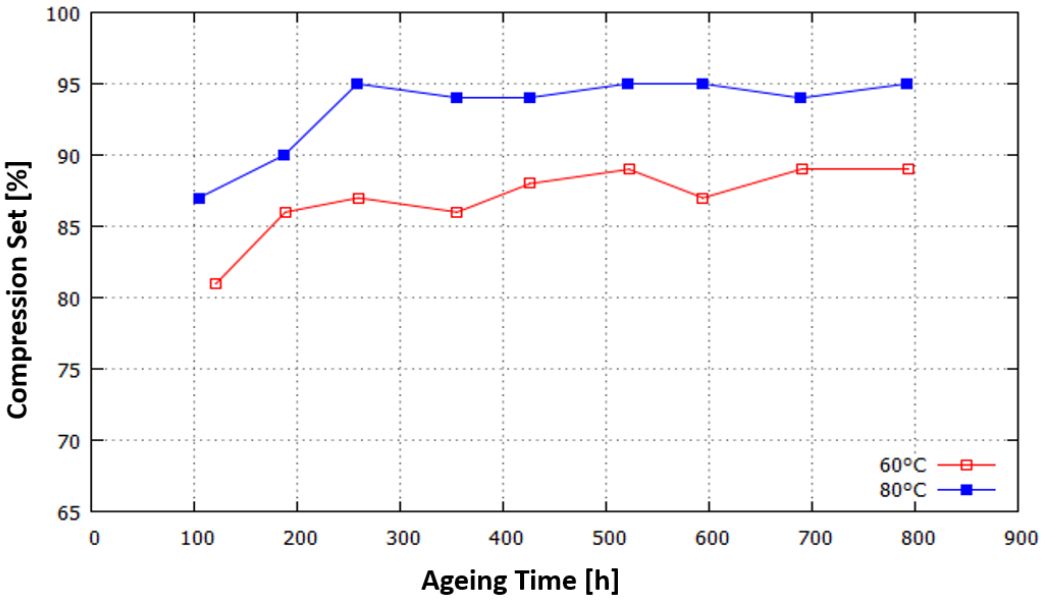

Figure 46: Compression set of polyurethane samples after ageing at 60 and 80 °C up to 33 days [38]

5.3.3 Discussion

Usually ageing induced degradation of mechanical properties is explained by means of changes in the cross-linking network. Relaxation tests in paragraph 5.3.2.1 depict that there is less variation between the individual temperatures after 24 h but a clear difference after 96 h. Figure 43 shows only a slightly higher tension and hence stiffness for 100 °C compared with 60 °C and 80 °C. Hence, for longer ageing higher stiffness could be expected with more pronounced differences

between the temperatures. Though Figure 44 presents an unexpected result after 96 h ageing with lower stiffness for 100 °C and higher stiffness for 60 °C than tests after 24 h showed. Nevertheless, such findings can be explained by network degradation and reformation occurring in parallel. At first, stiffening dominates the mechanical changes before degradation causes softening of the elastomer. The curve for 60 °C in Figure 44 is still dominated by network reformation whereas for 100 °C chain-scission is more pronounced either due to the necessary activation energy being reached or more proceeded due to the accelerated reactivity. It also is possible that induction periods cause such a behaviour as well as an inhomogeneous effect such as DLO which was described in previous chapters. Due to small number of tests shown here insufficient information is available to provide clear evidence. Nevertheless, it is shown that ageing can cause non-obvious impact on the relaxation behaviour of elastomers and linkage of ageing processes itself and consequences on mechanical properties is a challenge which cannot be answered in general for all types of elastomers.

Compression set behaviour of elastomers can be described with physical as well as chemical ageing whereby a clear distinction is often difficult to make since these processes usually run in parallel and thus complex effects and interactions can occur. During the tests for determining the compression set samples are permanently loaded by compressive stress due to the clamping device. Chain-scission and depletion of cross-linkings causes a decline in tension when the compression is maintained. In contrast, cross-linking reactions do not affect the tension during compression set testing unless volume shrinkage occurs. Hence, two processes run in parallel which can be used to explain compression set. First, the original molecular network is degraded which relieves the restoring tension. Furthermore, a new network structure is built up which is in balance in the compressed sample and hence counteracts a reversion of the compressed shape. If the sample is relieved, it regains the height at which these two forces balance each other. Since the ageing effects are thermally activated and saturation processes occur after longer time of exposure the permanent deformation in Figure 46 after dismounting from the clamping device can be explained.

6 Constitutive modelling of thermo-oxidative ageing

6.1 Absorption of oxygen in elastomers

In the beginning of this chapter the expressions 'solubility' and 'consumption' will be clearly differentiated once again. Here, solubility means the oxygen uptake of the material from the environmental atmosphere, whereas consumption is often used to define the chemical reaction of oxygen with the material. The former describes a physical process, the latter a chemical one. Sometimes oxygen consumption is also used to determine the amount of oxygen taken up by the elastomer as done in previous chapters. In the following, a constitutive model regarding solubility of oxygen in elastomeric material will be developed. The objective is the mathematical description of experimental findings presented in subsubsection 5.1.6. That means the characterisation of the oxygen absorption of elastomer materials as a function of ageing time and elevated temperatures, i.e. how many moles of oxygen per gram sample weight is absorbed by the elastomer during exposure in air.

The modelling approach is based on the fundamentals of oxygen absorption, which has been introduced in subsection 4.1. The findings of this chapter were published in [84]. The trigger of the absorption is the dissolution of oxygen molecules in the superficial layer of the elastomer, which results in an oxygen concentration gradient in the layer close to the surface. This represents the driving force for further penetration into the material known as diffusion. For exposure in environments containing air, solubility is a significant function of the partial pressure p_{ox} of oxygen. The equilibrium concentration C_s in the outer surface is given by Henry's law and describes the influence of the solubility rate coefficient S and the partial pressure p_{ox} (Equation (12)). Since C_s is the stimulus for further transportation of oxygen into the material, it is proportional to the oxygen absorption rate $\dot{m}_{ox}$ (the higher the concentration, the higher the solubility rate).

$$\dot{m}_{ox} \sim C_s = S\, p_{ox} \tag{23}$$

S is the solubility rate coefficient, which is a characteristic parameter for the material used. Due to the assumption that morphological dense phases show lower permeability to gases, cross linking density also has an impact on the solubility. This effect is similar to the permeability of crystalline phases in semi-crystalline thermoplastics. In the case of amorphous elastomers, it can be written in a first approach:

$$S = S_a\,(1 - p_s) \tag{24}$$

The inner variable p_s represents the cross-linking density. The value one stands for a level of cross-linking which inhibits any uptake of oxygen molecules. S_a is the initial solubility rate if no changes occur in the amorphous material, which is a function of temperature [17]. Equation (25)

follows the previously introduced Equation (13) but makes clear that S_a represents the initial solubility.

$$S_a = S_0 \, e^{-\frac{E_s}{R\theta}} \tag{25}$$

S_0 describes the material's basic solubility rate, E_s is the activation energy of solubility, R is the universal molar gas constant and θ stands for the absolute temperature. For the samples exposed to elevated temperature conditions θ represents the ageing temperature. In summary, solubility can be formulated as shown by Equation (26).

$$S = S_0 \, e^{-\frac{E_s}{R\theta}} \, (1 - p_s) \tag{26}$$

The cross linking density in elastomers is supposed to be influenced by ageing processes, for instance chain scission or network degradation. Thus, it is assumed that the cross linking density is a function of the ageing progress p. In a first approach a simple linear relation between the ageing parameter p and the cross-linking p_s is assumed:

$$p_s \, (p) = p \tag{27}$$

For this case cross-linking density is supposed to increase with ongoing ageing and hence solubility is inhibited for a fully aged sample which can be determined from the following equation. Of course, this approach is not able to consider all physical effects entirely and in every detail. Especially, extreme values like total inhibition of oxygen uptake due to ageing has to be critically reflected and kept in mind.

Using cross-linking density is only one possibility to develop a phenomenological model for the absorption behaviour. Describing solubility as a function of ageing can also be explained with a different approach using the progress of ageing as a solubility reducing factor, since the ongoing oxidation reduces surface affinity and thus the oxygen absorption rate is decelerated. Moreover, in the case of oxygen take up and the rising oxygen concentration in the superficial layer the stimulus for oxygen adsorbing at the elastomers surface declines which can also be described by means of the ageing parameter p. All approaches mentioned support the formulation of solubility as stated in Equation (28).

$$S = S_0 \, e^{-\frac{E_s}{R\theta}} \, (1 - p) \tag{28}$$

Consequently, oxygen absorption rate can be written as

$$\dot{m}_{ox} = p_{ox}\, S_0\, e^{-\frac{E_s}{R\theta}}\, (1-p) \tag{29}$$

The accompanying evolution equation that describes phenomenologically the ageing progress p can be expresses by [38][67]:

$$\dot{p} = \nu_p\, e^{-\frac{E_p}{R\theta}}\, (1-p)^2 \tag{30}$$

ν_p represents a proportionality factor and can be imagined as a temperature independent velocity of the ageing progress. E_p is the activation energy of the ageing process. R and θ were already introduced previously as the universal molar gas constant and absolute temperature. The ageing rate is reduced with ongoing degradation which is represented by the term in brackets and can be imagined as reduced reactivity due to saturation effects.

This model is demonstrated on the example of Standard Vietnam Rubber whose oxygen absorption behaviour was determined via experiment in subsection 5.1 (see Figure 27 and Figure 28). Figure 47 shows the experiment's results for the oxygen absorption rate and the calculated output of the theoretical approach introduced before. Therefore, the evolution equation was solved by using ode45 MATLAB nonstiff differential equations solver and fitted to the experimental data.

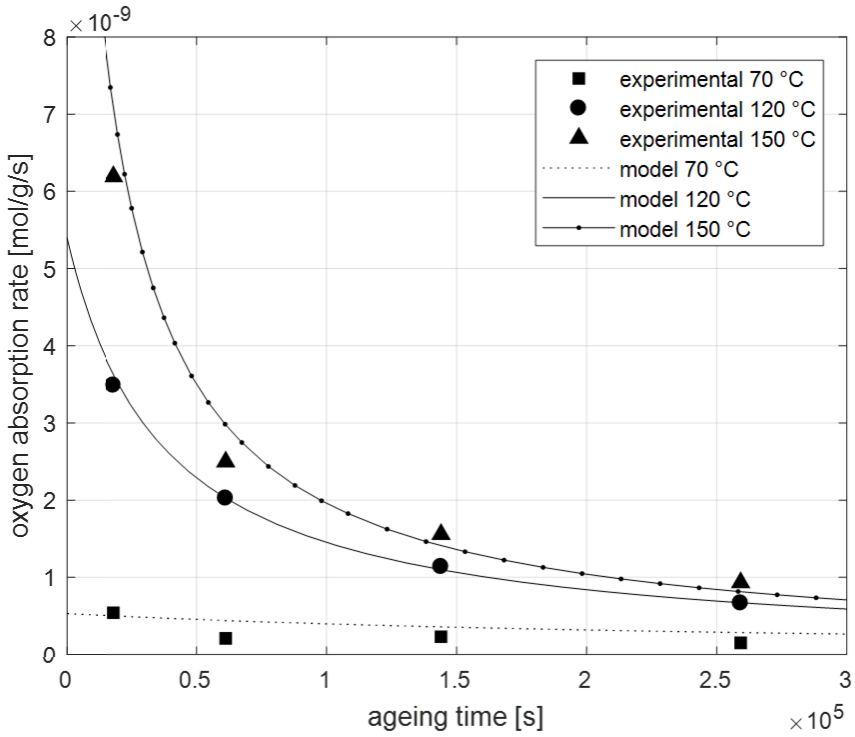

Figure 47: Description of experimentally determined oxygen absorption rate of Standard Vietnam Rubber by the modelling approach introduced (based on [84])

The parameters used for the modelling shown in Figure 47 are chosen as follows.

Table 3: Parameters for modelling of oxygen absorption behaviour

p_{ox} [kPa]	2.0	R [J/mol/K]	8.3145
S_0 [mol/g/s/Pa]	2.2×10^{-6}	ν_p [s^{-1}]	48
E_s [J/mol]	5.2×10^{4}	E_p [J/mol]	47000

Along with the description of the experimental data the model can be used to describe the oxygen absorption rate at further temperatures, for instance at 100 °C (Figure 48). Furthermore, the model is able to simulate absorption behaviour at more severe conditions. As an example, the output for higher temperatures can serve to explore an upper limit of oxygen absorption. Further increase of temperature results in the oxygen absorption rate approaching saturation. Therefore, Figure 48 also includes a simulation at an ageing temperature of 200 °C which is higher than all experimental investigations. The result shows that for high temperatures changes in oxygen uptake of elastomers become more and more irrelevant. This effect can be demonstrated and affirmed by the model for temperatures even higher than 200 °C, however at such temperatures elastomer decomposition begins. The latter is not considered in the model as validity range would be exceeded.

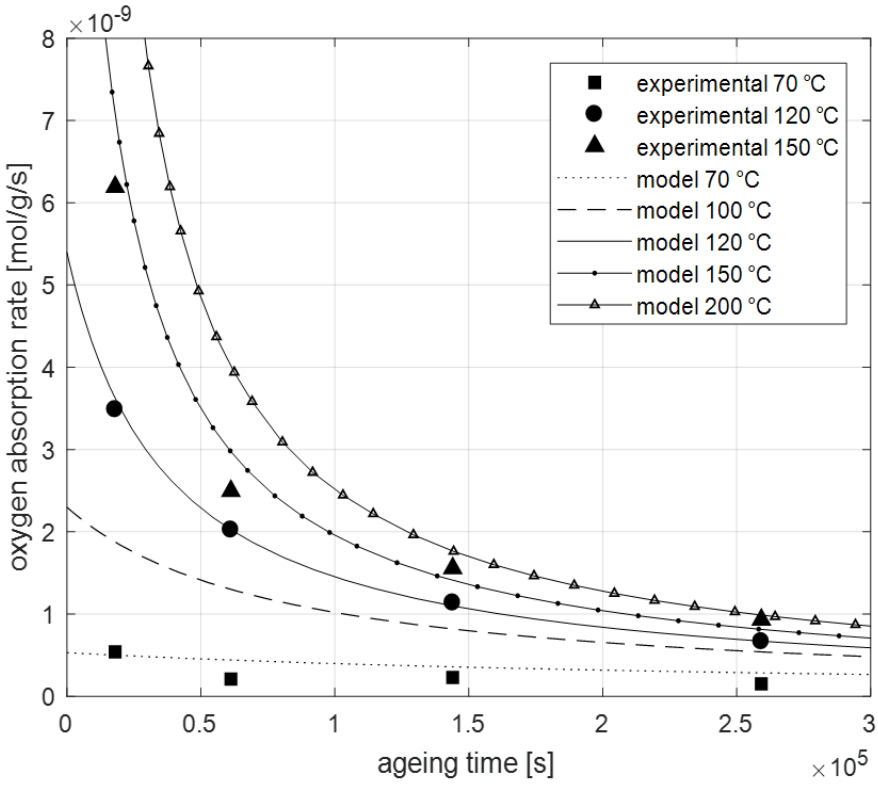

Figure 48: Oxygen absorption rate of Standard Vietnam Rubber over ageing time; model behaviour for further temperatures at 100 and 200 °C (based on [84])

Figure 47 and Figure 48 show that the modelling approach is able to replicate the experimentally obtained oxygen absorption rate. At the beginning, oxygen uptake is highly temperature dependent. With ongoing ageing time, the oxygen absorption rate decreases, which is highly pronounced for high temperatures and less significant for 70 °C. This observation is motivated by the dualism of the exponential temperature behaviour of Equation (28) and Equation (30), which counteract each other during the exposition at elevated temperatures. According to Equation (28) solubility is significantly increased by thermal energy as soon as the activation energy is reached. For a virgin sample (ageing time = 0), the effect of temperature is obviously shown in Figure 48. With ongoing exposure, the ageing parameter p increases according to Equation (30) and reduces the oxygen absorption (Equation (29)). This is more pronounced at high temperatures and thus the deceleration of oxygen absorption decreases further. As a result, the oxygen absorption rate reduces with ongoing ageing, which results in a similar absorption rate for all temperatures after a certain time (Figure 48).

6.2 Heterogeneous oxidation of elastomers

6.2.1 Modelling of reaction-diffusion behaviours

6.2.1.1 Diffusion of oxygen in elastomers

As stated in the previous chapters, chemical ageing of an elastomer by oxidation is generally defined as a process involving several steps including absorption, diffusion and chemical reactions. In contrast to the approach in subsection 6.1 oxidation is handled here as a diffusion driven process where oxygen is absorbed from the ambient environment in most applications. After oxygen molecules are adsorbed due to the affinity of the polymers surface for O_2 molecules, a concentration gradient occurs in the exterior layer, before the oxygen molecules subsequently start to diffuse into the interior of the material [83]. The most common approach to describe this kind of diffusion process is given by Fick‘s second law. Diffusion continues until an equilibrium state is reached or diffusion is prohibited otherwise. Fick‘s second law in its basic formulation reads as follows for the oxygen concentration C in elastomers, where the oxygen concentration C is formulated as a function of the location in the material and ageing time.

$$\frac{\partial C}{\partial t} = \nabla \cdot (D_{ox} \nabla C) \tag{31}$$

Equation (31) can be converted as shown in Equation (32).

$$\begin{aligned}
\frac{\partial C}{\partial t} &= \nabla \cdot (D_{ox}\, \nabla C) = \text{Div}\ (D_{ox}\, \text{Grad}\, C) \\
&= D_{ox}\, \text{Div Grad}\, C + \text{Grad}\, C \cdot \text{Grad}\, D_{ox} \\
&= D_{ox}\, \frac{\partial}{\partial x_i}\, \frac{\partial C}{\partial x_j}\, \vec{e_j} \cdot \vec{e_i} + \frac{\partial C}{\partial x_i}\, \vec{e_i} \cdot \frac{\partial D_{ox}}{\partial x_j}\, \vec{e_j} \\
&= D_{ox}\, \frac{\partial}{\partial x_i}\, \frac{\partial C}{\partial x_j}\, \delta_{ji} + \frac{\partial C}{\partial x_i}\, \frac{\partial D_{ox}}{\partial x_j}\, \delta_{ji} \\
&= D_{ox}\, \frac{\partial}{\partial x_i}\, \frac{\partial C}{\partial x_i} + \frac{\partial C}{\partial x_i}\, \frac{\partial D_{ox}}{\partial x_i} \\
&= \frac{\partial C}{\partial x_i}\, \frac{\partial D_{ox}}{\partial x_i} + D_{ox}\, \frac{\partial^2 C}{\partial x_i^2}
\end{aligned} \tag{32}$$

For a one-dimensional case, Fick's second law can be simplified as follows.

$$\frac{\partial C(x,t)}{\partial t} = \frac{\partial}{\partial x}\, \left(D_{ox}(x,t) \frac{\partial C(x,t)}{\partial x} \right) \tag{33}$$

Equation (33) describes the oxygen concentration as a function of position x and ageing duration t, where the diffusion coefficient is assumed not to be constant but can change during the process of ageing. In the following, the ambient oxygen concentration C_0 is assumed to be constant, which is true for most applications since air is the mostly present medium in the environment of elastomer components and supposed to be available in abundance.

6.2.1.2 Oxidative reactions

Once oxygen molecules have reacted chemically with the elastomer they are no longer available for further diffusion. This consumption of oxygen molecules is expressed by adding a reaction term r_{ox} to Equation (33) that is described in detail in a previous study [84] and presented by Equation (34).

$$\frac{\partial C}{\partial t} = \frac{\partial}{\partial x}\, \left(D_{ox} \frac{\partial C}{\partial x} \right) - r_{ox}(C, \theta) \tag{34}$$

The term r_{ox} represents the rate of oxygen consumption and is a function of ageing temperature and oxygen concentration. Furthermore, r_{ox} is subdivided in a chain scission $r_{ox,sci}$ part and a network reformation $r_{ox,ref}$ part (Equation (35)). Both types of chemical ageing reactions prevent oxygen from further diffusion since they create a chemical compound with the network of elastomer molecules.

$$\frac{\partial C}{\partial t} = \frac{\partial}{\partial x}\, \left(D_{ox} \frac{\partial C}{\partial x} \right) - r_{ox,sci}(C, \theta) - r_{ox,ref}(C, \theta) \tag{35}$$

Chain scission and network reformation are treated individually and depending on the circumstances either of the two processes can dominate. Both reaction rates are described by an Arrhenius approach (Equation (36) and Equation (37)).

$$r_{ox,sci} = \frac{C}{C_0}\, r_{0,sci}\, e^{-\frac{E_{r,sci}}{R\theta}} \tag{36}$$

$$r_{ox,ref} = \frac{C}{C_0}\, r_{0,ref}\, e^{-\frac{E_{r,ref}}{R\theta}} \tag{37}$$

$r_{0,sci}$ and $r_{0,ref}$ are constant factors influencing the velocity of the reactions. $E_{r,sci}$ and $E_{r,ref}$ represent the activation energies. With these parameters the kinetic reactivity of the oxidation can be adjusted. R stands for the universal gas constant and θ for the ageing temperature. Since both reactions - chains scission and network reformation - are based on the local availability of dissolved oxygen molecules the reaction rate is also a function of the oxygen concentration in the elastomer. If there is no oxygen, no oxidative reaction can occur. Thus, Equation (36) and Equation (37) are complemented by a quotient, which presents the availability of oxygen due to the ambient oxygen concentration. C/C_0 is zero if no oxygen is available at the considered point in the material. It is assumed that the maximum oxygen concentration which can be reached is ambient concentration C_0 (boundary condition). Therefore, the quotient becomes 1 at the elastomers surface. Equation (36) and Equation (37) show the reaction terms as formulated in an earlier stage of this work. One shortcoming, that this description of the reaction terms exhibits, is the fact that no saturation effect can be simulated. At a point in the material where unlimited oxygen supply is assumed, the reaction would continue without any decline in reaction rate. Hence, the saturation caused by the decreasing number of reaction partners in the polymers molecular structure could not be captured with this formulation of the reaction. Consequently, the progression of ageing has to be considered, which is achieved by modified reaction terms in Equation (38) and Equation (39).

$$r_{ox,sci} = \frac{C}{C_0}\, r_{0,sci}\, e^{-\frac{E_{r,sci}}{R\theta}}\ (1 - p_{sci})^{n_1} \tag{38}$$

$$r_{ox,ref} = \frac{C}{C_0}\, r_{0,ref}\, e^{-\frac{E_{r,ref}}{R\theta}}\ (1 - p_{ref})^{n_2} \tag{39}$$

In the case of a fully aged material no further oxidative reaction is enabled by the model. The exponents n_1 and n_2 are parameters used to adjust the effect of saturation as explained in more detail lateron.

The accompanying evolution equations that phenomenologically describe the progress of thermo-oxidative ageing can be formulated as follows [84]:

$$\dot{p}_{sci} = v_{p,sci}\, e^{-\frac{E_{p,sci}}{R\theta}}\ (1 - p_{sci})\ \frac{r_{ox,sci}}{r_{ox,sci,0}} \tag{40}$$

$$\dot{p}_{ref} = v_{p,ref}\, e^{-\frac{E_{p,ref}}{R\theta}}\ (1 - p_{ref})\ \frac{r_{ox,ref}}{r_{ox,ref,0}} \tag{41}$$

Equation (40) and Equation (41) are capable of describing the progress of oxidative reactions with respect to the ageing temperature θ and the oxidative reaction rates. In order to ensure compliancy of units the reaction rates are expressed in a normalised way, where $r_{ox,sci,0}$ and $r_{ox,ref,0}$ are here set to 1 for convenience only. It is obvious from Equation (40) and Equation (41) that the level of oxidation does not rise if no oxidative reaction takes place. Due to the equations introduced earlier the progress of ageing also depends on the oxygen concentration C and hence on the diffusion process.

6.2.1.3 Influence of antioxidants

Aim of most antioxidants is preventing the reaction of dissolved oxygen molecules or intermediate products with the elastomer before the molecular structure is affected according to subsection 4.4. In order to consider antioxidative reactions in the reaction-diffusion equation, a third reaction term r_{aox} is introduced.

$$\frac{\partial C}{\partial t} = \frac{\partial}{\partial x}\ \left(D_{ox} \frac{\partial C}{\partial x} \right) - r_{ox,sci} - r_{ox,ref} - r_{aox} \tag{42}$$

Analogue to the reaction rates of oxidation (Equation (36) and Equation (37)) antioxidative reactions are also described by a modified Arrhenius approach. The reaction rate is a function of the oxygen concentration since in the case of less oxygen being available the probability of oxidative reactions is reduced. The same applies for the availability of antioxidants which is assumed to be constantly distributed in a virgin sample and consumed by binding dissolved oxygen molecules or radicals (Equation (43)). Thus, the concentration or rather the effect of antioxidants decreases with the ongoing ageing progress. This is similar to the decreasing number of reaction partners at the polymers molecular structure in Equation (38) and Equation (39) but not coupled to the ageing parameter directly.

$$r_{aox} = \frac{C}{C_0}\ \frac{C_{ao}}{C_{ao,0}}\ r_{0,ao}\, e^{-\frac{E_{r,ao}}{R\theta}} \tag{43}$$

Furthermore, gradients occur locally due to the decreasing concentration of antioxidants which can provoke diffusion processes [34]. Consequently, the diffusion of antioxidants could also be described by Fick's second law and hence the concentration of antioxidants can be formulated

as a function of time and location. Such an extension of the model ought to be mentioned and discussed but experimental investigations on these effects and identification of parameters are difficult and tedious. Therefore, the effect of antioxidants will not included in the following modelling approach but should always be kept in mind and can be included easily due to the modular structure of the model.

6.2.1.4 Influence of oxidation on diffusivity

Besides the fact that the oxidative reactions consume the dissolved oxygen molecules they can also influence material properties, for instance by reducing the permeability to gases [32][62][87]. The mechanism was described in detail in subsection 4.3 and can occur in different ways and intensities. This phenomenon is considered in the model by describing the diffusion coefficient D_{ox} as a function of ageing temperature and progress of oxidation. Here, it is assumed that both types of oxidative reactions - chain scission and network reformation - reduce the diffusivity of the elastomer in the same way. Thus, the diffusion coefficient D_{ox} is formulated as a function of the ageing parameters chain scission p_{sci} and network reformation p_{ref} (Equation (44)). The progressing state of oxidation decreases the diffusivity, however a total diffusion stop is avoided since completely aged material is assumed to be still permeable. The model parameter μ is used to adjust the influence of the ageing parameters on the diffusion coefficient.

$$D_{ox} = D_0 \, e^{-\frac{E_D}{R\theta} \gamma} \qquad \text{with} \qquad \gamma = \mu \, p_{sci} \, p_{ref} \tag{44}$$

This approach allows to adjust the effect on permeation depending on the material and circumstances. Even in a fully aged elastomer, diffusion is not stopped but increasingly reduced up to a negligible influence only. Another approach to this is given by Kari who describes the diffusion coefficient as a function of the oxidation progress however a residual diffusivity always remains.

$$D_{ox} = D_0 \, e^{-\frac{E_D}{R\theta}} \left(\frac{1}{1 + \hat{p}_{ref}} \left(1 - p_{sci} + (1 - p_{ref}) \, \hat{p}_{ref}\right) (1 - \beta) + \beta \right) \tag{45}$$

For a virgin elastomer ($p_{sci} = p_{ref} = 0$) the above equation reads

$$D_{ox} = D_0 \, e^{-\frac{E_D}{R\theta}} \tag{46}$$

For a fully aged material ($p_{sci} = p_{ref} = 1$) Equation (45) is reduced to

$$D_{ox} = \beta \, D_0 \, e^{-\frac{E_D}{R\theta}} \tag{47}$$

Both approaches (Equation (44) and Equation (45)) include a temperature dependency of the diffusion coefficient expressed by an Arrhenius approach, where D_o is the basic diffusivity and E_D is the activation energy [37][130]. β represents the percentage of diffusivity which cannot be undercut not even for a fully aged elastomer. The parameter $\hat{p}_{ref}$ weights the influence of p_{ref} on the diffusivity D_{ox} in relation to the influence of p_{sci}. In the case of chain scission and network reformation affecting the diffusivity in a comparable manner ($\hat{p}_{ref} = 1$) Equation (45) can be rewritten as

$$D_{ox} = D_0 \left(1 + (\beta - 1)\,\frac{p_{sci} + p_{ref}}{2}\right) e^{-\frac{E_D}{R\theta}} = D_0 \left(1 - \alpha\,\frac{p_{sci} + p_{ref}}{2}\right) e^{-\frac{E_D}{R\theta}} \tag{48}$$

Here, α is a material parameter which describes the maximum percentage of the reduction of the diffusivity by ageing whereas β is the minimum percentage to which the diffusivity can be reduced.

In summary, the model delivers the position depending ageing parameters p_{sci} and p_{ref} over the geometry of the elastomeric sample. Thus, the model has the capacity to describe inhomogeneous oxidation as a function of ageing temperature and duration, oxygen concentration in the ambient environment and several specific material parameters.

In most cases the progress of ageing itself is not the point of interest and, furthermore, quite hard to imagine or to interpret. Hence, p_{sci} and p_{ref} are to be considered interim results which are subsequently used as an input for the description of the inhomogeneous changes of mechanical properties. The latter can then be used to define limits which give a quantitative measure for lifetime prediction.

6.2.1.5 Linkage of oxygen absorption and diffusion-reaction behaviour

After oxygen is absorbed there are four possibilities for subsequent progression: Oxygen is dissolved in the elastomer without any chemical reaction, it reacts with the elastomer (oxidative-reaction), it reacts with the antioxidant or it is desorbed by the elastomer again. The latter is not considered in this work. Hence, the amount of absorbed oxygen can be calculated by summing up the first three cases. The currently dissolved oxygen in the sample $m_{ox,di}$ is added to the total amount of oxygen molecules consumed by reactions after absorption $m_{ox,re}$. Reactions consuming the absorbed oxygen can be divided in network degrading reactions $r_{ox,sci}$ and network reforming reactions $r_{ox,ref}$ as well as binding oxygen molecules by means of antioxidation r_{aox}.

$$m_{ox} = m_{ox,di} + m_{ox,re} = \iiint C \mathrm{d}V + \int_0^t \iiint \left(r_{ox,sci} + r_{ox,ref} + r_{aox}\right) \mathrm{d}V\,\mathrm{d}t \tag{49}$$

The currently dissolved amount of oxygen is obtained by computing the volume integral of the whole elastomer sample. In the case of reactive consumption, the time integral is needed as well. Thus, the amount of oxygen being absorbed from the beginning of exposure until ageing time t can be calculated as an output of the diffusion-reaction model. That allows to compare the calculated amount of absorbed oxygen with the experimental data obtained by the method introduced in subsection 5.1.

6.2.1.6 Inhomogeneous temperature field

Elevating temperature is the preferred way to accelerate ageing of elastomers. Generally, there are two ways to apply heat to elastomers: the sample is exposed to an environment with a higher temperature or the temperature of the material is increased by self-heating due to dynamic loading (dissipative heating). In both cases the temperature in the material is not necessarily distributed homogeneously as assumed above by using the singular value θ. Rather the temperature has to be described as a function of the location and time, $\theta(x, y, z, t)$. Here it has been shown that the inhomogeneity of the temperature field can be insignificant if the ageing process is executed for long durations at constant temperatures without dynamic loads. Hence, for most laboratory tests on oxidation of elastomers the effect of inhomogeneous temperature can be neglected since a constant temperature field is established after a short period compared to the entire ageing time. Nevertheless, such boundary conditions are not representative for all technical applications and the effect of an inhomogeneous temperature field has to be weighed up for every specific case.

In order to consider heat conduction a constant initial temperature in the material is assumed and the ambient temperature is defined. The changing of temperature is described by a heat equation like the one used for the diffusion problem above. The heat conduction coefficient K can be assumed as a constant value, hence the heat conduction equation can be written as following.

$$\frac{\partial \theta}{\partial t} = \nabla \cdot (K \, \nabla \theta) = K \, \Delta \theta \tag{50}$$

Such a parabolic partial differential equation can be solved analogously to the diffusion-reaction-equation. As a result of this, temperature θ is described by an array which can change during the period of ageing. That means temperature θ, which is an important input parameter for the diffusion-reaction-equation is provided as a function of location and time.

This represents a further part of the modular concept which can be included in the simulation if required. Here, inhomogeneous temperatures will not be considered in further detail or included in the modelling since the number of parameters would raise significantly leading to higher calculation time, higher efforts in parameter determination and less clarity in the model. Nevertheless, ageing behaviour of dynamically loaded components with a geometry consisting of delicate and

bulky sections at the same time can necessitate considering inhomogeneous temperature fields.

6.2.2 Modelling oxidation induced changes of mechanical properties

Aim of this chapter is not the modelling of mechanical properties itself but the linkage of the previous description of ageing to the mechanical behaviour of elastomers.

6.2.2.1 Rheological approach

A common approach to describe the mechanical behaviour of elastomers is the use of rheological models which consist of spring, damper and temperature elements arranged in parallel and serial connections. The main advantage of such models is their modular design, the thermodynamically consistent behaviour as well as the easy transformation to three dimensional problems [38]. In the following a rheological model according to Figure 49 is used which enables the simulation of the mechanical properties of an elastomeric material [38][67].

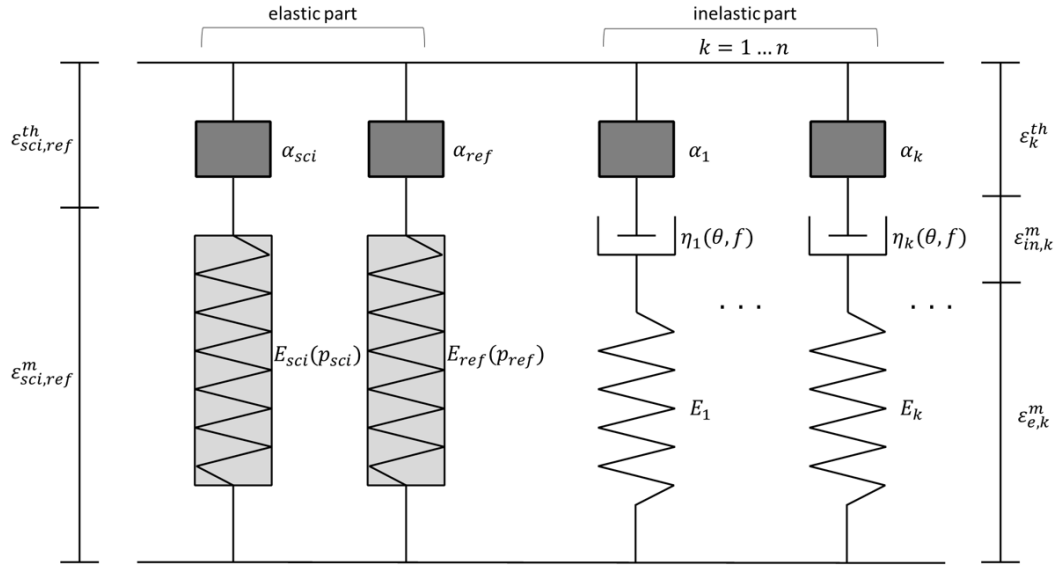

Figure 49: Rheological model to describe the mechanical properties as function of chemical and physical ageing [67]

The first two serial temperature and spring elements represent the basic elasticity of the system which are influenced by the chemical ageing processes of chain scission and network reformation. All other n parallel elements are assumed to be unaffected by the ageing processes. They are used to simulate the thermoviscoelastic behaviour including the contribution of the temperature dependency of the whole system. This model was introduced by Johlitz [67] to describe the mechanical behaviour of elastomeric bulk material after thermal exposure. He assumed thoroughly aged samples and homogeneously distributed ageing effects in the material. In order to include diffusion and reaction effects in this work the rheological model in Figure 49 is only

used to describe the inhomogeneous oxidation behaviour for finite parts of the sample instead of the mechanical properties of the whole sample. This is shown schematically in Figure 50 for one dimension. The elastomer sample is subdivided in nx equal parts, each represented by a rheological model as indicated in Figure 50. The inelastic part is described by a single Maxwell element for practical reasons and for the sake of clarity.

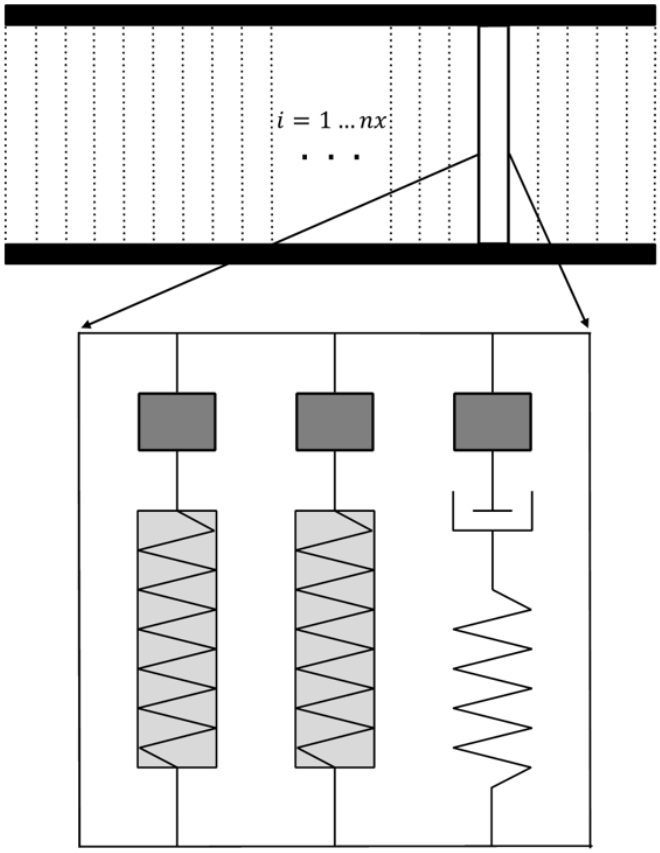

Figure 50: Modelling of an inhomogeneous aged elastomer sample by a parallel connection of rheological models each containing two springs for basic elasticity including ageing effects and one Maxwell element

The mechanical response of the whole sample (here shown for one dimension only) is then expressed as a parallel connection of nx subsystems which are equidistantly distributed. Each of the individual subsystems contains two elements for basic elasticity including oxidative effects and n elements for viscoelasticity. Thus, the overall behaviour of a sample under tensile loading can be expressed as a sum of its components, equilibrium stress σ_{eq} and non-equilibrium stress σ_{neq}, and reads as follows:

$$\sigma_{total} = \sum_{i=1}^{nx} \left(\sum_{k=1}^{2} \sigma_{eq,k,i} + \sum_{k=1}^{n} \sigma_{neq,k,i} \right) \tag{51}$$

Each elastic part can be divided in a chain scission and a network reformation element.

$$\sum_{k=1}^{2} \sigma_{eq,k,i} = \sigma_{1,i} + \sigma_{2,i} = \sigma_{sci,i} + \sigma_{ref,i} \tag{52}$$

Strain ε is assumed constant over the samples cross-section and is divided in a mechanical and a thermal part.

$$\varepsilon = \varepsilon^{m}_{sci} + \varepsilon^{th}_{sci} = \varepsilon^{m}_{ref} + \varepsilon^{th}_{ref} \tag{53}$$

The oxidative impact of chain scission is considered by describing the elastic modulus of the first element's spring as a function of the ageing parameter p_{sci} at the respective position i. Hence, tension can be written as

$$\sigma_{sci,i} = E_{sci,0}\ (1 - p_{sci,i}) \left(\varepsilon - \varepsilon^{th}_{sci}\right) \tag{54}$$

with

$$\varepsilon^{th}_{sci} = \alpha_{sci}\,(\theta - \theta_0) \tag{55}$$

α_{sci} represents the coefficient of thermal expansion, θ the current temperature and θ_0 the reference temperature. For simplicity's sake, temperature θ can be assumed to be constant over the whole sample (see also paragraph 6.2.1.6). Influences of oxidation on the viscoelastic behaviour are not included in this work [20].

The second element for basic elasticity describes the network reformation. Therefore, the elastic modulus of the second spring is implemented as a function of the ageing parameter p_{ref}. Since it is assumed that network reformation takes place in a state of no stress [19][20] the stress-strain relation is formulated according to [67][131] which differs from the formulation in Equation (54).

$$\sigma_{ref,i} = \int_0^t E_{ref,0}\, p_{ref,i}(s) \left(\dot{\varepsilon}(s) - \dot{\varepsilon}^{th}_{ref}(s)\right) \mathrm{d}s \tag{56}$$

Equation (56) can be transformed to a tension rate expression (Equation (57)) to ensure there is only an input of network reformation on mechanical tension if the deformation is changed. This is an important fact when considering the different effects of intermittent and continuous relaxation tests. In the latter case oxidation generates a new network, which is built in an unstressed condition and has no impact on the result of the test.

$$\dot{\sigma}_{ref,i} = E_{ref,0}\, p_{ref,i}\, \left(\dot{\varepsilon} - \dot{\varepsilon}^{th}_{ref}\right) \tag{57}$$

with

$$\varepsilon^{th}_{ref} = \alpha_{ref}\, (\theta - \theta_0) \tag{58}$$

Hence, the mechanical properties of inhomogeneously aged samples are described by a parallel connection of single models (Figure 50) which differ in the heterogeneous development of the ageing parameters p_{sci} and p_{ref}. Depending on the individual application, either the mechanical response of the sample as a whole is needed (e.g. for the design of a vibration absorber) or the maximum state of local ageing in the material is required when considering lifetime prediction or fatigue behaviour for example of sealings.

Besides their elastic behaviour, elastomers also show viscoelastic effects, which are considered via a serial connection of damper, spring and temperature elements (Maxwell elements) as shown in Figure 49. For the sake of completeness, the description of viscoelastic effects will be briefly introduced here. After applying external stress to the Maxwell element, the damper prevents the instantaneous response due to its viscous behaviour and the spring gets stretched. As time progresses, the stress in the spring provokes a relaxation of the Maxwell element until an equilibrium state is reached. In order to ensure a customisable modelling approach, which enables the adjustment of the model to various viscoelastic behaviours, several Maxwell elements can be connected in parallel as implied in Figure 49. According to Johlitz [38][67], the non-equilibrium stress of the k-th Maxwell element is

$$\sigma_{neq,k,i} = E_k\, \varepsilon^m_{e,k} = E_k \left(\varepsilon - \varepsilon^m_{in,k} - \varepsilon^{th}_k\right) \tag{59}$$

Equation (59) depicts a dependency of location i, however in this work it is assumed that there is no heterogeneous effect on viscoelasticity, that means $\sigma_{neq,k,i} = \sigma_{neq,k}$. Besides the distinction of deformation in a thermal and mechanical part, $\varepsilon^t_k h$ and ε^m_k, the latter is also split up in elastic $\varepsilon^m_{e,k}$ and inelastic strain $\varepsilon^m_{in,k}$. Elasticity is represented by the spring and inelasticity by a damper of viscosity η. Thermal deformation is treated as above

$$\varepsilon^{th}_k = \alpha_k\, (\theta - \theta_0) \tag{60}$$

The evaluation of the second principle of thermodynamics motivates the evolution equation

$$\dot{\varepsilon}^m_{in,k} = \frac{E_k}{\eta_k} \left(\varepsilon - \varepsilon^m_{in,k} - \varepsilon^{th}_k\right) \tag{61}$$

In order to consider the elastomer's thermoviscoelasticity, physical ageing effects as well as the changing behaviour of transiting the glass transition zone, an advanced Williams–Landel–Ferry (WLF) equation is used (Equation (62)). For further information see [38][67][132][133].

$$\eta_k = \eta_{0,k}\, e^{-C_3(f-f_{\theta_G})}\, e^{-\frac{C_1\,(\theta-\theta_G)}{C_2+(\theta-\theta_G)}} \tag{62}$$

Viscosity is described as a function of the free-volume f, which can be imagined as a dimensionless inner parameter characterising the macromolecules' mobility. In order to compute the progression of f the following evolution equation is used.

$$\dot{f} = \frac{1}{\tau}\,(f_\theta - f)) \tag{63}$$

τ refers to a specific relaxation time and f_θ is a reference value of free-volume, which is described by

$$f_\theta = f_{\theta_G} + \alpha_f\,(\theta - \theta_G) \tag{64}$$

The model is able to describe the temperature dependent properties as well as effects of physical ageing. It can easily be added to the elastic part described before and enables the simulation of viscoelastic material behaviour. Here, viscoelasticity is modelled without being influenced by any ageing effects [20]. That means that the inelastic behaviour is assumed to be the same over the whole sample without any influence of oxidation. The inelastic part of the tension $\sigma_{neq,k,i}$ is equally added to every section according to Equation (51).

6.2.2.2 Mooney Rivlin approach

Another way to describe the influence of heterogeneous oxidation on the mechanical properties of elastomers is a modified Mooney Rivlin approach which is a common method in polymer science [18][70][86]. With the elongation $\lambda = l/l_0$ and the material parameters C_1 and C_2 the stress strain relationship can be written as follows.

$$\sigma_{MR} = 2\,\left(C_1 + \frac{C_2}{\lambda}\right)\,\left(\lambda^2 - \lambda^{-1}\right) \tag{65}$$

The first material parameter, C_1 is directly linked to the elastomer's cross-linking density whereas C_2 is additionally influenced by the degree of molecular chain entanglement[18][86]. Hence, it is supposed here, that oxidation primarily influences the material parameter C_1. Another technical aspect, which is considered in the following equation, is the limitation of the network reformation

to an upper limit β according to Kari [79][80]. Thus, the network reformation is not able to fully compensate the chain scission process for $0 \leq \beta < 1$, since an upper limit is defined or dominates for $\beta > 1$. For the sake of clarity, a dependency of C_2 on oxidative processes is neglected but not precluded in this work. In Equation (66) the parameter C_1 is reduced by chain scission, which is represented by p_{sci}, and increased by network reformation p_{ref} up to a maximum of $\hat{p}_{ref}$. Both ageing parameters can evolve inhomogeneously, thereby leading to an inhomogeneous Mooney Rivlin stress σ_{MR}.

$$\sigma_{MR} = 2 \left(C_1 \ (1 - p_{sci} + p_{ref} \, \beta) + \frac{C_2}{\lambda} \right) \left(\lambda^2 - \lambda^{-1} \right) \tag{66}$$

Since the network reformation takes place in a state of no stress, Equation (66) has to be rewritten to consider this as follows.

$$\sigma_{MR} = 2 \left(C_1 \ (1 - p_{sci}) + \frac{C_2}{\lambda} \right) \left(\lambda^2 - \lambda^{-1} \right) + \int_0^t 2 \, C_1 \, p_{ref} \, \beta \, \left(\lambda^2 - \lambda^{-1} \right)^{\cdot} \mathrm{d}s \tag{67}$$

In order to describe the elastomers' overall answer, the tension is determined for all finite parts of the profile and subsequently added up to obtain the sample's total answer for one-dimensional cases.

$$\sigma_{total} = \sum_{n=1}^{nx} \sigma_{MR,i} \tag{68}$$

Although this is a one-dimensional approach and therefore does not represent the real condition, it highlights the fundamental behaviour of the influences of oxidation on elastomers. It can also be used as a foundation for modelling two or three-dimensional behaviour as well as for more advanced models combining further physical effects (e.g. an inhomogeneous temperature field in the sample) based on the modular structure.

6.2.3 Numerical implementation

6.2.3.1 Reaction-Diffusion equation (1D)

Equation (24), Equation (25) and Equation (26) are combined in a reaction-diffusion equation depicting the foundation of the heterogeneous oxidation in this work. By applying the product rule Equation (69) can be transformed into Equation (70).

$$\frac{\partial C}{\partial t} = \frac{\partial}{\partial x} \left(D_{ox} \frac{\partial C}{\partial x} \right) - \frac{C}{C_0} \left(r_{0,sci} \, e^{-\frac{E_{r,sci}}{R \, \theta}} + r_{0,ref} \, e^{-\frac{E_{r,ref}}{R \, \theta}} \right) \tag{69}$$

$$\frac{\partial C}{\partial t} = D_{ox}\frac{\partial C^2}{\partial^2 x} + \frac{\partial D_{ox}}{\partial x}\,\frac{\partial C}{\partial x} - \frac{C}{C_0}\left(r_{0,sci}\,e^{-\frac{E_{r,sci}}{R\,\theta}} + r_{0,ref}\,e^{-\frac{E_{r,ref}}{R\,\theta}}\right) \tag{70}$$

The numerical solution is realised by means of an implicit Cranck-Nicolson algorithm in combination with a central difference quotient. Subscript i represents the spatial and j the time variable. The oxygen concentration C which is used for the reaction rate on the right side is formulated as the average of the current and the subsequent timestep to retain the implicit method.

$$\begin{aligned}\frac{C_{ij+1} - C_{ij}}{\Delta t} &= D_{ij}\,\frac{C_{i+1j+1} - 2C_{ij+1} + C_{i-1j+1} + C_{i+1j} - 2C_{ij} + C_{i-1j}}{2\Delta x^2} \\ &+ \frac{D_{i+1j} - D_{i-1j}}{2\Delta x}\,\frac{C_{i+1j} - C_{i-1j} + C_{i+1j+1} - C_{i-1j+1}}{4\Delta x} \\ &- \frac{1}{2}\left(C_{ij} + C_{ij+1}\right)\frac{1}{C_0}\left(r_{0,sci}\,e^{-\frac{E_{r,sci}}{R\,\theta}} + r_{0,ref}\,e^{-\frac{E_{r,ref}}{R\,\theta}}\right)\end{aligned} \tag{71}$$

Equation (71) is transformed into Equation (72) to separate terms of the current time step from that of the subsequent one.

$$\begin{aligned}&\left[\frac{1}{\Delta t} + \frac{D_{ij}}{\Delta x^2} + \frac{1}{2C_0}\left(r_{0,sci}\,e^{-\frac{E_{r,sci}}{R\,\theta}} + r_{0,ref}\,e^{-\frac{E_{r,ref}}{R\,\theta}}\right)\right] C_{ij+1} \\ &\quad - \left(\frac{D_{ij}}{2\Delta x^2} + \frac{D_{i+1j} - D_{i-1j}}{8\Delta x^2}\right) C_{i+1j+1} - \left(\frac{D_{ij}}{2\Delta x^2} - \frac{D_{i+1j} - D_{i-1j}}{8\Delta x^2}\right) C_{i-1j+1} \\ &\quad = \left[\frac{1}{\Delta t} - \frac{D_{ij}}{\Delta x^2} - \frac{1}{2C_0}\left(r_{0,sci}\,e^{-\frac{E_{r,sci}}{R\,\theta}} + r_{0,ref}\,e^{-\frac{E_{r,ref}}{R\,\theta}}\right)\right] C_{ij} \\ &\quad + \left(\frac{D_{ij}}{2\Delta x^2} + \frac{D_{i+1j} - D_{i-1j}}{8\Delta x^2}\right) C_{i+1j} + \left(\frac{D_{ij}}{2\Delta x^2} - \frac{D_{i+1j} - D_{i-1j}}{8\Delta x^2}\right) C_{i-1j}\end{aligned} \tag{72}$$

Hence, the problem can also be written with the tridiagonal matrix $[\mathbf{A}]$ in the form

$$[\mathbf{A}]C_{ij+1} = [\mathbf{B}]C_{ij} + [d] \tag{73}$$

$$[\mathbf{A}] = \begin{bmatrix} b_1 & c_1 & 0 & & & & \\ a_2 & b_2 & c_2 & \dots & & 0 & \\ 0 & a_3 & b_3 & & & & \\ & \vdots & & \ddots & & \vdots & \\ & & & & b_{nx-2} & c_{nx-2} & 0 \\ & 0 & & \dots & a_{nx-1} & b_{nx-1} & c_{nx-1} \\ & & & & 0 & a_{nx} & b_{nx} \end{bmatrix} \tag{74}$$

According to Equation (72) the elements of Equation (73) and Equation (74) are defined as following

$$a_i = -\Big(\frac{D_{ij}}{2\Delta x^2} - \frac{D_{i+1j} - D_{i-1j}}{8\Delta x^2}\Big) \tag{75}$$

$$b_i = \frac{1}{\Delta t} + \frac{D_{ij}}{\Delta x^2} + \frac{1}{2C_0}\left(r_{0,sci}\, e^{-\frac{E_{r,sci}}{R\,\theta}} + r_{0,ref}\, e^{-\frac{E_{r,ref}}{R\,\theta}}\right) \tag{76}$$

$$c_i = -\Big(\frac{D_{ij}}{2\Delta x^2} + \frac{D_{i+1j} - D_{i-1j}}{8\Delta x^2}\Big) \tag{77}$$

and the right-hand side

$$\begin{aligned}[\mathbf{B}]C_{ij} + [d] = &\left[\frac{1}{\Delta t} - \frac{D_{ij}}{\Delta x^2} - \frac{1}{2C_0}\left(r_{0,sci}\, e^{-\frac{E_{r,sci}}{R\,\theta}} + r_{0,ref}\, e^{-\frac{E_{r,ref}}{R\,\theta}}\right)\right] C_{ij} \\ &+ \Big(\frac{D_{ij}}{2\Delta x^2} + \frac{D_{i+1j} - D_{i-1j}}{8\Delta x^2}\Big)\, C_{i+1j} + \Big(\frac{D_{ij}}{2\Delta x^2} - \frac{D_{i+1j} - D_{i-1j}}{8\Delta x^2}\Big)\, C_{i-1j}\end{aligned} \tag{78}$$

Subsequently a LU-factorisation of matrix $[\mathbf{A}]$ is executed and the right-hand side is updated to include boundary conditions. As already mentioned, a constant oxygen concentration C_0 is assumed in the ambient environment. Hence, Dirichlet boundary conditions are used.

Further, in every single time step the diffusion coefficient is updated by Equation (44) or rather Equation (45). Therefore, the ageing parameters are needed which are derived according to the evolution equations mentioned (Equation (40) and Equation (41)). The evolution equations are solved numerically by means of the implicit finite difference method which reads for the chain scission as follows.

$$\frac{p_{sci,ij+1} - p_{sci,ij}}{\Delta t} = v_{p,sci}\, e^{-\frac{E_{p,sci}}{R\,\theta}}\, (1 - p_{sci,ij+1})\, \frac{r_{ox,sci}}{r_{ox,sci,0}} \tag{79}$$

$$p_{sci,ij+1} = \frac{p_{sci,ij} + \Delta t\, v_{p,sci}\, e^{-\frac{E_{p,sci}}{R\,\theta}}\, \frac{C_{ij}}{C_0}\, \frac{r_{o,sci}}{r_{ox,sci,0}}\, e^{-\frac{E_{r,sci}}{R\,\theta}}}{1 + \Delta t\, v_{p,sci}\, e^{-\frac{E_{p,sci}}{R\,\theta}}\, \frac{C_{ij}}{C_0}\, \frac{r_{o,sci}}{r_{ox,sci,0}}\, e^{-\frac{E_{r,sci}}{R\,\theta}}} \tag{80}$$

The numerical solution for the network reformation is implemented the same way and is therefore not shown here.

6.2.3.2 Rheological model (1D)

While the tension's chain scission part σ_{eq} can be easily calculated by means of Equation (54) since ageing parameter p_{sci} is obtained from the reaction-diffusion equation, the network reformation part σ_{neq} of the tension is formulated as a rate expression (Equation (57)). Therefore, the latter is solved by means of an implicit finite difference method.

$$\frac{\sigma_{ref,ij+1} - \sigma_{ref,ij}}{\Delta t} = E_{ref,0}\, p_{sci,j} \left(\frac{\varepsilon_{ij+1} - \varepsilon_{ij}}{\Delta t} - \frac{\varepsilon^{th}_{ref,ij+1} - \varepsilon^{th}_{ref,ij}}{\Delta t} \right) \tag{81}$$

With the assumption that temperature does not change over time of exposure the last term of Equation (81) disappears and the stress of the next time step is calculated by

$$\sigma_{ref,ij+1} = \sigma_{ref,ij} + E_{ref,0}\, p_{sci,j} (\varepsilon_{ij+1} - \varepsilon_{ij}) \tag{82}$$

6.2.3.3 Mooney Rivlin (1D)

In order to solve the Mooney Rivlin equation for every section i (Figure 50) Equation (66) is rewritten and split up into two additional parts. Then the network reformation part can be transformed in a tension rate expression and solved numerically. After this the two parts are recombined.

The first part of the stress equation considers chain scission and entanglement.

$$\sigma_{1,ij} = 2 \left(C_1 (1 - p_{sci,ij}) + \frac{C_2}{\lambda_{ij}} \right) (\lambda_{ij}^2 - \lambda_{ij}^{-1}) \tag{83}$$

The second part considers the network reformation and is transformed in a tension rate expression.

$$\sigma_{2,ij} = \int_0^t 2C_1\, p_{ref,ij}\, \hat{p}_{ref}\, (\lambda_{ij}^2 - \lambda_{ij}^{-1})^{\cdot}\, ds \tag{84}$$

$$\dot{\sigma}_{2,ij} = 2C_1\, p_{ref,ij}\, \hat{p}_{ref}\, (\lambda_{ij}^2 - \lambda_{ij}^{-1})^{\cdot} \tag{85}$$

The tension rate expression is solved by means of finite difference method.

$$\frac{\sigma_{2ij+1} - \sigma_{2ij}}{\Delta t} = 2C_1\, p_{ref,ij}\, \hat{p}_{ref} \frac{(\lambda_{ij+1}^2 - \lambda_{ij+1}^{-1}) - (\lambda_{ij}^2 - \lambda_{ij}^{-1})}{\Delta t} \tag{86}$$

$$\sigma_{2ij+1} = \sigma_{2ij} + 2C_1\, p_{ref,ij}\, \hat{p}_{ref} \left((\lambda_{ij+1}^2 - \lambda_{ij+1}^{-1}) - (\lambda_{ij}^2 - \lambda_{ij}^{-1}) \right) \tag{87}$$

Finally, the two parts, which were only split due to numerical reasons, are brought back togheter.

$$\sigma_{MR,ij} = \sigma_{1,ij} + \sigma_{2,ij} \tag{88}$$

6.2.3.4 Reaction-Diffusion equation (2D)

In order to get a better understanding of heterogeneous ageing the output of the model being introduced, is visualised in two dimensions. That means ageing parameters are calculated and plotted over the whole cross-section of a bar shaped sample. Therefore, the model introduced above is modified for two dimensional cases and solved by means of the Alternating Direction Implicit (ADI) method.

Hence, diffusion-reaction equation was written for two dimensions.

$$\begin{aligned} \frac{\partial C(x,y,t)}{\partial t} = \frac{\partial}{\partial x}\left(D_{ox}(x,y,t)\, \frac{\partial C(x,y,t)}{\partial x} \right) + \frac{\partial}{\partial y}\left(D_{ox}(x,y,t)\, \frac{\partial C(x,y,t)}{\partial y} \right) \\ - r_{ox,sci}(C,\theta) - r_{ox,ref}(C,\theta) \end{aligned} \tag{89}$$

$$\frac{\partial C}{\partial t} = D_{ox}\, \frac{\partial C^2}{\partial^2 x} + \frac{\partial D_{ox}}{\partial x}\, \frac{\partial C}{\partial x} + D_{ox}\, \frac{\partial C^2}{\partial^2 y} + \frac{\partial D_{ox}}{\partial y}\, \frac{\partial C}{\partial y} - \frac{C}{C_0} \left(r_{0,sci}\, e^{-\frac{E_{r,sci}}{R\,\theta}} + r_{0,ref}\, e^{-\frac{E_{r,ref}}{R\,\theta}} \right) \tag{90}$$

Here, oxygen concentration C is a function of the location in x and y direction as well as the ageing duration. Further equations and relationships are the same as those chosen for the one-dimensional case, reaction rates are calculated according to Equation (36) and Equation (37), changing diffusivity is described by Equation (44). Equation (40) and Equation (41) represent the evolution of the ageing parameters.

The Crank-Nicolson method is standard practice for one-dimensional problems. The solution is quite straightforward for one-dimensional problems since a tridiagonal system has to be solved for every time step, which is a fast and attainable way. Solving two-dimensional problems is possible but it is not trivial since the implicit method requires the solution of a two-dimensional Poisson

equation which is much more complicated and effortful to solve. An alternative is provided by the Alternating Direction Implicit (ADI) method which splits every time step up in two single steps. This method is also known as the implicit Peaceman-Rachford algorithm of alternating directions [134]. This numerical procedure works in such a way that a 2D problem is transformed into two 1D problems which can be solved with an implicit approach. In summary this means the numerical solution can be simplified to two tridiagonal systems per time step where first the concentration is calculated in the x-direction and then the y-direction [135].

Here, the ADI method is used to solve the reaction-diffusion equation (Equation (90)) of the model shown above. The solution is achieved by separating the partial differential equation into two steps. The first step provides the oxygen concentration C in the intermediate time step $m+\frac{1}{2}$. i and j are used as variables to describe location dependency in the x and y direction.

$$\begin{aligned} C_{i,j}^{m+\frac{1}{2}} = C_{i,j}^{m} &+ \frac{D_{ox}{}_{i,j}^{m}\,\Delta t}{2h^2}\left(C_{i-1,j}^{m+\frac{1}{2}} + C_{i+1,j}^{m+\frac{1}{2}} - 2C_{i,j}^{m+\frac{1}{2}} + C_{i,j-1}^{m} + C_{i,j+1}^{m} - 2C_{i,j}^{m}\right) \\ &+ \frac{\Delta t}{2\Delta x^2}\left(D_{i+1,j}^{m} - D_{i,j}^{m}\right)\left(C_{i+1,j}^{m+\frac{1}{2}} - C_{i,j}^{m+\frac{1}{2}}\right) \\ &+ \frac{\Delta t}{2\Delta y^2}\left(D_{i,j+1}^{m} - D_{i,j}^{m}\right)\left(C_{i,j+1}^{m} - C_{i,j}^{m}\right) \\ &- \frac{\Delta t}{4}\left(C_{i,j}^{m+\frac{1}{2}} + C_{i,j}^{m}\right)\left(\frac{r_{0,sci}}{C_0}\,e^{-\frac{E_{r,sci}}{R\,\theta}} + \frac{r_{0,ref}}{C_0}\,e^{-\frac{E_{r,ref}}{R\,\theta}}\right) \end{aligned} \tag{91}$$

Since Equation (91) is used for the calculation of the oxygen concentration at an interim time-step of $m+\frac{1}{2}$, $\frac{1}{2}\Delta t$ represents the half duration between two time steps. The concentration $C_{i,j}^{m+\frac{1}{2}}$ is an interim solution used by the ADI method and calculated at every grid point of the area with $i,j = 1,\ldots,$N. N stands for the number of grid points in the x and y direction and h represents the constant distance between two points in the horizontal as well as the vertical direction. The diffusion coefficient is updated every complete time step according to Equation (44) and assumed to be constant over a single iteration step. The oxygen concentration used for the reaction term is chosen as a mixture of the explicit and implicit calculation.

After the interim concentration $C^{m+\frac{1}{2}}$ is obtained by Equation (91) ADI method uses a second step to calculate the final oxygen concentration C^{m+1} after an entire time-step.

$$
\begin{aligned}
C_{i,j}^{m+1} = C_{i,j}^{m+\frac{1}{2}} &+ \frac{D_{ox}{}_{i,j}^{m}\,\Delta t}{2h^2}\left(C_{i,j-1}^{m+1} + C_{i,j+1}^{m+1} - 2C_{i,j}^{m+1} + C_{i-1,j}^{m+\frac{1}{2}} + C_{i+1,j}^{m+\frac{1}{2}} - 2C_{i,j}^{m+\frac{1}{2}}\right) \\
&+ \frac{\Delta t}{2\Delta x^2}\left(D_{i+1,j}^{m} - D_{i,j}^{m}\right)\left(C_{i+1,j}^{m+\frac{1}{2}} - C_{i,j}^{m+\frac{1}{2}}\right) \\
&+ \frac{\Delta t}{2\Delta y^2}\left(D_{i,j+1}^{m} - D_{i,j}^{m}\right)\left(C_{i,j+1}^{m+1} - C_{i,j}^{m+1}\right) \\
&- \frac{\Delta t}{4}\left(C_{i,j}^{m+\frac{1}{2}} + C_{i,j}^{m+1}\right)\left(\frac{r_{0,sci}}{C_0}\,e^{-\frac{E_{r,sci}}{R\,\theta}} + \frac{r_{0,ref}}{C_0}\,e^{-\frac{E_{r,ref}}{R\,\theta}}\right)
\end{aligned}
\tag{92}
$$

The calculation of Equation (91) contains the solution of N tridiagonal equation-system using some summarised expressions (Equation (93), Equation (94) and Equation (95)) for better readability.

$$
\alpha_{i,j} = \frac{D_{ox}{}_{i,j}^{m}\,\Delta t}{h^2} \tag{93}
$$

and

$$
\beta_{sci} = \frac{r_{0,sci}}{C_0}\,e^{-\frac{E_{r,sci}}{R\,\theta}} \tag{94}
$$

and

$$
\beta_{ref} = \frac{r_{0,ref}}{C_0}\,e^{-\frac{E_{r,ref}}{R\,\theta}} \tag{95}
$$

$$
\begin{aligned}
&-\frac{\alpha_{i,j}}{2}\,C_{i-1,j}^{m+\frac{1}{2}} + \left(1 + \alpha_{i,j} + \frac{\Delta t}{4}\,\beta_{sci} + \frac{\Delta t}{4}\,\beta_{ref} + \left(\frac{\alpha_{i+1,j}}{2} - \frac{\alpha_{i,j}}{2}\right)\right) C_{i,j}^{m+\frac{1}{2}} \\
&\qquad + \left(-\frac{\alpha_{i,j}}{2} - \left(\frac{\alpha_{i+1,j}}{2} - \frac{\alpha_{i,j}}{2}\right)\right) C_{i+1,j}^{m+\frac{1}{2}} \\
&\qquad = \frac{\alpha_{i,j}}{2}\,C_{i,j-1}^{m+\frac{1}{2}} + \left(1 - \alpha_{i,j} - \frac{\Delta t}{4}\,\beta_{sci} - \frac{\Delta t}{4}\,\beta_{ref} - \left(\frac{\alpha_{i,j+1}}{2} - \frac{\alpha_{i,j}}{2}\right)\right) C_{i,j}^{m} \\
&\qquad + \left(\frac{\alpha_{i,j}}{2} + \left(\frac{\alpha_{i+1,j}}{2} - \frac{\alpha_{i,j}}{2}\right)\right) C_{i,j+1}^{m}
\end{aligned}
\tag{96}
$$

Analogously to this, the solution of Equation (92) contains another N tridiagonal equation system (Equation (97)).

$$
\begin{aligned}
&-\frac{\alpha_{i,j}}{2}\, C_{i,j-1}^{m+1} + \left(1 + \alpha_{i,j} + \frac{\Delta t}{4}\,\beta_{sci} + \frac{\Delta t}{4}\,\beta_{ref} + \left(\frac{\alpha_{i,j+1}}{2} - \frac{\alpha_{i,j}}{2}\right)\right) C_{i,j}^{m+1} \\
&\qquad + \left(-\frac{\alpha_{i,j}}{2} - \left(\frac{\alpha_{i,j+1}}{2} - \frac{\alpha_{i,j}}{2}\right)\right) C_{i,j+1}^{m+1} \\
&\qquad = \frac{\alpha_{i,j}}{2}\, C_{i-1,j}^{m+\frac{1}{2}} + \left(1 - \alpha_{i,j} - \frac{\Delta t}{4}\,\beta_{sci} - \frac{\Delta t}{4}\,\beta_{ref} - \left(\frac{\alpha_{i+1,j}}{2} - \frac{\alpha_{i,j}}{2}\right)\right) C_{i,j}^{m+\frac{1}{2}} \\
&\qquad + \left(\frac{\alpha_{i,j}}{2} + \left(\frac{\alpha_{i+1,j}}{2} - \frac{\alpha_{i,j}}{2}\right)\right) C_{i+1,j}^{m+\frac{1}{2}}
\end{aligned}
\tag{97}
$$

As a result, 2N tridiagonal systems of dimension N must be solved at every time step to get from m to $m+1$ when using the ADI method, which can be solved by Thomas algorithm. The coefficient matrix differs for each tridiagonal system since the $\alpha_{i,j}$ depend on $D_{ox}{}_{i,j}^{m}$ which is a function of location and time. After finishing the calculation of a single time step the oxygen concentration $C_{i,j}$ with $i,j = 1,\ldots,$N is obtained which is used to update the ageing parameters $E_{p,sci}$ and $E_{p,ref}$ and subsequently the diffusion coefficient D_{ox} at every grid point. The ADI method is unconditional stable and its accuracy is of second order with respect to time and space [135].

6.2.3.5 Linkage of oxygen absorption and diffusion-reaction behaviour (2D)

The total amount of oxygen being absorbed by an elastomer sample during ageing is the sum of the entire amount of oxygen being currently solved in the elastomer and all oxygen molecules ever reacted with the elastomer. The former is calculated by the summation of the present oxygen at every spatial element of the whole sample. This is done by multiplication of the oxygen concentration with the volume [mol/m^3] or rather the area [mol/m^2] of every element and summing them up.

$$
{m_{ox,di}}^{m} = \iiint C\, dV = \Delta x^2 \sum_{i=1}^{N} \sum_{j=1}^{N} C_{i,j}^{m} \tag{98}
$$

The total amount of oxygen reacted after absorption is calculated by summing up the consumption of every previous time step since the start of exposure.

$$
m_{ox,re} = \int_0^t \iiint \left(r_{ox,sci} + r_{ox,ref} + r_{aox}\right) dV\, dt \tag{99}
$$

With m being the number of timesteps and the neglect of any antioxidant Equation (99) reads as follows.

$$m_{ox,re}{}^{m} = \Delta t \sum_{t=1}^{m} \left(\Delta x^2 \sum_{i=1}^{N} \sum_{j=1}^{N} (r_{ox,sci}{}_{i,j}^{t} + r_{ox,ref}{}_{i,j}^{t}) \right) \tag{100}$$

with

$$r_{ox,sci}{}_{i,j}^{t} = \frac{C_{i,j}^{t}}{C_0} \, r_{0,sci} \, e^{-\frac{E_{r,sci}}{R\,\theta}} \, (1 - p_{sci}{}_{i,j}^{t}) = C_{i,j}^{t} \, \beta_{sci} \, (1 - p_{sci}{}_{i,j}^{t}) \tag{101}$$

and

$$r_{ox,ref}{}_{i,j}^{t} = \frac{C_{i,j}^{t}}{C_0} \, r_{0,ref} \, e^{-\frac{E_{r,ref}}{R\,\theta}} \, (1 - p_{ref}{}_{i,j}^{t}) = C_{i,j}^{t} \, \beta_{ref} \, (1 - p_{ref}{}_{i,j}^{t}) \quad . \tag{102}$$

Equation (101) and Equation (102) use the modified reaction equation introduced in Equation (38) and Equation (39). Without this the saturation effect could not be described as explained in paragraph 6.2.1.2. This was a finding which was determined during the development of this work. The model also works with the reaction rate shown in Equation (36) and Equation (37) but calculating the oxygen absorption was not possible since the saturation effects mentioned, were considered by a different part of the model (evolution equations). The modified reaction rate formulation must be used for the whole model which means it has to be used for the diffusion reaction equation as well. This is not shown here for reasons of clarity. When applied later in this work it will be addressed and discussed further.

The amount of absorbed oxygen can be plotted over the ageing duration and represents a by-product of the model. The result can be used to compare the model output with oxygen consumption tests.

6.2.4 Results

6.2.4.1 Heterogeneous oxidation

The model introduced above is illustrated here with plots of representative parameters. Input variables are chosen in the scale of previous works [38][84] and adjusted to provide a comprehensive view of the intention of the model. Due to significance of temperature on the oxidative ageing of elastomers, five different ageing temperatures were modelled and compared. Unless otherwise stated, Equation (36) and Equation (37) are used for reaction terms, Equation (44) is used for the diffusion coefficient and effects of antioxidants are neglected. The parameters are chosen as stated in Table 4.

Table 4: Parameters used for modelling of heterogeneous oxidation profiles in Figure 51

D_o [m^2/s]	4.0×10^{-2}	E_D [J/mol]	10	t_{max} [s]	1000
$r_{o,sci}$ [mol/l/s]	100	$r_{o,ref}$ [mol/l/s]	100	L [−]	1
$E_{r,sci}$ [J/mol]	20000	$E_{r,ref}$ [J/mol]	20000	$E_{sci,0}$ [MPa]	2.0
$\nu_{p,sci}$ [1/s]	380	$\nu_{p,ref}$ [1/s]	380	$E_{ref,0}$ [MPa]	15.0
$E_{p,sci}$ [J/mol]	32000	$E_{p,ref}$ [J/mol	30000		

The ageing temperatures are chosen at 293, 323, 373, 423 and 473 Kelvin. 293 K (20 °C) ambient temperature is shown as a reference since below this temperature oxidation of elastomers is highly decelerated and less relevant. Higher temperatures are chosen in equidistant steps beginning from 323 K (50 °C). According to previous work [84] the first visualisation of the model is done by plotting the ageing parameter p_{sci} as a function of the one-dimensional location in the sample, the ageing temperature and the ageing duration (Figure 51). Since the parameters are chosen to be almost equal for both chain-scission and network reformation (Table 4) the outputs p_{sci} and p_{ref} appear almost the same and hence the latter are neglected here. In this case the only difference consists in the activation energies $E_{p,sci}$ and $E_{p,ref}$. Of course, assuming r_o, E_r and ν_p to be totally equal for both processes of chain scission and network reformation does not correspond to reality.

The maximum ageing duration shown in Figure 51 is 1000 seconds which is a fictitious value and used only to show the basic functionality of the model. Of course, this ageing time cannot be compared to real ageing behaviour of elastomers. For fitting the model to experimental data, the numerical values of the model can be adjusted, accordingly the oxidation is described on a longer time scale.

Figure 51 shows conclusively the influence of temperature on the oxidation behaviour. Below a certain temperature, oxidation is only slightly pronounced and almost homogeneously distributed over the sample (293 K and 323 K). When the temperature is increased, the activation energies are exceeded and the oxidative reactions as well as diffusivity are increased relevantly. Elevated temperatures do not only accelerate the diffusivity but also may cause a decline due to oxidative reactions which further results in a more inhomogeneous distribution of oxidation. For 373 K the diffusivity is decreased to a level where in the core of the sample oxidation is almost stopped after a duration of approximately 600 seconds. At even higher temperatures (here 423 and 473 K) the diffusion coefficient decreases in such a way that diffusion is reduced to a minimum by the progress of ageing. Thus, DLO (subsection 4.3) occurs and prevents oxygen from further diffusion into the interior of the sample. For 473 K the maximum level of ageing is reached after 40 to 80 seconds and thus no subsequent oxidative reactions take place in the core of the material.

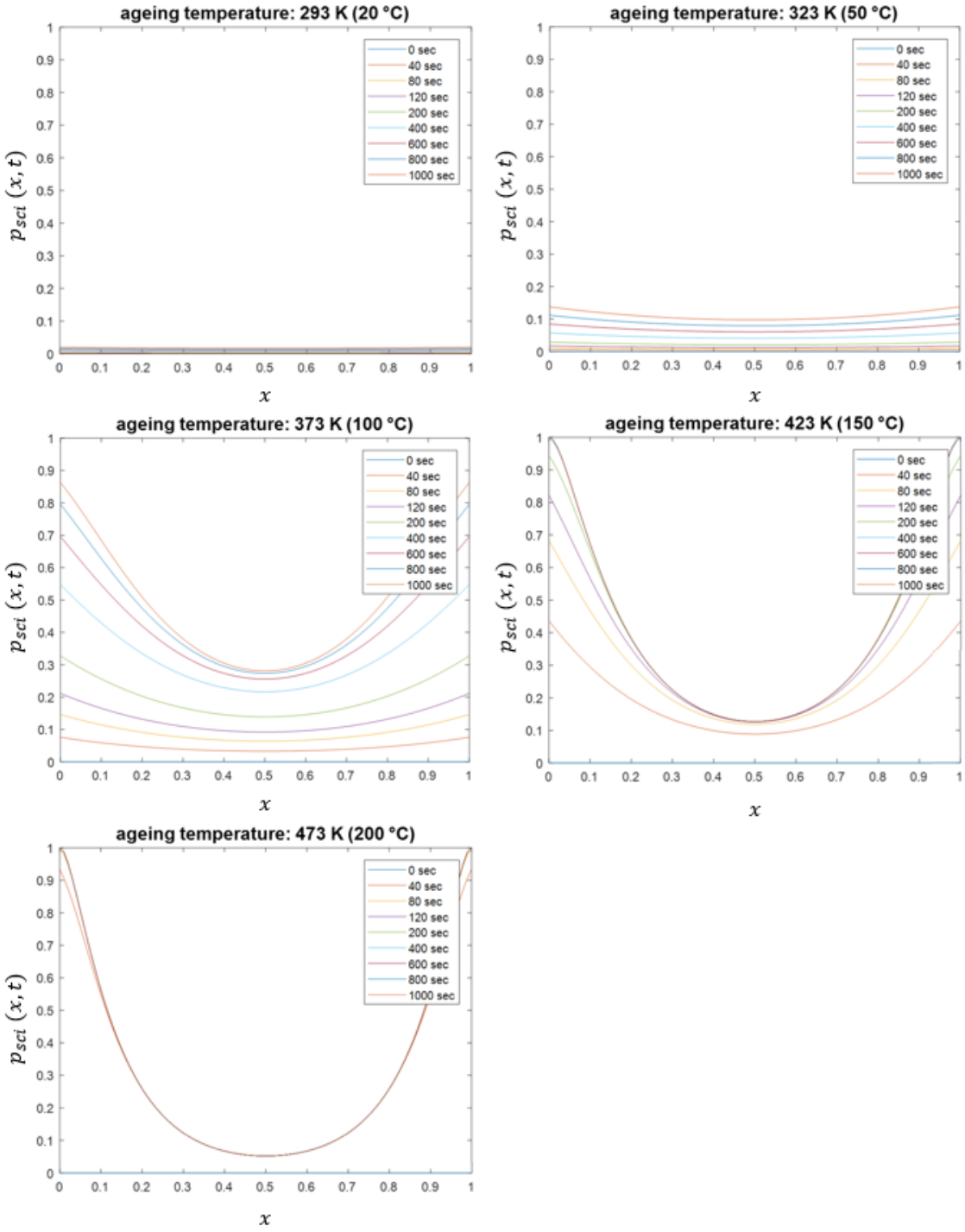

Figure 51: Ageing parameter for chain scission p_{sci} plotted for different ageing temperatures as a function of ageing duration and the location x in the sample

This becomes even clearer by examining the oxygen concentration profiles during the progress of oxidation. Figure 52 shows the profiles of dissolved oxygen in the elastomer for 373 K and 473 K. For the chosen set of parameters, the diffusion process dominates at the beginning of exposure and the highest oxygen concentration is reached shortly after ageing starts. While there are also oxidative reactions occurring at the beginning of the ageing process, enough oxygen is provided

by diffusion to increase the oxygen concentration even in the centre of the sample. In the ongoing process, oxygen is consumed by oxidative reactions and the diffusivity decreases. Consequently, less oxygen is provided by diffusion than is consumed by chemical reaction, which reduces the oxygen concentration. At 473 K the initial oxidation rate is so high that a high amount of oxygen is consumed, and deeper diffusion decelerated. After a very short period the surface layer is fully aged and hence diffusivity almost diminished. For such high temperatures, DLO inhibits oxygen from reaching the core region of the sample.

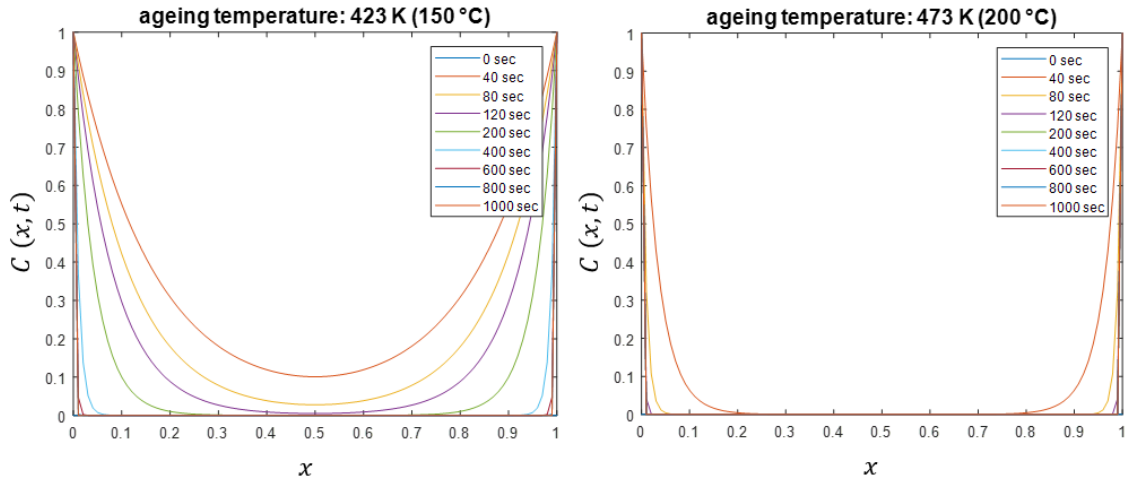

Figure 52: Oxygen concentration plotted for temperatures 373 K and 473 K as a function of ageing duration and the location x in the sample

To further investigate the present results, the visualisation of a cross section in the sample is used. This follows the same principles and applies the same model as for one-dimensional graphs but employs a different numerical solution as shown in paragraph 6.2.3.4. Two dimensional plotting offers the opportunity to establish a comprehensive visual impression of thermo-oxidative ageing of a bar-shaped sample's cross-section and DLO. Especially coloured visualisation of the ageing parameters by means of heat mapping helps to understand the effects of diffusion-reaction behaviour. Figure 53 gives an example for the spatial development of the ageing parameter p_{sci} as a function of temperature and ageing time. Duration and temperature are chosen as published in a previous work [136]. To improve the amount of information only, the number of time steps was reduced, and ageing duration was extended for Figure 53. This produces a clear graphic rendition, where different time-steps and temperatures can be compared and all mentioned effects can be observed.

Besides equidistant plots up to 1000 s, further plots showing p_{sci} after 5000 s are added. As a first snapshot, ageing states after 330 s are shown in the first column which clearly present the effect of temperature. While oxidation progresses steadily towards the interior of the sample for 20 °C and 60 °C, elevated temperatures provoke a different behaviour. As expected, the initial oxidation rate is higher for 100 °C but after 660 s the ageing state shows to be changing less rapidly. The same can be observed for 150 °C where minimal alterations are noticeable between the plotted timesteps. Regarding the column of 5000 s highlights clearly the effect of DLO on

the ageing parameter p_{sci} and shows that higher temperatures are not necessarily accompanied with a higher oxidation level.

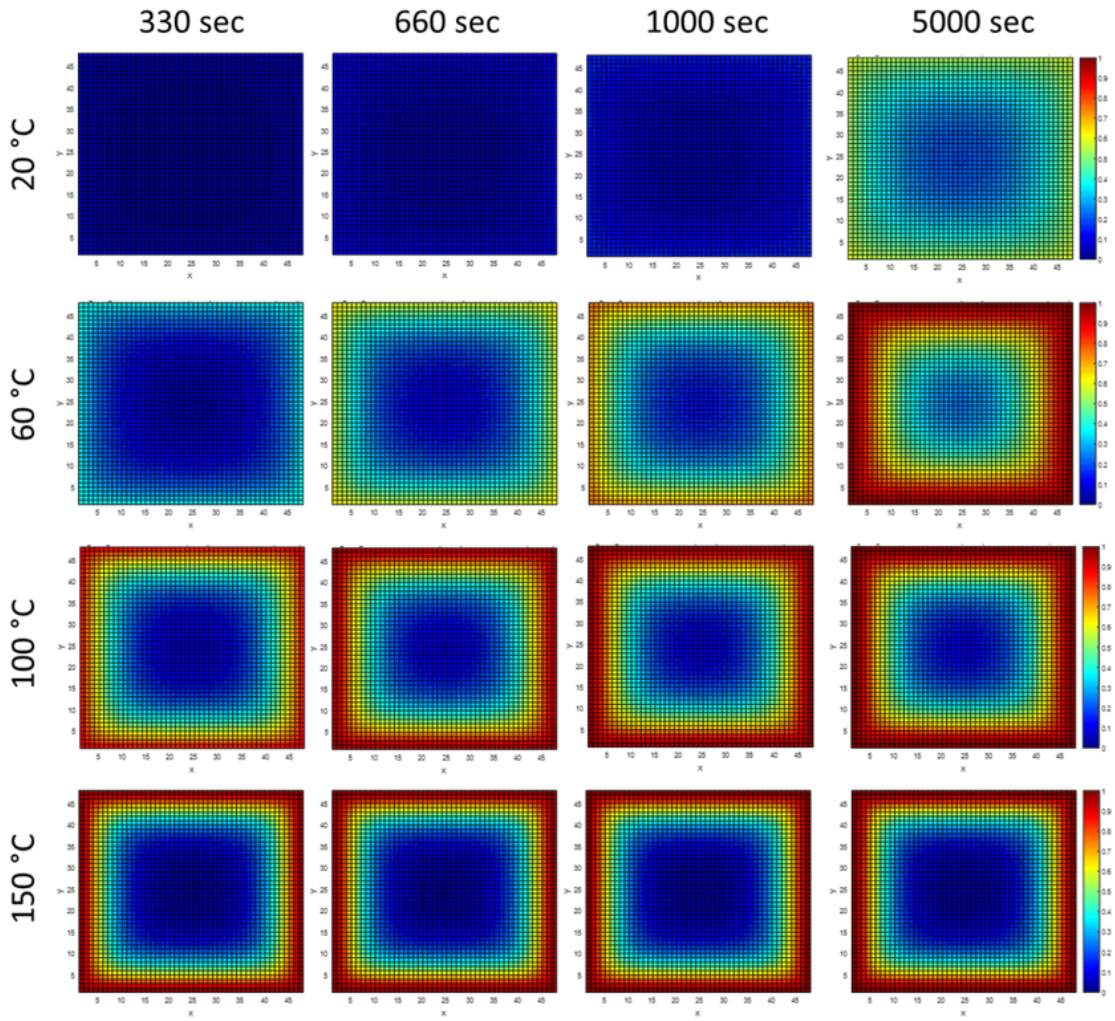

Figure 53: 2D-plot of the ageing parameter p_{sci} for different ageing temperatures and durations

6.2.4.2 Mechanical properties

The created profiles of p_{sci} and p_{ref} are also used as an input for the description of the mechanical properties of aged elastomer according to Equation (54) and Equation (56). Viscoelasticity is not taken into consideration at this point for reasons of clarity. Since it is assumed that network reformation takes place under a condition of no stress, the method of mechanical loading during the ageing process has to be taken into account. Therefore, the sample is loaded by strain-controlled deformations during thermal exposure displayed in Figure 54. In the first case the sample is spontaneously deformed to a strain level of 10 % from 100 seconds on until the end of ageing duration. In the second case the sample is aged stress- and strain-less and 10 % deformation is applied at the end of the ageing progress.

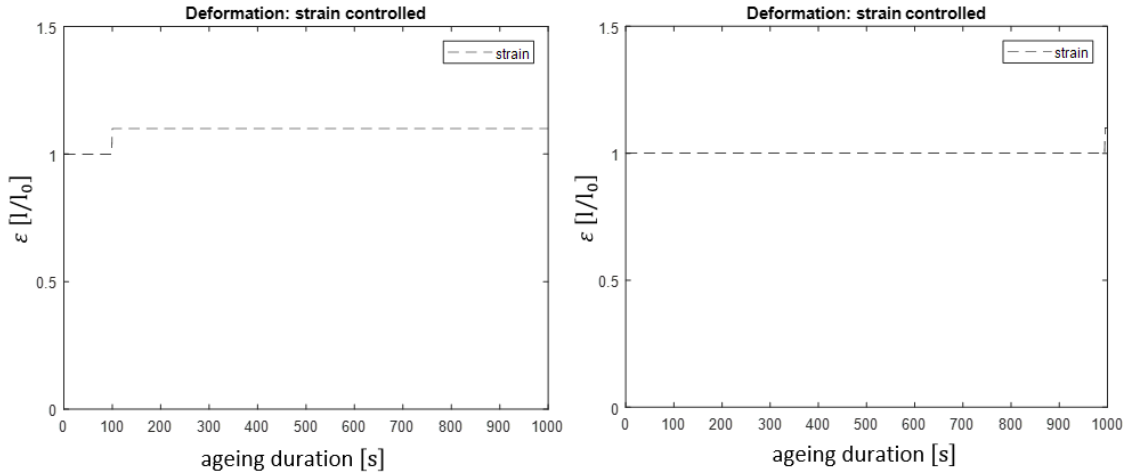

Figure 54: Strain controlled deformation during exposure to visualise different impacts of network reformation; left 54.1: stretching the sample by 10 % after 100 s, right 54.2: stretching the sample by 10 % at the end of exposure (intermittent relaxation)

Figure 55 shows the tension profiles after the sample's exposure according to Figure 54.1. The contribution from chain scission σ_{sci} and network reformation σ_{ref} are plotted as well as the final tension profile σ_{total}. For the case of deformation at the beginning of exposure (ageing duration = 0 s), a network reformation contribution does not exist.

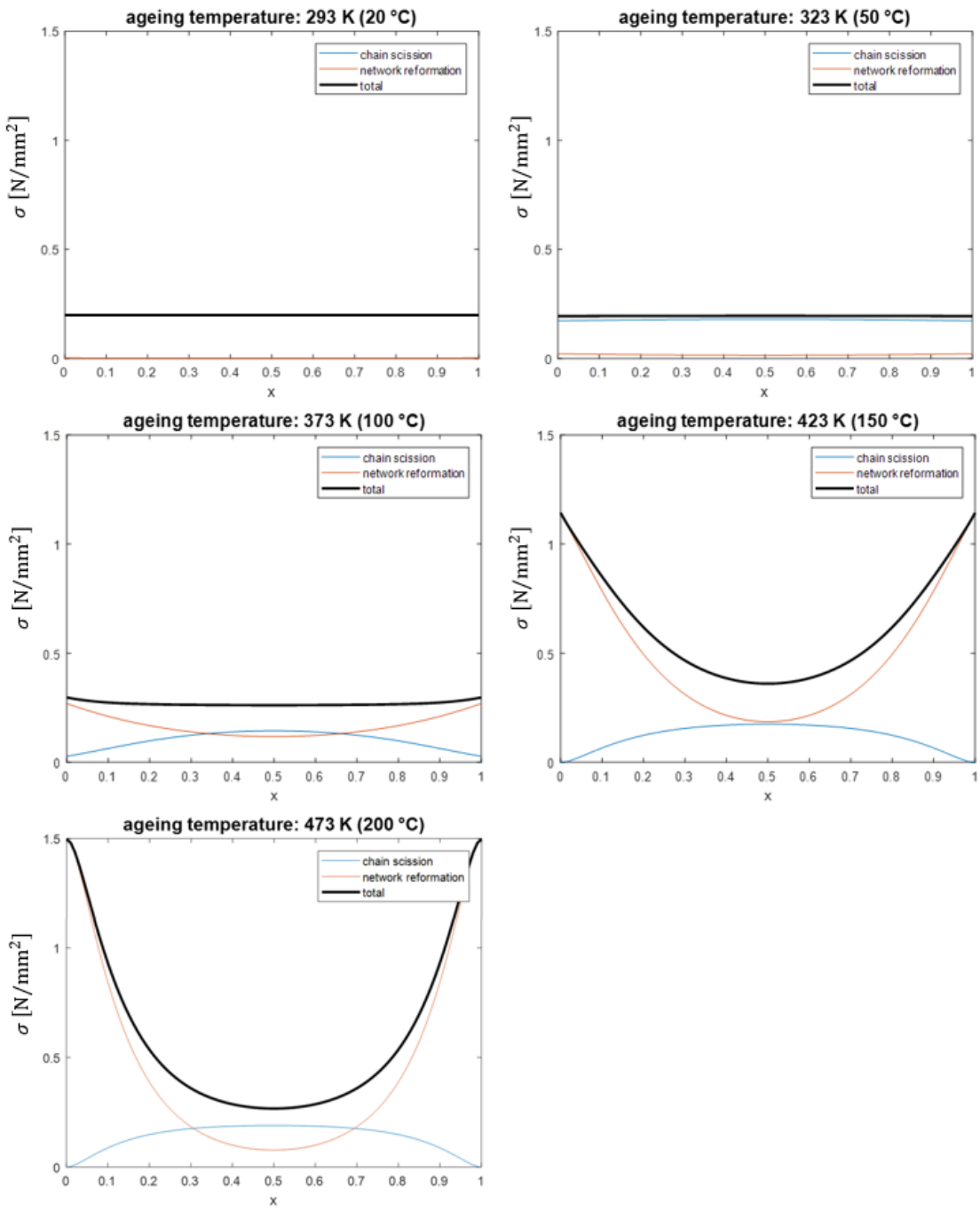

Figure 55: Tension profiles of chain scission, network reformation and the resulting tension after ageing for 1000 s at different temperatures. Strain was applied according to Figure 54.1.

In order to clarify the influence of the ageing temperature, the resulting tension profiles are plotted together in one diagram (Figure 56). The higher the temperature is the more pronounced become the heterogeneous material properties. As already discussed for the ageing parameters, oxidation starts only if the temperature exceeds a certain threshold. The plot represents the local tension in the sample when assuming a unidirectional stretching with the ends of the sample firmly clamped, for instance by gluing the elastomer to steel plates (see Figure 56).

Figure 56 illuminates that for elastomers which are exposed to elevated temperatures a reliable lifetime prediction is only possible by considering potential heterogeneous ageing effects. As depicted in the graph, the increased stiffness at the surface regions has a significant influence on the overall tensile behaviour as well as on the fatigue behaviour of the whole sample. Although the changes of the entire mechanical properties can still be no issue the high stresses at the surface may provoke crack formation or adhesion failure of an adhesive sealing.

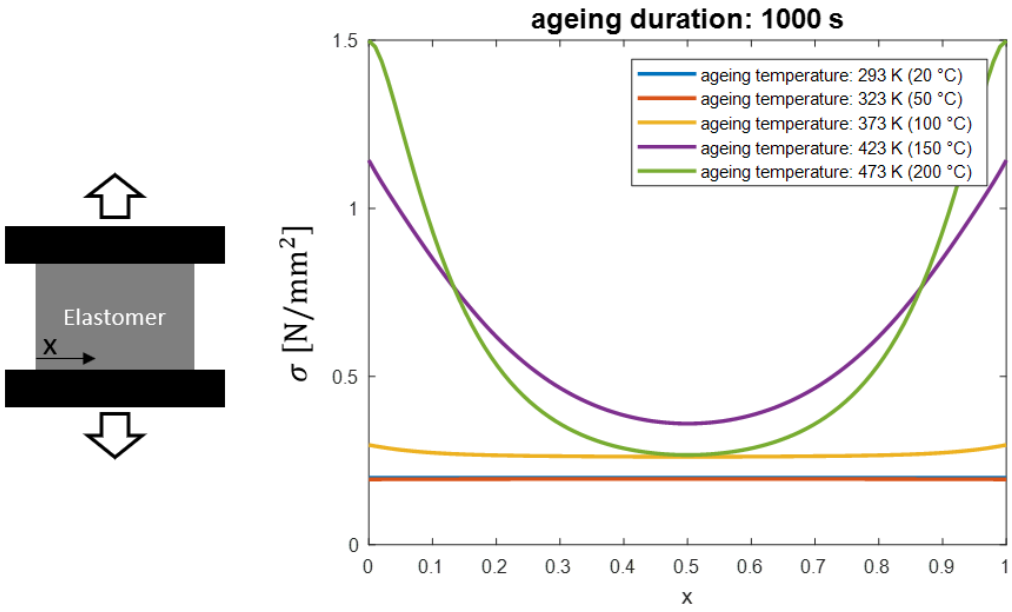

Figure 56: Profiles of the resulting tension (chain scission + network reformation) after ageing for 1000 s at different temperatures. Unidirectional stress was applied by firm clamping and according to Figure 54.1.

Usually elastomer samples are not cut into slices for running tensile tests with the whole set, but the intact sample is used for tests after exposure. Hence, the mechanical properties of the sample as a whole are measured. In order to be able to compare such results with the output of the model introduced here, the mechanical answer shown in Figure 55 is transformed by adding the stresses of finite parts of the sample according to Equation (51) and Figure 50. This united tension answer is plotted over the whole time of ageing and subsequently normalised to the peak value. Due to the applied strain shown in Figure 54.1 the results represent a kind of continuous relaxation test and are shown in Figure 57.

The example depicts that a general approach to describe the relaxation behaviour is not possible if a distinctive state of heterogeneous ageing exists. Since the thermal strain element is not taken into account in this isothermal experiment, temperature dependent material properties are not considered here.

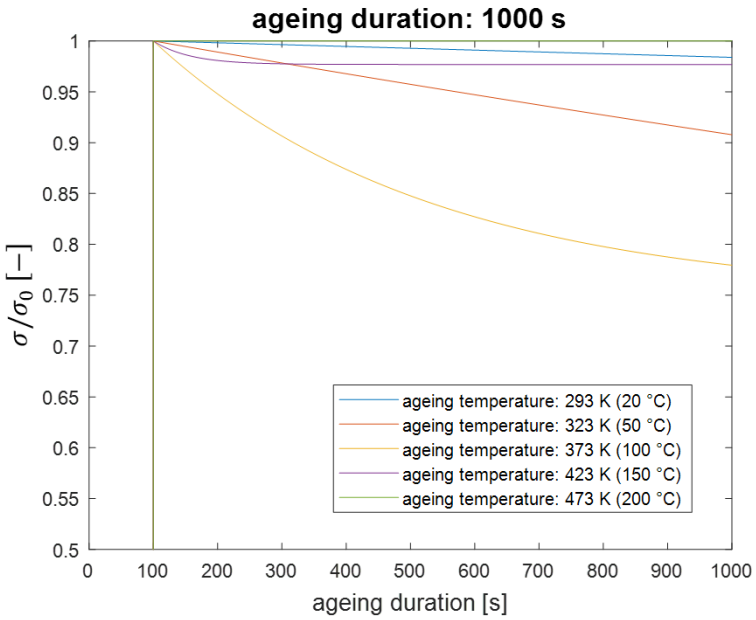

Figure 57: Normalised stress curves at different temperatures as a function of ageing time; Strain of 10 % is applied after 100 seconds of ageing

In comparison to the behaviour shown above, Figure 58 exhibits the tension profiles after the application of strain at the end of exposure as displayed in Figure 54.2. When applying strain to the sample after the oxidation process has taken place, both network parts - chain scission and reformation – are strained. That means that the stress results in Figure 58 consider all newly built network. Thus, the stress profiles differ significantly and are generally higher for respective temperatures as compared to those in Figure 56.

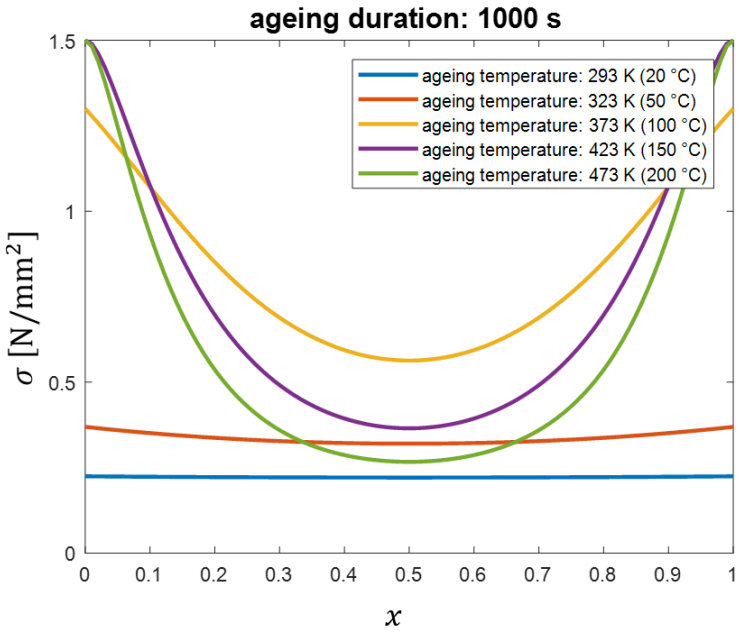

Figure 58: Tension profiles of the resulting tension (chain scission + network reformation) after ageing for 1000 s at different temperatures. Unidirectional stress was applied by firm clamping and according to Figure 54.2.

Comparing Figure 58 and Figure 56 highlights the influence of network reformation on the tension profiles. For low temperatures (293 K and 323 K) intermittent testing (Figure 58) exhibits homogeneous but higher tensions. A 373 K tension profile is much higher after intermittent testing than for continuous testing and heterogeneity is already well pronounced. For 423 K and 473 K heterogeneity occurs for intermittent as well as continuous testing. For these temperatures, the tension level in the centre of the sample is similar for both types of testing.

6.2.4.3 Size effect

For most investigations size effects are omitted since they make the comparison of specific influences complicated. Density and tension for example are formulated relative to the respective volume or area. In the case of thermo-oxidative ageing, the size effect can be important and should not be neglected. Here, the size effect describes a behaviour which results from diffusion-reaction processes and DLO. In practical terms, oxidation of a large elastomer bridge dampers and a small O-ring gasket cannot be easily compared although environmental conditions are in theory equal. This is shown in Figure 59 by comparing two bar-shaped samples which only differ in edge length. The ageing parameter p_{sci} is plotted over the cross-section and the average value is calculated.

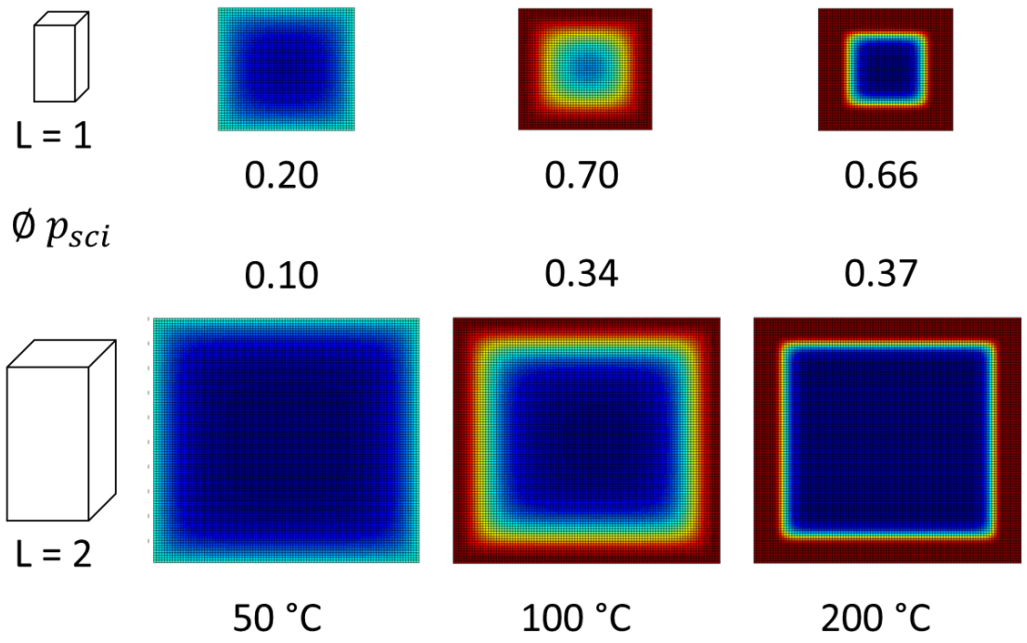

Figure 59: Size effect shown by the comparison of two bar-shaped samples with edge length L = 1 and L = 2

The plots as well as the average values of the ageing parameters ($\varnothing p_{sci}$) show that the diffusion-reaction process is unaffected by the dimension as long as an unaged area exists in the core. The example shows that the oxidised surface has an equal thickness for both sample sizes for each temperature. Thus, the aged part of a smaller sample has a higher share of the whole and therefore the average ageing parameter is higher. Since oxygen is provided from two sides at a corner oxidation is higher in these regions. For smaller dimension this effect also yields a higher ratio than for bigger ones. As a result, the bigger sample is less affected by oxidation than the smaller one. In Figure 59 the effect is shown for a simple geometry. The influence of this behaviour increases if the shape has a higher surface to volume ratio.

6.2.4.4 Heterogeneous oxidation of peroxide cured NBR

In this chapter the introduced model is applied for the simulation of heterogeneous ageing behaviour of peroxide cured NBR. Respective experimental has been generated as shown in paragraph 5.2.2.2, Figure 41. For this, the model is adjusted and fitted to the data obtained by FTIR-investigation. The modifications were made based on findings that have been gained during the application and fitting shown in this chapter. The content of this chapter was published in [137].

The reaction-diffusion equation with reaction terms for chain-scission and reformation is used as introduced in Equation (35). The antioxidants term is omitted since there is no experimental data available to make a reasonable consideration. Hence, the effect of antioxidants being present

in the elastomer is included in the existing reaction terms. The reaction terms are chosen as stated in Equation (38) and Equation (39) with the saturation parameters n_1 and n_2 having the value 2.

$$r_{ox,sci} = \frac{C}{C_0}\, r_{0,sci}\, e^{-\frac{E_{r,sci}}{R\,\theta}}\, (1 - p_{sci})^2 \tag{103}$$

$$r_{ox,ref} = \frac{C}{C_0}\, r_{0,ref}\, e^{-\frac{E_{r,ref}}{R\,\theta}}\, (1 - p_{ref})^2 \tag{104}$$

The non-linear contribution of the ageing parameters p_{sci} and p_{ref} are considered proportional to the square. Thus, the reactivity reduces with the progressing ageing process since the amount of convenient reaction partners decreases. Increasing the ageing parameter is only be achieved by an oxidative reaction or rather $r_{ox} > 0$. In this case the evolution equation is simplified since temperature and saturation effects are already considered by the reaction terms. Consequently, the evolution equations read

$$\dot{p}_{sci} = v_{p,sci}\, \frac{r_{ox,sci}}{r_{ox,sci,0}} \tag{105}$$

$$\dot{p}_{ref} = v_{p,ref}\, \frac{r_{ox,ref}}{r_{ox,ref,0}} \tag{106}$$

Since diffusivity is influenced by the ongoing ageing process, the diffusion coefficient is not formulated as a constant value but rather the influence of oxidative reactions, temperature is also considered in accordance with Equation (48) having a lower limit of 30 %. That means diffusivity can be reduced 70 % by oxidation.

A major challenge is the linkage of ageing parameters as an output of the model and experimental data obtained by FTIR spectroscopy. In order to describe the degree of oxidation from both the theoretical and experimental side, it is assumed that carbonyl nitrile ratio is equalised with the ageing parameter p_{sci}. The aim of this equalisation is to prove the modelling approach and gain knowledge about how the parameters influence the physical and chemical processes described by the model.

Figure 60 shows the carbonyl nitrile ratio profiles of the elastomer tested and the fitted model curves for the corresponding temperatures. Parameters are chosen as stated in Table 5.

Table 5: Parameters used for modelling of carbonyl-nitrile-ratio of the NBR shown in Figure 60

D_o [m^2/s]	3.0×10^{-5}	E_D [J/mol]	3267
$r_{o,sci}$ [mol/l/s]	30	$r_{o,ref}$ [mol/l/s]	30
$E_{r,sci}$ [J/mol]	29000	$E_{r,ref}$ [J/mol]	29000
$v_{p,sci}$ [1/s]	0.27	$v_{p,ref}$ [1/s]	0.27

Adopting the model failed until it was assumed that oxygen was in the elastomer before exposure started. Oxygen concentration cannot be chosen to be zero at the beginning of ageing. To be more specific an initial value of 15 % of the oxygen concentration of the ambient air (i.e. 3.15 %) was appropriate. Cross-linking and chain-scission were assumed to be equal regarding kinetics and the effects on diffusivity.

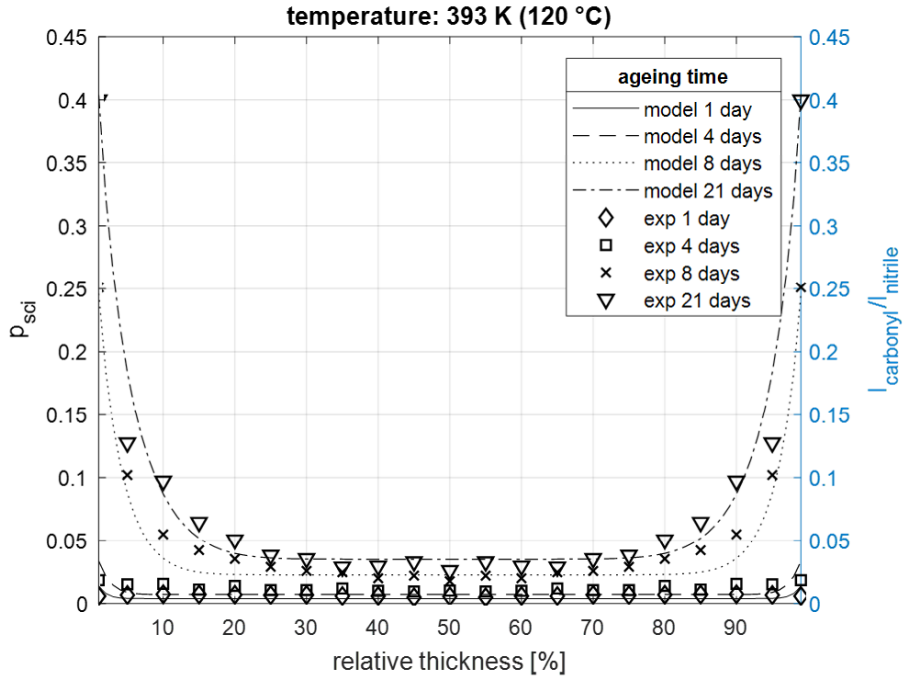

Figure 60: Carbonyl nitrile ratio of the NBR aged at 120 °C (exp) and model curves of ageing parameter p_{sci} (model)

The model describes a good approximation of carbonyl-nitrile profiles but more significant are the assumptions and discoveries which have been made on the way to this result. A more in depth discussion of these findings will follow in subsection 6.3.

6.2.4.5 Oxygen absorption

As shown in paragraph 6.2.3.5 oxygen absorption progress can be attained as an interim result of the diffusion-reaction process. Such an interim result can be used to validate the model or the parameter identification as well as any experimental results collected at this specific interim point. Modelling can be enhanced by acquiring additional knowledge of the model's individual

steps. Thus, specific steps can be optimised, changed or simplified resulting in the model better approximating the real chemical and physical processes occurring. This can reduce the degree of phenomenology and helps to bring together different specialities like mechanics, chemistry or material science.

Here, the ageing parameter and the amount of oxygen absorbed are plotted in parallel to one another. Figure 61 shows the ageing parameter profiles similar to those introduced before and the corresponding amount of oxygen absorbed during the time of ageing (bottom right). The individual graphs show the amount of oxygen molecules being absorbed during the process of ageing. Hence, at the very beginning the graphs start at the zero and rise steadily. In Figure 61 parameters are chosen such that diffusion dominates and DLO is less pronounced for the purpose of illustration. According to the modelling approach, absorption rate never increases during ageing but for the majority of cases declines, i.e. a saturation effect occurs. In the bottom right diagram of Figure 61 this becomes clear from the steadily decreasing gradient of the 200 °C curve with ongoing ageing time.

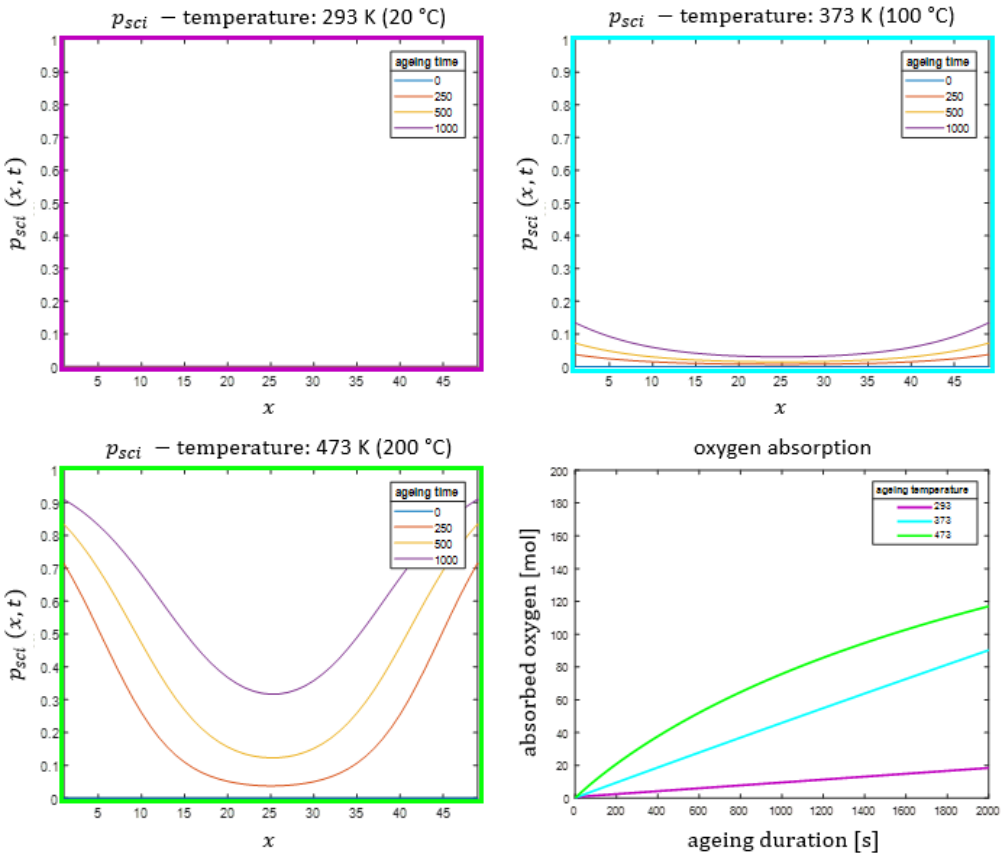

Figure 61: Oxygen absorption over ageing time as an additional output of the model

Figure 61 depicts the influence of temperature on the oxygen absorption. For 20 °C and 100 °C the amount of oxygen absorbed, rises linearly whereas at 200 °C a declining absorption rate can be observed which bases on DLO effect triggered by elevated temperature. The oxygen absorption clearly correlates with the ageing parameter profiles. For 20 °C up to 1000 s the ageing parameter

is apparently not affected and still rises only slightly for 100 °C. At a high temperature (200 °C) the ageing parameter immediately increases at the outer regions but after 1000 s the interior caught up. Hence, the diffusion-reaction process is less influenced by DLO and more by the availability of oxygen molecules or rather simple diffusion. In Figure 62 the same circumstances are chosen as in Figure 61 but with higher reactivity of the oxidation process. This was realised by elevating the basic reactivities and lowering activation energy for both the chain-scission and the network reformation. The parameters used for both figures are listed in Table 6.

Table 6: Parameter list for illustration of oxygen absorption as an interim step of model

$D_o\,[m^2/s]$	4.0×10^{-3}	Figure	61	62
E_D [J/mol]	10	$r_{o,sci}$ [mol/l/s]	300	500
$v_{p,sci}$ [1/s]	380	$E_{r,sci}$ [J/mol]	25000	22000
$v_{p,ref}$ [1/s]	380	$r_{o,ref}$ [mol/l/s]	300	500
$E_{p,sci}$ [J/mol]	38000	$E_{r,ref}$ [J/mol]	25000	22000
$E_{p,ref}$ [J/mol]	38000	γ	20	

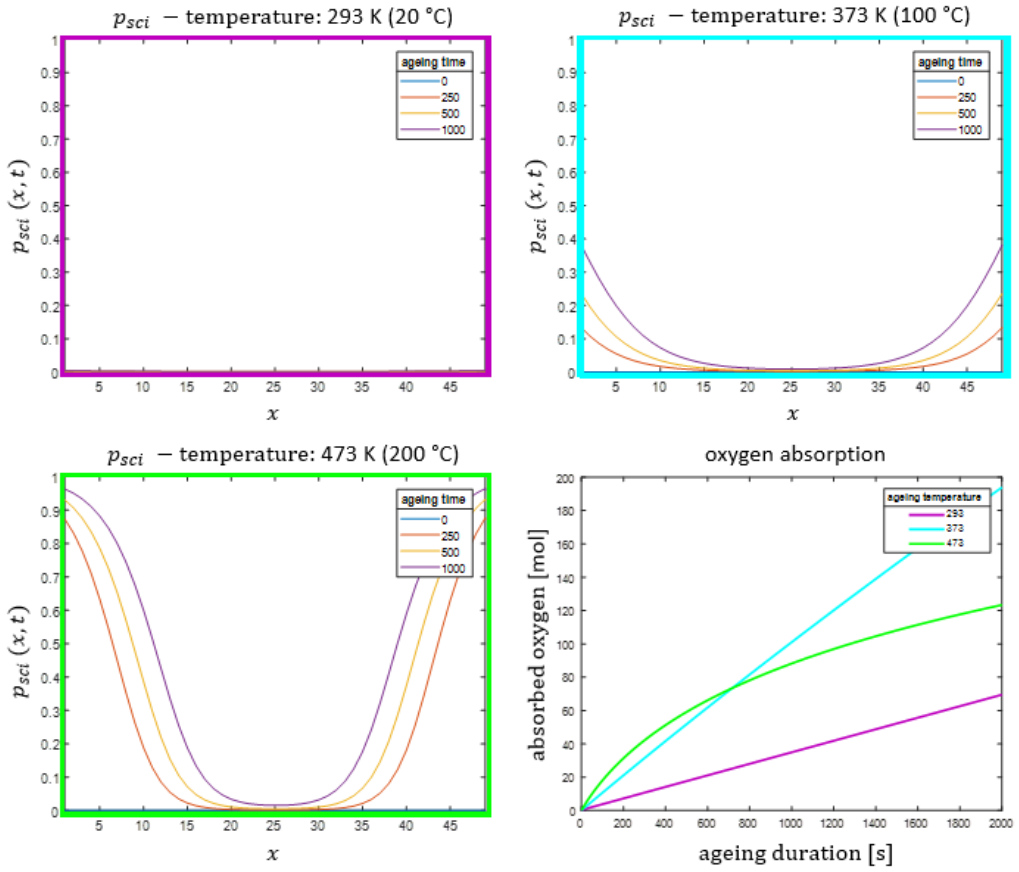

Figure 62: Oxygen absorption over ageing time with higher reactivity of oxidation

The results show that the general statement of higher temperatures provoking a higher amount of oxygen uptake reaches its limit in the case of DLO. This conlusion was already drawn in subsubsection 5.1.6 after the analysis of the experimental results from testing the statement with

different elastomer types. Oxygen absorption at 20 °C and 100 °C show quite linear behaviours but differ in the absorption rate. This is in line with the ageing parameter profiles which are still neglectable for 20 °C but more pronounced for 100 °C. Comparing the 100 °C profiles of Figure 61 and Figure 62 shows a slight DLO behaviour since the ageing parameter at the core is lower in Figure 62 than in Figure 61. For 200 °C ageing is very inhomogeneous with a highly oxidised surface and the core remains almost unaffected. Oxygen absorption starts with a high rate due to the diffusion process being accelerated by high temperature. With ongoing ageing time oxygen absorption rate at 200 °C declines even below the absolute amount of absorbed oxygen at 100 °C which is caused by an ageing induced deceleration of diffusivity. The highly pronounced DLO effect can be clearly seen in the ageing parameter profiles as well.

6.3 Discussion

The modelling approach regarding oxygen absorption (subsection 6.1) attempts to describe the experimental data determined from the measurements described in subsection 5.1. The concept of the model is based on Henry's law and supposes a correlation of the equilibrium oxygen concentration at the elastomers surface and the oxygen absorption rate. In other words, the higher the concentration at the surface the higher the amount of oxygen being absorbed by the elastomer in that moment. This assumption reaches its limit in the case of a high concentration at the surface with low amount or without oxygen being absorbed in that specific moment. For the case of DLO occurring the oxygen molecules are hindered further in their diffusing into the material. Hence, concentration can be high at the surface although absorption rate is low. This saturation effect in the superficial layer is not considered in the oxygen abortion model and motivates the development of an advanced model that considers diffusion effects (as presented in the subsequent chapters). Nevertheless, oxygen absorption rate is described by means of an oxygen absorption gradient S and a driving parameter p_{ox}. Thus, heterogeneous ageing or rather oxidation itself is not considered in that approach but the effects on oxygen absorption are included in the evolution equation. This is also believed to be the reason why a modified expression using the square to describe the reduction of the ageing parameter p fits better to the experimental data than a linear formulation. From a physical or rather chemical point of view this seems incorrect since the evolution equation includes additional effects which was not the original intention and further the phenomenological character of the model is increased.

The evolution equation was modified by using the square to describe the reduction of the ageing parameter p. This was determined to fit the experimental results better. More precisely, the bracket in Equation (30) describes how the ageing velocity is reduced with an ongoing degree of ageing. Therefore, three basic possibilities can be distinguished which are shown in Figure 63.

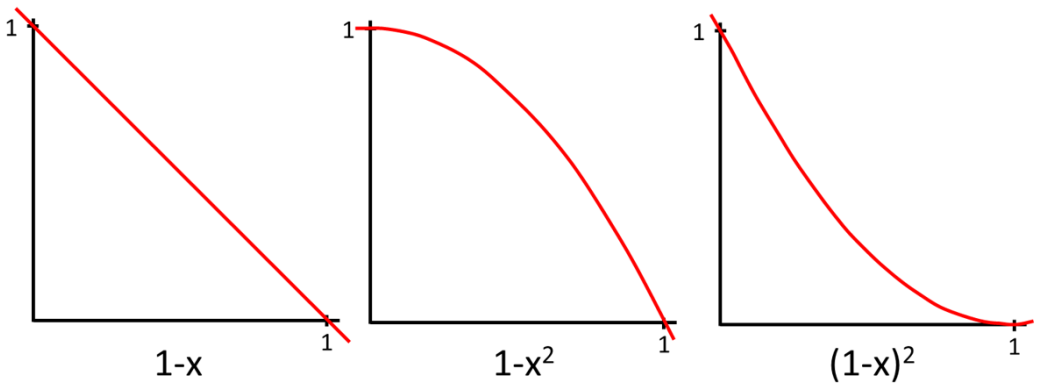

Figure 63: Visualisation of three different approaches for the saturation effect in the evolution equation

For "1-x" the rate of ageing decreases linearly with the progress of ageing which is the simplest way of describing a saturation effect. The number of reaction partners decreases since they already have reacted with oxygen or other sub-products of oxidation and hence the velocity of oxidation is reduced. This does not consider any inhomogeneous effects or spatial differences but represents an external observation of the elastomer sample. For the oxygen absorption behaviour presented, two other approaches are shown in Figure 63 which will be discussed here. The 'saturation term' "1-x^2" starts with a lower deceleration of the process at the beginning which can be seen in the smoother gradient of the graph closer to the x value of zero than for higher x-values up to 1. This approach can be used to model effects which depend on the value x but are initially less influenced when x starts at the value zero and for low numbers of x. For increasing x, the influence is also increased and accelerates which can be seen in the high negative gradient close to x is 1. The opposite can be achieved by using "$(1\text{-}x)^2$". At the beginning the influence is strong for even small changes in x. This effect slows down for x increasing until the gradient reaches the value zero. The latter is used in the model for oxygen absorption to describe the velocity term in the evolution equation. At the beginning ageing parameter p increases very fast since $(1\text{-}p)^2$ is close to 1 (Equation (30)). Each oxidative reaction decreases the number of reaction partners and decelerates the absorption process, which results in a decreased velocity. During exposure the influence of the degree of ageing decreases. DLO can also influence this behaviour when diffusivity is reduced in the surface layer of the elastomer sample. Initially each reaction taking place in the superficial layer reduces the diffusion coefficient and oxygen concentration is increased due to hindered diffusion of oxygen molecules deeper into the material. This effect decelerates diffusion which is expressed by slowed down decrease of ageing parameter p for higher degrees of ageing.

The model was introduced by describing solubility as a function of the cross-linking density. Usually solubility is most influenced by the affinity of oxygen to absorb at the elastomers surface. Cross-linking density is known to have an effect on the transportation process or rather diffusion, which has also influence on the permeation behaviour. As described in the previous chapters introducing the fundamentals absorption and diffusion can hardly be separated experimentally

but linear correlation of solubility and cross-linking density must be questioned. Further, cross-linking density can be increased and declined by chain-scission and network reformation in parallel, but here a steadily rising cross-linking density is assumed. As discussed previously the approach includes several effects and the explanation of solubility as a function of the degree of ageing would hit the core better. In general, Equation (29) assume oxygen absorption rate becoming zero for a fully aged sample. This is synonymous to a complete oxygen absorption stop after a certain time or progress of ageing and should be handled with care.

Although the model fits the measured curves well the geometrical shape of the sample is not included but the weight of the sample only. Since oxygen absorption is a process which is driven by or through the sample's surface the geometry or rather the shape can influence the amount of oxygen being taken up. Consequently, the modelling approach should be not generalised regarding shape and dimension and a more detailed view on spatial effects is needed. Since the model does not provide any output about inhomogeneous effects an extension of the model including diffusion processes was done subsequently.

Moreover, the model returns a very high oxygen absorption at the beginning of exposure (Figure 48) for elevated temperatures, due to the exponential influence of temperature. At this point the mathematical model seems to reach the limit of its validity since the model does not consider the upper limit for oxygen absorption. This effect is only suspected at the very beginning and should be questioned critically. Due to the short exposure time the amount of oxygen absorbed is quite low and hence the effect on the total amount of oxygen absorbed is minimal. Nevertheless, upper and lower limits of oxygen absorption are not described by the model which should be kept in mind when interpreting and discussing the results.

All in all, the theoretical approach is able to describe the experimental measurements and provides a tool to model the observed behaviour. Moreover, several aspects arise which are critically discussed here, and new ideas come up to improve the approach as shown subsequently. Due to the points mentioned oxidation was looked at from a different perspective including its diffusion processes in subsubsection 6.2.1. The main objective was to consider the inhomogeneous effects such as DLO. Therefore, the process of oxidation was handled following the chain of causation (Figure 64). This approach aims on the logical sequence of oxygen penetrating the elastomer, interacting with it and change its properties.

Figure 64: Chain of causation of thermo-oxidative ageing of elastomers

Thermo-oxidative ageing is assumed to be influenced by temperature and oxygen partial pressure in the ambient environment. This represents a simplification and real applications often struggle with more complex circumstances, for instance the additional influence of ozone and mechanical loads. The process of oxygen penetrating in the interior of the elastomer is described by Fick's

second law which does not consider adsorption processes based on surface affinity or other more complex physical effects like physisorption (see subsection 4.1). This is a simplification and does not take into account any emission of oxygen. Subsequent reactions with the elastomer are split into two groups, chain-scissioning and network reformation. Investigations by means of chemical analytics showed that thermo-oxidative reactions cause diverse alterations in the chemical structure and the simple fact that several reaction schemes exist indicates the complexity of this topic. The fact that all oxidative reactions are described by two equations (Equation (36) and Equation (37)) based on Arrhenius approaches which use four parameters for adjustment suggest the potential for a more detailed consideration of chemical details. Further, Equation (36) and Equation (37) include the availability of oxygen as a trigger and accelerator but no saturation effect of the polymer. Thus, with temperature being high enough to reach activation energy and oxygen being available, oxidation occurs with a constant rate without reaching any limit of consuming reaction partners on the elastomers side. This does however not reflect reality since saturation effects occur when oxidation binds reactants of the elastomer. This shortcoming was observed when oxygen absorption was obtained as an interim result of the diffusion-reaction model. Consequently, a modification of the equation was performed (Equation (38) and Equation (39)). Such a modification of the model is achieved by a critical reflection of the individual steps of the chain of causation and their interaction. If possible, experimental results are used to validate the interim steps of the model. Another example on this kind of modification concerns the evolution equation which was adjusted in 6.2.4.4. Since the current application brought new data on the problem, the equation which is based on former works can be simplified to reduce the number of parameters and brings the model closer to the occuring physical and chemical processes.

Due to the way the model is designed, oxidation immediately starts when oxygen is available. Effects like probability of reaction increasing with time are not considered. Hence, the model does not consider any potential effects of an induction period or similar.

Antioxidants are treated in a similarly simplified way as oxidative reactions and are formulated as a further reaction term in the reaction-diffusion equation. All these terms compete regarding the availability of oxygen molecules. Other influences of antioxidants which reduce diffusion or bind interim products of the oxidation scheme are excluded here. Parallel oxidation reactions are not hindered even if the reactivity of the antioxidative reactions is accelerated. As soon as oxygen is available in the elastomer, both oxidative and antioxidative reactions occur. Antioxidants are not separately included in the simulation of experimental results here because detailed information about the chemical processes of antioxidants and their consequences on ageing are not available. Consequently, the effects of the antioxidants have to be included in the reaction kinetics of chain scission and network reformation. Previous experimental results show the effect of antioxidants on an exposed elastomer sample (subsubsection 5.1.6) which motivates a deeper investigation and the inclusion of the effect in the future.

Since heterogeneous oxidation is dominated by diffusion, changes of the diffusion coefficient play an important role. Here, the diffusion coefficient is considered as a non-constant parameter,

dependant on time and space. Although different approaches on how diffusion can be described as a function of temperature and ageing progress have been introduced, this phenomenon is still a big challenge in elastomer science. The way diffusivity is influenced by ageing is still little studied and is likely to also differ depending on the type of elastomer. Effects of molecular network flexibility or the degree of curing are presumed to be influential, just like the presence of methyl and polar groups. Besides diffusivity, ageing is also assumed to affect adsorption behaviour which is not considered here. At high levels of oxidation embrittlement and hence cracking of the superficial layer can occur which transforms oxygen diffusion into an even more complicated process.

Temperature plays an important role in almost every step of ageing. Assuming the elastomers to have the same temperature as the ambient medium is mostly a good approximation but reaches its limit for high and quick temperature variations or dynamic loads causing dissipative heating. Adsorption, diffusion and any kind of chemical reaction are influenced by temperature. This is the reason inhomogeneous temperature effects have been taken into consideration here and were introduced by paragraph 6.2.1.6. The modular structure of the modelling approach allows a flexible adjustment and consideration of such effects. In order to implement it, additional data is required such as the thermal conduction coefficient. To what extent this phenomenon is influenced by ageing effects will not be discussed here but implies how far the model can be extended.

Main output of the model are the ageing parameters p_{sci} and p_{ref} which represent the state of ageing in an all-encompassing way. It stands to reason that this is a simplification which cannot illustrate the whole complexity of ageing and oxidation. Nevertheless, two main influencing parts are identified, chain-scission and network reformation. One of this parts is breaking down the molecular network while the other is reinforcing it. This distinction is based on the main objective of this work to simulate mechanical properties of elastomers and the question if it becomes softer or harder during exposure. Since this is essential when describing the ageing of elastomers, the linkage between ageing parameters and mechanical properties is included. The approaches are widely used and are only meant to highlight the modelling output. For this, spending a lot of effort in a very complex diffusion-reaction model which includes detailed knowledge about for instance reaction kinetics and their influence on tensile properties is wastage if the main interest focuses on fatigue behaviour. In this case reducing the whole oxidation process to two parameters describing network changes can be suboptimal since information gets lost. In summary this means the whole chain of causation should be considered and critically reflected for each individual problem.

The numerical implementation is achieved by means of the Crank-Nicolson method, a difference quotient as well as the ADI method. The methods are used due to their good stability, performance and accuracy for the problems at hand. No already existing code is used to solve the introduced problems, instead the algorithm is implemented step by step. Thus, the developed code is adjustable to the problem and it shows the results of the single steps during the numerical solving process. Furthermore, the individual equations are highly dependent on input

from other equations and the iterative development of the model required a highly flexible development environment which was ensured by the implemented code. Since the solving of the equations follows well known methods it will not be further discussed here.

The results of the model were presented in several figures with freely chosen parameters for reasons of illustration of the model as well as parameters adjusted for fitting experimental data. The 1D-plot for 423 K in Figure 51 points out a high velocity of oxidation from the beginning of exposure up to 200 s. After that the surface region (app. $x < 0.05$ and $x > 0.95$) depicts a very high level of ageing (p_{sci} close to the value 1) but further exposure does no longer influence the interior of the sample. For 473 K this effect is even more pronounced. The surface layer quickly reaches a high or even fully aged state and the interior is shielded by a kind of protection layer which prevents oxidation in the centre of the sample. That becomes even more obvious when observing the maximum degree of oxidation after the maximum ageing time shown here (1000 s) in the very middle of the sample ($x = 0.5$). At ambient temperature (293 K), the rate of oxidation is very low and quite homogeneous compared to elevated temperatures. It increases with increasing temperatures due to the acceleration of the oxidative reactions and the diffusion process. This behaviour shows up to 373 K. With higher ageing temperatures (423 and 473 K) the ageing parameter at $x = 0.5$ does not reach comparable values after a similar time of ageing which can be explained by the DLO effect preventing oxygen molecules from passing to the interior of the sample. Therefore, oxidation of elastomers is always accompanied by a dualism of elevated temperature increasing the diffusivity and the oxidative reactions, which decrease the diffusion coefficient (compare fundamentals of DLO in subsection 4.3). Figure 51 makes clear, that the model shows a more expressed heterogeneity for elevated ageing temperatures.

DLO causes a greater ageing of the surface area, but little to no ageing of a samples core area. Thus, a high gradient of oxidation transpires between these two different sections, especially at high temperatures, this can be observed in Figure 51. Other than in the transition area the gradient is not as high. The model introduced here is able to describe this behaviour. This can be confirmed by the changing curvature of the plots. The point of inflection can be chosen as a mark for the transition between surface area and interior.

Figure 51 shows the fictitious ageing parameter p_{sci} representing the degree of oxidation and not the concentration profile of dissolved oxygen which is shown in Figure 52. The oxygen concentration profiles are determined by solving the reaction-diffusion equation and are needed for the calculation of the reaction rate. The current oxygen concentration profile however, is not representative for the state of ageing or the progress of ageing. Furthermore, the oxygen profiles do not provide any information about altering mechanical properties. Nevertheless, example concentration profiles are shown in Figure 52 to give indications as to the way the model works. Diffusivity is not as high for real elastomers but here the basic functionality and the interaction of oxygen concentration and ageing parameter should be illustrated. Figure 52 shows the dualism of diffusion and consumption as mentioned previously when introducing DLO. At 100 °C diffusion is initially very high before oxidative reactions start and decelerate further diffusion. The amount of oxygen entering the elastomer decreases and in parallel oxygen is consumed by

oxidative reactions. This provokes a reduction in the dissolved oxygen during exposure as shown in Figure 52. For 200 °C this effect is even more pronounced, and oxygen is consumed faster and reduction in diffusivity occurs earlier. Plotting oxygen concentration illustrates an interim result of the model. Most often ageing parameters or mechanical properties are more significant for the user but when modelling as close to the real chemical and physical realities as possible, plotting additional information like the concentration of dissolved oxygen can provide further validation.

DLO is once more depicted by 2D-visualisation in Figure 53. Although the model is the same as for 1D it provides further information. For example, it shows how oxidation provokes advanced ageing in the corners of the sample since oxygen is provided from two sides. The output clarifies once more how DLO can prevent the interior from being affected by oxidation. The comparison of temperatures at 60 °C and 150 °C after 5000 s provides further clarification with the visualisation of DLO resulting in a lower average ageing parameter despite higher temperatures. More complex geometries are not shown here since different numerical methods would be required. The influence of geometry and dimension is suggested by the size effect (paragraph 6.2.4.3).

Simulation of mechanical properties depict a higher tension at the surface than in the interior. This makes crack formation more likely in the surface layer which has influence on the fracture and fatigue behaviour as stated previously in this work. This concludes that heterogeneous ageing is of significant consequence. Crack formation provokes a spatial changed oxygen absorption behaviour and enables oxygen penetration into the cracks and reaching regions below the surface. This can happen even for a sample with a low average ageing level since heterogeneity of oxidation is very high. The mechanical properties presented here, only include the influence of the ageing parameters. Other effects such as the loss of plasticisers are not considered here. The figures presented in paragraph 6.2.4.2 base on the assumption that network reformation is the dominating process. This is not a general rule and can differ depending on among other things the type of elastomer.

The model introduced was applied to simulate heterogeneous ageing of peroxide cured NBR in an oxygen containing environment. The description in paragraph 6.2.4.4 explains how the model was adjusted to best fit the experimental data. Several assumptions had been made and equalising the ageing parameter for chain scission and the carbonyl to nitrile ratio represents a simplification of real processes. At this point it should be clarified that all approaches in this work do not have any claim to absolute correctness or precise depiction of nature. Rather this work shows a possible way to handle such problems with a modular model which follows the chain of causation as closely as possible. The example shows that a modified reaction term including the saturation effect was necessary to simulate the oxygen absorption. More specifically this means the saturation part was transformed from the evolution equation to the reaction term. This transformation had no significant effect of the final result, however changes in the interim results can be observed. The decision to define saturation parameters n_1 and n_2 was made on the base of fitting the curves to the experimental data as closely as possible. The definition of the parameters was entirely empirical and has no relation to the chemical or physical evidence

found during testing.

Even with the achievment made with this model there remains still a lot of potential for further works. Selecting single physical or chemical processes in order to analyse them further and gain more knowledge would bring guaranteed improvement to the model. Similarly, diffusivity was handled in an iterative way the modelling being then adjusted accordingly. Figure 60 showed that the model's ability to simulate the experimental data is good. Nevertheless, the knowledge gained during the development of the model was more valuable than the result obtained by simulating peroxide cured NBR.

Despite a good overall result, inaccuracies can be found. For example, at very high degrees of oxidation at the surface between approximately 10 and 25 % depth. Such effects could be due to a more complex influence of oxidation or other ageing processes on diffusivity or on adsorption. At this point DLO is not described in a perfect way since the carbonyl to nitrile ratio sharply decreases at 0 to 5 % depth and declines at a lower rate in a depth of 10 to 25 %. Moreover, simulation of the homogeneous ageing for low ageing durations depicts some difficulties close to surface layer. A potential improvement could be the inclusion of phenomena such as the induction period by antioxidants or advanced description of reaction kinetic.

7 Critical reflection and outlook

The work presented aims at providing a comprehensive view on thermo-oxidative ageing of elastomers without the limitation to a certain type of elastomer. Therefore, a broad fundamental understanding of polymer ageing was established at the beginning before the focus was shifted to the deterioration of elastomers. Oxidation was elaborated and presented in detail as an important kind of elastomer degradation to provide the basis for the subsequent investigations and discussions. This was achieved by following the chain of causation from the environmental and triggering conditions to changing material properties and lifetime limiting consequences. Special attention was given to approaching the topic via several disciplines. Aspects of engineering, material science, mechanics and chemistry were used to understand and explain oxidative phenomena. In this, a dualism in the description of ageing mechanism between a basic and an applied scientific approach occured. Both have their justification and the more advantageous choice must be determined depending on the individual application. Following the way of the oxygen molecules penetrating the elastomer material and reacting with the polymer structure formed the basis for the way of experimental investigation and modelling. In order to handle the complexity of the ageing of elastomers a modular model was used with a diffusion-reaction equation as the core element. Although the work focuses predominately on thermo-oxidative ageing, other types of ageing were introduced in parallel to illustrate similarities, interactions and differences. Oxidation has been presented in a more or less isolated way to clarify its ageing mechanism and to keep an understandable level. Nevertheless, the findings showed that elastomer deterioration during usage or storage is a multidisciplinary and complex phenomenon.

Experimental results show that findings can be difficult to interpret since usually several effects of ageing interact and overlap. This makes analysis and general statements difficult especially when comparing different kinds of elastomers. Consequently, it is not possiple to develop a single model being unrestrictedly valid for all kinds of elastomers as well as environmental conditions and admixed additives. Although this work provides a detailed look on fundamental chemical and physical processes, a lot of questions are still open to be answered in subsequent works. For example, the mechanism and influence of antioxidants, the oxygen's diffusion process or the chemical oxidative reaction are still not answered completely and are expected to differ depending on the type of elastomer. This highlights the need for chemical expertise, more analytical investigation and further research in the field of polymer ageing. Beside a deeper understanding for ongoing reaction processes, the work shows that the adsorption of oxygen from the ambient environment has to be investigated in more detail since it represents the starting point of oxidation and can influence all subsequent steps of the ageing process. Hence, the effects of physisorption and chemisorption and how they are affected by ongoing ageing should be in the focus of future investigations.

The experimental methods chosen in this work do not claim to be comprehensive for investigating a specific type of elastomer ageing but instead try to give an insight to the whole process of oxidation. In order to analyse the first step, the oxygen absorption, a test setup was de-

signed based on a respirometer. Although much effort was spent in the construction and the development of the testing procedure, the possibility of further improvements and extensions arose during testing. The setup was designed to cover a wide range of testing procedures which are still not exhausted yet. For instance, continuous testing represents a potential way of investigation but is still a challenge. The oxygen absorption measurements reach their limit if information about spatial distribution is required or inhomogeneous oxidation is investigated. A spatial measurement of the dissolved oxygen which is not possible with the developed setup would provide more thorough information on the oxidation behaviour and help to further improve modelling. The present work shows that in many cases oxidation cannot be treated as a homogeneous phenomenon but behaves highly inhomogeneously. Thus, size and geometry of the elastomer component have impact on the overall ageing process and elastomer ageing should not be handled as a bulk effect. Therefore, experimental investigations focusing on the heterogeneous oxidation have been executed including computer tomography and infrared spectroscopy. The former represents a novel approach to investigate ageing phenomena by providing density mappings. The latter is an entrenched method for the analysis of chemical changes and yields oxidation profiles at the cross-section of an aged elastomer. Although the results of both methods provide a deep insight in heterogeneous ageing a combination or comparison of both outcomes clarifies which deficiencies still exist. A quantitative explanation of density changes by the results of FTIR-spectroscopy is still a challenge and shows the limits of the current state of knowledge. Density changes are not only caused by chemical processes but also by physical ones which makes it even more difficult to compare the results of both methods. This also shows that experimental investigations usually focus on a certain set of parameters and hence represent a limited section of ageing only. Converse observations of density changes during exposure at different temperature underline the temperature dependency and show significant gaps in the understanding which require further research. Focusing on oxidative reactions confirms FTIR-spectroscopy as a powerful tool for examining chemical changes and occurred reactions. Here, detailed information on the thermally activated reaction steps of oxygen with the elastomer's molecular structure or on the functionality of antioxidants and other additives is still to be gathered. Unfortunately, investigating inhomogeneous oxidation by FTIR-spectroscopy necessitates destructive testing and is limited for filled elastomers. In this context a critical question arises: Is it necessary to know about the chemical and physical details during ageing or is it sufficient to have a highly phenomenological description of the problem? The answer to this question depends on the individual situation and has to be chosen as the case arises.

The modelling approach presented in this work tries to replicate the chemical and physical steps as realistically as possible to reduce the degree in phenomenology and approximate the actual processes. Taking an honest look on the model shows that there is still a lot of potential for further enhancements. The degree of phenomenology is, if at all, only slightly reduced. The present work leads to the question if the reduction of phenomenology is the overarching objective. On the one side, profound information about the ageing mechanism increases the accuracy of the results but on the other side goes along with a more and more specialised model being valid for a certain type of material and limited boundary conditions only. Sometimes a less extensive model is sufficient and meets the requirements on simulation. In this work, the modelling of oxygen absorption

(subsection 6.1) does not distinguish between chain-scission and network reformation and a single ageing parameter is used. Going further shows that even using two ageing parameters is a significant simplification to represent the complex state of oxidation. Also, if the state of ageing is reduced to two parameters and used as an input for the description of material properties, loss of information cannot be ruled out. The model for the diffusion-reaction process does not yet include a more sophisticated consideration of the absorption or rather solubility process. Uncertainty exists if the ongoing ageing affects solubility, diffusion behaviour or even both. These examples show the still existing potential for further improvements of the modelling approach, but a deep understanding of the physical and chemical processes is a necessary prerequisite.

On the one hand future works can aim at detailed investigation of individual ageing effects and on the other hand at their interaction. This requires the consolidation of various fields of research, e.g. mechanics, material science, engineering and chemistry. Especially chemistry bears a lot of potential since information about the ageing reactions can be obtained. This provides information for the improvement of the modelling and helps to reduce phenomenology. Further, countermeasures to prevent the chemical steps of degradation can be optimized, for example antioxidants. Besides a closer understanding of ageing and its modelling, the information can also be utilised to optimise the usage of elastomers in engineering applications. During design it is important to know about the influences of the environment on the respective component to choose the right type of elastomer or to inhibit certain external loads if possible. For example, the effect of mechanical loads on diffusion or oxidation in general has to be analysed more deeply. A multidisciplinary approach will most likely help to reach an advanced level in the description of elastomer ageing.

In this work, experimental investigations and modelling were shown for thermo-oxidation only but should not be limited to these ambient conditions. The extension to other types of ageing and external loads like ozone or lubricants are possible tasks for subsequent works. Special focus should be given to inhomogeneous effects. Further, investigations and further research should be conducted in the field of inhomogeneous temperature fields which occur during dynamic loads or varying external temperatures. Moreover, physical and chemical ageing can be considered in parallel if good modelling results on short and long-time scales are required.

The modular structure of the model introduced in this work provides an adjustable and clear way to approach the simulation of oxidative phenomena. In future enhancements, this modular structure can be improved and extended to further ageing effects. For example, a core ageing model considering heterogeneous effects could be used as fundamental model and extended by modules depending on the type of elastomer or application. For better consideration of size and geometry effects a 3D implementation of the model would help to obtain good simulation results even for complex shaped elastomer components.

In general, the degree of phenomenology can be reduced more and more by gaining new information about the ageing process with all its challenges. For this, the existing approach which uses chain-scission and reformation as basic parts to describe elastomer ageing can be extended.

This helps to improve the prediction of the elastomer components' end of usage and to ensure a save and economical application. To be able to apply the results of such predictions, criteria for the end of usage are necessary in order to meet the requirements of the respective application. This includes criteria for fatigue behaviour and crack formation as well as their propagation to the field of elastomer ageing which represents a severe challenge for future research.

Bibliography

[1] Michael J. Tarkanian and Dorothy Hosler. America's first polymer scientists: Rubber processing, use and transport in mesoamerica. *Latin American antiquity*.

[2] Doris Klee, Jörg Lahann, and Wilhelm Plüster. Dünne Beschichtungen auf Biomaterialien. In Erich Wintermantel and Suk-Woo Ha, Editors, *Medizintechnik*, pages 863–877. Springer Berlin Heidelberg, Berlin, Heidelberg, 2009.

[3] S. Raab, A. M. Ahmed, and J. W. Provan. Thin film pmma precoating for improved implant bone-cement fixation. *Journal of biomedical materials research*, 16(5):679–704, 1982.

[4] A. Higgins. Adhesive bonding of aircraft structures. *International Journal of Adhesion and Adhesives*, 20(5):367–376, 2000.

[5] Edward M. Petrie. Adhesives for the assembly of aircraft structures and components. *Metal Finishing*, 106(2):26–31, 2008.

[6] S.G Burnay. An overview of polymer ageing studies in the nuclear power industry. *Nuclear Instruments and Methods in Physics Research Section B: Beam Interactions with Materials and Atoms*, 185(1-4):4–7, 2001.

[7] Michael Raupach and Till Fritz Büttner. *Concrete repair to EN 1504: Diagnosis, design, principles, and practice*. CRC Press, Boca Raton [u.a.], 2014.

[8] Katrin Reincke, B. Langer, Döhler S., U. Heuert, and W. Grellmann. Alterung und Beständigkeitsuntersuchungen von Elastomerwerkstoffen. *Kautschuk Gummi Kunststoff*, (10):60–67, 2014.

[9] John M. Hutchinson. Physical aging of polymers. *Progress in Polymer Science*, 20(4):703–760, 1995.

[10] Victor A. Soloukhin, José C. M. Brokken-Zijp, van Asselen, Otto L. J., and Gijsbertus de With. Physical aging of polycarbonate: Elastic modulus, hardness, creep, endothermic peak, molecular weight distribution, and infrared data. *Macromolecules*, 36(20):7585–7597, 2003.

[11] Gottfried W. Ehrenstein and Sonja Pongratz. *Beständigkeit von Kunststoffen*. Edition Kunststoffe. Hanser, München, 2007.

[12] Alexander Lion and Michael Johlitz. A thermodynamic approach to model the caloric properties of semicrystalline polymers. *Continuum Mechanics and Thermodynamics*, 28(3):799–819, 2016.

[13] C. Mittermeier, M. Johlitz, and A. Lion. A thermodynamically based approach to model physical ageing of amorphous polymers. *Archive of Applied Mechanics*, 85(8):1025–1034, 2015.

[14] Elizabeth N. Hoffman, Donald Fisher, William L. Daugherty, Eric T. Skidmore, and

Kerry A. Dunn. Aging performance of model 9975 package fluorelastomer o-rings: conference paper. *Conference: INMM 52nd Annual Meeting*, 2011.

[15] Roger A. Assink, Mathew Celina, Julie M. Skutnik, and Douglas J. Harris. Use of a respirometer to measure oxidation rates of polymeric materials at ambient temperatures. *Polymer*, 46(25):11648–11654, 2005.

[16] Lars Steinke. Ein Beitrag zur Simulation der thermo-oxidativen Alterung von Elastomeren, Volume 749 of *Fortschritt-Berichte VDI : Reihe 5, Grund- und Werkstoffe, Kunststoffe*. VDI-Verl., Düsseldorf, 2013.

[17] Jacques Verdu. *Oxidative ageing of polymers*. ISTE and Wiley, London and Hoboken, NJ, 2012.

[18] X. Colin, L. Audouin, and J. Verdu. Kinetic modelling of the thermal oxidation of polyisoprene elastomers. part 3: Oxidation induced changes of elastic properties. *Polymer Degradation and Stability*, 92(5):906–914, 2007.

[19] A. V. Tobolsky, I. B. Prettyman, and J. H. Dillon. Stress relaxation of natural and synthetic rubber stocks. *Journal of Applied Physics*, 15(4):380, 1944.

[20] Arthur V. Tobolsky. *Mechanische Eigenschaften und Struktur von Polymeren*. Berliner Union, Stuttgart, 1967.

[21] M. Celina, J. Wise, D.K Ottesen, K.T Gillen, and R.L Clough. Correlation of chemical and mechanical property changes during oxidative degradation of neoprene. *Polymer Degradation and Stability*, 68(2):171–184, 2000.

[22] Manfred Achenbach and Andreas Konrath. Alterung von Elastomeren - Anwendung auf Dichtungen. *Kautschuk Gummi Kunststoff*, 66(10):54–62, 2013.

[23] M. Celina, J. M. Skutnik Elliott, S. T. Winters, R. A. Assink, and L. M. Minier. Correlation of antioxidant depletion and mechanical performance during thermal degradation of an htpb elastomer. *Polymer Degradation and Stability*, 91(8):1870–1879, 2006.

[24] Christine Prieß, V. Katzenmaier, R. Kreiselmaier, B. Traber, and K. Beck. Analyse des oxidativen Alterungsverhaltens elastomerer Werkstoffe: Gegenüberstellung von NMR, Spannungsrelaxation und Chemilumineszenz. *Kautschuk Gummi Kunststoff*, pages 16–21, 2014.

[25] Richard J. Pazur and J. G. Cormier. The effect of acrylonitrile content on the thermo-oxidative aging of nitrile rubber. *Rubber Chemistry and Technology*, 87(1):53–69, 2014.

[26] Mathew C. Celina. Review of polymer oxidation and its relationship with materials performance and lifetime prediction. *Polymer Degradation and Stability*, 98(12):2419–2429, 2013.

[27] A. Kumar, S. Commereuc, and V. Verney. Ageing of elastomers: a molecular approach based on rheological characterization. *Polymer Degradation and Stability*, 85(2):751–757, 2004.

[28] John Scheirs, Stephen W. Bigger, and Norman C. Billingham. A review of oxygen uptake techniques for measuring polyolefin oxidation. *Polymer Testing*, 14(3):211–241, 1995.

[29] M. Celina, A. C. Graham, K. T. Gillen, R. A. Assink, and L. M. Minier. Thermal degradation studies of a polyurethane propellant binder. *Rubber Chemistry and Technology*, 73(4):678–693, 2000.

[30] Richard J. Pazur and T. Mengistu. Activation energies of thermo-oxidized nitrile rubber compounds of varying acrylonitrile content. *Rubber Chemistry and Technology*, 2018.

[31] Samuel Ding, Atul Khare, Michael T.K. Ling, Craig Sandford, and Lecon Woo. Polymer durability estimates based on apparent activation energies for thermal oxidative degradation. *Thermochimica Acta*, 367-368:107–112, 2001.

[32] J. Wise, K. T. Gillen, and R. L. Clough. Quantitative model for the time development of diffusion-limited oxidation profiles. *Polymer*, 38(8):1929–1944, 1997.

[33] Y. N. Torrejon and U. Giese. Consumption and reaction mechanisms of antioxidants during thermal oxidative aging. *Kautschuk Gummi Kunststoff*, 65(3):25–31, 2012.

[34] Christoph Naumann and Jörn Ihlemann. Simulation von oxidativen Alterungsprozessen in Elastomerbauteilen. *Kautschuk Gummi Kunststoff*, (10):68–75, 2014.

[35] L. Steinke, J. Spreckels, M. Flamm, and M. Celina. Model for heterogeneous aging of rubber products. *Plastics, Rubber and Composites*, 40(4):175–179, 2013.

[36] Jieying Zhi, Qinglin Wang, Mengjie Zhang, Manjia Li, and Yuxi Jia. Coupled analysis on heterogeneous oxidative aging and viscoelastic performance of rubber based on multi-scale simulation. *Journal of Applied Polymer Science*, 25:47452, 2019.

[37] Heinrich Rothert, Michael Kaliske, and Lutz Nasdala. Entwicklung von Materialmodellen zur Alterung von Elastomerwerkstoffen unter besonderer Berücksichtigung des Sauerstoffeinflusses, Volume 2 of *Mitteilungen des Instituts für Statik und Dynamik der Universität Hannover*. ISD, Hannover, 2005.

[38] Michael Johlitz. *Zum Alterungsverhalten von Polymeren: Experimentell gestützte, thermochemomechanische Modellbildung und numerische Simulation.* Habilitationsschrift, Universität der Bundeswehr München, Neubiberg, März 2015.

[39] Michael Johlitz, Benedikt Dippel, and Alexander Lion. Dissipative heating of elastomers: A new modelling approach based on finite and coupled thermomechanics. *Continuum Mechanics and Thermodynamics*, 28(4):1111–1125, 2016.

[40] Benedikt Dippel. Experimentelle Charakterisierung, Modellierung und FE-Berechnung thermomechanischer Kopplungen: am Beispiel eines rußgefüllten Naturkautschuks. Ph.D. thesis, Universität der Bundeswehr München, Neubiberg, 2015.

[41] V. Le Saux, P. Y. Le Gac, Y. Marco, and S. Calloch. Limits in the validity of arrhenius predictions for field ageing of a silica filled polychloroprene in a marine environment. *Polymer Degradation and Stability*, 99:254–261, 2014.

[42] Xuan Liu, Jiaohong Zhao, Rui Yang, Rossana Iervolino, and Stellario Barbera. A novel in-situ aging evaluation method by FTIR and the application to thermal oxidized nitrile rubber. *Polymer Degradation and Stability*, 128:99–106, 2016.

[43] Tetsuya Kawashima and Toshio Ogawa. Prediction of the lifetime of nitrile-butadiene rubber by FT-IR. *Analytical Sciences*, 21(12):1475–1478, 2005.

[44] Pierre Yves Le Gac, Mathew Celina, Gérard Roux, Jacques Verdu, Peter Davies, and Bruno Fayolle. Predictive ageing of elastomers: Oxidation driven modulus changes for polychloroprene. *Polymer Degradation and Stability*, 130:348–355, 2016.

[45] Sebastian Koltzenburg, Michael Maskos, and Oskar Nuyken. *Polymere: Synthese, Eigenschaften und Anwendungen.* Springer-Lehrbuch. Springer Spektrum, Berlin [u.a.], 2014.

[46] Wilhelm Keim. *Kunststoffe: Synthese, Herstellungsverfahren, Apparaturen.* Wiley-VCH, Weinheim, 2006.

[47] Hans Domininghaus and Peter Elsner, editors. *Kunststoffe: Eigenschaften und Anwendungen; mit 275 Tabellen.* Springer, Heidelberg [u.a.], 8., neu bearb. und erw. aufl Edition, 2012.

[48] A. Herzig, M. Johlitz, and A. Lion. Ageing phenomena in polymers: A short survey. In Wulff Possart and Markus Brede, editors, *Adhesive Joints*, pages 167–204. John Wiley & Sons Incorporated, Newark, 2018.

[49] L. Audouin, V. Langlois, J. Verdu, and de Bruijn, J. C. M. Role of oxygen diffusion in polymer ageing: kinetic and mechanical aspects. *Journal of Materials Science*, 29(3):569–583, 1994.

[50] K. T. Gillen, M. Celina, and R. L. Clough. Density measurements as a condition monitoring approach for following the aging of nuclear power plant cable materials. *Radiation Physics and Chemistry*, 56(4):429–447, 1999.

[51] V.A. Fernandes and D.S.A. De Focatiis. A swelling study of process-induced and deformation-induced anisotropy of filled rubbers. In Bohdana Marvalová and Iva Petriková, editors, *Constitutive Models for Rubbers*, pages 141–146. CRC Pr I Llc, London, 2015.

[52] C.-Y. Hui, K.-C. Wu, Ronald C. Lasky, and Edward J. Kramer. Case-II diffusion in polymers. I. Transient swelling. *Journal of Applied Physics*, 61(11):5129, 1987.

[53] N. Rabanizada, M. Johlitz, and A. Lion. Chemical aging of elastomers under different environmental conditions. *Proceedings of the International Conference "ANTEC"*, 2013.

[54] K. Narynbek Ulu, B. Huneau, E. Verron, and P.-Y. Le Gac. Infleunce of air and seawater on fatique behaviour of natural rubber. In Bohdana Marvalová and Iva Petriková, editors, *Constitutive Models for Rubbers*, pages 403–409. CRC Pr I Llc, London, 2015.

[55] J. Verdu, X. Colin, L. Audouin, J. Rychly, and L. Matisová-Rychlá. Chemiluminescence from the thermal oxidation of polyisoprene and polybutadiene I. Influence of oxygen pressure on the chemiluminescence of polyisoprene during its oxidation. *Polymer Degradation and Stability*, 91(6):1387–1394, 2006.

[56] Laurence W. McKeen. Introduction to permeation of plastics and elastomers. In Laurence W. McKeen, editor, *Permeability Properties of Plastics and Elastomers*, pages 1–20. Elsevier, 2012.

[57] Nathalie Lucas, Christophe Bienaime, Christian Belloy, Michèle Queneudec, Françoise Silvestre, and José-Edmundo Nava-Saucedo. Polymer biodegradation: Mechanisms and estimation techniques – a review. *Chemosphere*, 73(4):429–442, 2008.

[58] K. Vasanthi. Biodegradable polymers - a review. *Polymer Sciences*, (3), 2017.

[59] Xuan Liu, Jiaohong Zhao, Rui Yang, Rossana Iervolino, and Stellario Barbera. Effect of lubricating oil on thermal aging of nitrile rubber. *Polymer Degradation and Stability*, 151:136–143, 2018.

[60] Manfred D. Lechner, Klaus Gehrke, and Eckhard H. Nordmeier. *Makromolekulare Chemie: Ein Lehrbuch für Chemiker, Physiker, Materialwissenschaftler und Verfahrenstechniker*. Springer Spektrum, Berlin, 5. aufl. Edition, 2014.

[61] Haiqing Lin and Benny D. Freeman. Gas permeation and diffusion in cross-linked poly(ethylene glycol diacrylate). *Macromolecules*, 39(10):3568–3580, 2006.

[62] Van Amerongen, G. J. Influence of structure of elastomers on their permeability to gases. *Journal of Polymer Science*, 5(3):307–332, 1950.

[63] Ignazio Blanco. Lifetime prediction of food and beverage packaging wastes. *Journal of Thermal Analysis and Calorimetry*, 125(2):809–816, 2016.

[64] Ignazio Blanco. End-life prediction of commercial PLA used for food packaging through short term TGA experiments: Real chance or low reliability? *Chinese Journal of Polymer Science*, 32(6):681–689, 2014.

[65] Zbigniew Dobkowski. Lifetime prediction for polymer materials using OIT measurements by the DSC method. *Polimery*, 50(03):213–215, 2005.

[66] John Scheirs. *Compositional and failure analysis of polymers: A practical approach*. Wiley, Chichester, 2000.

[67] Michael Johlitz. On the representation of ageing phenomena. *The Journal of Adhesion*, 88(7):620–648, 2012.

[68] Wolfgang Kaiser. *Kunststoffchemie für Ingenieure: Von der Synthese bis zur Anwendung*. Hanser, München, 4., neu bearbeitete und erweiterte Auflage Edition, 2016.

[69] Martin Bonnet. *Kunststofftechnik: Grundlagen, Verarbeitung, Werkstoffauswahl und Fallbeispiele*. Lehrbuch. Springer Fachmedien, Wiesbaden, 2., überarb. und erw. aufl Edition, 2014.

[70] Claus Wrana. *Polymerphysik: Eine physikalische Beschreibung von Elastomeren und ihren anwendungsrelevanten Eigenschaften*. Springer Spektrum, Berlin [u.a.], 2014.

[71] Michael Johlitz, Johannes Retka, and Alexander Lion. Chemical ageing of elastomers: Ex-

periments and modelling. In Stephen Jerrams and Niall M. Murphy, editors, *Constitutive models for rubber VII*, volume 7, pages 113–118. CRC Press, Boca Raton, 2012.

[72] C. Henneuse-Boxus and T. Pacary. Emissions from plastics, volume 161 of *Report / Rapra Technology Ltd.* Rapra Technology, Shrewsbury, 2003.

[73] V. Mehling and H. Baaser. Simulation of self–heating of dynamically loaded elastomer components. In G. Heinrich, editor, *Constitutive models for rubber VI*. CRC Press, Boca Raton [Fla.] and London, 2010.

[74] Erhard Hornbogen, Gunther Eggeler, and Ewald Werner. *Werkstoffe: Aufbau und Eigenschaften von Keramik-, Metall-, Polymer- und Verbundwerkstoffen.* Springer-Lehrbuch. Springer, Berlin [u.a.], 9., vollst. neu bearb. aufl. Edition, 2008.

[75] Khairi Nagdi. *Gummi-Werkstoffe: Ein Ratgeber für Anwender; Arten, Gemeinsamkeiten, Zusammensetzung, Eigenschaften, Beständigkeiten, Anwendungen, Prüfungen, Klassifizierung, Chemie.* Vogel, Würzburg, 1. aufl. Edition, 1981.

[76] Walter Gohl. *Elastomere: Dicht- u. Konstruktionswerkstoffe.*, Volume 5 of *(Kontakt & Studium.* Expert Verl., Grafenau/Württ., 3., überarb. aufl. Edition, 1983.

[77] James E. Mark and Burak Erman. *Science and technology of rubber.* Elsevier Academic Press, Amsterdam and Boston, 3rd ed. edition, 2005.

[78] Katrin Reincke. Elastomere Werkstoffe - Zusammenhang zwischen Mischungsrezeptur, Struktur und mechanischen Eigenschaften sowie dem Deformations- und Bruchverhalten. Berichte aus der Kunststofftechnik. Shaker Verlag, Aachen, 1. aufl. Edition, 2016.

[79] Leif Kari. Dynamic stiffness of chemically and physically ageing rubber vibration isolators in the audible frequency range: Part 2 - waveguide solution. *Continuum Mechanics and Thermodynamics*, 21:741, 2017.

[80] Leif Kari. Dynamic stiffness of chemically and physically ageing rubber vibration isolators in the audible frequency range. *Continuum Mechanics and Thermodynamics*, 21:741, 2017.

[81] Michael Johlitz and Alexander Lion. Chemo-thermomechanical ageing of elastomers based on multiphase continuum mechanics. *Continuum Mechanics and Thermodynamics*, 25(5):605-624, 2013.

[82] François Bénière. Diffusion in and through polymers. *Defect and Diffusion Forum*, 194-199:897–908, 2001.

[83] Peter W. Atkins and Ralf Ludwig. *Kurzlehrbuch Physikalische Chemie: [mit 600 Übungen].* Bachelor. Wiley-VCH, Weinheim, 4. aufl. Edition, 2008.

[84] A. Herzig, L. Sekerakova, M. Johlitz, and A. Lion. A modelling approach for the heterogeneous oxidation of elastomers. *Continuum Mechanics and Thermodynamics*, 68(2):197, 2017.

[85] Kenneth T. Gillen and Roger L. Clough. Rigorous experimental confirmation of a theoretical model for diffusion-limited oxidation. *Polymer*, 33(20):4358–4365, 1992.

[86] Arnaud Vieyres, Roberto Pérez-Aparicio, Pierre-Antoine Albouy, Olivier Sanseau, Kay Saalwächter, Didier R. Long, and Paul Sotta. Sulfur-cured natural rubber elastomer networks: Correlating cross-link density, chain orientation, and mechanical response by combined techniques. *Macromolecules*, 46(3):889–899, 2013.

[87] R. L. Clough and K. T. Gillen. Oxygen diffusion effects in thermally aged elastomers. *Polymer Degradation and Stability*, 38(1):47–56, 1992.

[88] J. D. Edwards and S. F. Pickering. Permeability of rubber to gases. In Montgomery T. Shaw and William J. MacKnight, editors, *Introduction to polymer viscoelasticity*, pages 1–6. Wiley Interscience, New York [u.a.], 2005.

[89] M. Celina, J. Wise, D. K. Ottesen, K. T. Gillen, and R. L. Clough. Oxidation profiles of thermally aged nitrile rubber. *Polymer Degradation and Stability*, 60(2-3):493–504, 1998.

[90] A. Herzig, M. Johlitz, and A. Lion. Consumption and diffusion of oxygen during the thermoxidative ageing process of elastomers. *Materialwissenschaft und Werkstofftechnik*, 47(5-6):376–387, 2016.

[91] K. T. Gillen, R. L. Clough, and N. J. Dhooge. Density profiling of polymers. *Polymer*, 27(2):225–232, 1986.

[92] Alexander Herzig, Michael Johlitz, and Alexander Lion. Experimental investigation on the consumption of oxygen and its diffusion into elastomers during the process of ageing. In Bohdana Marvalová and Iva Petriková, editors, *Constitutive Models for Rubbers*, pages 23–28. CRC Pr I Llc, London, 2015.

[93] Rui Yang, Jiaohong Zhao, and Ying Liu. Oxidative degradation products analysis of polymer materials by pyrolysis gas chromatography–mass spectrometry. *Polymer Degradation and Stability*, 98(12):2466–2472, 2013.

[94] Nicolas Saintier, Georges Cailletaud, and Roland Piques. Cyclic loadings and crystallization of natural rubber: An explanation of fatigue crack propagation reinforcement under a positive loading ratio.

[95] Richard J. Pazur and T. Mengistu. Effect of thermo-oxidation on permeation resistance of bromobutyl compounds. *Rubber Chemistry and Technology*, 90(1):195–206, 2017.

[96] Liliane Bokobza. Mechanical and electrical properties of elastomer nanocomposites based on different carbon nanomaterials. *C*, 3(4):10, 2017.

[97] Frederikke B. Madsen, Shamsul Zakaria, Liyun Yu, and Anne L. Skov. Mechanical and electrical ageing effects on the long-term stretching of silicone dielectric elastomers with soft fillers. *Advanced Engineering Materials*, 18(7):1154–1165, 2016.

[98] P. N. Lowell and N. G. McCrum. Diffusion mechanisms in solid and molten polyethylene. *Journal of Polymer Science Part A-2: Polymer Physics*, 9(11):1935–1954, 1971.

[99] Roger Alan Assink, Julie M. Elliott, and Mathias C. Celina. *Thermal aging of the polyurethane foam for the H1259 storage container*. 2006.

[100] Timothy J. Strovas, Sarah C. McQuaide, Judy B. Anderson, Vivek Nandakumar, Marina G. Kalyuzhnaya, Lloyd W. Burgess, Mark R. Holl, Deirdre R. Meldrum, and Mary E. Lidstrom. Direct measurement of oxygen consumption rates from attached and unattached cells in a reversibly sealed, diffusionally isolated sample chamber. *Advances in Bioscience and Biotechnology*, 01(05):398–408, 2010.

[101] Rona L. Thompson, Andrew C. Manning, David C. Lowe, and David C. Weatherburn. A ship-based methodology for high precision atmospheric oxygen measurements and its application in the southern ocean region. *Tellus B*, 59(4), 2007.

[102] Daisuke Goto, Shinji Morimoto, Shigeyuki Ishidoya, Akinori Ogi, Shuji Aoki, and Takakiyo Nakazawa. Development of a high precision continuous measurement system for the atmospheric O2/N2 ratio and its application at aobayama, Sendai, Japan. *Journal of the Meteorological Society of Japan. Ser. II*, 91(2):179–192, 2013.

[103] Alexander Herzig, Michael Johlitz, and Alexander Lion. An experimental set-up to analyse the oxygen consumption of elastomers during ageing by using a differential oxygen analyser. *Continuum Mechanics and Thermodynamics*, 2014.

[104] Britton B. Stephens, Peter S. Bakwin, Pieter P. Tans, Ron M. Teclaw, and Daniel D. Baumann. Application of a differential fuel-cell analyzer for measuring atmospheric oxygen variations. *Journal of Atmospheric and Oceanic Technology*, 24(1):82–94, 2007.

[105] R. K. Josephson, J. G. Malamud and D. R. Stokes. Efficiency of asynchronous muscle.

[106] Angelika Mennecke. *Evaluation und Optimierung eines Luftprobennahmesystems für flugzeuggestützte Messungen des atmosphärischen 02/N2 - Verhältnisses*. Diploma thesis, Friedrich-Schiller-Universität Jena, Jena, 2006.

[107] Julia Steinbach. Enhancing the usability of atmospheric oxygen measurements through emission source characterization and airborne measurements. Doctoral thesis, Friedrich–Schiller–Universität Jena, Jena, 2010.

[108] Kenneth T. Gillen, Mathew Celina, and Robert Bernstein. Validation of improved methods for predicting long-term elastomeric seal lifetimes from compression stress–relaxation and oxygen consumption techniques. *Polymer Degradation and Stability*, 82(1):25–35, 2003.

[109] TetraTec Instruments GmbH. Laminar flow elemente: Durchflussmessung mit LFES.

[110] T. Zaharescu and C. Podina. Thermal degradation of butyl rubber. *Journal of Materials Science Letters*, 16(9):761–762, 1997.

[111] M. Celina, G. A. George, D. J. Lacey, and N. C. Billingham. Chemiluminescence imaging of the oxidation of polypropylene. *Polymer Degradation and Stability*, 47(2):311–317, 1995.

[112] M. Celina, A. B. Trujillo, K. T. Gillen, and L. M. Minier. Chemiluminescence as a condition monitoring method for thermal aging and lifetime prediction of an htpb elastomer. *Polymer Degradation and Stability*, 91(10):2365–2374, 2006.

[113] A. Momose. Micro X-ray CT. *Structure Characterization in Real Space*, pages 547–558, 2012.

[114] Juan Pazmino, Valter Carvelli, and Stepan V. Lomov. Micro-CT analysis of the internal deformed geometry of a non-crimp 3d orthogonal weave e-glass composite reinforcement. *Composites Part B: Engineering*, 65:147–157, 2014.

[115] Paul R. Morrell, Mogon Patel, and Simon Pitts. X-ray CT microtomography and mechanical response of foamed polysiloxane elastomers. *Polymer Testing*, 31(1):102–109, 2012.

[116] Firas Awaja, Minh-Tam Nguyen, Shengnan Zhang, and Benedicta Arhatari. The investigation of inner structural damage of UV and heat degraded polymer composites using X-ray micro CT. *Composites Part A: Applied Science and Manufacturing*, 42(4):408–418, 2011.

[117] F. Cosmi and A. Bernasconi. Micro-CT investigation on fatigue damage evolution in short fibre reinforced polymers. *Composites Science and Technology*, 79:70–76, 2013.

[118] T. Alshuth and S. Robin. Hochauflösende 3D-Röntgen-Computertomographie (CT): Eine neue, leistungsfähige Methode zur Charakterisierung von Elasomerwerkstoffen und Bauteilen. *Kautschuk Gummi Kunststoff*, pages 382–387, 2010.

[119] Mohamed Baba, Jacques Lacoste, and Jean-Luc Gardette. Crosslinking on ageing of elastomers III. A new method for evaluation of crosslinking based on density measurements. *Polymer Degradation and Stability*, 65(3):421–424, 1999.

[120] Helmut Günzler and Alex Williams. *Handbook of analytical techniques*. Wiley-VCH, Weinheim and New York, 2001.

[121] Thomas Lehmann. IR-spektroskopie: Infrarotspektroskopie: Institut für Chemie und Biochemie. Institut für Chemie und Biochemie, 2010.

[122] Sébastien Rolere, Siriluck Liengprayoon, Laurent Vaysse, Jérôme Sainte-Beuve, and Frédéric Bonfils. Investigating natural rubber composition with fourier transform infrared (FT-IR) spectroscopy: A rapid and non-destructive method to determine both protein and lipid contents simultaneously. *Polymer Testing*, 43:83–93, 2015.

[123] Ludmila Vozarova, Michael Johlitz, and Alexander Lion. Nitrile rubber - the influence of acrylonitrile content on the thermo-oxidative aging: Proceedings of the 10th european conference on constitutive models for rubber (ECCMR), Munich, Germany, 28-31 August 2017. In Alexander Lion and Michael Johlitz, editors, *Constitutive models for rubber X*, pages 91–94, Boca Raton, Florida, 2017. CRC Press.

[124] Tuyet-Trinh Do, Mathew Celina, and Peter M. Fredericks. Attenuated total reflectance infrared microspectroscopy of aged carbon-filled rubbers. *Polymer Degradation and Stability*, 77(3):417–422, 2002.

[125] Fei-Zhou Li, Mu-Rong Gao, and Bian Guo. Investigation of ageing behaviour of nitrile-butadiene rubber with added graphene in an accelerated thermal ageing environment. *Kemija u industriji*, 67(1-2):29–37, 2018.

[126] Jiaohong Zhao, Rui Yang, Rossana Iervolino, and Stellario Barbera. Changes of chemical structure and mechanical property levels during thermo-oxidative aging of NBR. *Rubber Chemistry and Technology*, 86(4):591–603, 2013.

[127] Victor M. Litvinov and Prajna P. De. *Spectroscopy of rubber and rubbery materials*. Rapra Technology Ltd, Shawbury, U.K, 2002.

[128] Philipp Bruns and Christian Hopmann. The effect of crosslinks on the mechanical properties of elastomers: Experimental characterization and modeling. *Proceedings of the SPE ANTEC Conference Orlando*, pages 2871–2875, 2015.

[129] J. Duarte and M. Achenbach. On the modelling of rubber ageing and performace changes in rubbery components. *Kautschuk Gummi Kunststoff*, pages 172–175, 2007.

[130] S. Kamaruddin, A. H. Muhr, P. Y. Le Gac, Y. Marco, and V. Le Saux. Modelling naturally aged NR mouldings. 2013.

[131] A. Lion and M. Johlitz. On the representation of chemical ageing of rubber in continuum mechanics. *International Journal of Solids and Structures*, 49(10):1227–1240, 2012.

[132] A. Lion, C. Liebl, S. Kolmeder, and J. Peters. Representation of the glass-transition in mechanical and thermal properties of glass-forming materials: A three-dimensional theory based on thermodynamics with internal state variables. *Journal of the Mechanics and Physics of Solids*, 58(9):1338–1360, 2010.

[133] A. Lion and J. Peters. Coupling effects in dynamic calorimetry: Frequency-dependent relations for specific heat and thermomechanical responses — a one-dimensional approach based on thermodynamics with internal state variables. *Thermochimica Acta*, 500(1-2):76–87, 2010.

[134] D. W. Peaceman and Jr. H. H. Rachford. The numerical solution of parabolic and elliptic differential equations. *Journal of the Society for Industrial and Applied Mathematics*, 3(1):28–41, 1955.

[135] Li, Jichun, Chen, Yi-Tung. Computational partial differential equations using Matlab.

[136] A. Herzig, M. Johlitz, and A. Lion. Modelling of reaction-diffusion induced oxidation of elastomers in two spatial dimensions by means of ADI method. In Alexander Lion and Michael Johlitz, editors, *Constitutive models for rubber X*, pages 33–38, Boca Raton and London and New York and Leiden, 2017. CRC Press.

[137] A. Herzig, M. Johlitz, R. J. Pazur, J. Lopez-Carreon, and C. G. Porter. Thermal ageing of peroxide-cured NBR, part II: Diffusion-limited oxidation and constitutive modelling. In Bertrand Huneau, Jean-Benoît Le Cam, Yann Marco, and Erwan Verron, editors, *Constitutive Models for Rubber XI: Proceedings of the 11th European Conference on Constitutive Models for Rubber (ECCMR 2019), June 25-27, 2019, Nantes, France*, pages 587–592, 2019. CRC Press (CAM) and CRC Press.

List of Figures

List of Tables